Università degli Studi di Ferrara

DOCTORAL COURSE IN
"MOLECULAR MEDICINE"

CYCLE XXXIV

DIRECTOR Prof. Di Virgilio Francesco

Determination of the soluble form of the P2X7 receptor in aqueous humour, vitreous humour and serum under normal and pathological conditions: sP2X7R as an indicator of ocular inflammatory status.

Scientific/Disciplinary Sector (SDS) MED/30

Candidate
Dott. Carla Enrica Gallenga

_____
(signature)

Supervisor
Prof. Di Virgilio Francesco

_____
(signature)

Years 2018/2021

ABSTRACT

Background

P2X7R is a nucleotide receptor that binds extracellular ATP and is present on the cytoplasmic membrane of numerous cell types, including all inflammatory and immune cells. P2X7R plays a key role in inflammation, mediating activation of the NLRP3 inflammasome and release of cytokines such as IL-1β, and in regulating several cell death mechanisms. Espression of P2X7R was found in both the bulb and the ocular adnexa. Furthermore, on the ocular surface P2X7R is activated by chemical or mechanical sources of exogenous stress, leading to inflammation, apoptosis and cell proliferation. At the retinal level, abnormalities in P2X7R function have been linked to neuronal loss in glaucoma and neuroinflammatory processes in age-related macular degeneration and diabetic retinopathy. Based on a careful analysis of the recent literature on the involvement of P2X7R in the pathogenesis of various ocular diseases, this observational interventional study was conducted, aiming to:

- asses the presence of the soluble form of the purinergic P2X7 receptor (sP2X7R) in aqueous humour and vitreous humour;
- compare sP2X7R levels in healthy conditions and in the presence of various ocular or systemic pathological conditions with ocular involvement, underlying an inflammatory pathogenesis, such as: glaucoma, Fuchs endothelial dystrophy, pseudoexfoliatio, age-related macular degeneration, diabetes mellitus and retinal detachment;
- compare sP2X7R levels in aqueous humour and vitreous humour with those in serum.

Methods

The patients enrolled in the study are represented by subjects undergoing eye surgery at the Ophthalmic Clinic Unit of the Sant'Anna Hospital of Ferrara. In the group of pathological subjects there are aqueous humour and serum samples taken from patients with different ocular pathologies who underwent planned cataract extraction surgery and vitreous humour and serum samples from patients with retinal detachment who underwent vitrectomy surgery. The control group included aqueous humour and serum samples from patients undergoing cataract extraction surgery in the absence of other eye disease and vitreous and serum samples taken from patients undergoing vitrectomy for macular hole or macular pucker.

Results

In this study, the presence of a soluble form of the P2X7 receptor (sP2X7R) was assessed, which was found to be detectable in aqueous humour and vitreous humour using a specific ELISA kit. The concentrations of sP2X7R in aqueous humour control group are in the range of 3.89-93.87 pg/ml and in pathologic groupd the concentration range from 3.55 to 277.4 pg/ml. In vitreous humour the range is 4.21-76.92 pg/ml in the control group, whilist in pathological condition the range was 28.52 to 284.57 pg/ml.

The Kruskal-Wallis Chi-squared on the equality of the medians of the groups, both control and pathology groups of the acqueous samples, (Kruskal-Wallis chi-squared = 18.254, df = 10, p-value = 0.05082) estimates a p-value slightly above the test reliability limit (p=0.05), confirming that the median value of the sP2X7r concentration measured in the pathology groups, when all the data are considered together, is significantly different from the control group. Despite the finding of high maximum concentrations of P2X7r in its soluble form in the disease groups, analysing each pathology group compared to the control group, statistical analysis using Dunn's Test to perform the pairwise comparison of the groups with the Bonferroni's correction factor, failed to confirm a statistically significant difference.

The non-parametric hypothesis test performed with the Kruskal-Wallis Test on the equality of the median of the groups in Figure 20 (Kruskal-Wallis chi-squared = 4.6481, df = 3, p-value = 0.1995) does not allow the initial hypothesis to be rejected with probability p-value = 0.1999 (Talbe 17). The test result therefore does not allow the assertion that there is a significant difference between the P2X7r content in the vitreous of healthy patients and patients with the studied eye diseases

Conclusions

In this study the presence of the soluble form of the P2X7 receptor in aqueous humour and vitreous humour was tested for the first time, and the ELISA kit used proved to be a reliable tool. In the global examination of pathologic groups it can be stated that sP2X7R is a marker of ocular inflammatory status in, but the stratification analysis failed to prove a significant correlation with the single pathology.

Those data reflect a local and time-limited reality, but could lay the groundwork for further investigation.

CHAPTER 1: THE P2X7 RECEPTOR

Generalities on the P2X7 receptor

The P2X7 receptor (P2X7R) is a member of the P2X receptor subfamily (P2XR), which is part of the P2 nucleotide receptor (P2R) family. The P2X7R, which is present on the cytoplasmic membrane, binds extracellular ATP and, depending on the agonist concentration and time of stimulation, can behave either as a selective cation channel or as a non-selective membrane pore capable of allowing the passage of molecules with masses up to 900 Da [1] [2].

The receptor is widely distributed in human tissues and expressed in numerous cell types including neurons, dendritic cells, fibroblasts and endothelial cells. In addition, P2X7R is expressed by all inflammatory and immune cells, belonging to both innate and adaptive immunity. Its activity has been best characterised in the monocyte-macrophage lineage, including dendritic cells, microglia and osteoclasts, but it is also present in T lymphocytes, B lymphocytes and their precursors [3] [4].

The P2X7 receptor has been extensively demonstrated to play a key role in both inflammation and immunomodulation under both septic and sterile conditions [5] [6], including the inflammatory response developed in allergic reactions [7]. In addition, P2X7R mediates the activation of the NLRP3 inflammasome, the release of cytokines, such as IL-1β and IL-18, chemokines and oxygen free radicals [5], promotes the proliferation and differentiation of T lymphocytes [8] and the activation of several transcription factors. In addition, depending on cell type and agonist binding, P2X7R can act as a cytotoxic receptor regulating various cell death mechanisms such as apoptosis, pyroptosis and necrosis [9] [10]. Its function in neoplastic cell growth processes and tumour progression has been documented. This makes P2X7R a potential target for anti-inflammatory and anti-tumour therapies [11] [12].

Although the function of the receptor has been well characterised under pathological conditions, in which high concentrations of ATP in the extracellular environment trigger multiple inflammatory processes, accumulating evidence suggests that P2X7R also has a basal level of tonic activation in healthy cells and tissues, supported by physiological amounts of endogenously released ATP, where it probably regulates cellular ion balance, supports mitochondrial metabolism and thus ATP synthesis, promotes motility and supports cell proliferation and differentiation [13] [14].

Inflammation and DAMPs

Inflammation is an essential defence mechanism involving components of innate immunity and is a key homeostatic response to protect the body from exogenous or endogenous sources of tissue or cellular damage. The main targets of the inflammatory response are:

- localising and eliminating the initial cause of the injury, such as pathogenic micro-organisms or toxins, and the products of that injury (e.g. damaged cells and necrotic tissues)
- initiate reparative processes, promoting healing.

It develops through reactions that take place at various levels: vascular responses; responses based on the coordinated activity of specialised cells of the lymphoid and myeloid lines, which are responsible for the innate and adaptive immune response; responses linked to the intervention of plasma proteins of inflammation.

Inflammation may be acute or chronic, depending on the nature of the stimulus, the duration of the reaction and the result achieved in terms of elimination of the noxious agent and damaged tissue. Usually when the acute inflammation, which mainly involves neutrophil granulocytes, succeeds in eliminating the noxious stimulus, the reaction is extinguished. However, if the target is missed, a chronic response may occur. Chronic inflammation, which may follow acute inflammation or have a slow and insidious onset, lasts longer and is associated with the presence of macrophages and lymphocytes, the formation of new blood vessels, fibrosis and tissue destruction.

However, inflammation can become a source of damage or disease because the same inflammatory mechanisms have the capacity to damage healthy tissues as well, where conditions arise in which inflammatory reactions are inappropriately directed towards host tissues or, because they are not adequately controlled, damage healthy cells and tissues. Inflammatory reactions are at the basis of many types of diseases and therefore many research efforts are aimed at identifying mediators and biomarkers that allow early recognition of the inflammatory process or factors that may be potential therapeutic targets to prevent or treat the resulting damage [15].

A crucial role in triggering the inflammatory process is played by PPRRs (**Primitive Pattern Recognition Receptors**), receptors present on the surface of innate immunity

cells such as monocytes, macrophages, dendritic cells and neutrophils, which are able to recognise and bind two classes of molecular patterns: PAMPs, Pathogen-associated molecular patterns, expressed or released by pathogenic microorganisms, and DAMPs, Damage-associated molecular patterns, expressed or released by host cells during damage or cell death. The acronym DAMPs refers to different classes of molecules that are normally sequestered intracellularly and released after cellular damage; once in the extracellular space, DAMPs activate the immune system by interacting with specific receptors to trigger protective and regenerative responses [16]. One of the oldest and most conserved DAMPs is extracellular ATP, which performs this role by binding to purinergic P2X receptors, of which P2X7R is one of the most relevant.

The role of ATP in inflammation

Adenosine-5'triphosphate (ATP) is a ribonucleotide consisting of a nitrogenous base, adenine, a pentose sugar, ribose, and three phosphate groups. The hydrolysis of the two pyrophosphate bonds, which bind the three phosphate groups to each other, allows a considerable amount of energy to be released. For this reason, it is universally recognised that ATP plays a central role in maintaining the energy homeostasis of cells: While it is the main product of reactions such as oxidative phosphorylation, cellular respiration and fermentation, it can also be regarded as an energy donor in most endoergonic processes, i.e. a series of reactions in which energy from the hydrolysis of pyrophosphate bonds is used to support cell survival and to enable cell proliferation and motility [17]. Mammalian cells contain intracellular ATP concentrations of between 5-10 mmol, and even higher levels of ATP are stored within special storage structures such as synaptic vesicles. At non-adrenergic and non-cholinergic nerve endings in the central and peripheral nervous systems, ATP acts as a neurotransmitter by binding to purinergic receptors, while at the level of dense platelet granules, once released it amplifies ongoing platelet activation through an autocrine and paracrine mechanism [18] [19].

Signalling by extracellular ATP

In complex multicellular organisms, cells communicate through different types of molecules, which are used in a variety of ways: they can diffuse in intercellular space, they can be transferred through intercellular channels shared between one cell and another, or they can be released into extracellular space via the vesicular system. Theoretically, all living cells are able to release variable amounts of this nucleotide into

the extracellular environment to exchange information between cells of the same kingdom (eukaryote-eukaryote or prokaryote-procaryote cell), but also across different kingdoms (prokaryote-eukaryote) [20]. Although it is generally accepted that purine nucleotides appeared among the primordial mediators of cell-cell communication, it is only in recent decades that the role of ATP as a ubiquitous extracellular messenger and in particular its character as an inflammatory mediator of the immune system has been highlighted.

In recent years, the mechanism of signalling via extracellular ATP has received extensive experimental support, especially after the development of techniques that allow direct measurement of ATP concentration in different pathophysiological contexts such as the tumour microenvironment (TME), the inflammatory microenvironment (IME), at ischaemic sites and in regions of tissue injury [21] [22].

The most important and recent advance in this field has been the introduction of the pmeLUC (plasma membrane luciferase) probe, a chimeric protein that, being sensitive to ATP concentrations in the micro-millimolar (µmol-mmol) range and insensitive to other nucleotides, allows the semi-quantitative measurement of extracellular ATP levels in living organisms [23]. As a result of this groundbreaking research work, the role of extracellular ATP in inflammation and immunity has been supported by direct in vivo demonstration that inflammatory sites contain high concentrations (hundreds of µmol/L) of ATP, as opposed to the interstitium of healthy tissues where the concentration is below the nanomolar (nmol) range [24].

There are several stimuli and mechanisms by which ATP is released into the extracellular environment to perform its mediating function. ATP can be released from damaged or dead cells through damage to the cytoplasmic membrane, which is why it is considered one of the first and most important DAMPs. Given that ATP from the cellular processes of glycolysis or oxidative phosphorylation is normally present at very high physiological intracellular concentrations (mmol/L) and higher than in the physiological extracellular environment, where it is found in minimal quantities, it can be deduced that this difference in concentrations across the negatively charged plasma membrane generates a strong gradient towards the extracellular environment. This gradient is both chemical and electrical because at physiological concentrations of $Mg^{2+}$and Ca^{2+}, one ATP molecule carries two negative charges. Given these premises, it can be deduced that any breach in the integrity of the plasma membrane will cause a timely outflow of large quantities of ATP which, being soluble in an aqueous environment, will quickly diffuse into the extracellular environment due to its low molecular weight and electrical charge [25]. In

the extracellular space, ATP undergoes rapid enzymatic degradation by ecto-nucleotidases, soluble or plasma membrane-associated enzymes that not only control the half-life of ATP as a receptor agonist, in order to avoid over-stimulation or desensitisation of the purinergic receptor, but also generate its metabolites such as
ADP or adenosine, which are also ligands of specific purinergic receptors [26]. The main metabolite of ATP is adenosine, which is a potent immunosuppressive agent capable of attenuating the inflammatory reaction and can be considered as a component of a negative feedback signalling system, an additional control factor of most homeostatic systems [27]. In addition to efflux in passive mode, ATP can also be released from intact cells through active mechanisms involving different pathways that can be dependent on vesicular transport, as in constitutive or regulated exocytosis, or using transmembrane channels and proteins, such as pannexin-1 and connexin-43, the CALHM (Calcium homeostasis modulator) ion channel and the P2X7 receptor (P2X7R) [28] [29]. Several pro-inflammatory stimuli have been found to trigger the extracellular release of ATP, although the signalling pathways involved in many cases have not been identified or fully characterised. Immune cells are able to release ATP in response to bacterial PAMPs such as endotoxins (e.g. LPS, lipopolysaccharide) to signal the presence of microorganisms, but at the same time bacterial colonies are able to release ATP to shape the mucosal immune response and establish a controlled tolerance between commensal microorganisms [30]. It has been shown that the accumulation of LPS in the cytosol of human macrophages triggers the release of ATP through the activation of pannexin1 [31] [10]. No less important is the fact that infections by intracellular bacteria and protozoa trigger the release of high amounts of ATP, which on the one hand promotes the propagation of damage and on the other hand triggers an immune response [32]. It is worth mentioning that reactive oxygen species (ROS) are involved in multiple intracellular signalling pathways [33], just as hypoxia, a condition commonly found at inflammatory sites, is another well-known factor in promoting ATP release [34]. From the above considerations, it can be understood that the high intraextracellular gradient of ATP, its release into the intercellular environment in response to different stimuli, its high solubility in water, its rapid degradation by membrane nucleotidases that regulate its extracellular concentration, and the presence of specific purinergic receptors, make ATP a true extracellular messenger, a ubiquitous mediator involved in septic and sterile inflammation. This signalling system has a high signal-to-noise ratio (SNR), so the release

of even small amounts of ATP from the cell generates a very strong signal because it leads to a high increase in extracellular fractional concentrations [11].

Purinergic receptors

Generalities

Purines and pyrimidines, the building blocks of all living organisms, are the main constituents of nucleotides and nucleosides, ubiquitous molecules that perform a variety of functions as basic building blocks of nucleic acids, coenzymes, allosteric modulators, energy intermediates, intracellular and extracellular messengers [35]. During evolution, complex multicellular organisms, from plants to higher mammals, have developed a signalling system that exploits the release of ATP as an extracellular messenger; interestingly, although in plants and animals they evolved from different proteins by gene recombination [36], receptors for extracellular ATP are widely expressed in all *phyla,* where they regulate similar protective responses for cell survival and tissue homeostasis. A radical change has occurred in recent years where a large body of scientific evidence has shown that nucleotide signalling governs some of the most essential immune responses; In particular, it has been observed that ATP accumulation in IME and TME produces multiple effects and supports various processes such as inflammatory cell migration, specifically macrophage and neutrophil chemotaxis, antigen-driven proliferation of T lymphocytes, cell differentiation to Th1 or Th2, and killing of intracellular pathogens, activation of NADPH-oxidase [37], maturation and activation of the NLRP3 inflammasome and release of IL-1β and IL-18, and can also facilitate the release of cytokines, chemokines and growth factors, production of ROS and nitrogen radicals, stimulation of stromal or tumour cell growth and even possess direct toxicity effects [38] [39].

Classification

Purinergic receptors are divided into two families: P1 receptors, selective for adenosine, comprising four subtypes, A1, A2A, A2B and A3, and P2 receptors, selective for purine nucleotides, comprising two subfamilies with distinct pharmacological profiles: metabotropic G-protein-associated P2YRs and ionotropic P2XRs. Eight members of the P2YR subfamily (P2Y1, 2, 4, 6, 11-14) and seven members of the P2XR subfamily (P2X1-, 2, 4, 6, 11-14) were identified.

7).

P2Y receptors (P2YR) show a higher affinity for ADP, UDP, UTP, UDP-glucose, or UDP-galactose, except for P2Y11R which is the only ATP-selective one. In contrast, the P2XRs have ATP as their preferred physiological agonist, whereas they are inactive for other nucleotides [40].

P2XRs are ionotropic receptors whose subunits associate to form ion channels for the transit of monovalent (Na^+, K^+) and bivalent (Ca^{2+}) cations. The subunits (P2X1-7) can combine to form homo-multimers or hetero-multimers. When three ATP molecules bind to the extracellular portion of a P2X receptor, a conformational change takes place that generates a rapid opening, in the millisecond range, of a channel that makes the plasma membrane permeable to positively charged ions, causing an increase in intracellular Ca^{2+} and Na^+ and a simultaneous decrease in the intracellular K^+ concentration. Opening of the channel leads to depolarisation of the cell membrane and initiation of $^{2+}$Ca-dependent signalling events downstream. Only the P2X7R has the peculiarity of forming a non-selective membrane pore when exposed for longer to higher concentrations of the agonist. P2X receptors are widely expressed in different human and animal tissues: at pre- and post-synaptic endings of the nervous system, or in various types of muscle cells, such as those of cardiac muscle, skeletal muscle and smooth muscle fibrocells of the bladder and vas deferens, but also in epithelial cells, endothelium and platelets [41] [42]. Little is known about the functions of P2X5R and P2X6R in the immune system, with the exception of the up-regulation of P2X5R in CD34+ leukaemic myeloid cell subpopulations and T lymphocytes [43] [44]. In contrast, the role of P2X1, P2X4 and P2X7 receptors has been better characterised in human immune cells. P2X1R has been associated with the regulation of metabolism, T-lymphocyte proliferation and neutrophil overflow. P2X4R has been implicated in the activation of the transcription factor NFAT and the modulation of T-lymphocyte responses [45]. In this panorama, the P2X7 receptor stands out as the only member of the family

P2XR with a firmly established role in multiple inflammatory and immune responses. Nevertheless, P2Y receptors are also variously implicated in several inflammation-related, ATP-associated responses, such as chemotaxis, release of proinflammatory cytokines and stimulation of platelet granule component release. Incidentally, the different selectivity of P2YRs suggests that other nucleotides could also act as DAMPs [46] [47].

Table 1. Classification of P2 receptors (Di Virgilio et al., 2017)

Receptor	Preferred agonist	Coupled mechanisms	Transduction mechanism	Intracellular signalling
P2YRs				
P2Y1	ATP, ADP	Gq/G	PLC activation and IP3 production	Ca^{2+} increase
P2Y2	ATP, UTP			
P2Y4	UTP			
P2Y6	UDP			
P2Y11	ATP	G/G-Gs $_{q11}$	PLC activation and IP3 production Stimulation of adenylate cyclase	Increase in Ca^{2+}/ cAMP
P2Y12	ADP	$_{J/o}$	Inhibition of adenylate cliclase	Decrease in cAMP
P2Y13	ADP			
P2Y14	UDP-glucose UDP-galactose			
Receptor	**Preferred agonist**	**Assembled subunits**	**Mechanism of transduction**	**Intracellular signalling**
P2XRs				
P2X1	ATP	P2X1, P2X2, P2X4, P2X5	Cation-selective ion channel	Increase in Ca^{2+} and Na^{+}
P2X2		P2X2, P2X3, P2X6		
P2X3		P2X3, P2X2		
P2X4		P2X4, P2X6		
P2X5		P2X5, P2X1		
P2X6		P2X6, P2X2, P2X4		
P2X7		P2X7	Ion selective channel for cations, Membrane pore non-selective	Increase in Ca^{2+} and Na^{+}, Decrease in K^{+}

Genetics, protein structure and function of the P2X7 receptor

The P2X7R is an ATP-dependent homotrimeric membrane ion channel, i.e. formed by the assembly of three identical P2X7 subunits. Rapid stimulation with low concentrations of physiological (ATP) or synthetic agonist Bz-ATP [2',3'-O-(4-benzoylbenzoyl) -ATP], generates the opening of a cation channel 0.7-0.8 nm in diameter that allows the influx of Na^+ and Ca^{2+} and the efflux of K^+, leading to a large increase in intracellular Na^+ concentration and depolarisation of the plasma membrane. Ca influx $^{2+}$increases the intracellular Ca^{2+} concentration, thereby activating calcium-dependent signalling pathways, while K^+ efflux, by lowering the cytosolic Ca concentration, promotes the activation of additional processes such as assembly and activation of the NLRP3 inflammasome. Prolonged stimulation with high concentrations of ATP (0.5-1 mmol) causes the opening of a non-selective pore with a larger diameter (4nm) that is permeable to hydrophilic solutes of molecular weight up to 900 Da, which are normally not diffusible through the membrane, such as choline, methylglucamine, ethidium bromide, YO-PRO-1 or lucyfer yellow. This also causes the efflux of low molecular weight cytoplasmic solutes, including ATP itself. The purinergic P2X7 receptor does not undergo desensitisation, so the pore formed by ATP stimulation remains open as long as the agonist is present in the extracellular environment, and closes after its removal. Macropore formation, which requires the presence of the intracellular C-terminal tail of P2X7, has been associated with NLRP3 inflammasome activation and P2X7R-mediated cytotoxicity [48] [49] [50].

In fact, recent work shows, through detailed electrophysiological analysis of the human and murine P2X7R, that the increase in conductance through the macro-pore, rather than occurring only after prolonged stimulation by the agonist, occurs without delay after P2X7R 'gating' allowing both large (e.g. YOPRO-1) and small cationic fluxes to pass simultaneously [51] [52]. YOPRO-1) and small cation fluxes and that permeability to organic solutes is an early and intrinsic property of the channel itself that does not require progressive dilation of the channel [51] [52].

The gene encoding for P2X7R is located in humans at the level of the long arm of chromosome 12, at 12q24.3, centromeric and close to the gene for P2X4R (12q24.32). The sequence homology between P2X7 and P2X4 monomers is 41%. A number of single nucleotide polymorphisms (SNPs) have been identified and some of these genetic variants, present in the coding region, result in gain-of-function or loss-of-function

versions of the receptor, some of which are associated with different disease conditions. The selection of mutated alleles may in fact be due to selective environmental pressure exerted by infectious agents or chronic inflammatory conditions [53] [54].

Nine different human isoforms of P2X7 subunits resulting from alternative splicing processes were identified and the full-length canonical form was named isoform A (P2X7A). The human truncated B variant is probably the isoform that has been best characterised in terms of its pathophysiological role and has been associated with cell growth, mesenchymal cell differentiation and tumour progression. Truncated variants are mostly non-functional, but it has been seen that some of them can behave as positive or negative modulators of the canonical A isoform [55] [56] [57].

Each P2X7 monomer is a protein of 595 amino acids that assembles into a trimeric complex to form the three-dimensional functional form of P2X7R. The P2X7 monomer has a short intracellular N-terminal residue (26 aa), an extended extracellular loop (282 aa), two transmembrane helices TM1 and TM2 (approximately 24 aa each) and a long cytoplasmic carboxy-terminal tail (239 aa). The extracellular loop contains pockets for binding to agonists and antagonists. In the C-terminal tail, there is a sequence homology site for the TNF receptor (TNFR1) and an LPS binding site homologous to that found on serum LPS binding proteins in the acute phase. The carboxy-terminal tail is crucial for the formation of the membrane pore that gives P2X7R its high conductance, and the presence of extra amino acids in this portion distinguishes it from other P2XR receptors [50]. Without this tail, the P2X7B splicing variant forms a receptor lacking the ability to form the macropore, while retaining ion channel activity [57].

Information on the tertiary structure and general architecture of the P2XR receptor family in both the closed (apo) and open (ATP-bound) forms was obtained by homology from the resolution of the crystallised structure of P2X4R in zebrafish, of the human P2X3R and the P2X7R in the panda (Ailuropoda melanoleuca) and this allowed us to specify the three-dimensional structure of the P2X7R, the ATP binding site, the interaction between the subunits and the mechanism of membrane pore opening [58] [59] [60].
The three-dimensional structure of the P2X3, P2X4 and P2X7 monomers was assimilated to the shape of a dolphin and the various subunit domains were made to correspond to the anatomical parts of the dolphin: the two transmembrane helices (TM) form the tail and the segments of the extracellular region form the various body sections i.e. head, side fins and dorsal fin. (Figure 1). Dolphin anatomy is now generally adopted to identify specific

regions in the tertiary structure of P2X7 subunits and also to describe the architecture of the P2X7R.

The ATP binding sites are located on the extracellular domains, at the interface between two adjacent subunits, between the dorsal fin of one subunit and the tail and left fin of the adjacent subunit, while the ion channel is formed by the TM2 helix of each subunit [58]. Comparison of the apo and ATP-linked crystallised structure suggests the mechanism of "gating and channel opening:

Binding to ATP triggers a major conformational rearrangement whereby the monomers change their orientation towards each other, thus behaving like rigid bodies without altering their configuration. During this process, the head domain of the monomers approaches the dorsal fin of the adjacent units, while the TM domains change their orientation towards each other, thus generating a pore formed by lateral fenestrations lined by the TM2s of each monomer. The process of channel formation allows for the rapid flow of Na^+ and Ca^{2+} inwards and the flow of K^+ outwards. Both inward and outward ion fluxes are critical in the implementation of P2X7R-activated responses. The onset of the current is followed by a phase of inactivation, called desensitisation, and recovery. In the other receptors of the family, prolonged exposure to the agonist would cause inactivation of the receptor, but a peculiar feature of the human P2X7R (and also possible in P2X2R and P2X4R) is the absence of desensitisation under continuous agonist stimulation, which instead promotes further rearrangement with reorientation of the three monomers that allows transmembrane flow to hydrophilic molecules. This progressive increase in activity is a property called facilitation [61] [62].

Homology models based on the structure of P2X3R explain that ATP binding of P2X7R causes a reorientation of the three monomers and the formation of a so-called 'cytoplasmic cap' consisting of the N- and C-terminal segments and partially covering the end of the transmembrane pore. Another interesting property of the increased conductance of P2X7R is its reversibility upon ATP removal. This property has been exploited to trap normally non-permeable low molecular weight aqueous solutes such as nucleotide analogues, fluorescent probes and anticancer drugs in the cytoplasm of different cell types [63] [5].

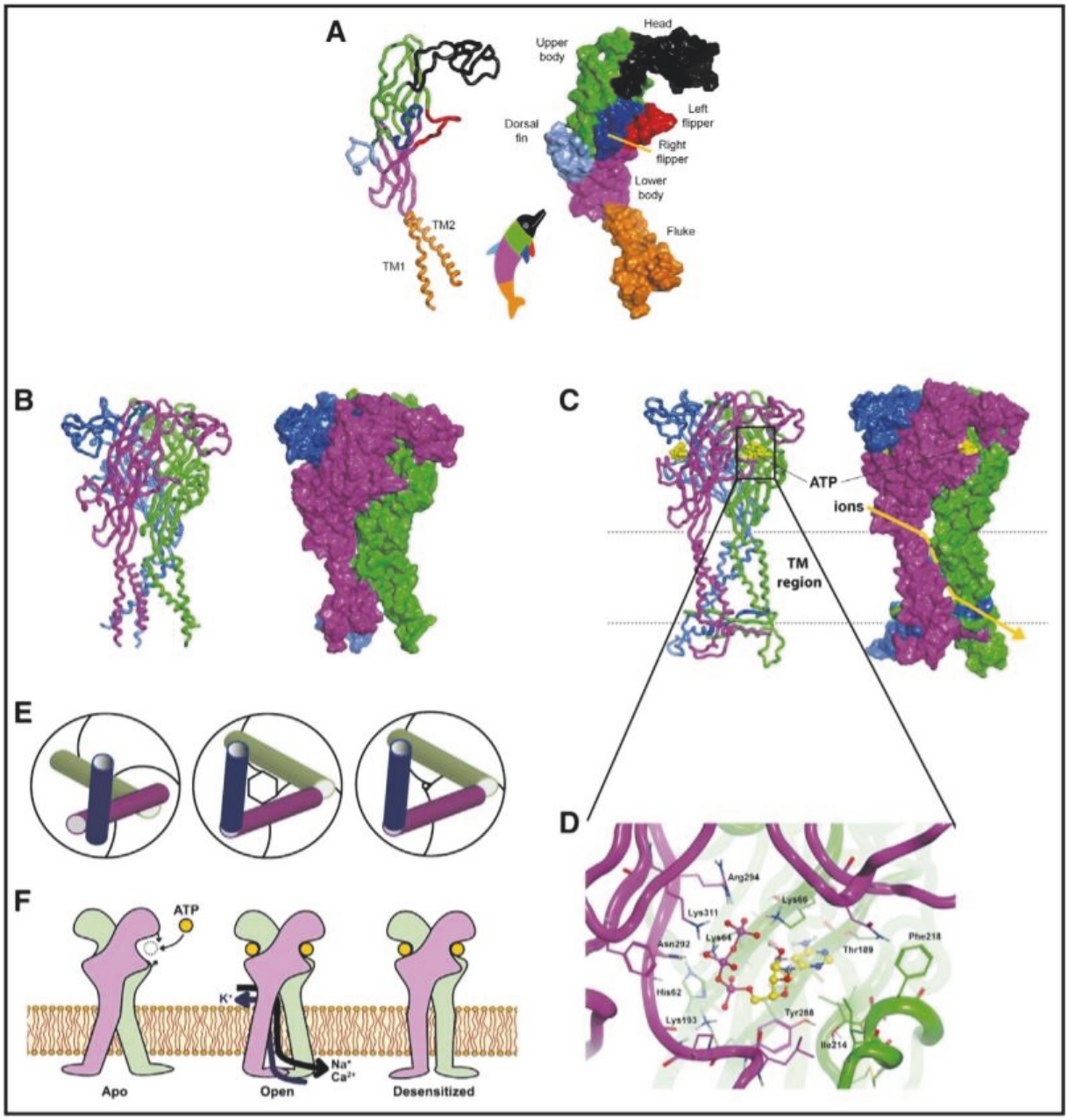

Architecture of human P2X7R reconstructed using homology models based on the crystallised structure of human P2X3R. (A) The monomer in its secondary structure (left) and representation of the molecular surface (right); the shape of the monomer compared to the figure of a dolphin, subdivided into the various regions. (B) Schematic representation of trimeric P2X7R in the closed state and (C) in the open state. (D) Detail of the ATP-binding site. (E) (F) Schematic representations of the conformational changes of the receptor in the transition from the closed, to the open and to the desensitised state. (Di Virgilio et al., 2017)

The role of the P2X7 receptor in inflammation

The P2X7R receptor is unanimously recognised as the main ATP sensor during inflammation and the most potent stimulus for NLRP3 inflammasome activation and thus mediates the maturation and secretion of Interleukin-1β (IL-1β) of the early phase of the immune response [64]. Synthesis of pro-IL-1β, a 31 kDa immature protein, begins with activation of the nuclear transcription factor NF-κB. Maturation into the bioactive 17 kDa form requires cleavage by caspase-1, which in turn is activated from pro-caspase-1 through formation of the inflammasome. Without this conversion, pro-IL-1β is rapidly degraded by the proteasome [65] [66]. The NLRP3 inflammasome is a multi-protein intracellular complex formed by the assembly of four components that create a heterotetramer consisting of a central NLRP3 protein, which is a structural, scaffold protein, to which other proteins are associated when the immune cell is activated: an adaptor protein ASC, pro-caspase-1 and the sensor protein Nima-kinase 7 (NEK7). The NLRP3 inflammasome is activated by ATP but can also assemble in response to PAMPs from infectious agents, other DAMPs or chemical and physical agents that cause cellular damage [67]. When the NLRP3 component is activated, the adaptor protein ASC is recruited, which brings NLRP3 into contact with pro-caspase-1. Activation of caspase-1 is an autocatalytic phenomenon. By bringing several caspase-1 elements next to each other, as these are proteolytic enzymes, they are self-activated by self-proteolysis releasing the activated caspase-1, which can act on pro-IL-1 and produce mature IL-1. This assumes that since the formation of the initial heterotetramer, for proteolytic activation by self-proteolysis to occur, several heterotetramers must come into contact with each other, bringing into contact several pro-caspase-1 molecules. In fact, the mature inflammasome is a penta- or heptameric structure composed of the aggregation of 5 or 7 heterotetramers that form a cytoplasmic superstructure [68].

Membrane pore function is a prerequisite for NLRP3 activation, suggesting that a major reduction in intracellular K^+ is required to trigger the process, although the underlying molecular mechanism has not yet been elucidated [69]. Recent evidence suggests that localised modification of the intracellular ionic microenvironment directs the recruitment of inflammasome components and facilitates their assembly in the vicinity of the P2X7R itself, and that decreased intracellular K^+ enhances the interaction of NLRP3 with the NEK7 protein, a sensor of the ionic concentration of the microenvironment in which the inflammasome is located. NEK7 is required for P2X7R-driven inflammasome assembly

and evidence of this is the fact that ATP-stimulated NLRP3 activation is abrogated in NEK7-deficient bone marrow-derived macrophages [70].

In addition, P2X7R is a strong stimulus for the externalisation of active IL-1β as it is the main driver of multiple release mechanisms, such as passive release following cell death or secretion through lysosomes, exosomes or plasma membrane-derived microvesicles [71] [72].

Following the results of some recent evidence, an alternative model of P2X7R activation in inflammation has been formulated according to which the binding of PAMPs to membrane receptors or sensors in the cytoplasm triggers the controlled release of ATP and autocrine/paracrine stimulation of P2X7R. This leads to the inference that stimulation of P2X7R activates intracellular effector systems (e.g. the NLRP3 inflammasome) and further amplifies the effect of other pro-inflammatory agents by releasing ATP, which in turn acts as an inflammatory stimulus [73].

P2X7R also promotes inflammation through the activation of different intracellular pathways

which may also be associated with inflammasome formation. One example is the activation of the transcription factor NF-κB, probably through an adaptor protein that interacts with the C-terminal domain of P2X7R, to enable the expression of genes encoding for several components of the inflammatory chain including IL-1, TNF-α and cyclooxygenase (COX) enzymes [74]. Expression of COX-2 and activation of COX-1 by P2X7R has been associated with the occurrence of fever and inflammatory pain, which is why it could be considered a potential target for new drugs, alternative to non-steroidal anti-inflammatory drugs (NSAIDs), such as aspirin [75] [76]. Other signalling pathways associated with P2X7R are Ca-dependent^{2+} activation and translocation into the NFAT core to promote lymphocyte and osteoblast proliferation, a process that can also promote tumour cell multiplication [77] [78]. Other pro-inflammatory cytokines secreted upon P2X7R activation include IL-6 and IL-1α, albeit through inflammasome-independent pathways, and other inflammatory mediators such as prostaglandin E2, leukotriene B4 and thromboxane A2. Furthermore, stimulation of macrophages via P2X7R leads to the release of VEGF (vascular endothelial growth factor) suggesting its involvement in regeneration and neoangiogenesis processes [79] [80].

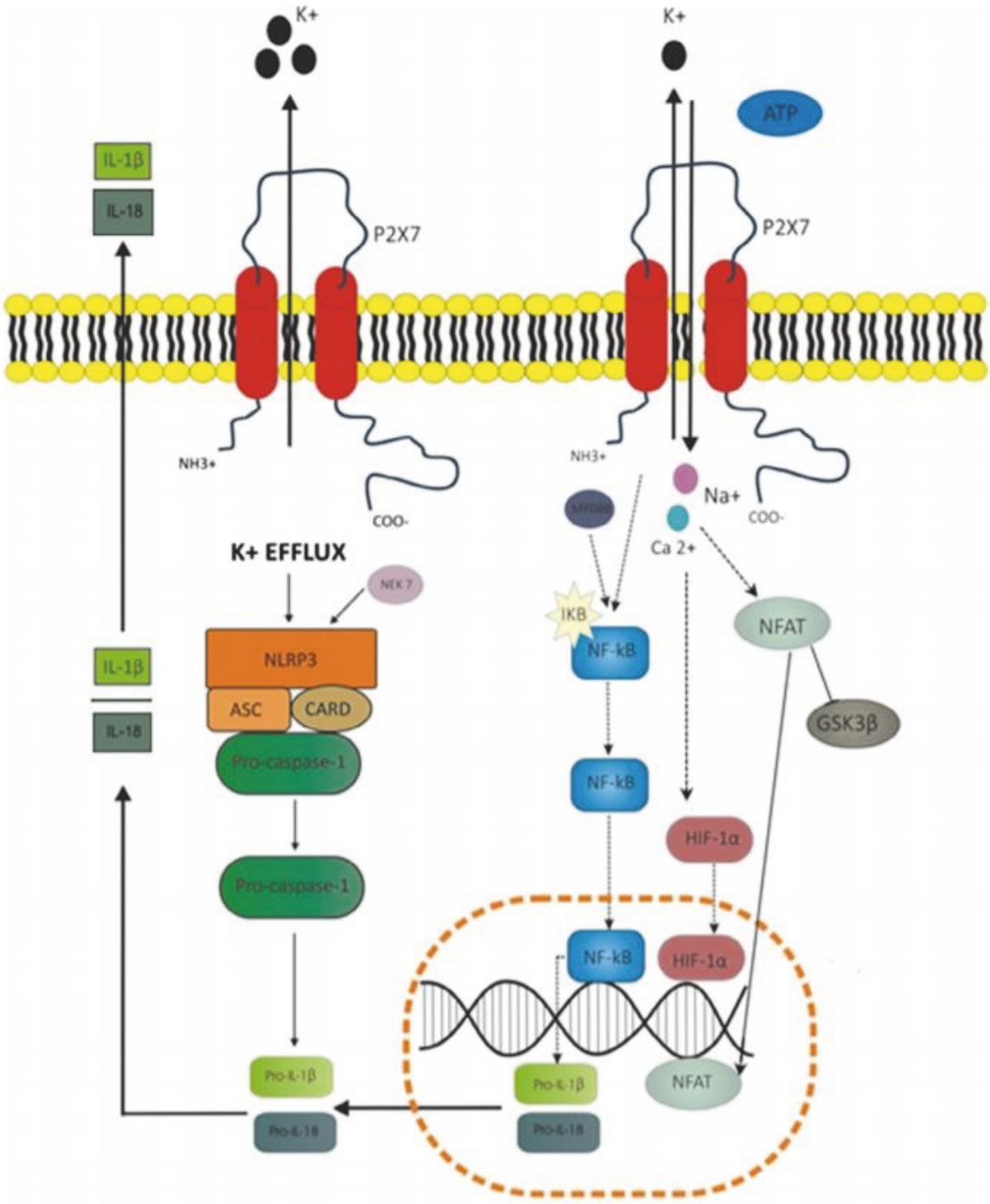

Inflammatory signalling pathways activated by P2X7R: activation of NLRP3 inflammasome, synthesis and release of IL-1β and IL-18; activation of NF-κB via MyD88 and promotion of IL-1β gene expression; NFAT $^{2+}$factor-dependent activation leading to IL-2 synthesis, lymphocyte proliferation and down-regulation of GSCKβ factor. In addition, stimulation of P2X7R promotes activation of HIF-1α and subsequent VEGF release.

(Adinolfi et al., 2018)

The role of the P2X7 receptor in cell death

The P2X7 receptor is considered a cytotoxic receptor and a potent activator of cell death, which can occur by different mechanisms depending on cell type, agonist concentration and duration of binding. In the absence of bacterial-derived products, as is the case in sterile inflammation, the most common type of cell death triggered by P2X7R is necrosis [5]. P2X7R is not only linked to cell necrosis, but its stimulation in mouse lymphocytes has been observed to lead to oedema and cell lysis. It has also been shown that the P2X7 receptor, activated by binding to ATP, allosteric modulators or pathogens, promotes pyroptosis in mononuclear cells, a type of caspase-1-dependent inflammatory cell death [81]. In human cells, pyroptosis can be triggered by caspases-1, -4 and -5 [82]. Stimulation of the receptor by ATP can lead to the release of cytochrome-C from the mitochondria and the cleavage of caspases-3, -8 and -9, which are directly linked to the mechanism of apoptosis [83].

Soluble form of P2X7 receptor

Research recently conducted at the University of Ferrara has led to evidence that a soluble form of the full-length P2X7R receptor (sP2X7R) is released into the blood under both healthy and pathological conditions. Specifically, sP2X7R was found to be present in both plasma and serum regardless of storage mode. In contrast to the low concentrations found in healthy control subjects, levels of the soluble form are much higher in different pathological conditions including infectious diseases, ischaemia, cancer and other conditions such as autoimmune diseases and trauma. By measuring levels of C-reactive protein (CRP), considered a systemic inflammatory marker, it was observed that sP2X7R levels correlated with CRP levels. Furthermore, taking into account a PCR cut-off of 3mg/dL, considered to indicate a systemic inflammatory state, a significant increase in sP2X7R concentration was found in subjects with PCR>3 mg/dL. These results indicate that the measurement of plasma sP2X7R could complement the assessment of PCR and other markers currently used to investigate a subject's inflammatory status. Possible sources of the plasma soluble form of the receptor include peripheral blood mononuclear cells (PBMCs) isolated from peripheral blood. PBMCs isolated from healthy subjects release sP2X7R into the culture medium after stimulation with BzATP [2',3'-O-(4-benzoylbenzoyl)-ATP], an ATP analogue, and to a greater extent after pre-stimulation with LPS, simulating an inflammatory condition on an infectious basis in vitro. Finally, the study showed that plasma sP2X7R is present to a large extent associated with

microvesicles/microparticles (MVs/MPs), i.e. heterogeneous populations of particles of different sizes and cellular origin [84].

CHAPTER 2: P2X7R AND EYE DISEASES

P2X7R locations and functions in the eye

Purinergic receptors are abundantly distributed in the various ocular segments and perform many functions in the physiological field, but dysregulation of the biomolecular processes involving them can also contribute to the development of ocular pathologies.

The P2X7R receptor is expressed both in the eyeball and in the ocular adnexa. On the ocular surface, this receptor is activated by chemical or mechanical sources of exogenous stress, such as by contact with ophthalmic solutions containing preservatives or surfactants, or by corneal abrasion, leading to inflammation apoptosis and cell proliferation. In the case of corneal injury, the P2X7R receptor acts, in coordination with P2Y2R, to ensure appropriate tissue repair by promoting epithelial cell adhesion to the basement membrane, coordinating Ca^{2+} mobilisation, rearrangement of the cytoskeleton and formation of a normal stromal collagen structure. At the retinal level, the P2X7R receptor and abnormalities in its function have been potentially linked to neuronal loss occurring in glaucoma and hereditary retinal degeneration, as well as contributing to neuroinflammatory processes occurring in age-related macular degeneration and diabetic retinopathy [85].

Table 2. Expression of the P2X7R receptor in the eye structures of different species. (Dutot et al.,2017)

Fabric	Cells	m-RNA	Protein	Species
Cornea	Corneal epithelial cells			Human
	Section of cornea		+	Mouse
	Corneo-limbal epithelial cells	+	+	Human
Conjunctive	Conjunctival epithelial cells		+	Human
	Calico cells		+	Rat
Crystalline	Lenticular fibres	+	+	Rat
	Epithelial cells		+	Human
Retina	Müller cells	+	+	Human
	Section of retina	+	+	Rat
	Retinal Ganglion Cells	+		Rat
	Retinal pigment epithelium cells (ARPE-19 cell line)		+	Human
	Retinal pigment epithelium cells (primary culture)	+	+	Human
	Retinal pigment epithelium cells	+	+	Mouse
	Photoreceptors	+	+	Rat
Ciliary body	Epithelial cells	+		Bovine

P2X7R as a therapeutic target

The P2X7 receptor has recently attracted particular interest as a potential therapeutic target due to its wide involvement in ocular diseases. Several highly selective P2X7R inhibitors are currently available, some of which are in phase 1 and 2 clinical trials for the treatment of certain chronic inflammatory diseases [86] [87] [88] [89]. Understanding the exact functioning of the molecular mechanisms associated with the P2X7R receptor in the context of ocular diseases would be important in order to adopt new therapeutic strategies to prevent the onset of visual symptoms or slow down the progression of disease processes towards more advanced stages and thus limit their impact in terms of visual disability.

Topical administration of medication, in most cases in the form of eye drops, is usually used to treat diseases of the anterior segment of the eye, particularly the cornea and conjunctiva. In this regard, hyaluronic acid or sodium hyaluronate (HA) is considered to be a potent modulator of the P2X7 receptor, and pre-treatment with this molecule is able to reduce P2X7R-mediated oxidative and apoptotic damage induced by sodium lauryl sulphate, an anionic surfactant with irritating power, and benzalkonium chloride, a quaternary ammonium salt that is widely used as an antimicrobial preservative [90] [91].

Although oral administration is not a very efficient way of delivering a therapeutic molecule to the eye, the administration of omega-3-rich fatty acids, such as docosahexaenoic acid DHA and eicosapentanoic acid EPA, combined with Brilliant Blue G, a potent selective P2X7 receptor antagonist, has been shown to prevent the neurocytotoxic effect of amyloid β in age-related macular degeneration (AMD) [92].

To date, no P2X7R inhibitors are commercially available for the treatment of retinal diseases, but several antagonists of this receptor, which attenuate IL-1β production, have been found to cross the blood-brain barrier. The NJ55308942 molecule reduces Ca^{2+} conductance through P2X7R and IL-1β release from blood monocytes and cultured microglia. In addition, in experimental animal models, following oral administration at increasing doses of this compound, there is an increase in the number of P2X7 receptors occupied by microglia, suggesting that it is able to cross the blood-brain barrier. Consistently, treatment with JNJ55308942 in mouse models of chronic stress reduced inflammation and the subsequent clinical signs associated with it [93]. Given the similarities in the structure of the blood-brain barrier with the blood-retinal barrier, it is likely that several brain-permeable receptor antagonists, including JNJ-55308942 or JNJ-5417446, could be effective in the treatment of P2X7R-associated retinal disease [94].

Recently, dimeric nanoparticles have been developed that are able to reduce or increase P2X7R conductance, inhibit membrane pore formation and IL-1β release in macrophages and T cells, and in experimental in vivo models of allergic contact dermatitis and glomerulonephritis have been shown to be effective in attenuating the inflammatory process [95].

Against this background, further studies are needed to analyse the potential of various P2X7R antagonists and inhibitors in ophthalmological diseases.

The following is a review of the most recent knowledge concerning a potential involvement of the P2X7R receptor in the pathogenesis of several ocular diseases.

Diabetic eye diseases

Diabetes mellitus is one of the most prevalent metabolic diseases in the world. The potentially fatal condition affects more than 422 million people worldwide and its prevalence is expected to grow to 592 million by 2035 [96] [97].

Diabetes mellitus develops when the endocrine pancreas is no longer able to synthesise insulin and/or when the body becomes resistant to it due to persistently high blood glucose

levels. The 3 main types of diabetes are Diabetes Mellitus type 1, Diabetes Mellitus type 2 and Diabetes Mellitus type 3.

Diabetes Mellitus Type 2 and gestational diabetes. Chronic hyperglycaemia and failure to control the condition leads to various microangiopathic complications at the tissue level, the most common of which in the visual system are diabetic keratopathy and diabetic retinopathy [98].

Diabetic keratopathy

Diabetic keratopathy or diabetic corneal epitheliopathy is a degenerative corneal disease. Some of the clinical features present at the corneal level in a patient with diabetes are: delayed corneal re-epithelialisation with impaired wound healing, reduced corneal sensitivity (hypo-anesthesia), neurotrophic ulcers and corneal oedema. These features are mainly caused by the fact that local hyperglycaemic conditions lead to multiple effects on corneal tissue, including: changes in corneal epithelial basement membrane composition, deposition of advanced glycation products (AGEs), damage to corneal nerve endings, reduced tear secretion and oxidative stress.

It is also known that the hyperglycaemic environment leads to abnormalities at the stromal level and at the level of endothelial cells, whose morphological changes and altered cell density are some of the factors that lead to neovascularisation and increased corneal thickness [99]. Furthermore, during the initial phase of diabetes, morphological changes are observed in the nerve fibres, which become thicker and degenerate due to the accumulation of advanced glycation end products (AGEs).

In addition to chronic hyperglycaemia, the cornea is also subject to high levels of inflammation and oxidative stress, hallmarks of diabetes in all tissues. The interaction between AGEs and their receptors (RAGE) causes the formation of oxygen free radicals and the release of pro-inflammatory cytokines. In the human eye, AGEs have been detected in the corneal stroma, Descemet's membrane, the basement membrane of the corneal epithelium, the lens and the lamina cribrosa. In a study in mouse models of diabetes induced by streptozotocin injections, AGEs immunoreactivity levels in the cornea were higher than in non-diabetic controls, and were localised to the epithelium, corneal stroma and endothelium, as reflected in the expression of the oxidative DNA damage marker 8-OHdG. Furthermore, treatment with the AGEs inhibitor aminoguanidine prevented the development of diabetic corneal structural abnormalities, such as degeneration of intracellular organelles, formation of cytoplasmic vacuoles and

oedema in the corneal stroma. In Western blot analysis, caspase-3 protein expression was significantly increased in diabetic corneas compared to non-diabetic controls, indicating that corneal cells also undergo apoptosis. In addition, the activation of NF-κB and its elevated presence in diabetic corneas suggest that the AGE/RAGE interaction leads to NF-κB activation, which promotes increased oxidative stress and transcription of pro-apoptotic cytokines, thereby mediating corneal tissue damage in diabetes [100].

Mankus et al. found that P2X7 receptor expression is increased in corneal epithelium samples from diabetic donors compared to age-matched controls [101].
Using a mouse model of pre-diabetes type 2 with diet-induced obesity (DIO), changes in corneal sensory nerves and P2X7R expression were characterised under diabetic conditions. A significant reduction in sub-basal nerve plexus density associated with increased tortuosity and decreased diameter was observed. In addition, P2X7 mRNA expression was significantly higher in the corneal epithelium of DIO mice and, after abrasion, the increase in transcription was more intense in the central regions of the abraded area, where the cells migrated after injury, and in the peripheral areas surrounding the abrasion. The re-epithelialisation process was slower and incomplete in DIO mice compared to controls, suggesting that dysregulation of P2X7R expression may be associated with the altered healing process in diabetic corneas. While in non-diabetic controls P2X7R is more highly expressed at the main wound margin, it is less specifically distributed in DIO mice. This feature allows us to hypothesise that normally the purinergic receptor may play a role in promoting protein migration and cytoskeletal rearrangements at the healing margin of a corneal wound, whereas in diabetic conditions this activity is dysregulated [102].

Diabetic retinopathy

Diabetic retinopathy is the most frequent microvascular complication of diabetes mellitus and includes all the pathological and functional changes observed in the retina as a result of chronic exposure to hyperglycaemia. It affects approximately one third of patients with type 1 and type 2 diabetes, with the risk increasing in proportion to the duration of the disease and the levels of glycated haemoglobin HbA1c. Diabetic retinopathy is the leading cause of visual impairment in the working-age population, accounting for 15-17% of cases of blindness [103].

Development of diabetic retinopathy

The progressive development of diabetic retinopathy follows different clinical stages that are set out in the International Classification or Severity Scale of Diabetic Retinopathy and Diabetic Macular Oedema drawn up in 2003 [104].

Table 3. Diabetic retinopathy (DR.) severity scale (Wilkinson et al., 2003)

Clinical stage	Retinal injuries
Non RD	No injuries
Mild non-proliferative RD	Microaneurysms only
Moderate non-proliferating RD	Any or all of the following signs: microaneurysms, retinal haemorrhages, hard exudates, cottony nodules; not associated with other lesions of severe non-proliferative RD
Severe non-proliferating RD	Any of the following signs and no signs of proliferative retinopathy: more than 20 intraretinal haemorrhages in all 4 quadrants; significant venous *beading* in 2 or more quadrants: IRMA (intraretinal microvascular abnormalities) prominent in 1 or more quadrants
Very severe non-proliferating RD	Two or more criteria for severe non-proliferating RD
Proliferating RD	One or more of the following: neovascularisation vitreous/pre-retinal haemorrhages
High-risk proliferating RD	One or more of the following: neovases on the disc greater than or equal to 1/3 of the disc area retinal neovases at least ½ the size of the haemovitreous disc area

Table 4. International diabetic macular oedema (EMD) severity scale. (Wilkinson et al., 2003)

Level of severity of macular oedema	Ophthalmoscopic signs
Mild EMD	Retinal thickening or hard exudates at the level of the posterior pole, but distant from the centre of the macula
Moderate EMD	Retinal thickening or hard exudates approaching the centre of the macula, but not involving the centre
Severe EMD	Retinal thickening or hard exudates involving the centre of the macula

Pathogenesis of diabetic retinopathy: the role of inflammation

During diabetic disease, various systemic metabolic changes develop, such as dyslipidaemia and hyperglycaemia, which are the starting points in the pathogenesis of the complications of this disease. In the eye, chronic exposure to high levels of glycaemia leads to the activation of various biochemical mechanisms such as the polyol and hexamine pathways, the activation of protein kinase C isoforms and the non-enzymatic glycation of proteins, which are the molecular basis for the initiation of pathological processes characteristic of diabetic retinopathy such as retinal microangiopathy, inflammation and neurodegeneration, causing structural and functional changes in the retina leading to irreversible impairment of visual function.

OXIDATIVE STRESS AND MITOCHONDRIAL DYSFUNCTION

Hyperglycaemia induces disruption of the electron transport chain at the level of the inner membrane of the mitochondria leading to the production of oxygen free radicals (ROS), such as superoxide anion. ROS are harmful to the mitochondria themselves by inducing oxidative damage at the level of the mitochondrial DNA leading to a dysfunction of the respiratory chain and thus to increased production of ROS and the auto-oxidation of glucose. Over time, ROS production saturates the capacity of antioxidant systems and leads to exposure of retinal cells to oxidative stress. Intracellular oxidative modifications of lipids, proteins and DNA promote further mitochondrial damage, inflammation, apoptosis and subsequent tissue effects. ROS-induced mitochondrial dysfunction also causes a reduction in ATP production and an increase in mitochondrial membrane

permeability, which leads to the release of apoptotic factors such as cytochrome c within the cell cytoplasm, inducing apoptosis in pericytes and endothelial cells. In parallel, hyperglycaemia promotes non-enzymatic glycation of serum, cellular and tissue proteins, leading to the formation of AGEs, the end products of advanced glycation. AGEs are able to bind to specific receptors called RAGE and activate the transcription factors NF-κB, STAT (signal transducer and activator of transcription), AP-1 (activator protein 1) that trigger inflammatory processes, neurodegeneration and loss of pericytes at the retinal level, components of the retinal vascular walls [105] [106].

NEUROVASCULAR ALTERATIONS

Oxidative stress together with the inflammatory process induces neurotoxicity leading to apoptosis of **retinal** ganglion cells (RGCs) and hyperactivation of glial cells, in a process called neuroinflammation. Retinal ganglion cell damage is the result of oxidative stress, inflammation and hypoxia and emerges early, before the onset of obvious vascular lesions and before pericyte apoptosis [107] [108].

Neuronal death or dysfunction of retinal neuronal cells promotes the process of **reactive gliosis** indicated by the up-regulation of glial fibrillary acidic protein (GFAP) in astrocytes and Müller cells. Reactive gliosis is associated with increased activation of immune-related signalling pathways leading to increased production of pro-inflammatory factors and growth factors, contributing to vascular injury [109]. An elevated level of GFAP has been detected in the aqueous humour of diabetic patients without clinical signs of diabetic retinopathy or in patients with non-proliferative diabetic retinopathy.

The first vascular changes observed are the loss of pericytes and thickening of the basal membrane [110]. The loss of the pericytes of the retinal capillary wall, which normally line the outside of the capillary endothelium, guaranteeing greater mechanical resistance, would appear to be responsible for the breakdown of the blood-retinal barrier and the loss of vascular tone. This causes a progressive deformation and widening of the vessels, an increase in permeability and proliferation of endothelial cells due to the deficit of TGF-β, which was produced by the pericytes. These changes lead to the formation of microaneurysms and intraretinal haemorrhages, two of the first clinical features observable ophthalmoscopically in RDNP. In addition, thickening of the basement membrane and disjunction of the *tight junctions* are the factors determining *leakage* from the retinal capillaries with passage of the intravascular contents, mainly represented by lipids, proteins and inflammatory mediators, into the interstitial space.

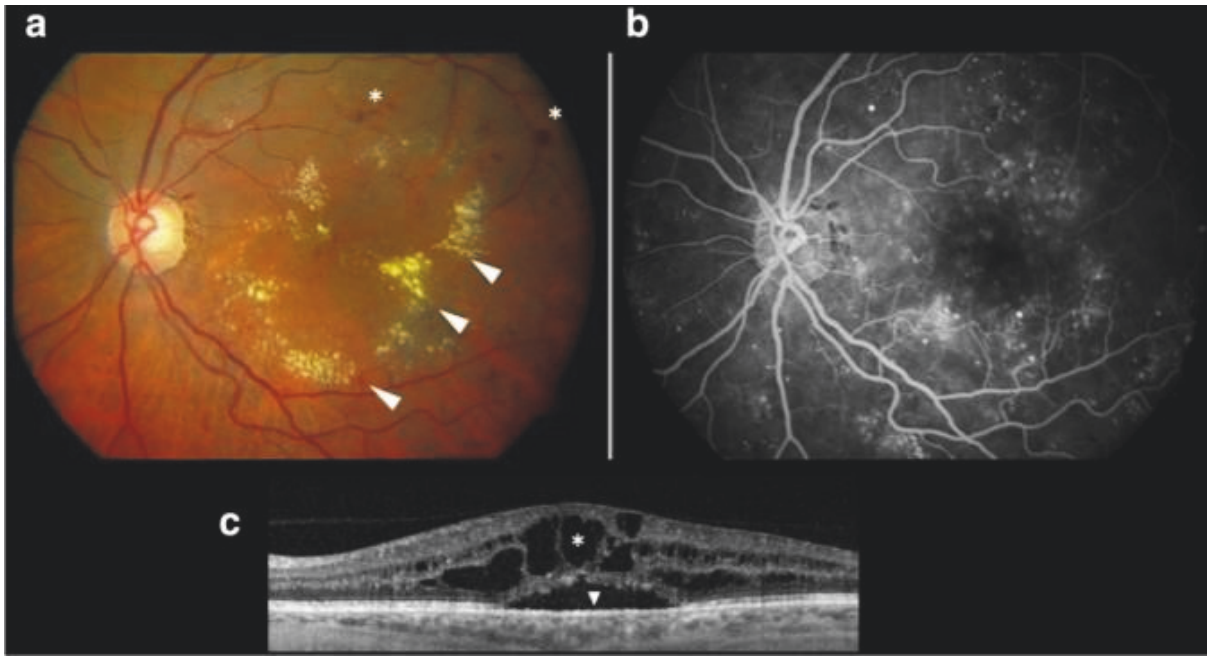

Figure 3. (a) Fundus ocularis photograph, (b) Fluorangiography and (c) SD-OCT of a patient with Non-Proliferative Diabetic Retinopathy (RDNP) and Diabetic Macular Edema (EMD). In (a) hard exudates (arrows), microaneurysms and retinal haemorrhages (asterisks) can be observed. In (b) we observe multiple spots of hyperfluorescence prevailing in the areas where aneurysmal lesions and vascular leakage are present. In (c) we observe an SD-OCT where multiple intraretinal cysts (asterisk) and subfoveal neuroretinal detachment (arrow) are present. (Mesquida et al., 2019)

On the other hand, retinal glial cells, i.e. Müller cells and microglia, EPR, and macrophages lead to the secretion of vascular growth factors such as VEGF-A and pro-inflammatory cytokines, such as IL-1β, TNF-α, IL-6, IL-8, MCP-1(monocyte chemoattractant protein 1), contributing to vascular dysfunction. Persistent secretion of inflammatory mediators can lead to the establishment of a state of chronic inflammation, which has two main effects on the retina: the breakdown of the blood-retinal barrier and leukostasis.

An alteration in the blood-retinal barrier results in an increase in vascular permeability, which has as its clinical consequence the appearance of hard exudates, due to the leakage of plasma constituents, especially lipids and proteins. As a result, fluids accumulate in the macula, leading to diabetic macular oedema, which, if left untreated, has the potential to impair visual function [111].

Pro-inflammatory factors lead to increased expression of adhesion factors on the surface of endothelial cells, in particular ICAM-1 (intercellular adhesion molecule 1) and VCAM-1 (vascular cell adhesion molecule 1), where activated leukocytes adhere, triggering a process called leukostasis.

Leukostasis is the determinant of retinal capillary occlusion and activation of the thrombogenesis process. The resulting ischaemia is one of the most severe complications of this pathological process and determines a progression of retinopathy towards an advanced form of proliferative type, where new vessels develop within the retina or optic disc. Indeed, hypoxia is able to activate the production of HIF-1α (hypoxia inducible factor) in endothelial and glial cells, which feeds the process of angiogenesis by increasing the production of VEGF-A in endothelial cells, glial cells, astrocytes and EPR cells, the secretion of which is also favoured by ROS, hyperglycaemia itself, AGEs and inflammatory cytokines such as IL-1β and IL-6 [112].

The importance of inflammation in this phenomenon has been demonstrated by the fact that blocking inflammation reduces neovascularisation. In mouse models of choroidal neovascularisation, elimination of the factor MCP-1, which is responsible for recruiting monocytes to hypoperfused areas, and elimination of ICAM-1 or CD18 leads to a significant reduction in the process of neoangiogenesis: Similarly, inhibition of cyclooxygenase-2 (COX-2), which normally produces prostanoids, reduces VEGF production and the resulting vascular *leakage* in animal models of diabetic retinopathy and reduces neovascularisation in mouse models of proliferative ischaemic retinopathy [113].

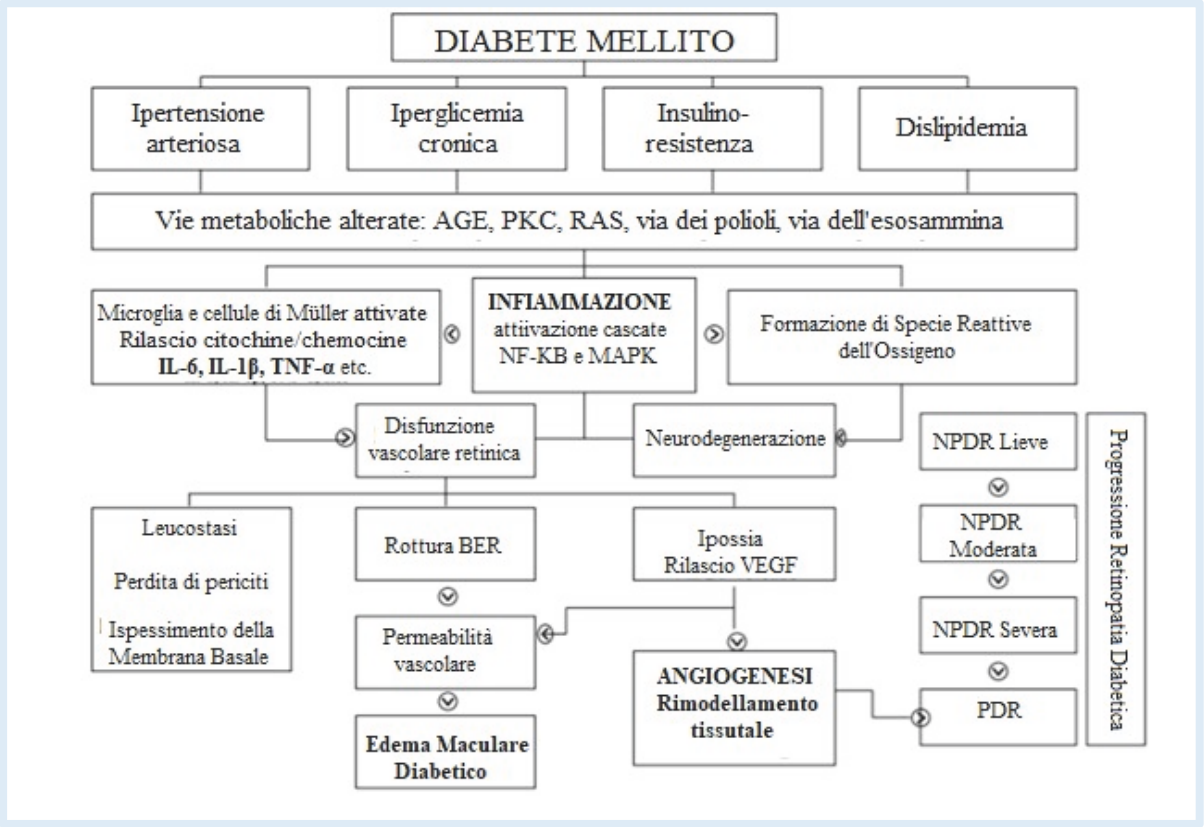

Schematic representation of the pathogenesis of damage and its progression in diabetic retinopathy. (Mesquida et al.,2019)

MICROGLIA AND NEUROINFLAMMATION

Neuroinflammation' is a process that plays a major role in the pathogenesis of diabetic retinopathy. The fundamental mechanism by which the process of neuroinflammation begins in response to tissue nerve disturbances caused by the metabolic dysregulations of diabetes is microglial activation. Under normal conditions microglia cells are represented by dormant macrophages located in the inner layers of the retina.

In response to hyperglycaemia, dyslipidaemia, AGEs and oxidative stress, these cells become activated, retract their dendrites and assume an amoeboid phenotype whereby they infiltrate the deeper layers of the retina where they initially take on an anti-inflammatory role mediated by M2 cells to delay disease progression. However, persistent exposure to diabetic conditions leads to the decline of the M2 response with the respective emergence of M1 cells that assume a pro-inflammatory role and, by activating the NF-κB and ERK pathways, contribute to neuronal damage by releasing neurotoxic factors such as glutamate, iNOS, caspases and TNF-α, IL-6, IL-1β and VEGF [114] [115].

CYTOKINES AND ANGIOGENESIS

In support of the role of inflammation in the pathogenesis of diabetic retinopathy, several studies have shown a specific expression profile of various cytokines and proinflammatory factors in serum, aqueous humour and vitreous humour using *protein array* analysis techniques. Local pro-inflammatory biomarkers in ocular fluids, whose main source of production is retinal glial cells, correlate more precisely with the various stages of diabetic retinopathy and diabetic macular oedema than do their corresponding serum levels. These comparisons showed that:

- IFN-γ, IL-1α, IL-3 and MCP-2 are higher in diabetic patients without clinical signs of DR than in non-diabetic controls.
- Factors IL-1β, IL-3, IFN-γ, IFN-γ induced protein 10 (IP-10) and monocyte chemotactic protein 2 (MCP-2) are significantly increased in diabetic patients compared to controls;
- Granulocyte-Macrophage Colony Stimulating Factor (GM-CSF), IFN-γ, IL-10, IP-10, Regulated And Normal T cells Expressed and Secreted (RANTES) and Soluble Tumour Necrosis Factor Receptor (sTNF-R) II are highly elevated in diabetics with mild DR compared to control cases;
- Macrophage Inflammatory Protein (MIP-1b), GM-CSF, RANTES and sTNF-RII increase more in diabetics with mild DR than in diabetics without DR. In more advanced stages of diabetic macular oedema and proliferative diabetic retinopathy, increased concentrations of IL-6, VEGF, IL-12, IL-8, IP-10, MCP-1, platelet-derived growth factor (PDGF) and ICAM-1 are reported in the aqueous humour, while IL-6, IL-8, TNF-α, IL-1β, VEGF, ICAM-1, MCP-1 and complement factors are increased in the vitreous humour [116].

In addition to participating in the processes of neurodegeneration and apoptosis, the increased expression of pro-inflammatory cytokines in the diabetic environment promotes the creation of new vessels through the recruitment of endothelial cells, which are in turn induced to produce pro-angiogenic factors. Endothelial cells are extremely susceptible to cytokines, in particular IL-1β, TNF-α, and IFN-γ, which induce the production of IL-8, MCP-1, and Regulated and normal T cells Expressed and Secreted (RANTES) in them. In vitro studies have shown that endothelial cells respond more to cytokines than to elevated glucose levels, suggesting that diabetes-induced retinal vascular injury is primarily due to cytokine release from neighbouring cells rather than the direct effect of hyperglycaemia on endothelial cells themselves [117].

P2X7R in the pathogenesis of diabetic retinopathy

P2X7R has been described at the level of ganglion cells, photoreceptors, amacrine cells, EPR and Müller cells and many studies in recent decades have linked P2X7R-related functions to the pathogenesis of diabetes.

In a recent study in mouse models, in which diabetes was induced by streptozotocin (STZ) injections, a significant increase in P2X7R expression was observed approximately one month after the onset of induced diabetes and simultaneously the percentage of P2X7R-positive peripheral blood mononuclear cells (PBMCs) was increased compared to controls [118].

The inflammatory microenvironment contains high concentrations of extracellular ATP, sufficient to trigger the opening of P2X7R and the release of the cytokines IL-1β and IL-6, membrane metalloproteases and the production of ROS. In this regard, in mouse models of diabetes it has been observed that genetic deletion of P2X7R or its pharmacological inhibition protects against CD-40-induced release of TNF-α, IL-1β, ICAM, and NOS-2 over-expression in Müller cells [119]. Moreover, P2X7R activation represents a powerful trigger for VEGF release. Indeed, the expression of the NLRP3 inflammasome, which can be activated by P2X7R stimulation, is increased in the vitreous fibrovascular membrane of patients with diabetic retinopathy and dysregulation of NLRP3 in hyperglycaemic transgenic mice leads to vascular *leakeage* and retinal neovascularisation [120].

In a recent study in animal models of type 1 diabetes, it was found that hyperglycaemia induces increased P2X7R expression in the retina and that selective P2X7R antagonism reverses some of the diabetes-induced inflammatory effects in the retina, such as increased microvascular permeability and neovascularisation. This protective effect is accompanied in parallel by a strong inhibition of VEGF release and a normalisation of retinal IL-6 levels, thus supporting the hypothesis that P2X7R-related signalling plays a key role in promoting the inflammatory process and oxidative stress in the development and progression of diabetic retinopathy. [121]. Exposure of pericytes to high concentrations of glucose induces the activation of a P2X7R-mediated signalling pathway that promotes the acquisition by these cells of an inflammatory phenotype, as evidenced by the secretion of TNF-α and IL-1β. In the same study that demonstrated this phenomenon, it was also found that hyperglycaemia-induced damage in retinal pericytes leads to cell lysis, accompanied by the release of ATP into the extracellular environment, which in turn binds P2X7R on neighbouring cells, activating the inflammasome and

taking on the function of an inflammatory damage signalling device through an autocrine-paracrine mechanism [122]. It was found that P2X7R ligand concentrations are not sufficient to induce apoptosis in controls, while they are able to induce cell death in retinal capillaries extracted from diabetic mice, suggesting that hyperglycaemia is able to increase the vulnerability of retinal vascular cells to P2X7R activation [123]. The ability of P2X7R to induce apoptosis in endothelial cells and retinal capillary pericytes, termed purinergic vaso-toxicity, is mediated by transmembrane pore formation, typically resulting from sustained stimulation of this receptor, and appears to play a crucial role in the development of microaneurysms, exudates and diabetic macular oedema due to disruption of the blood-retinal barrier [124].

A new investigation has shown that Lamivudine, a recently discovered nucleoside reverse transcriptase inhibitor of P2X7R, is able to attenuate the progression of vascular and neurodegenerative lesions of diabetic retinopathy in mouse models, in which, compared to non-diabetic controls, administration of this molecule inhibits the formation of acellular capillaries and simultaneously allows maintenance of neuroglial function [118].

Using drugs that target P2X7R could be an interesting prospect for the treatment of diabetic retinopathy in the future. Diabetic macular oedema is currently treated with intravitreal injections of biological drugs that antagonise VEGF, such as Bevacizumab, Ranibizumab and Aflibercept, or intravitreal implants of devices containing corticosteroids, such as Dexamethasone. These therapies are highly effective, but also impractical and invasive for patients who have to undergo monthly eye injections, so therapies based on small molecules that can be administered via minimally invasive routes, such as oral therapies or eye drops, would be desirable. Several pharmaceutical companies have developed highly selective P2X7R inhibitors, some of which are in phase 1 and 2 clinical trials for the treatment of certain chronic inflammatory diseases. Some of these molecules are permeable across the blood-retinal barrier and may be available in the future for the treatment of diabetic retinopathy.

Age-related macular degeneration

Age-related macular degeneration is a degenerative disorder affecting the central area of the retina, known as the macula, responsible for high-resolution colour vision, and is the major cause of severe and irreversible visual decline in people over 65 years of age in industrialised countries. This maculopathy affects about 10% of the population over 65 and more than 25% of people over 75.

The retinal pigment epithelium (EPR) is made up of a layer of pigmented cells located on the outside of the neurosensory retina and has multiple functions that are essential for maintaining homeostasis at the level of the photoreceptors, such as protecting the retina from excessive exposure to light, forming the blood-retinal barrier together with the vascular endothelium, and also playing an immune defence role at the level of the macula. The EPR undergoes numerous changes with age, which become clinically detectable on ophthalmoscopic examination when **there are** focal extracellular deposits of yellowish polymorphous material at the interface between the retinal pigment epithelium and the inner collagenous zone of Bruch's membrane. Drusen are made up of several potentially harmful molecules including: lipofuscin, a pigment composed mainly of lipids with esterified and non-esterified cholesterol, more than 120 different proteins such as amyloid-β, apolipoprotein E (APOE), clusterin, TIMP-3 (tissue metalloproteinase inhibitor 3) protein, proteins involved in complement regulation, immunoglobulins, acute phase proteins such as vitronectin and fibrinogen, together with zinc and iron ions. With ageing there is a progressive accumulation within the EPR cells of intracellular bodies containing lipofuscin that should normally be eliminated by the choriocapillaries [125].

Classification

There are several classification systems for AMD, used for clinical or research purposes, including:

- conventional classification, dictated by clinical and evolutionary characteristics [126]:

- Dry' form. The most common form, found in 90% of AWD diagnoses. It has a gradual progression with bilateral asymmetrical eye involvement and in 10% of cases it progresses to the wet form.

  The presence of **soft drusen** and areas of focal hypo- and hyperpigmentation is characteristic. Soft drusen appear on **ophthalmoscopic examination** as yellowish-white subretinal deposits with generally ill-defined borders and a tendency to confluence.

  The advanced stage is called **geographic atrophy (AG)** or areolar atrophy and is characterised by a progressive reduction in neuroepithelial thickness with defined-edge chorioretinal atrophy affecting the retinal pigment epithelium,

choriocapillaris and photoreceptors. There are no signs of macular scar thickening (disciform scar) nor of oedema, haemorrhage or exudation.

On **fluroangiography,** atrophic areas appear hyperfluorescent and associated with hypofluorescent areas. Focal pigment accumulations may vary in shape: punctiform, reticular or linear and appear as hypofluorescent areas on fluorangiography.

The loss of central vision occurs slowly over the years. In very early stages symptoms are modest and reading difficultiesmay occur due to blurred vision or altered size of some letters (micro- or macropsies); in more advanced stages positive scotoma, an area of vision loss in the centre of the visual field, and metamorphopies, in which straight lines may appear distorted or broken in places, may appear.

- Wet' form. This is less common, affecting around 10% of cases. It has a more rapid course, leading to a significant reduction in vision within days weeks, and symptoms are often unilateral due to the tendency to affect one eye at a time.

The clinical picture at onset is characterised by a sudden reduction in visual acuity and the appearance of metamorphoses, positive central scotoma and blurred central vision. Peripheral vision and colour vision are generally unaffected. However, the patient may become legally blind in the affected eye (visual acuity < 20/200 in the better eye with corrective lenses), especially if treatment is not given.

The main pathophysiological alteration is **choroidal neovascularisation** (NVC), caused by an imbalance between angiogenetic and antiangiogenetic factors. It is characterised by the proliferation of abnormal blood vessels that originate in the choroid, penetrate through Bruch's membrane and spread below the EPR and/or below the neuroretina and, in association with the proliferation of fibroblasts, form a fibrovascular complex that alters the normal architecture of the choriocapillaris, Bruch's membrane, EPR and photoreceptors, leading to the formation of subretinal scars.

Characteristic is the presence of retinal and subretinal macular oedema, grey-green dyschromia under the macula, haemorrhage in the retina, subretina or below the EPR, retinal or subretinal lipid exudation. Focal macular oedema or haemorrhage may lead to the elevation of a macular area or localised detachment

of the retinal pigment epithelium. Finally, untreated neovascularisation results in submacular disciform scarring and subretinal fibrosis.

Based on **fluorangiographic** appearance, NVC can be divided into two subgroups:

Classical NVC: in early stages a delimited area of hyperfluorescence is visible and in late stages shows dye leakage; Occult NVC: characterised by the presence of late hyperfluorescence of undetermined origin or by detachment of the fibrovascular EPR.

- **Histological** classification divides NCV into 3 categories:
  - **Type 1** (or 'occult'), when the neovascularisation is localised below the EPR. Characterised by occult leakage to the FAG.
  - **Type 2** (or 'classic'), when the neovascularisation is localised above the EPR, in the subretinal space.
  - **Type 3** defined as retinal angiomatous proliferations (RAP), in which the neovascularisation develops in the context of the retinal layers and then progressively develops towards the subretinal space, creating a shunt with the choroidal circulation.

- **AREDS** classification, Age-Related Eyes Disease Study, used in clinical practice and in clinical and epidemiological studies [127]. (Table 5)

Table 5. Classification scheme of Age-Related Macular Degeneration according to AREDS (Age-Related Eye Disease Studies). (Al-Zamil et al., 2017)

Classification Category	Clinical signs	
NO DMLE	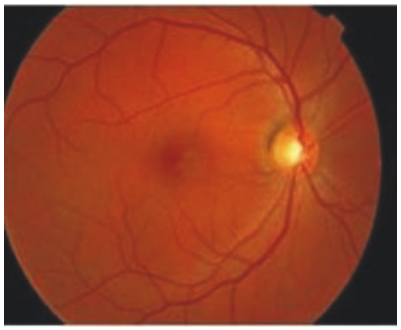	0-5 small drusen (<63µm in diameter)
DMLE iniziale	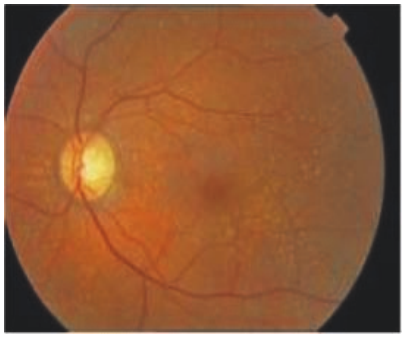	Multiple small drusen or a few drusen of intermediate size (63-124µm in diameter) or pigmentary abnormalities of the macula
Intermediate DMLE	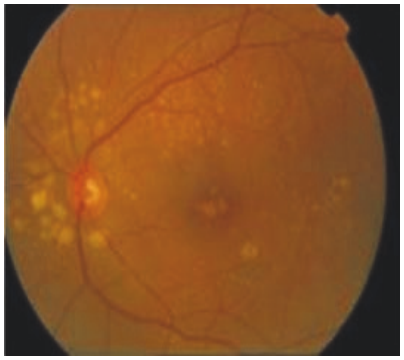	Diffuse intermediate drusen or at least one large drusen (≥125 µm) or Geographical atrophy not involving the central fovea
Advanced DMLE	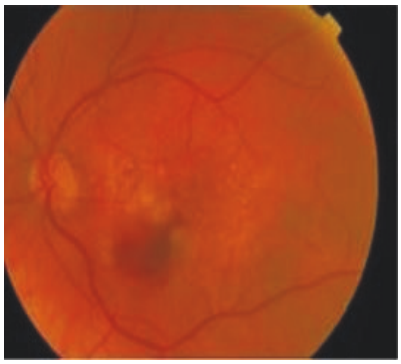	Geographical atrophy involving the central fovea or any signs of neovascularisation choroidal: subretinal haemorrhages, serous retinal detachment or detachment of pigment epithelium retinal, lipid exudates or fibrovascular scars.

Aetiopathogenesis of Age-Related Macular Degeneration

The multifactorial pathogenesis of AMD consists of multiple activated molecular processes that have as their common denominator the dysregulation of the immune-inflammatory system.

Advancing age is accompanied, on the systemic side, by the emergence of a chronic low-level inflammatory state, known as 'Inflammaging', which can be seen as an increase in serum levels of pro-inflammatory cytokines. As we age, various oxidative insults increase and accumulate, and the controlled mechanism of para-inflammation also increases. Systemic para-inflammation concerns the immune response

Local ocular para-inflammation is the response of the eyes to insults occurring at the macular level, through which homeostasis is maintained at the level of the macula during the normal ageing process. The para-inflammatory response can become dysregulated as a result of multiple factors such as genetic predisposition, epigenetic changes or the intervention of environmental factors. The resulting chronic inflammation results in the loss of the immune privileged position possessed by the retina: there is activation of retinal immune cells, in particular microglia and dendritic cells, activation of the complement cascade and the inflammasome, with production of various pro-inflammatory cytokines that then damage the EPR and photoreceptors and lead to the development of AMD. Chronic sustained inflammation at the macular level can also lead to scar formation resulting in loss of central vision.

While ageing is the risk factor with the greatest impact, environmental factors that increase oxidative stress such as cigarette smoking, low antioxidant diets and phototoxicity from UV exposure also contribute significantly to the increased risk of onset and progression of AMD, along with the presence of various gene polymorphisms [128] [129].

IMMUNOGENTICS AND COMPLEMENT

Using wide-screening genomic techniques, some 52 genetic variants on different chromosomes related to AMD have been identified, many of which encode proteins involved in the regulation of the inflammatory and complement cascade in the immune system, but also proteins involved in mitochondrial function, collagen production, extracellular matrix production and angiogenesis.

The most important genetic risk factor associated with approximately 50% of cases of AMD is the Y402H polymorphism of the CFH gene on the 1q32 locus whose function is

to downregulate the alternative complement pathway. Thus, the presence of this gene variant leads to reduced complement factor H activity with activation of the complement cascade and triggering of the inflammatory process at the subretinal level [130]. Smoking can also lower CFH levels, which means that smokers have an increased risk of developing AMD [131]. Dysregulation of the immune system and complement is in fact one of the fundamental pathophysiological alterations in the development of maculopathy and also plays a major role in the mechanism of parainflammation of the retina undergoing ageing. Certain activation products of the complement cascade, such as C3a, C5a have been identified in the drusen of eyes affected by AMD and are also elevated in the serum of patients with AMD, compared to controls in the same age group. In some studies, exposure of choriocapillary endothelial cells to C5a in vitro has been shown to upregulate ICAM-1, an adhesion molecule that binds leukocytes, and C5a has also been shown to promote IL-22 and IL-17A secretion in human $CD4^+$ T cells isolated from patients with exudative AMD. Indeed, IL-17A in vitro induces angiogenesis in choroidal endothelial cells and induces apoptosis and pyroptosis in ARPE-19 cells, which are part of a cell line derived from the retinal pigment epithelium. With the results of this research, it is possible to explain how cytokines derived from complement activation can induce neovascularisation and cell death at the macular level, two characteristics of neovascular AMD [132] [133] [134].

OXIDATIVE STRESS

Due to their high metabolic activity combined with high oxygen consumption and their polyunsaturated fatty acid content, EPR cells are usually prone to produce ROS, but daily exposure to sunlight and cigarette smoke contribute to making the EPR particularly sensitive to oxidative stress. A major function of EPR is heterophagy, a homeostatic mechanism aimed at autophagic degradation of materials from photoreceptor outer segments (POS) damaged by oxidative stress. Exposure to environmental factors, combined with a genetic predisposition for dysregulation of protective mechanisms, results in the continuous phagocytosis of this waste material by the cells of the retinal pigment epithelium, which are, moreover, aged and undividable. This leads to the accumulation in lysosomes of a non-degradable and self-fluorescent metabolite called lipofuscin, which inhibits the autophagy process by blocking the function of lysosomal enzymes and, in combination with oxidative stress, leads to the initiation of retinal inflammation. Lipofuscin is one of the key components of drusen and therefore it has

been hypothesised that it is these typical lesions that trigger the pathogenic inflammatory reactions that allow AMD to progress [135].

Studies have shown increased serum levels of oxidative markers such as malondialdehyde (MDA), and 8-hydroxy-2-deoxyguanosine (8-OHdG) in subjects with AMD compared to controls. In addition, cultured retinal pigment epithelium cells from eyes with AMD showed increased levels of ROS, AGEs and markers of oxidative damage in nuclear and mitochondrial DNA [136].

The EPR also possesses antioxidant systems that protect cells and photoreceptors from oxidative damage. Among these, the NRF2 (nuclear factor-erythroid 2-related factor 2) transcription factor-mediated signalling system, which is involved in maintaining mitochondrial metabolism by regulating several Krebs cycle enzymes, has been found to be altered and associated with retinal pigment epithelium degeneration in patients with AMD who are chronically exposed to cigarette smoke [137]. In addition, in vitro studies have shown that the antioxidant lutein can minimise the immune-inflammatory processes induced by oxidative stress in the retina by suppressing the activation of the NF-κB factor and inhibiting the expression of enzymes such as iNOS and COX-2, the main sources of free radicals [138].

MICROGLIA, MACROPHAGES AND IMMUNOSENESCENCE

Retinal microglia cells together with dendritic cells and choroid macrophages are among the immune cells that play an essential role in counteracting retinal malfunctions and allowing the maintenance of retinal homeostasis during ageing. In the neuroretinal structures, the para-inflammatory response mechanism, characterised by the breakdown of the blood-retinal barrier, is activated by a series of subclinical damages that lead to the production of endogenous molecules called "Allarmine", which, at ocular level lead to the activation of microglia and their migration to the subretinal level, while at choroid level the proliferation of macrophage cells occurs accompanied by the activation of the complement at the EPR-basal membrane interface [139]. Several studies have identified the presence of two different macrophage lines on pathological analysis of eyes with AMD: M1 macrophages, which are proinflammatory, have been associated with geographical atrophy while M2 macrophages, found at the level of NVC formations, express the proangiogenic protein VEGF, suggesting their involvement in the development of these neovascular lesions [140]. With ageing, adaptive immunity cells, such as T lymphocytes, also undergo changes known as immunosenescence, and it has

been shown that there is *downregulation* of CD28, a co-inflammatory molecule involved in the formation of antigen-specific responses, and *upregulation* of markers typically found in natural killer (NK) cells, such as CD56, which have a non-specific reactivity. An increased number of $CD56^+$ T cells was detected in the serum of patients with AMD compared to controls. Furthermore, $CD4^+$ T cells play a combined role with complement in establishing an inflammatory reaction underlying pathogenesis [141].

CYTOKINES AND INFLAMMASOME

High concentrations of multiple pro-inflammatory cytokines have been found in both ocular tissues and fluids and in the serum of subjects with AMD compared to age-matched controls, suggesting that the level of 'inflammaging', i.e. the low-grade systemic inflammatory response related to the ageing process, is more severe in patients with AMD. At the systemic level, IL-1β, TNF-α and IL-17 are elevated, where the production of the latter appears to be related to the increase in complement factor C5a [142].

Increased systemic concentrations of IL-6, IL-18 and TNF-α correlate with CFH gene haplotypes and IL-6 levels correlate with both the onset and progression of maculopathy. In addition, IL-6, which has pro-inflammatory and pro-angiogenic properties, is increased in aqueous humour from eyes of patients with neovascular AMD. The cytokines IL-22 and IL-17A, produced by the Th17 type of CD4-$helper^+$ T lymphocytes, are elevated in the serum of patients with exudative AMD and were found in disease-typical lesions and not in normal macular tissue. In vitro, IL-22 induces apoptosis of human EPR cells, while IL-17A increases the production of proinflammatory cytokines produced by ARPE-19 cells, such as IL-6, IL-8 and CCL2, and induces angiogenesis in human choroidal endothelial cells [143].

A typical example of an age-related inflammatory response in the EPR is the activation of the NLRP3 inflammasome, which has been correlated with the pathogenesis of AMD because it is found in epithelial cells in lesions of both advanced forms of AMD. Several intra- or extracellular stimuli that are present in the eye during ageing can activate the NLRP3 inflammasome, such as AluRNA, β- substance, β- and β-substance.

amyloid, A2E (a chromophore retinoid contained in lipofuscin and aldehyde derivative of vitamin A involved in retinal ROS production and subsequent mitochondrial damage), lipofuscin and oxidised lipoproteins. Depending on the stimulus NLRP3 is able to produce IL-18, IL-1β or both [144] [145] [146] [147] [148].

In a recent study, it was found that in vitro exposure of EPR cells to UVB induces ROS production and DNA damage. This contributes to IL-1β production via a signalling pathway involving the NLRP3 inflammasome, activated by K^+ efflux triggered by extracellular ATP, whose production is increased by UVB exposure. IL-18 production in the same cells is stimulated by UVB and ROS but through cellular pathways independent of the inflammasome [149].

A study group of patients with geographic atrophy showed higher concentrations of a non-coding RNA sequence called AluRNA in EPR cells and lower concentrations of DICER1 RNAase, an enzyme capable of cleaving and inactivating Alu-RNA. Alu-RNA is able to activate the NLRP3 inflammasome leading to the production of IL-8, which activates, via MyD88, caspase 8 responsible for apoptosis of EPR cells.

[150]. As shown in a study conducted in mouse models of EPR, activation of NLRP3 by Alu-RNA does not occur via Toll-like receptors (TLRs), although these are present in the retina, but via P2X7R [151].

Another study conducted in vivo in mouse models also found that activation of NLRP3 by β-amyloid, a component of drusen, is linked to activation of pathways leading to apoptosis of EPR cells and pyroptosis of choroid cells [152]. Furthermore, research has shown that amyloid-β induces apoptosis of Müller glial cells via a P2X7R receptor-mediated signalling pathway and that this cytotoxic effect is inhibited by incubating retinal cells with lipid solutions containing high levels of omega-3, such as docosahexanoic acid DHA and eicosapentanoic acid EPA, combined with Brilliant Blue G, a potent selective P2X7 receptor antagonist, protecting them from neurodegeneration [92].

Another study showed that in EPR cells and ARPE-19 cells, in which inflammasome activation had been induced with different types of stimuli such as lysosomal membrane permeabilisation, hydrogen peroxide-induced oxidative damage lipofuscin-mediated phototoxicity and activation of the P2X7 receptor by BnzATP, demonstrated that the application of selective NLRP3 inhibitors inactivates the inflammasome regardless of the stimulus applied to activate it [153].

The role of P2X7R in the pathogenesis of AMD

Based on in vitro studies, a study group has proposed a model of a P2X7R-dependent signalling pathway involved in the mechanisms of senescence and apoptosis of the retinal

pigment epithelium and in the pathogenesis of the two typical forms of AMD. Endogenous and exogenous tissue insults such as trauma, infection, oxidative stress and inflammation lead to ATP production and promote tissue expression of P2X7R. Extracellular ATP-activated P2X7R promotes ROS production, accelerating the process of EPR senescence and amplifying the inflammatory process underlying the early stages of maculopathy. Activated P2X7R induces apoptosis in EPR cells through a mechanism mediated by the influx of extracellular Ca^{2+} and the formation of the membrane pore pannexin-1 and also leads to dysfunction of the lysosome-phagosome system, which triggers an altered autophagy mechanism. Indeed, P2X7R has been observed to lead to ROS production by macrophages, induce lysosome alkalinisation, lipid oxidation and reduce phagosome clearance in ARPE-19 cells [154] [155]. ATP binding to the receptor also triggers K^+ efflux which induces activation of the NLRP3 inflammasome leading to IL-18 secretion. All these pathways are involved in the mechanism of EPR degeneration and the genesis of the dry form of AMD. On the other hand, P2X7R can lead to the activation of p38 which in turn mediates the secretion of IL-8, Monocyte Chemoattractant Protein-1 (MCP1) and Vascular Endothelial Growth Factor (VEGF). IL-8 and VEGF are pro-angiogenic factors that promote the growth of neovases leading to the wet form of AMD. MCP-1 is a chemokine capable of attracting activated mononuclear phagocytes that on the one hand kill the cells

EPR contributing to the dry form and on the other hand induce vascular growth, participating in the neoangiogenesis of the wet form [156]. Subsequent research conducted in vivo, including the use of knockout animal models for P2X7R or pharmacological inhibitors of the receptor, has confirmed this model, demonstrating that P2X7R is a key protein in the macular degenerative process that characterises AMD. Among these studies, we would like to mention the one mentioned above in which, in a mouse model of a non-neovascular form of AMD, Alu-RNA indicates the activation of NLRP3 via P2X7, leading to degeneration of pigment epithelium cells. In addition, the same research group, again using mouse models, demonstrated that the application of the nucleoside reverse transcriptase inhibitor NRTIs, a drug commonly used against HIV, inhibits the P2X7R-NLRP3 inflammasome complex in dry Alu-RNA-induced forms of AMD and improves the outcome of the laser-induced neovascular form [157] [158].

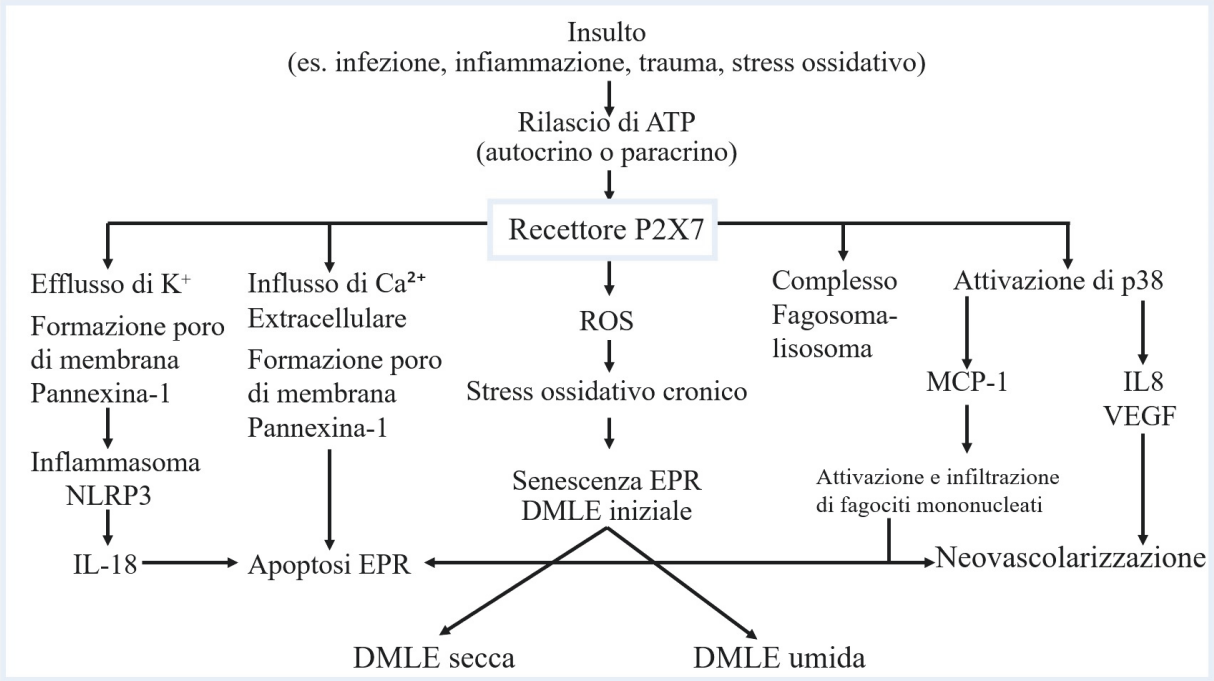

Schematic representation of P2X7 receptor-mediated signalling pathways involved in the pathogenesis of AMD. (Yang & Chen, 2014)

Increased levels of ATP were found in aqueous humour samples from exudative AMD patients with subretinal haemorrhages and in corresponding mouse models, application of the P2X7 receptor antagonist Brilliant Blue G (BBG) prevented photoreceptor apoptosis, suggesting that ATP-mediated P2X7 activation may contribute to the development of these lesions in subjects with advanced exudative AMD [159].

In P2X7R/SOD-1 double knockout mice, the absence of P2X7R can be shown to prevent the accumulation of microparticles within the EPR and the choroid and block the action of oxidative stress in the retina [160].

Furthermore, oxysterols, oxidised derivatives of cholesterol, have been shown to accumulate in drusen during AMD and P2X7 receptor activation plays a key role in oxysterol-induced retinal degeneration in human pigment epithelium cells [161].

Finally, underlining the importance of P2X7R in the pathogenesis of AMD, genetic investigations have shown that a haplotype containing two rare genetic variants of P2X7R and P2X4R is associated with an increased susceptibility to the onset of AMD [162].

Based on this information and using a 'P2X7 null' mouse model in which a loss of P2X7R function was induced, a recent study suggested that the P2X7 receptor normally acts as a scavenger in retinal macrophages and microglia and that in the absence of P2X7R, altered

phagocytosis by these cells leads to the accumulation of photoreceptor-derived debris at Bruch's membrane and age-related loss of EPR cells and photoreceptors [163].

Glaucoma

The term glaucoma refers to a heterogeneous group of optic neuropathies characterised by the progressive degeneration of retinal ganglion cells (RGCs) and their axons, which make up the optic nerve, due to altered fluid dynamics in the anterior and vitreous chambers of the eye. Glaucoma is considered the leading cause of blindness in the world and it is predicted that more than 76 million people will be affected by 2020. Early diagnosis is made difficult by the fact that symptoms often appear late in the course of the disease, so that therapeutic measures are applied when irreversible loss of retinal neurons has already begun. In general, the decline in visual function becomes detectable when more than 30% of RGCs have been lost, although it has been observed that symptoms, i.e. gradual loss of peripheral vision followed by progressive loss of central vision, are reported by patients even later [164].

Types of glaucoma

In the past, increased intraocular pressure (IOP) was considered the primary marker for the diagnosis of glaucoma, but it has been observed that many individuals with elevated IOP do not show clinical signs of glaucoma and optic nerve damage, and up to 50% of glaucoma patients have IOP within normal ranges.

Primary glaucoma is related to anatomo-functional alterations of the eye that compromise ocular hydrodynamics and can be distinguished into three types [165]:

- Primary open angle glaucoma (**POAG**)

It is the most common form of glaucoma and accounts for more than 80% of cases in the Western Hemisphere. Risk factors for primary open-angle glaucoma include: older age, positive family history, African ethnicity, thinner central corneal thickness, systemic hypertension, diabetes and myopia. Clinically, POAG is diagnosed when the following are present: open angle, IOP>21 mmHg and visual field loss associated with degeneration of ganglion cell axons (optic neuropathy). The corneal iris angle, i.e. the anatomical angle formed between the iris and the cornea, is open in POAG as it is in the normal eye, but

the aqueous humour drainage mechanism at the level of the trabecular meshwork is altered, while production at the level of the ciliary body is usually normal.

- Normal **pressure glaucoma** (**NTG**)

It is present in about 30% of patients with POAG. Intraocular pressure is within the normal range, 10-21 mmHg, but optic nerve damage and visual field deficits typical of glaucoma are present, following an "hourglass pattern". Risk factors include female sex, race (more common in Japanese than Caucasians), vascular dysregulation and low blood pressure. Normal tension glaucoma evolves very slowly, but progression can be continuous even with very low blood pressure. The presence of haemorrhages in the optic papilla is often characteristic of disease progression [166]. Patients are likely to express *gain-of-function* mutations in genes involved in sensitivity to mechanical stimuli, which would make them hyper-sensitive to modest increases in IOP.

- Primary **closed angle** glaucoma (**PCAG**) The disease is caused by disturbances of the iris, crystalline lens and retro-lenticular structures that prevent the drainage of aqueous humour by narrowing the corneal iris angle. It is more common in Asian populations, women and people with high hypermetropia due to reduced anterior chamber depth. In about one third of patients with angle-closure glaucoma, an abrupt increase in IOP (often above 30 mm Hg) causes acute symptoms: violent eye pain, nausea and vomiting, conjunctival hyperemia, corneal oedema, pupillary mydriasis requiring immediate medical attention. An acute glaucoma attack, if not treated promptly, can lead to blindness in a short time.

Secondary glaucoma reflects pathological mechanisms that elevate IOP above the normal range due to pathological increased aqueous humour production at the ciliary body and/or reduced drainage at the trabecular level. Variants include pseudoexfoliative glaucoma, neovascular glaucoma, pigmentary glaucoma and steroid-induced glaucoma. Other types of glaucoma are associated with cataract formation, some ocular tumours, uveitis, myopia and early-onset glaucoma (juvenile glaucoma). In inflammatory or uveitic glaucoma, glaucoma may result from obstruction of the drainage structures in the anterior segment as a secondary consequence of ocular inflammation [167].

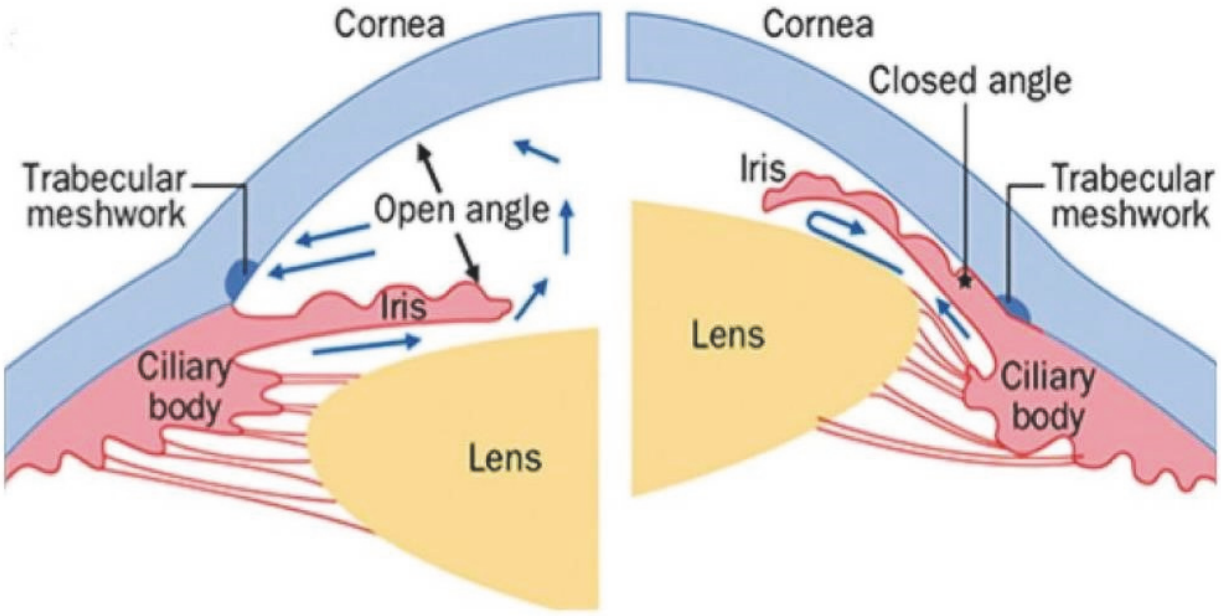

Figure 6. Schematic representation of open angle glaucoma (left) and closed angle glaucoma (right). In PCAG, dislocation of the lens and iris obstructs the outflow of aqueous humour at the level of the trabecular system. (Wiggs & Pasquale, 2017).

Glaucoma pathogenesis: the role of inflammation

The mechanisms underlying the pathogenesis of glaucoma have for decades been identified as abnormalities in the regulation of intraocular pressure (IOP) and/or altered mechanical sensitivity of the eye cells. Although the contribution of IOP is responsible for a significant proportion of glaucoma cases, approximately 30-70%, it has been observed that at any level of ocular pressure, even normal, lesions typical of the disease can be observed, and that, despite careful therapeutic control of IOP, 15-25% of glaucoma cases progress to more advanced optic neuropathy. For these reasons, the pathogenetic role of neuroinflammation, oxidative stress and alterations in the blood-retinal barrier is emerging in terms of increasing importance [168].

VASCULAR ALTERATIONS AND OXIDATIVE STRESS

The impact of intraocular pressure in the pathogenesis of glaucoma is generally explained through two complementary theories: the mechanical theory, in which increased IOP causes direct compression of retinal ganglion cell (RGCs) axon fibres at the lamina cribrosa, where the axons join to exit the eyeball at the level of the optic papilla.

According to the vascular theory, the increased IOP would cause compression of the capillaries resulting in reduced blood flow to the optic papilla and leading to chronic ischaemic optic nerve damage [169].

Many authors suggest that there is a multifactorial vascular insufficiency underlying glaucomatous optic neuropathy and that among the factors involved, in addition to the aforementioned mechanical vascular compression, is a reduced ability to self-regulate blood flow at the papilla level. In this regard, it has been observed that due to multifactorial predisposing causes such as genetics, ageing and lifestyle, the blood-retinal barrier and the blood-brain barrier surrounding the optic nerve are impaired in glaucomatous eyes. This leads to dysregulation of the vessel wall, resulting in the leakage of molecules that may be responsible for the establishment of the local inflammatory response, and an inability of the autoregulatory mechanism to maintain the blood supply to the papilla and optic nerve. This particular situation occurs during stressful conditions that can be generated either by an increase in IOP or by a reduction in local perfusion pressure due to low blood pressure. An impairment of the autoregulatory system then causes periods of relative ischaemia leading to reperfusion injury when flow is restored.

A consequence of relative ischaemia is an increase in the concentration of endothelin-1 (ET1) in the retina, where by activating caspase 3 it may be one of the factors responsible for RGC cell death, and in the choroid where it induces capillary vasospasm intensifying the hypoxic condition due to reduced perfusion. It has been observed that ET-1 may also stimulate the enzyme NO-synthase (NOS) to produce nitric oxide, thereby increasing oxidative stress and contributing to neuronal death, as well as inducing GFAP production at glial level, stimulating astrocyte and Müller cell proliferation [170].

Under hypoxic stress conditions in the retina, HIF-α expression is induced, which on the one hand is a regulatory mechanism to protect RGCs, but on the other hand induces the production of NO, VEGF and activation of the NF-κB signalling pathway, which correlates with the synthesis of various inflammatory mediators including TNF-α and IL-6. HIF-α also correlates with RGC death because it is accompanied by increased expression of p53 and various pro-apoptotic caspases [171].

The presence of HIF-α and hypoxia can also dysregulate the mitochondrial respiratory chain leading to increased production of reactive oxygen species (ROS), which in turn create a vicious cycle that leads to damage to various cellular components, including the mitochondria, with the release of pro-apoptotic factors. Increased levels of oxidative stress markers from DNA oxidation and lipid peroxidation have been documented in

glaucoma patients or mouse models with elevated IOP. In addition to facilitating apoptosis of RGCs, oxidative DNA damage can also occur in the cells of the trabecular system, leading to increased resistance to aqueous humour outflow and thus contributing to elevated IOP and visual impairment [172].

MICROGLIA, ASTROCYTES AND MÜLLER CELLS

When damage or pathological phenomena occur in the retina, as in the glaucomatous process or with an increase in IOP, the retinal surveillance immune system, composed of microglia, astrocytes and Müller cells, is activated to protect the neurons. In particular, studies over the last few decades have shown that the phenomenon of neuroinflammation related to the pathogenesis of glaucoma takes place at various points in the visual system including: the vitreous chamber of the eye, i.e. at the level of the retina and the optic papilla, in the optic tract and at the level of the brain tissue, in particular at the level of the superior colliculus and the lateral geniculate nucleus, and at the level of the immune system of the peripheral blood, due to the infiltration of blood lymphocytes at the level of the optic papilla and the retina [173]. The cells that suffer the most significant damage are the retinal ganglion cells (RGCs), which belong to the layer of multipolar cells of the retina whose axons form the optic nerve at the optic papilla. Their dendrites, on the other hand, enter into synapses with the amacrine cells and the bipolar cells of the inner plexiform layer, located externally, and through which they receive visual information collected by the retinal photoreceptor cells, cones and rods.

Astrocytes and Müller cells have been found to be activated under conditions of ocular hypertension. In particular, studies in animal models of chronic ocular hypertension have shown that levels of GFAP, produced by activated astrocytes, are elevated as early as 2 hours after IOP elevation, and in DBA/2J mice, traditionally used as glaucoma models, Müller cell activation was detected even before IOP elevation.

IOP. GPAF is a mediator that stimulates proliferation and infiltration of glial cells, a process known as astrogliosis [174].

One of the theories correlating astrocyte activation with neuronal death of RGCs is that neurotoxic mediators can propagate through the connectins, the main components of the *gap junctions* that connect astrocytes [175]. Ischaemia can induce astrocytes to alter axon transport and induce biomolecular changes at the level of the lamina cribrosa and the extracellular matrix. In addition, ischaemic conditions stimulate the release of potentially

toxic factors for neighbouring neurons such as NO, TNF-α, TGF-β and glutamate, contributing to glaucomatous neuropathy [176].

In the early stages of the disease process, the activation of Müller cells is intended to maintain the homeostasis and integrity of the retina, as they express several receptors related to cell growth and survival; however, when over-activated, they are able to release several damaging factors including TNF-α, IL-1 and NO, leading to the activation of receptors related to cell death and altering the homeostasis of potassium and H2O in the retina. Müller cells usually perform the function of removing extracellular glutamate from retinal tissue to prevent its diffusion beyond synaptic spaces via GLAST, the main glutamate transporter, whose expression is reduced in glaucomatous conditions, contributing to the pathological process of excitotoxicity, neuronal death and photoreceptor degeneration [177].

Microglia, retinal immunocompetent cells that act as sensors of neuronal damage, are among the first cell lines to be activated after the first glaucomatous damage events, before retinal ganglion cell degeneration occurs. In response to a damaging stimulus, microglia proliferate at the retinal level and at the level of the optic papilla and undergo a morphological change, assuming an ameboid inflammatory phenotype with the release of pro-inflammatory cytokines such as IL-6 and TNF-α and reactive oxygen species such as nitric oxide (NO), harmful to RGCs, and increased expression of phagocytosis-related CD68+ proteins and major histocompatibility membrane complexes MHC I and MHC-II. The extent of activated microglia cells correlates with the extent of axonal degeneration at the optic nerve head induced by the glaucomatous process [178] [179]. Various findings in animal models of glaucoma suggest that microglia activation occurs early and prior to elevation of intraocular pressure or signs of neuronal damage. Moreover, in experiments, inhibition of the activity of these cells by pharmacological molecules such as Minocycline or Azithromycin, an antibiotic with immunomodulatory properties, is able to stop the death of RGCs, improving their survival, modulating the local inflammatory state and preventing disease progression. In addition, in a model of acute ocular hypertension, induced by the injection of saline into the anterior chamber, it was observed that deletion of the CX3CR1 chemokine receptor reinforces neurotoxicity by modulating microglial activation [180].

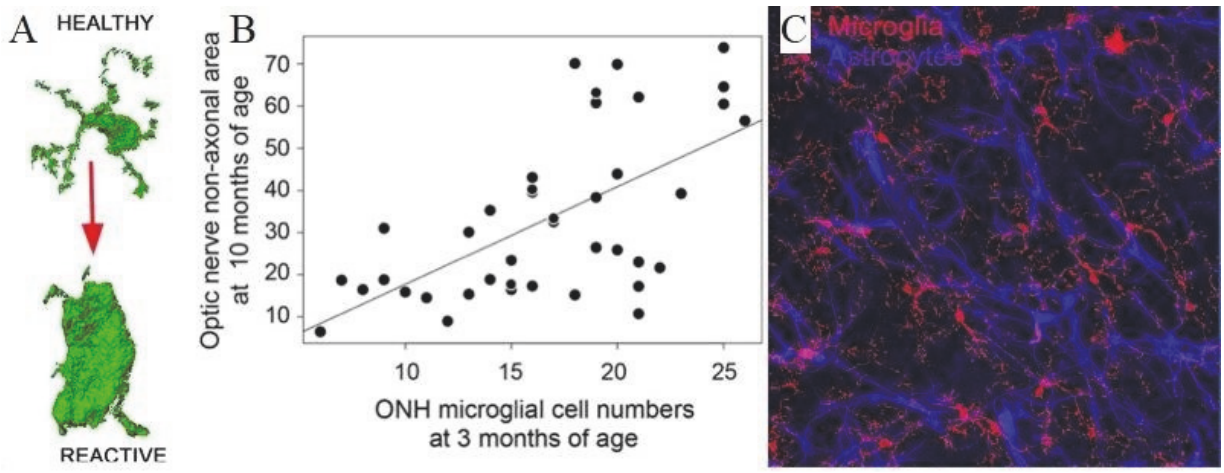

Figure 7. (A) Example of phenotypic change of microglial cell from quiescent branched to reactive amoeboid. (B) Murine model of chronic glaucoma in which the number of microglia at the optic nerve head in the early stages of glaucoma correlates with the following late axonal loss. (C) Early stage glaucoma: microglia are labelled with CD11b (red), astrocytes with GFAP (blue) and both cell types show signs of hypertrophy with enlarged soma and thickened processes. (Križaj D, What is glaucoma?; Webvision: The Organization of the Retina and Visual System, 2019)

Interestingly, investigations in experimental glaucoma models have shown that increased IOP is associated with higher numbers of M1-like microglia, with a pro-inflammatory phenotype, while few M2-CD86+ microglia have been detected between ganglion cells and optic nerve fibres. In the regulation of inflammatory responses, a reciprocal dialogue is established between microglia and astroglial cells: it has recently been reported that activated M1-like cells release IL-1α, C1q and TNF-α that induce the expression of the reactive A1 phenotype in astrocytes, which also has a neuroinflammatory function, leading to the expression of several genes, such as those involved in the complement cascade, that have destructive effects on synapses. Various components of the classical complement pathway, such as C1 and C3, are found to be increased in glaucoma mainly at the level of the optic papilla and the inner plexiform layer where they may play a protective role by coming into contact with the dendrites of retinal ganglion cells [181]. Infiltration of monocyte-macrophage cells has also been shown to occur coinciding with the onset of glaucoma in DBA/2J mice [182].

Importantly, other cell types, including neurons, astroglia and infiltrating leukocytes such as T cells, also participate in the neuroinflammatory process, and unravelling the molecular pathways that underlie the phenotype acquired by retinal cells in glaucoma

could be useful in finding better targets for treatment. To date, most of the information available in favour of the neuroinflammatory hypothesis has come from animal models and it will be important in the future to explore the biomolecular mechanisms involved in this process both in human subjects and in experimental models relevant to this disease.

PRO-INFLAMMATORY SIGNALLING PATHWAYS IN GLAUCOMA

From the point of view of the triggering of the inflammatory pathway, multiple investigations have led to the recognition of three main signalling pathways:

- **Toll-Like Receptor** (TLRs) mediated signalling pathway

Activation of innate immunity receptors TLRs in glial cells, microglia and astrocytes can occur through binding to oxidative stress products induced by glaucomatous conditions. Tenascin-C, an endogenous activator of TRL4, is a DAMP whose expression is elevated in astrocytes during glaucomatous optic neuropathy. Several studies have reported increased TLR2, TLR3 and TLR4 immunoreactivity of microglia and astrocytes in the retina and that stimulation of these receptors leads to activation of the NF-κB and MyD88 mediated signalling pathway, which amplify the secretion of proinflammatory cytokines IL-1 and IL-6 contributing to the creation of an inflammatory environment and degeneration of RGCs [183] [184] [185].

- **Tumor necrosis factor-α** (TNF-α)-mediated signalling pathway.

The pro-inflammatory cytokine TNF-α is produced by astrocytes and microglia in the retina and optic nerve. Its release is induced by increased IOP, ischaemia and oxidative stress. Certain genetic polymorphisms have been linked to an increased risk of developing glaucoma. Several investigations have found increased levels of this mediator in the aqueous humour and serum of glaucoma patients. Intraocular injections of TNF-α in mouse models with normal eyes have been observed to induce death of oligodendrocytes and RGCs and axonal damage of the optic nerve comparable to that in glaucoma patients. TNF-α expresses its functions by binding to TNF-R1 and TNF-R2 receptors and in glaucomatous conditions has been shown to play a role in inducing neuronal death of RGCs, as genetic ablation of these receptors results in neuroprotection of retinal cells and the optic nerve in experimental glaucoma models [186] [187] [188].

- **P2X7** receptor-mediated signalling pathway

P2X7 receptor expression was found in retinal amacrine cells, retinal ganglion cells (RCGs), microglia and astrocytes from animal models of glaucoma. Increased levels of ATP and P2X7R activation have been demonstrated in in vitro and in vivo models of ocular hypertension. ATP is released from cells as a result of apoptosis and necrosis caused by elevated IOP or ischaemia during glaucoma. It has been hypothesised that the P2X7R receptor is capable of activating several molecular signalling pathways involved in microglia activation, RGCs cell death and the creation of an inflammatory environment. In a study in which injection into the eyeball of BzATP, a P2X7R agonist, was used to establish an animal model of chronic ocular hypertension, the level of Iba1, the characteristic marker of microglia, was found to be significantly increased, suggesting that stimulation of P2X7R in glaucoma could drive microglia cells into a reactive form. In this regard, pretreatment with a P2X7R receptor antagonist, Brilliant Blue G (BBG) reduces microglia activation and also provides some level of neuroprotection by preventing retinal ganglion cell death [189].

Other research in animal models of glaucoma has shown not only that P2X7R activation is linked to microglia proliferation and activation but that RGCs death occurs through a P2X7R-NLRP3 mediated pathway. Indeed, the addition of a P2X7R inhibitor called A438079 or an NLRP3 inhibitor called Mcc950 on the one hand reduces the number of microglia cells present and on the other increases the survival rate of RGCs. Furthermore, the application of the NLRP3 inhibitor alone does not reduce the presence of transcripts of certain proinflammatory cytokines, implying that microglia are able to produce TNF-α, IL-6, IL-1β, IL-18 and IL-11 through stimulation of P2X7R, but through an independent NLRP3 pathway [190].

Pannexin-mediated mechano-sensitive ATP release stimulates P2X7Rs on RGCs and astrocytes leading to Ca^{2+} overload and caspase activation and, in addition, P2X7R stimulation due to mechanical stress on astrocytes or RGCs leads to IL-6 release [191].

In retinas from DBA/2J mice, increased P2X7R activation in RGCs correlates with *loss of function of* the ERG gene and increased expression of caspase-3, mediated by increased activation of MAPK, JNK and p38, suggesting that P2X7R is involved in a pro-apoptotic mechanism, induced by elevated intraocular pressure, leading to RCGs cell death. Recently, it has been shown that in vivo P2X7R is involved in the mechanism of NMDA-induced retinal damage leading to glaucomatous death of RCGs cells [192].

Stimulation of P2X7R in vivo has also been shown to lead to NMDA receptor activation, which is followed by a large influx of Ca^{2+} into RGCs, leading to neuronal death and retinal damage [193].

In conclusion, the results of these studies suggest that the P2X7R receptor is involved in the pathogenetic mechanisms leading to the onset and progression of glaucoma, being responsible for the processes of neurodegeneration, inflammation and gliosis, which prevent proper tissue regeneration. Inhibition of P2X7R-activated signalling pathways by specific pharmacological antagonists could therefore be an interesting therapeutic proposal for the prevention and treatment of glaucoma in the years to come.

Pseudo-exfoliative syndrome or PEX

Pseudoexfoliative syndrome, commonly abbreviated as PEX, is an age-related systemic disorder resulting from the deposition of pseudoexfoliative material (PXF) in various organs and tissues.

PEX affects around 60 million people worldwide, its incidence increases rapidly after the age of 50 and its geographical distribution is more concentrated in countries with a high incidence of PEX.

Scandinavia, Greece and parts of Africa, where several epidemiological studies have shown a higher frequency in specific ethnic groups [194].

PXF is an amyloid-like, grey-white, extracellular fibrillar material resulting from abnormal metabolism of the extracellular matrix and formed histologically from various matrix, basement membrane and elastic fibre constituents such as fibrillin-1, elastin, laminin, fibronectin, LTBP1 and LTBP2 (latent TGF-β binding proteins), clusterin and the cross-linking enzyme LOXL1 [195]. Fibrillar deposits have been found in or on the surface of all structures of the anterior chamber of the eye and appear to be produced by the epithelium of the pre-equatorial zone of the lens, corneal endothelium, endothelium of the trabecular meshwork, pigmented epithelium of the iris, and almost all cell types of the iris stroma, such as fibrocytes, melanocytes, endothelial cells, pericytes and smooth muscle cells [196].

The deposition of white-fur material on the surface of the lens is the most consistent and important diagnostic sign of PEX. The classic pattern of the advanced stage consists of three distinct zones on the anterior surface of the lens that become visible when the pupil is fully dilated: a central disc that corresponds approximately to the diameter of the pupil,

a granular and stratified peripheral zone and a free intermediate zone created by rubbing the iris against the surface of the lens during pupillary movement [197].

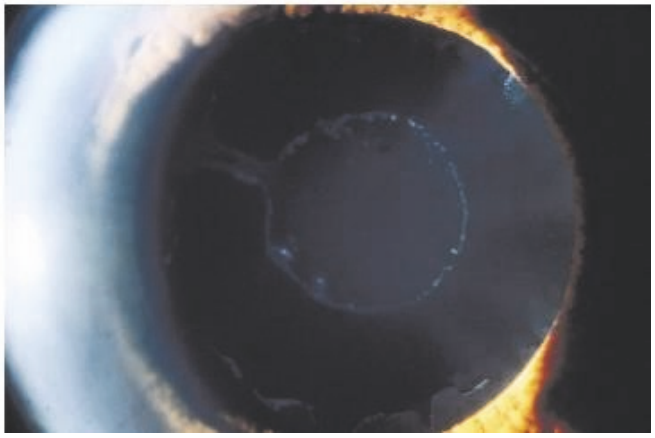

Figure 8. Classic presentation of lens with PEX. (Ritch & Schlötzer-Schrehardt, 2001)

PEX is the most common cause of secondary open-angle glaucoma, called pseudo-exfoliative glaucoma (PXG), which compared to primary open-angle glaucoma (POAG), has a greater increase in intraocular pressure (IOP), reduced visual function with more advanced visual field loss at diagnosis, worse prognosis and poor response to therapy [198].

Obstruction of the trabecular meshwork by pseudo-exfoliative material or accumulation of free iris pigment at the irido-corneal angle are generally considered to be the most plausible causes of increased IOP caused by blockage of the outflow of aqueous humour. The severity of glaucoma and subsequent optic nerve damage has been related to the amount of PXF material present in the iuxtacanalicular region of the trabecular system in studies of organ donor eyes. However, it is still unclear why a proportion of patients with PEX develop glaucoma, although most will probably never do so [199] [200] [201] [202]. In addition, PEX carriers are at high risk of developing various ocular pathological conditions that include angle-closure glaucoma, accelerated cataract formation, zonular weakness, droplet keratopathy or spheroidal degeneration, retinal vein occlusion and even decreased pupil dilation [203] [204].

Alterations in the vascularisation and blood-ocular barrier of the iris occurring in PEX would lead to alterations in aqueous humour composition and consequently may dysregulate the metabolism of the lens leading to cataract formation. Weakness of the zonular apparatus combined with poor pre-operative pupillary mydriasis leads to an increased risk of intraoperative complications in cataract extraction surgery [205] [206].

Systemic fibrillar deposition includes the skin, heart, vessels, lungs, bladder, kidneys and meninges, and several epidemiological studies have shown that affected individuals are at increased risk of cardiovascular disorders such as coronary artery disease, hypertension, cerebrovascular diseases, abdominal aortic aneurysm, peripheral vessel disease, renal artery stenosis, but also Alzheimer-like dementia, sensorineural hearing loss and, recently, erectile dysfunction and pelvic organ prolapse [207] [208] [209] [210] [211] [212] [213] [214].

Aetiopathogenesis of Pseudoexfoliative Syndrome

The etiopathogenesis of the syndrome is multifactorial. The variability in prevalence among populations of different ethnicities and the tendency for family aggregation in which multiple members of the same family present with different manifestations of the syndrome have extended interest in hypothesising the involvement of various heritable risk factors. Single nucleotide polymorphisms (SNPs) in the LOXL1 gene were the first to be highlighted, followed by the polymorphism in the CACNA1A gene, which encodes for the α-subunit of a $^{2+}$ Cauliflower-dependent channel, whose concentrations are high in deposited material [215].

Altered expression of the enzyme LOXL1 (lysyl oxidase-like1), found in deposits in the ciliary body, lens capsule and other affected tissues, could be associated with dysregulation of elastin and collagen metabolism and lead to structural disorganisation of elastin in the lamina cribrosa of the eye [216]. Although SNPs of LOXL1 are very common in the general population, most carriers do not develop pseudoexfoliative syndrome, suggesting that other genetic, epigenetic and environmental factors may contribute to the development of the condition [166] [217].

Molecular studies have revealed multiple disrupted pathways in PEX involving TGF-β1 signalling, the function of matrix metalloproteinases MMPs and their endogenous inhibitors TIMP, which result in aberrant synthesis on the one hand and altered degradation of the extracellular material that makes up fibrillar deposits on the other [218] [219]. High plasma and aqueous homocysteine levels and reduced folate *intake, which* contributes to hyperhomocystinemia, are additional risk factors associated with the syndrome [220]. Dysregulated molecular pathways in the development of pseudoexfoliative glaucoma also include those that regulate mitochondrial function and the autophagy phenomenon, which is important for the degradation of *misfolded* proteins,

which would contribute to the accumulation of fibrillar material and a reduced response to oxidative stress [221].

PEX is an age-related disease and therefore chronic exposure to harmful factors such as infections, UV radiation, environmental allergens and trauma alters the balance between oxidant and antioxidant factors, exposing ocular tissues to oxidative stress. Many research works have shown that a deficit in the cellular capacity to mitigate oxidative stress and exposure to a chronic inflammatory state contribute to the pathogenesis of PEX. On the one hand, reactive oxygen species (ROS) such as hydrogen peroxide ($_2HO_2$), lipid peroxidation products and advanced glycation products are elevated in the aqueous humour and blood, on the other hand there is a concomitant reduction in the levels of proteins and antioxidant molecules such as ascorbic acid and reduced glutathione. Oxidative damage is a trigger for degeneration of the trabecular system, causing a significant increase in intraocular pressure (IOP), which underlies the pathogenesis of glaucoma and associated neuronal lesions, which are also sustained by the lack of adequate local antioxidant defences. In the presence of reactive oxygen species (ROS), nitric oxide produces toxic metabolites called peroxynitrites and the resulting oxidative stress induces a chronic inflammatory process sustained over time, which is also responsible for fibroblast cell proliferation and neurotoxicity. Lower levels of nitric oxide (NO) were found in patients with PXG than in those with PEX and this could lead to a double negative effect contributing to both the development and progression of glaucoma because on the one hand the ocular blood flow is increased due to the vasodilating effect of NO on the endothelium, but on the other hand, since it has a vasoconstricting effect on trabecular cells, a reduction in NO leads to a reduced outflow of aqueous humour [222]. In addition, oxidative stress, tissue ageing and increased IOP induce the transcription of the NF-κB factor, which is widely involved in amplifying the inflammatory cascade. In this regard, a study conducted on daily dietary supplementation of docosahexaenoic acid (DHA), an omega-3 fatty acid, showed benefits in patients with PXG in terms of improving retinal function due to its inhibitory effect on NF-κB activation and cytokine synthesis and its protective antioxidant effect on the retinal pigment epithelium and photoreceptors [223].

Local oxidative stress triggers a chronic state of inflammation accompanied by the production of several pro-inflammatory cytokines such as IL-6, IL-17, TNF-α. In the pathogenesis of PEX, pro-inflammatory cytokines are involved in the regulation of the immune response, in the deposition and remodelling of the extracellular matrix, in

increased vascular permeability and in stimulating the secretion of other profibrotizing cytokines. Several studies have shown increased levels of TNF-α, IL-6, IL-17 in the aqueous humour of patients with early PEX and increased serum levels of IL-6 in both early and late PEX, thus suggesting that IL-6 contributes to the maintenance of the inflammatory process both locally and systemically and to the initiation of the fibrotic process underlying the pathogenesis of PXG. The levels of IL-17 and TNF-α in the aqueous humour remain high up to the stage of glaucoma while those of IL-6 continue to maintain an upward trend even after the onset of glaucoma.

There is a reciprocal stimulation of the above cytokines in that: IL-6 activates the local synthesis of TNF-α and IL-17 by stimulating Th1 and Th17; among the most relevant effects of IL-17 are the stimulation of stromal cells to secrete IL-6, IL-8, the granulocyte growth factor GCS-F (granulocyte colony-stimulating factor), prostaglandin E2 and nitric oxide and the regulation of IL-6 and TNF-α release by macrophages; the increased levels of TNF-α during the development of PEX suggest that chronic inflammation underlies this process and further intensifies the process of fibrosis and release of fibrotic material due to inhibition of collagen phagocytosis by fibroblasts [224]. The fibrotic process, which characterises the development of PEX and contributes to the injury of the trabecular system in pseudoexfoliative glaucoma, begins when the immune inflammatory response and wound repair process develops in tissues damaged by oxidative stress. Damage to epithelial and endothelial cells is accompanied by the release of proinflammatory cytokines (IL-1, TNF-α, IL-6, IL-17) with activation of the fibrinolysis system of the coagulation cascade to repair the damaged vessel. Activated thrombin in turn activates fibroblasts, promoting their proliferation and differentiation into collagen-producing myofibroblasts. Thrombin acts in conjunction with TGF-β release to lead to clot formation and increase vascular permeability to promote extravasation and recruitment of leukocytes to the lesion. The basement membrane, which lies beneath the epithelium and endothelium, retains the recruited leukocytes and matrix metalloproteinases MMPs degrade and release some of the basement membrane constituents increasing the extravasation of inflammatory cells at the damaged site. Inflammatory cells exploiting TNF-α can lead to the local synthesis of TGF-β, which together with CTGF (connective tissue growth factor) increases the secretion of EGF and IGF and accelerates the proliferation and differentiation of fibroblasts into myofibroblasts. These physiological processes are dysregulated and abnormally increased

in the pathogenetic process leading to PEX and PXG [225] [226]. A recent study also showed that the concentration of the proinflammatory protein

YKL-40 was found increased in aqueous humour, but not in serum, indicating that it may be used as a localised inflammatory marker at PEX [227]. Also worthy of mention is the role of hypoxia due to occlusion of the iris vessels with pseudo-exfoliative material and gradual degeneration of vascular cells. It has been shown that conditions of iris hypoperfusion and hypoxia in the anterior chamber can up-regulate LOXL1 expression and that high levels of vasoregulatory molecules such as endothelin-1, a potent vasoconstrictor, and proangiogenic molecules such as VEGF are present in the aqueous humour of patients with PEX [228] [229].

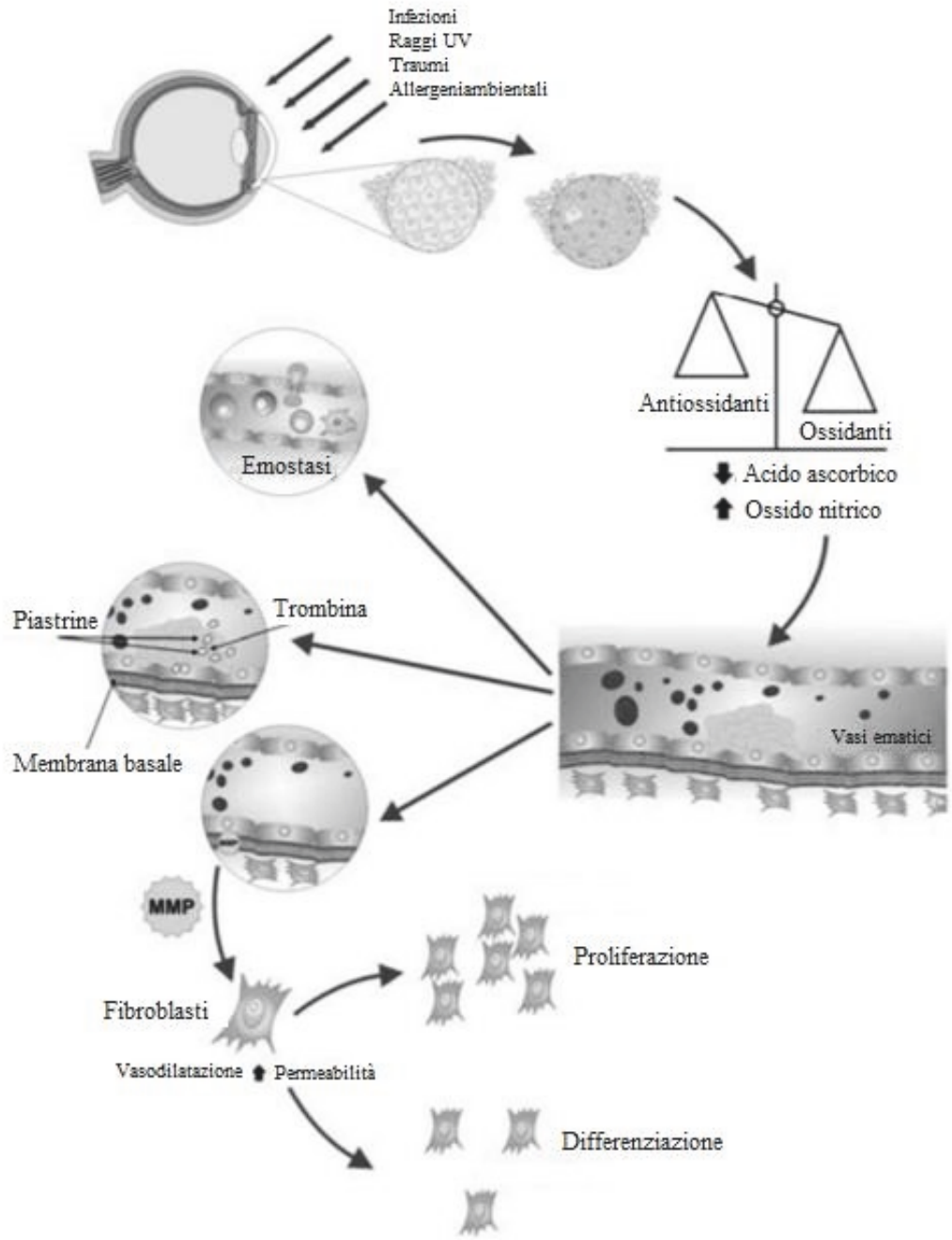

Figure 9. Schematic representation of the fibrotic process triggered by oxidative stress during the pathogenesis of Pseudoexfoliative Syndrome. (Sarenac Vulovic et al., 2016).

Fuchs endothelial corneal dystrophy

Fuchs' endothelial corneal dystrophy is the most common form of primary posterior corneal dystrophy and is the most frequent indication for corneal transplantation in the world [230]. This disease is characterised by a progressive loss via apoptosis of corneal endothelial cells and the sub-endothelial formation of extracellular matrix outgrowths, called **guttae**, at the level of Descemet's membrane.

Fuchs' dystrophy affects around 4% of the population and typically occurs in the fourth to fifth decade of life with a higher frequency in women.

Most patients in the early stages of dystrophy are not symptomatic: the presence of centrally located guttae in the cornea may be an incidental finding during a routine ophthalmological examination. Imaging detects a reduction in endothelial cell density, which should be at least 400-500 cells/mm^2 to allow physiological maintenance of function, with abnormalities in cell shape and size. The progression of the pathology leads to an increase in the number of guttae, which become peripheral and confluent, an increase in corneal thickness and a corresponding reduction in corneal function. The reduction in cell density triggers the loss of ion transport activity, causing the corneal endothelium to be unable to maintain an appropriate fluid balance between the stroma and the aqueous humour resulting in oedema and loss of corneal transparency [231].

At this stage, worsening stromal oedema leads to a decline in visual function with blurred vision, especially during the day, due to reduced evaporation of fluid from the corneal surface and a consequent increase in oedema during the night. In the advanced stages, epithelial and sub-epithelial blistering can be observed, the rupture of which can cause pain and tearing, and increased inflammation in the anterior chamber, which can contribute to increased sensitivity to glare. Reduced corneal innervation can lead to neurotrophic keratopathy characterised by erosions, ulcers and corneal scar formation, but this is an uncommon clinical finding in countries with advanced diagnostic, monitoring and treatment techniques [232] [233].

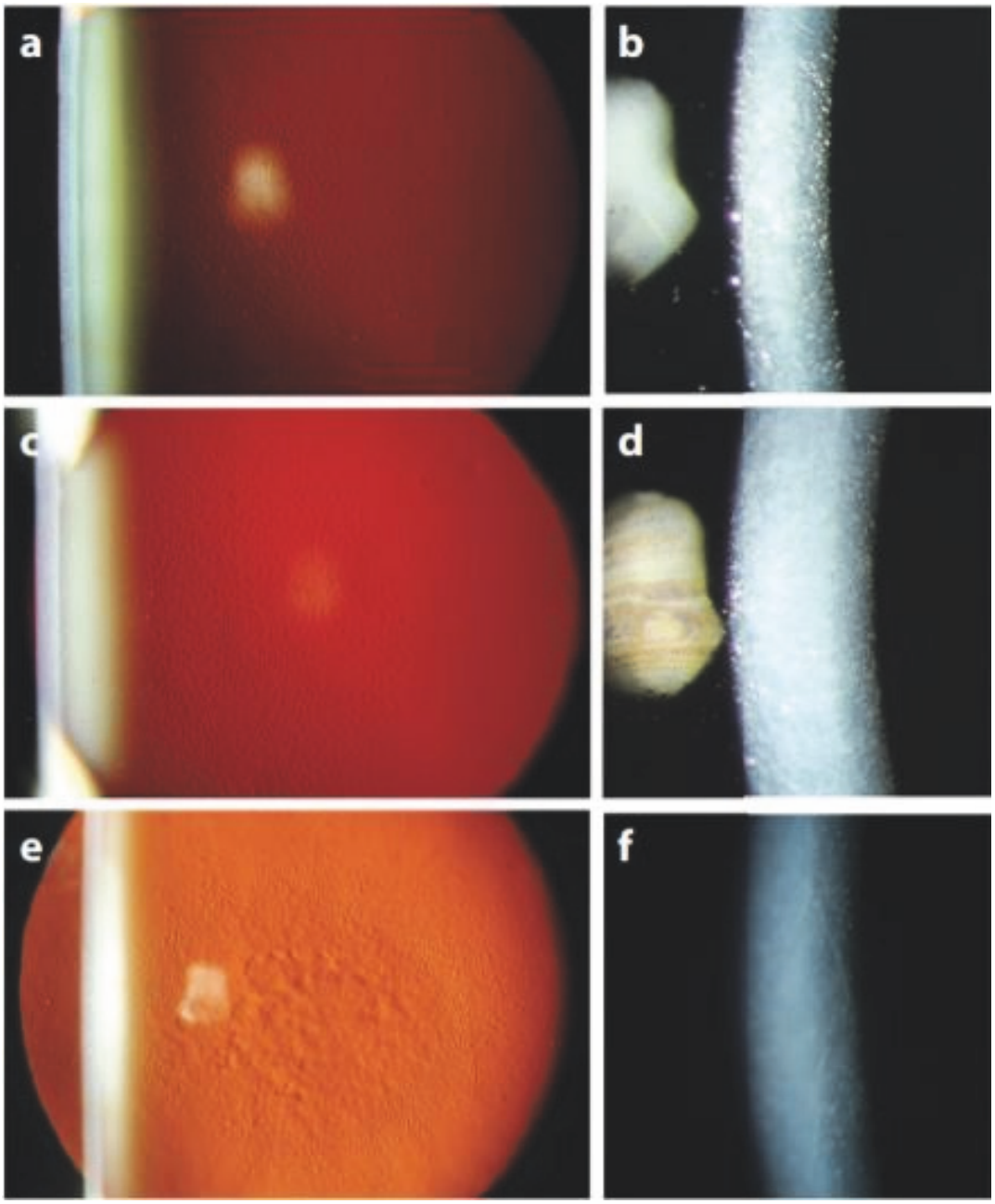

Figure 10. Progression of Fuchs' endothelial corneal dystrophy observed with backlight and slit lamp biomicroscopy. (Matthaei et al., 2019)

(a)(b) Early stage of corneal dystrophy in which central guttae of Descemet's membrane with clear, compact stroma are observed.

(c)(d) As the disease progresses, the appearance of guttae at the periphery and stromal oedema cause loss of transparency of the cornea.

(e)(f) Advanced stage in which epithelial bullae, stromal oedema and corneal haze are present.

Aetiopathogenesis of Fuchs' endothelial corneal dystrophy

From a pathogenetic point of view, Fuchs' dystrophy is a complex multifactorial disease in which the interaction between genetic and environmental factors leads to the activation of processes of cell apoptosis and aberrant deposition of extracellular matrix. Sixteen gene mutations and/or single nucleotide polymorphisms of sporadic or hereditary origin have been identified. The proteins encoded by these altered genes cover a wide range of cellular functions such as DNA damage repair, regulation of the apoptosis process and secretion of the extracellular matrix [234].

Oxidative stress is the major determinant in the pathogenesis of Fuchs' dystrophy and contributes, together with genetic and epigenetic factors, to the progressive degeneration of corneal endothelial cells, the loss of their hexagonal shape and the reduction in their density.

A number of exogenous factors, such as prolonged daily exposure to ultraviolet radiation and pollution, cigarette smoking and diabetes, promote an imbalance between oxidant and antioxidant factors in a genetically predisposed individual, thus increasing oxidative stress [235]. Many studies conducted in recent decades have found an increase in the corneal concentration of ROS and their cytotoxic derivatives, such as advanced glycation products (AGEs) and nitrotyrosine, and other markers of oxidative DNA damage, such as 8-hydroxy-2'-deoxyguanosine (8-OHdG). Oxidative stress leads to an accumulation of non-repairable DNA damage that blocks the proliferative capacity of cells and leads to premature senescence [236] [237].

Analyses carried out using molecular biology methods such as PCR have also demonstrated a transcriptional *down-regulation* of antioxidant factors such as Peroxiredoxin 2,-3,-5 (Prx-2,-3,-5) and Superoxide dismutase (SOD) and of the transcription factor Nrf2, which coordinates the expression of various proteins involved in defence against oxidative stress in the nucleus [238] [239].

The absence of Nrf2 induces perturbations in tissue homeostasis and activates molecular pathways involved in p53-dependent apoptosis in corneal cells [240]. An increased level of oxidatively damaged mitochondrial DNA and *misfolded* proteins found in the vicinity of guttae confirms the association between endothelial apoptosis and macromolecular damage caused by oxidative stress. ROS-induced cell apoptosis is also involved in the activation of NF-κB-mediated proinflammatory signalling pathways [241].

In addition, the intracellular elevation of ROS leads to dysregulation of mitochondrial function and cellular synthetic capacity. Indeed, at the level of the guttae, senescent

corneal endothelial cells have been found to become metabolically active and assume a fibroblastic phenotype, caused by the production of profibrotic mediators such as TGF-β1, which induce the endothelial-mesenchymal transition and the consequent increased subendothelial deposition of extracellular matrix. TGF-β1 is also involved in the initiation of apoptotic processes mediated by 'unfolded protein response' (URP) because it causes an overload of matrix proteins at the endoplasmic reticulum by increasing the formation of *misfolded* proteins. The guttae in turn create a toxic microenvironment around them that propagates the oxidant/antioxidant imbalance underlying the pathogenesis of dystrophy [242] [243].

Uveitis

The term uveitis refers to an inflammatory process affecting exclusively or predominantly the uvea, the middle tunic of the eye, composed of the iris, ciliary body and choroid; in fact, during uveitis, all structures of the eye may be affected.
In industrialised countries, uveitis affects approximately 2 out of every 1,000 people, around 35 % of those affected suffer from severe visual impairment and this disease is the cause of 5 % of cases of legal blindness, mainly due to ocular hypertonia, macular oedema and retinal ischaemia [244] [245].

Classification of uveitis

On the basis of the anamnestic and objective information collected, four different classifications of uveitis have been drawn up to guide the differential diagnosis [246]:

- **Clinical** classification. Based on the time of onset of ocular disease and the clinical course, uveitis can be subdivided into acute, which identifies uveitis with an acute onset and limited duration of less than 3 months, such as HLA-B27-associated anterior uveitis; recurrent, which is characterised by repeated episodes separated by periods of remission lasting more than 3 months without treatment; and chronic, which is of persistent duration of more than 3 months or recurring in a period of less than 3 months after treatment is discontinued.

- **Anatomical** classification. Uveitis is defined as anterior when there is pathological involvement of the anterior segment of the eye and is called iritis

when it involves only the iris and iridocyclitis when it involves the iris and ciliary body; intermediate uveitis involves the posterior part of the ciliary body, the vitreous cavity and the pars plana, the most peripheral portion of the retina; posterior uveitis involves the posterior segment of the eye and depending on the initial localisation one may speak of retinitis, retinochoroiditis, chorioretinitis or neuroretinitis. Panuveitis occurs when the inflammation affects all segments of the eye simultaneously.

- **Aetiological** classification. Infectious uveitis is due to bacterial, viral, fungal and parasitic infections. Infectious agents can enter the eye from the outside

  (exogenous uveitis) or reach it via the blood stream (endogenous uveitis). The Non-infectious uveitis may be related to known systemic or local disease processes, mainly immune-mediated or autoimmune. The systemic diseases most frequently associated with non-infectious uveitis are: HLA-B27 associated uveitis, juvenile idiopathic arthritis, rheumatoid arthritis, inflammatory bowel disease, sarcoidosis, Behçet's disease (BD), psoriasis or tubular-interstitial nephritis (TINU). Approximately 25%-45% of uveitis in Western countries are not related to systemic diseases or to known ocular pathological entities and are therefore defined as

  "idiopathic'.

Pathogenesis of uveitis: the role of inflammation

Uveitis is a complex and heterogeneous group from an etiopathogenetic point of view as many genetic, environmental, comorbidity-related or underlying systemic disease factors play a role in determining its final phenotype.

Under normal physiological conditions, the aqueous humour, the cornea and certain types of immune cells form a natural immune barrier to prevent the invasion of foreign pathogens.

Inflammation in these tissues occurs when trauma occurs, when pathogenic microorganisms enter the ocular structures through a local injury or through the bloodstream, or when autoimmune responses are triggered after exposure to self-antigens. During these events the immune response is stimulated leading to the activation and proliferation of autochthonous immune cells in the eye.

In the pathological process leading to uveitis, a dysregulation of adaptive immunity, which normally represents the first line of defence of the autoimmune system, may develop. In recent decades, ocular dendritic cells have acquired an increasing role in the pathogenesis of uveitis. Dendritic cells are present at the peripheral margins and iuxtapapillary areas of the retina in mouse models, and in the human eye they are normally concentrated in the central corneal and limbal epithelium, the basal lamina and the sub-basal nerve plexus. These cells possess phagocytic abilities and when activated lead to the release of pro-inflammatory cytokines such as TNF-α, IL-12, IL-6. Human and murine dendritic cells express both MHC-II/HLA surface molecules, TLR4 and the receptor complex for LPS to it [247] [248] [249].

Under pathological conditions they behave as antigen presenting cells (APC) and in a mouse model of uveitis, activated ocular dendritic cells were found at the level of the choroid, where they probably lead to the maturation of antigen-specific Th1 and Th17 cells. In addition, in animal models it was observed that many autoimmune cells such as NK cells, serum dendritic cells and $CD4^+$ cells infiltrate inflamed ocular tissues and interact with dendritic cells locally, promoting their mutual maturation. Interaction of ocular dendritic cells with NK cells leads to activation and maturation of both cell types and stimulates the secretion of cytokines such as INF-γ, TNF-α, IL-12, IL-15, 1L-18 [250].

Differentiation of Th17 cells is also stimulated by the presence of IL-1β, IL-6 and TGF-β produced by APC cells. In addition to IL-17, Th17 cells express IL-22, IL-17F, IL-21, GM-CSF, IL-6 and IFN-γ, all of which play important roles in inflammatory processes and autoimmunity.

In experimental models of autoimmune uveitis (EAU), treatment with anti-IL-17 antibody is sufficient to block the development of the disease. In humans, elevated levels of IL-17 have been identified in the eyes of patients with "birthshot" chorioretinopathy (BSCR), "Vogt - Koyanagi - Harada" (VKH) uveitis, HLA-B27 uveitis and Behçet's uveitis. In addition to driving the expression of inflammatory cytokines, IL-17 stimulates the expression of metalloproteases, which are responsible for tissue damage, and chemokines, which attract leukocytes to the inflammatory site [251]. Binding of TNF-α to its receptor TNFR1 triggers the activation of a complex cascade of cellular signals mediated by the TRAF (TNF receptor associated factor) protein: downstream, translocation of NF-κB to the cell nucleus and activation of MAPKs lead to the production of inflammatory mediators. In the

EAU, neutralisation of TNF-α suppresses the disease process and it has been shown that TNFR1-deficient mice are resistant to the development of uveitis [252].

In aqueous humour samples derived from human eyes, high levels of TNF-α in patients with HLA-B27 uveitis, idiopathic uveitis, VKH and Behçet's uveitis [251]. However, the levels of this cytokine in ocular fluids do not seem to reflect the degree of disease activity and do not correlate with the efficacy of systemic treatment with Adalimumab. Adalimumab is a humanised IgG monoclonal antibody that acts by inhibiting TNF-α and has been shown to be effective for the treatment of non-infectious intermediate, posterior and panuveitis uveitis, especially in adult patients who have had an inadequate response to corticosteroids or are intolerant to corticosteroid therapy [253] [252]. Several experimental studies in EAU models have demonstrated the importance of IL-6 in the pathogenesis of non-infectious uveitis. In an animal model of T-cell-mediated uveitis with IRBP-induced immunisation, researchers demonstrated that in IL-6-deficient mice, the absence of the cytokine resulted in a lack of stimulation of Th17 cells. On the other hand, systemic or intravitreal administration of anti-IL-6 receptor antibodies reduced the degree of inflammation in the uveitic process. This effect in EAU models appears to occur by suppressing the differentiation of both Th1 and Th17 cells, both of which are essential in the development of this animal model of uveitis [254] [255]. High levels of IL-6 are present in the aqueous humour of patients with uveitis, such as in uveitis caused by *Toxoplasma gondii*, in Fuchs' heterochromic cyclitis and in some forms of non-infectious uveitis, including Behçet's disease, VKH uveitis, sarcoidosis, idiopathic uveitis, acute retinal necrosis and HLA-B27 uveitis. In addition, IL-6 plays an important role in the development of ocular complications resulting from the uveitic process such as neovascularisation and macular oedema [256].

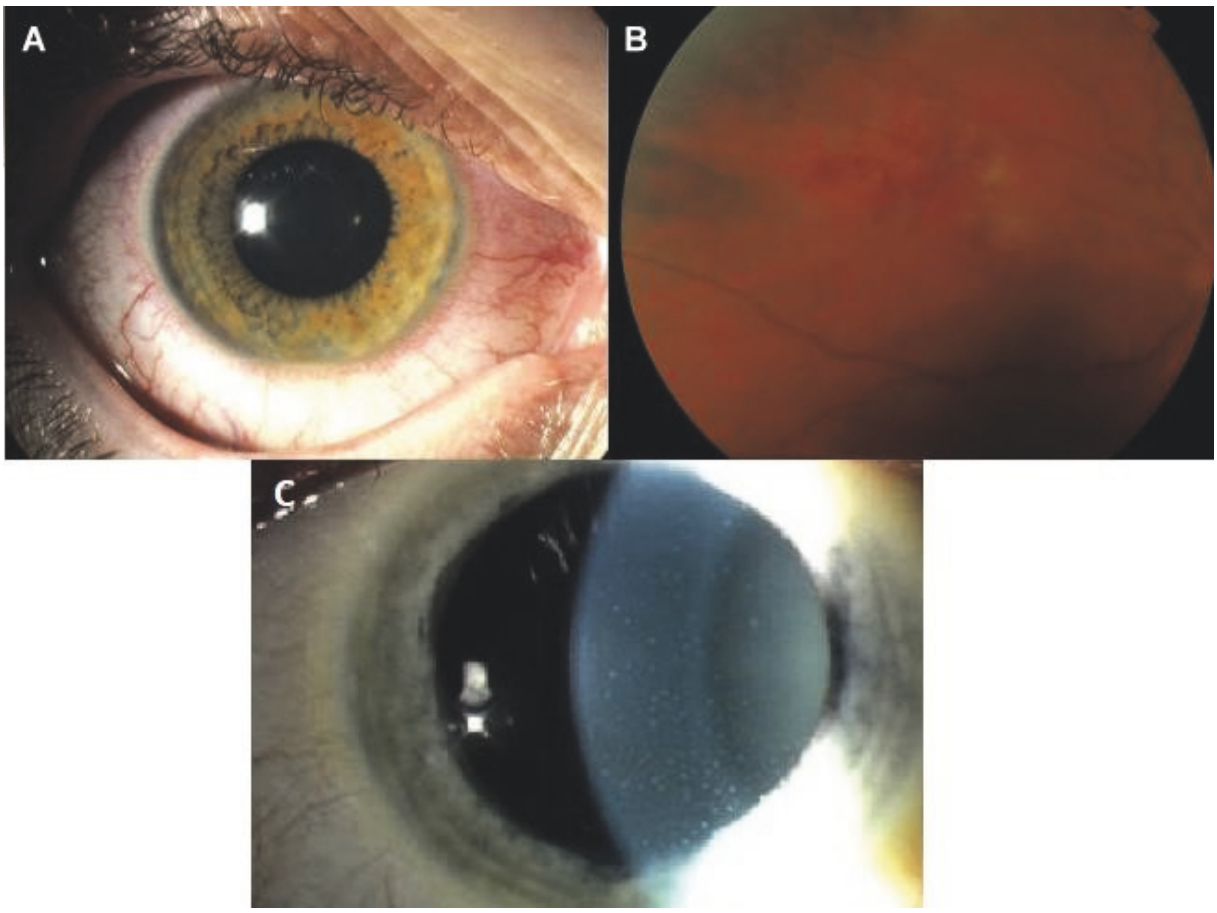

Figure 11. (A) Uveitis in Behçet's disease. Red eye with collection of white fluid in the anterior chamber of the eye, called hypopyon. (B) Uveitis in Behçet's disease. Area of ischaemia and retinal inflammation causing retinitis (in white) and haemorrhages (in red). (C) Uveitis in Fuchs' heterochromic cyclitis. Presence of typical keratic precipitates in the posterior portion of the cornea. (Kenneth et al., 2006)

A further study showed that VEGF and TNF-α factors, as well as IL-1β, can contribute to blood-retinal barrier breakdown in both experimental models of autoimmune uveitis and in patients with uveitis, probably by inducing the opening of *tight junctions* and increasing vesicular transport within endothelial cells. In contrast, IL-1β-blocking molecules inhibit the development of uveitis experimentally [257]. Many studies have linked the role of $CD4^+$ T cells to the pathogenesis of autoimmune uveitis, but this is actually a rather rare occurrence because, on the one hand, the thymus normally eliminates self-reactive $CD4^+$ T clones that form during cell development, while on the other hand the formation of T cells reacting against self antigens depends on the interaction of genetic predisposition factors with environmental factors. Regardless of the type of antigen they react against, whether self or external, $CD4^+$ T cells involved in uveitis development are activated by antigen-presenting cells, such as ocular dendritic cells or macrophages, that possess

antigenic peptides on the outer side of the membrane as part of major histocompatibility complex type II (MHC II) molecules. Once activated, they can differentiate into Th1 and Th2 cells. Several animal models of anterior and posterior uveitis have shown a prevalence of Th1-$CD4^+$ cells, which have a key role in triggering the inflammatory cascade. Their activation stimulates the secretion of IL-2 and consequently of other pro-inflammatory cytokines such as INF-γ and TNF-α, which have been found in the ocular fluids and peripheral circulation of patients with uveitis. Once these cells are active in the injured tissue, the inflammatory process is maintained through the production of chemokines and cytokines, including from local cells such as those of the retinal pigment epithelium. It has also been shown that, during inflammation, retinal pigment epithelium and choroid endothelium cells expose adhesion factors such as ICAM-1, VCAM-1 and ELAM-1, leading to adhesion and extravasation of leukocytes in the eye and subsequent immune-mediated tissue damage [258].

Macular Pucker or Epiretinal Membrane

Epiretinal membrane or macular pucker is a relatively common macular pathological condition characterised by the formation of a thin fibrocellular membrane along the surface of the inner limiting membrane of the retina. It may manifest ophthalmoscopically as a translucent membrane, which may wrinkle, leading to deformation and progressive distortion of the macula, or cell proliferation and scar tissue formation may exert traction on the retina and lead to detachment causing impairment of central vision. The visual deficit can be very variable, ranging from none to severe with a very slow period of evolution. One of the main symptoms is metamorphopias, i.e. distorted images, but blurred vision up to loss of detail may also be present.

Epiretinal membrane usually develops after the age of 50 and is more common among people aged > 75.

In most cases, epiretinal membrane develops in an eye with no history of ocular disease and is therefore termed 'idiopathic', while a smaller proportion of patients develop pucker due to ocular inflammatory disease, retinal detachments, trauma and retinal vascular disease [259] [166]. It is usually preceded by vitreoschisis and posterior vitreous detachment (DPV); by tangentially stretching the retina it can cause macular hole.

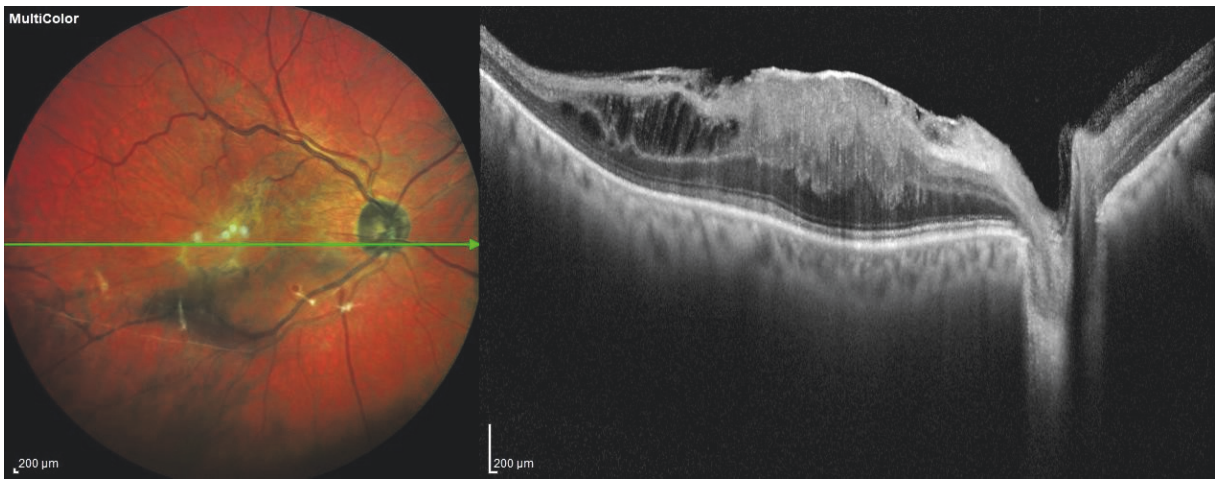

Figure 12. Fundus oculi (left) and OCT (right) of macular pucker. (O.U. Ophthalmology Clinic,

A.O.U. Sant'Anna of Ferrara, Prof. P. Perri)

Pathogenesis

For the pathogenetic mechanisms underlying the development of the idiopathic form of epiretinal membrane, a number of theories have been written concerning both the functions of multiple cell types such as glial cells, retinal pigment epithelium cells, fibroblasts and hyalocytes, and the role of cytokines and growth factors. Studies have shown that the predominant cell types in macular pucker samples are Müller cells and hyalocytes and that immunohistochemical investigations of surgically removed membrane samples show strong positivity for GFAP, CD68, CD163, vimentin and CRALBP protein, indicating the presence of glial cells and hyalocytes [260]. A study using *real time PCR* genetic analysis of vitreous samples from patients with epiretinal membranes showed increased expression of genes coding for IL-6, TGF-β2, VEGF-A, CXCL1, GFAP, RELA and tenascin C (TNC) compared to controls [261].

RELA is a subunit of the nuclear transcription factor NF-κB, which is activated by many stimuli including hypoxia and the pro-inflammatory cytokines IL-1β and TNF-α. NF-κB and the pro-angiogenic factor IL-8 are expressed in glial and endothelial cells and their expression has been associated with epiretinal membrane formation in later life [262].

TGF-β2 is a growth factor that is elevated in the vitreous humour of patients with macular pucker and in its presence hyalocytes trans-differentiate into myofibroblasts, showing immunopositivity to the α-SMA (α-smooth muscle actin) contractile protein, suggesting a role in the contractions that the epiretinal membrane generates at the vitreoretinal interface [263].

IL-6 is a pro-inflammatory cytokine reported to be involved in the activation of Müller cells by stimulation by microglia and epiretinal membrane formation in eyes with proliferating diabetic retinopathy and vitreoretinal proliferation, while the factor CXCL-1 may be associated with the pathogenesis of macular pucker due to its role in inflammatory, angiogenetic and wound repair processes [264] [265].

The hypothesis suggested by the above study is that in a TGF-β2-rich environment, the ageing of ocular structures and the destructuring of the vitreous humour accompanied by possible posterior vitreous detachment could stimulate the expression of RELA-NF-κB, IL-6 and CXCLI. Consequently, NF-κB stimulates glial cells to produce VEGF-A, which together with tenascin-C, promotes endothelial growth and, via CXCL1, stimulates glial cell proliferation. The increased production by glial cells and astrocytes of GFAP leads to a process of progressive fibrosis that characterises the formation of the epiretinal membrane.

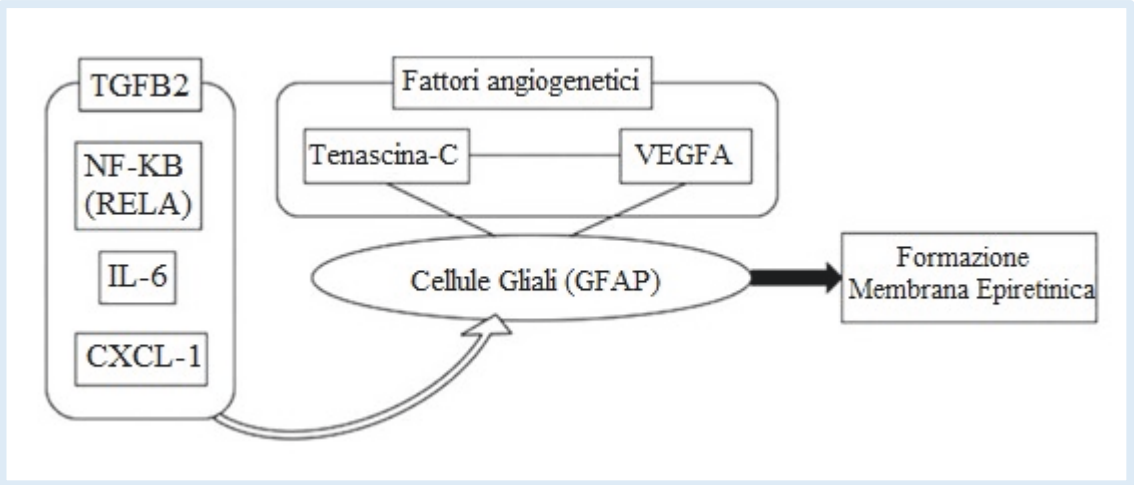

Figure 13. Illustrative diagram of the relationship between different factors whose genes have been found upregulated in eyes with idiopathic epiretinal membrane.

CHAPTER 3: PURPOSE OF THE STUDY

This interventional observational study aims to:

- Check for the presence of the soluble form of the purinergic P2X7 receptor (sP2X7R) in aqueous humour and vitreous humour.
- To compare the levels of sP2X7R in healthy conditions and in the presence of different ocular pathological conditions underlying an inflammatory pathogenesis, such as: glaucoma, uveitis, Fuchs' endothelial dystrophy, pseudoexfoliation (PEX), diabetic retinopathy, myopia, age-related macular degeneration and retinal detachment.
- Compare the levels of sP2X7R in aqueous humour and vitreous humour with those in serum.

These diseases of ophthalmological interest, which can lead to a significant reduction in visual function up to and including blindness, are determined or complicated by altered inflammatory processes. Therefore, the identification and measurement of the soluble form of this receptor in aqueous humour and vitreous humour could indicate an involvement of sP2X7R in processes leading to the development of serious eye diseases and designate sP2X7R as a marker of the ocular inflammatory state.
This evidence could be a prerequisite for targeted therapy.

Inhibition of the activity of this receptor, supported by the current availability of various pharmacological inhibitors of the P2X7 receptor.

CHAPTER 4: MATERIALS AND METHODS

Study groups

The patients involved in the study are those who underwent eye surgery at the Ophthalmic Clinic Unit of the Sant'Anna Hospital of Ferrara, from March 2019 to May 2022.
From February to September 2020, sample collection was suspended due to the shutdoown of the surgical activity caused by the Sars-COV 2 pandemic.
The cohort of patients was divided into 2 groups with the following inclusion and exclusion criteria:
Group 1 - inclusion criteria:

- Patients with different eye diseases who are scheduled to undergo cataract extraction by phacoemulsification procedure
- Patients with proliferating diabetic retinopathy, trauma, vitreal haemorrhage, retinal detachment with vitreoretinal proliferation who must undergo vitrectomy procedure
- Both sexes
- Age>18 years
- Patients giving consent for participation in the study.

Group 2 - inclusion criteria:

- Patients undergoing cataract extraction surgery in the absence of other eye diseases
- Patients undergoing vitrectomy for hole or macular pucker
- Both sexes
- Age>18 years
- Patients giving consent for participation in the study.

Refusal to participate in the study was considered as the only exclusion criterion for both groups.

Informed consent

Candidate patients were selected based on the above-mentioned inclusion criteria, taking into account the specific ocular pathological conditions under investigation in the study at the time of the scheduled eye surgery at the Ophthalmic Clinic Unit of the Sant'Anna Hospital of Ferrara. After being informed about the procedures and the aims of the study, informed consent was collected, in accordance with the Declaration of Helsinki and the indications of the Ethics Committee for Biomedical Research (Comitato Etico di Area Vasta Emilia Centro della Regione Emilia-Romagna (CE-AVEC); ethical committee ID number: *461/2019/Oss/AOUFe*).

Sample collection and storage procedures

Collection and preparation of aqueous and vitreous humour samples at the Ophthalmic Clinic of the A.O.U. Sant'Anna of Ferrara:

- Aqueous humour samples were obtained by collection after paracentesis to access the anterior chamber of the eye during cataract extraction surgery or "closed-bulb" in the case of other procedures such as vitrectomy. This method of collection carried out early in the procedure prevents contamination of the sample with fluids and viscoelastic materials, used during surgery.

  Limitation of the sampling procedure:

  It is important at this point to emphasise the difficulties and limitations of the extracting procedure of the aqueous humour from the anterior chamber.

  The anterior chamber is the aqueous humor-filled space inside the eye between the iris (posteriorly) and the cornea's innermost surface, the endothelium (anteriorly). The depth of the anterior chamber of the eye varies between 1.5 and 4.0 mm, averaging 3.0 mm. Its volume is about 250 microlitres (i.e. 0.25 ml) and aqueous humour is constantly produced by the ciliary bodies at a rate of approximately 2 μL/min within the anterior cavity.

  Extracting the aqueous humour from the anterior chamber logically reduces its depth, which is why the maximum amount that can be taken is around 0.1 to 0.2 ml, depending on the anatomical features and any ocular pathology present, so that the anterior chamber is not excessively deflated and the surgical procedure can then be continued safely. Most of the samples taken therefore have a volume of 0.05 ml. (min 0.05 ml, max 0.5 ml).

Of 210 patients screened for the study and who accepted and signed the informed consent to participate, 206 samples were taken during the intervention (4 samples were not sufficient for collection). Of these, 168 samples were collected in sufficient quantity for the analysis procedure to be carried out.

Minimum quantity of sample indicated per sampling: 0.05 ml.

Total number of samples collected: 206 samples

- Vitreous humour samples were obtained by sampling collected during minimally invasive 23-25 Gauge vitrectomy surgery. After placement of the 3 trocars to access the vitreous chamber, with the infusion line closed in order to avoid dilution of the sample, a 1 ml syringe was connected to the aspiration line, disconnected from the cutter to allow manual aspiration, the cutting speed was reduced to approximately 1000 cycles/min.

  The vitreous chamber contains the vitreous body and the average chamber volume is between of 4 to 4.4 mm^3. Therefore, vitreous humor samples of approximately 2–3 ml can be safely collected from each eye. As the volume of the vitreous chamber is larger, the amount of material that can be taken is thus higher (min 0.2 ml, max 2 ml).

  The limitation to the collection of material stems from the relatively lower frequency of these pathologies (compared to cataracts), so there are fewer interventions in clinical practice.

  Of 50 patients who were screened for the study and accepted and signed the informed consent to participate, 48 samples were collected during the intervention and subsequently analysed. Only 2 samples were insufficient for collection.

  Minimum quantity of sample indicated per sampling: 1 ml.

  Total number of samples collected: 48 samples.

- The biological fluids collected and catalogued, placed in special test tubes, were sent to the Chemical-Clinical Analysis Laboratory of the A.O.U. Sant'Anna of Ferrara and frozen at -80°C for preservation until use.

<u>Collection and preparation of serum samples at the Ophthalmology Clinic of the A.O.U. Sant'Anna in Ferrara:</u>

- Each of these patients was given a venous blood sample using tubes without anticoagulant before undergoing eye surgery. The venous blood sample was taken

from a peripheral venous access, which is placed in all patients attending the operating room, as a safety procedure for possible anaesthesia care during surgery.

- The test tubes were sent to the Laboratory for Chemical-Clinical Analysis of the A.O.U. Sant'Anna in Ferrara where the serum was separated by centrifugation at 300 rpm for 15 min at 4°C and divided into aliquots that were frozen at -80°C to preserve them until use.

Total number of samples collected: 210 total samples collected and analysed.

Sample analysis and measurement of sP2X7R concentration

The concentration of soluble P2X7R (sP2X7R) in vitreous humour, aqueous humour and serum samples was measured using the human P2X7 ELISA kit (Cusabio, Texas, USA) at the Experimental Medicine section of the Department of Medical Sciences, University of Ferrara.

ELISA is a quantitative enzyme immunoassay used to detect the presence of a substance using several antibodies to one of which an enzyme is bound. In the direct method, or variant

The "sandwich" wells used in this specific kit contain an antibody specific for the antigen being measured. The plasma/serum, aqueous humour or vitreous humour sample containing the antigen being tested is then added to the well, followed by a second antibody bound to a biotin molecule directed against the antigen bound to the first antibody. Next, a biotin-binding avidin solution is added, which is conjugated to a horseradish peroxidase (HRP). The peroxidase converts a specific substrate (TMB) into a coloured product that will highlight the well in which the antigen of interest is present.

The procedure began with the preparation of the **reagents**, which were brought to room temperature (18°C-25°C) before use. The tube containing the biotinylated antibody was centrifuged before opening and then serial dilution of 10 µL of 100x antibody with 990 µL of diluent was performed. The tube containing avidin-HRP reagent was centrifuged before opening and then 10 µL of 100x avidin-HRP was diluted with 990 µL of diluent. Wash buffer was prepared by bringing to room temperature and shaking the solution to dissolve any crystals present and then diluting 20 mL of 25x concentrated buffer in 480 mL distilled $_2$HO to obtain 500 mL of 1x wash buffer. The standard antigen solution was

prepared by centrifuging the tube at 6000-10000 rpm and the contents reconstituted with 1 ml of sample specific diluent to obtain the stock solution of 1600 pg/ml. The tube was kept in agitation for at least 15 minutes before dilutions were made. 250 µL of diluent was inserted into each tube and 2x dilutions were made from the stock solution, taking care to mix each tube well before subsequent transfer. The undiluted standard solution acts as a high concentration standard (1600 pg/ml) while the diluent alone acts as a zero standard (0 pg/ml).

This was followed by the preparation of the **samples** for testing. Samples were brought to room temperature and centrifuged. 100 µL of standard solution or 100 µL of sample was added to each well of the 96-well plate. The plate was then covered with an adhesive strip and incubated at 37°C for 2 hours. At the end, the contents of the wells were removed without rinsing and 100 µL of 1x biotinylated antibody was added to each well, the plate was covered with adhesive strip and incubated for 1 hour at 37°C. At the end of the incubation, 3 washes were performed with 200 µL of wash buffer each. After the last wash, the plate was inverted on absorbent paper for a few minutes to remove any residual buffer. 100 µL of 1x avidin-HRP was then added to each well, the plate was covered and left to incubate for 1 hour at 37°C. The washing procedure was then repeated 5 times. 90 µL of TMB substrate was added to each well. The plate was then incubated for 15-30 min at 37°C in the dark. At the end of the incubation, 50 µL of stop solution was added to each well.

Finally, the **optical density of** each individual well was determined at 450nm using a Multiskan FC spectrophotometer (Thermo Scientific), within 5 minutes of the addition of the stop solution. The tests were performed in duplicate and the antigen concentration for each well was calculated by reference to the standard curve.

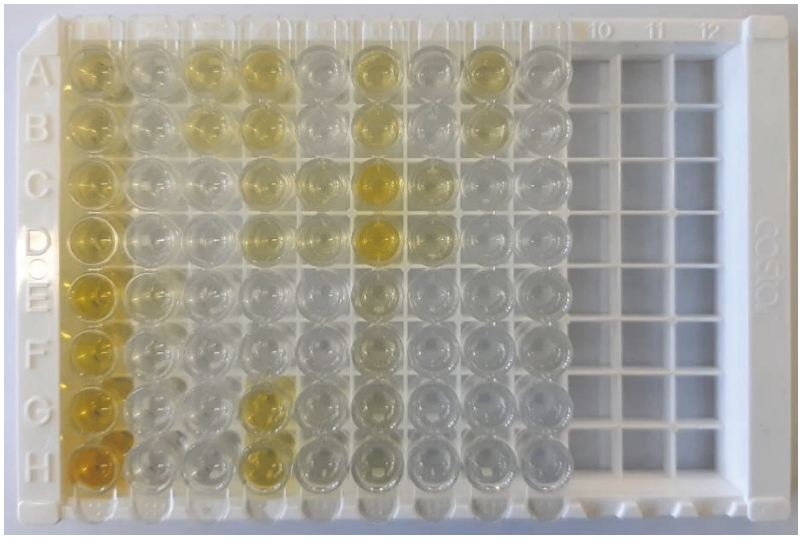

Figure 14. ELISA plate when reading the optical densities (OD) of the wells.

ELISA sP2X7R 17/06/2020

pg/ml	OD
0	0,073
12,5	0,116
25	0,152
50	0,285
100	0,367
200	0,758
400	1,298
800	2,199

x=(y-0,1234)/0,0027

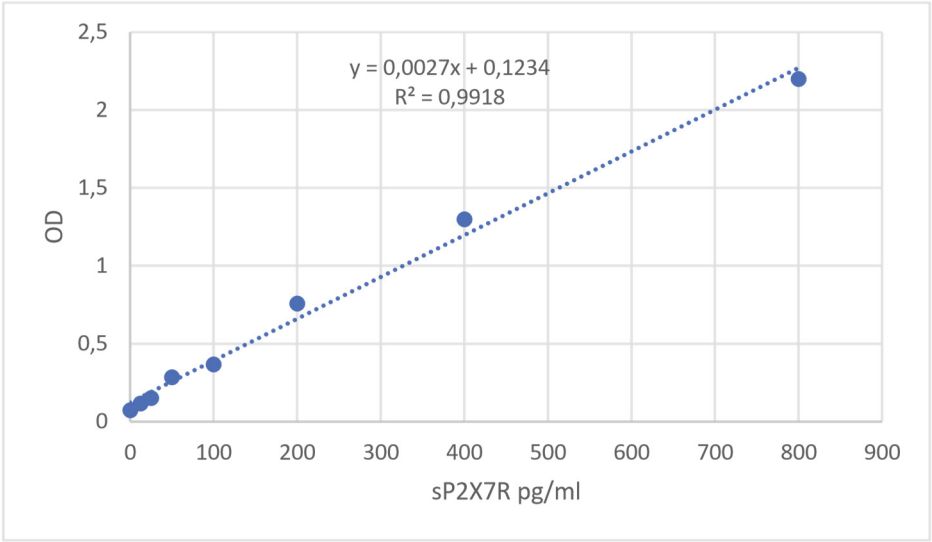

Figure 15. Table with the values of the concentrations of the sP2X7R standard solution (pg/ml) and the corresponding optical densities (OD). Graph obtained from concentrations and OD of sP2X7R standard solution. In red, equation to derive the analyte concentrations knowing the OD of the sample examined.

Analysis of population characteristics and statistical analysis

The analysis of population characteristics and statistical analysis were conducted using Graph Pad for Windows and Excel.

For the numerical variables, Student's t-test was used and the chosen significance level is 0.05; for the categorical variables, Fisher's exact test was used, reporting absolute frequencies and percentages.

For the analysis of non-parametric variables, the Kruskal-Wallis test was used [1]. Dunn's test is a continuation (post-hoc test) of the Kruskal-Wallis test on the comparison of ordered and ranked groups and takes into account Bonferroni's correction for multiple comparisons. For an explanation of the Dunn test and the non-parametric tests used in the report see "Alboukadel Kassambara. Package rstatix. Pipe-Friendly Framework for Basic Statistical Tests. CRAN November, 22". https://cran.r-project.org/web/packages/rstatix/rstatix.pdf.

All statistical analyses were performed in the R environment[2] .

[1] Kruskal, William H., and W. Allen Wallis. "Use of ranks in one-criterion variance analysis." Journal of the American statistical Association 47.260 (1952): 583-621

[2] R Core Team (2022). R: A language and environment for statistical computing. R Foundation for Statistical Computing, Vienna, Austria. URL https://www.R-project.org/.

CHAPTER 5: RESULTS

Population characteristics

The analysis of the demographic characteristics of the patients enrolled has already been assessed in a preliminary analysis, subject of a dissertation discussed in the academic year 2019-2020[3], in order to refine the sampling technique and preparation and the sample analisys. We therefore report those partial data in relation to demographic characteristics.

In order to analyse the characteristics of the test population, the samples collected were classified into two groups: the control group and the pathological group, consisting of all the aqueous and vitreous samples evaluated for each group.

The average age of the control group is 72.7 ± 10.8 years, while the pathological group has a mean age of 73.9 ± 12 years. The difference between the means of the groups was not statistically significant (P>0.74, Student's t-test).

In the control group (17 in total) there were 9 males (52.94%) and 8 females (47.06%). In the pathological group (23 in total) there were 13 males (56.52%) and 10 females (43.48%). The difference in sex distribution between the two groups was not statistically significant (P>0.99, Fischer's exact test).

With regard to laterality, the right eye was sampled in 7 cases (41.18%) in the control group and in 12 cases (52.17%) in the pathological group. While the eye affected by the sampling was the left one in 10 cases (58.82%) in the control group and in 11 cases (47.83%) in the pathological group. Also for this parameter the difference was not statistically significant (P>0.53, Fischer's exact test).

Finally, the presence of systemic comorbidities in the patients of the two groups was assessed: these were found in about 11 cases in the control group (64.71%) and in 13 cases in the pathological group (56.52%). The difference was not statistically significant, with a P value of 0.74 (Fischer's exact test).

From what has been analysed, it can be seen that the two populations under consideration have homogeneous characteristics.

[3] Grad Student: Alessandra Marrocco
Rapporteur: Prof Paolo Perri Co-rapporteur: Dr Carla Enrica Gallenga
"Determinazione della forma solubile del recettore P2X7 in umor acqueo, umor vitreo e siero in condizioni normali e patologiche: sP2X7R come indicatore dello stato infiammatorio oculare"

Table 6. Summary of population characteristics.

	Group of controls (tot. n 17)	Pathological group (tot. n 23)	P value (<0.05)
Age (years)	72,7 ± 10,8	73,9 ± 12	P>0,74
M-F (%)	9 - 8 (52,94% - 47,06%)	13 - 10 (56,52% - 43,48%).	P> 0,99
OD-OS (%)	7 - 10 (41,18% - 58,82%)	12 -11 (52,17% - 47,83%)	P> 0,53
Systemic Comorbidities	11 (64,71%)	13 (56,52%).	P> 0,74

Analysis of sP2X7R concentrations in aqueous humour

The datasets describing the aqueous humour and vitreous humour samples are given in Appendix A e B, each table has 16 columns and the same number of rows as the aqueous humour and vitreous humour samples taken, respectively. The measured value of the P2X7r receptor is reported in column 14 (P2X7r_pg_ml) in pg/ml. Columns 1-7 identify the subject who participated in the study with ID, date of birth, age, sex, right or left eye (OD/OS), type and date of surgery; columns 8-10 describe the sample indicating whether it was aqueous or vitreous humour, the total volume taken and the number of samples used for analysis. Columns 11-13 were reserved for the indication of the subject's primary pathology, secondary ocular pathology and any systemic pathology. Column 14 provides the measurement of the P2X7r receptor concentration in the sample taken, column 15 the results of any subsequent tests on the same sample, and column 16 the average of the values obtained.

The subjects from whom an aqueous humour sample was taken total 206 and the subjects from whom a vitreous humour sample was taken total 48.

In view of the significant difference between the subjects for whom a sample of a limiting volume for analysis (0.05 ml) was collected - especially for the aqueous humour samples - we decided to carry out a preliminary analysis to compare the distribution of P2X7r values in samples of different volumes.

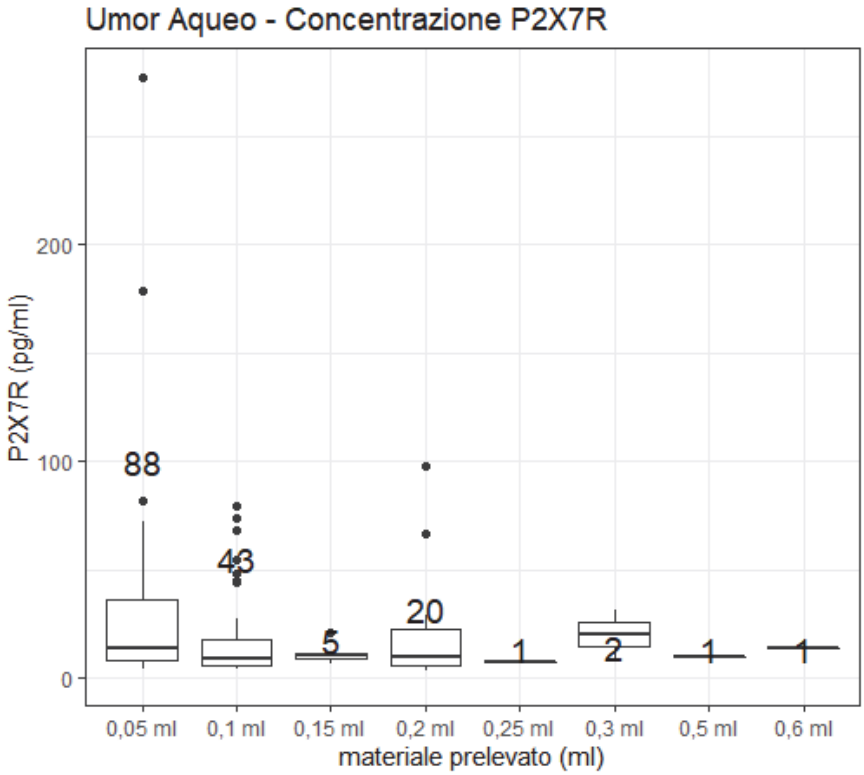

Figure 16. Box-plot of P2X7r concentration values (pg/ml) detected in aqueous humour samples

Figure 16 shows, in box-whisker plot form, the distribution of P2X7r values (pg/ml) detected in samples extracted from aqueous humour. The numbers associated with each box plot show that of the 161 values available, approximately 55% are from a sample volume of 0.05 ml and 27% and 12% respectively are samples with volumes of 0.1ml and 0.2ml; samples with volumes of 0.15ml and above 0.2ml are reduced to a few. The presence of very high outliers in the 0.05ml category makes the graph difficult to read, but it seems clear that in the most representative categories (0.05ml, 0.1ml and 0.2ml), the distribution of values is asymmetrical towards high values. As there was no reason related to the sampling technique to exclude the outliers highlighted for the 0.05 ml category, it was decided to preserve those subjects for whom a value above 100 pg/ml was observed. In the description of the sample, we will mainly refer to these three categories. On visual inspection the median value of the 0.1ml and 0.2ml groups appears to be of equal value, whereas the median value of the 0.05 group appears to be higher. For the completeness of the description we have shown in Table 7 the percentile values of each category of 'material taken' for the percentile values between the minimum value (0%) and the maximum value (100%) where next to the quartiles (25%, 50% and 75%) the percentiles 10% and 90% are taken. For the sampling categories with only one case, the percentile

values are the same and for the other categories, the median value was chosen as the representative value for the group. The 50% column of Table 7 shows that for the groups with a significant number of subjects (0.05ml, 0.1ml, 0.15 and 0.2ml) the median value is between 9 and 13 pg/ml and the Kruskal-Wallis chi-square test (chi-squared = 7.6279, df = 7, p-value = 0.3665) shows that the differences observed in do not depend on the available sample volume and the limitations of the sampling technique.

Table 7. Percentiles of the distribution of P2X7 values (pg/ml) detected in the aqueous humour samples.

Materiale Prelevato	Soggetti	Media	0%	10%	25%	50%	75%	90%	100%
0,05 ml	88	26.77	3.90	5.54	7.67	13.32	36.17	64.49	277.05
0,1 ml	43	17.57	3.90	4.29	5.93	8.68	17.31	47.18	79.24
0,15 ml	5	11.46	6.27	7.22	8.64	10.06	11.09	17.18	21.23
0,2 ml	20	18.95	3.56	4.51	5.51	9.69	22.29	32.78	97.43
0,25 ml	1	7.31	7.31	7.31	7.31	7.31	7.31	7.31	7.31
0,3 ml	2	20.23	8.98	11.23	14.61	20.23	25.85	29.22	31.47
0,5 ml	1	9.89	9.89	9.89	9.89	9.89	9.89	9.89	9.89
0,6 ml	1	13.40	13.40	13.40	13.40	13.40	13.40	13.40	13.40

The subjects for whom aqueous humour was taken were separated into healthy patients (control sample) and patients with disease (pathology samples), as depicted in Appendix B and listed in Table 8. Appendix B lists the patients for whom the appropriate attribute was assigned in the 'control/pathology' column; the number of patients belonging to the control group and the groups associated with the individual diseases is listed in Table 8, where the acronym used for the analysis is also indicated. Some non-specific pathologies causing a possible inflammatory state are indicated by the acronym MISC; these grouped pathologies account for approximately 0.018% of the sample examined. In this table not analysed samples are yet removed respect to the bulch collection.

Column M in Appendix B shows the P2X7r concentration values detected in the serum of the patients for whom an aqueous humour sample was taken. For a significant proportion of patients (approximately 60%), P2X7r could be detected in both samples, aqueous humour and plasma serum.

Table 8 Groups characteristics: description of the different groups, number of patients enrolled and sampled in each group, percentage of total.

Group definition	N of patients	%	details
CONT	69	0,411	No concomitant ocular pathology
G	17	0,101	Glaucoma
E	17	0,101	Endothelial dystrophy (Fuch's disease, guttae, low endotelial count)
M	16	0,095	Myopia
RDP	11	0,065	Proliferative diabetic retinopathy
DDRR	11	0,065	Regmatogenous retinal detachment
AMD	10	0,060	Age related macular degeneration, atrophic and/or exudative
PEX	7	0,042	Pseudoexfoliative syndrome
MP	5	0,030	Macular pucker
MISC	3	0,018	Miscellaneous (pathologies with inflammatory activation)
OVR	2	0,012	Retinal vascular occlusion
Tot	168	1	

The P2X7r values measured in the subjects belonging to the controls category (CONT) and the categories representing the pathologies listed in Table 8 are represented in the box-whisker plot in Figure 17 and are summarised in Table 9, where the mean value and percentiles between the minimum value (0%) and the maximum value (100%) are indicated; the 50% percentile or median of P2X7r is the reference value used to compare the controls and pathologies groups.

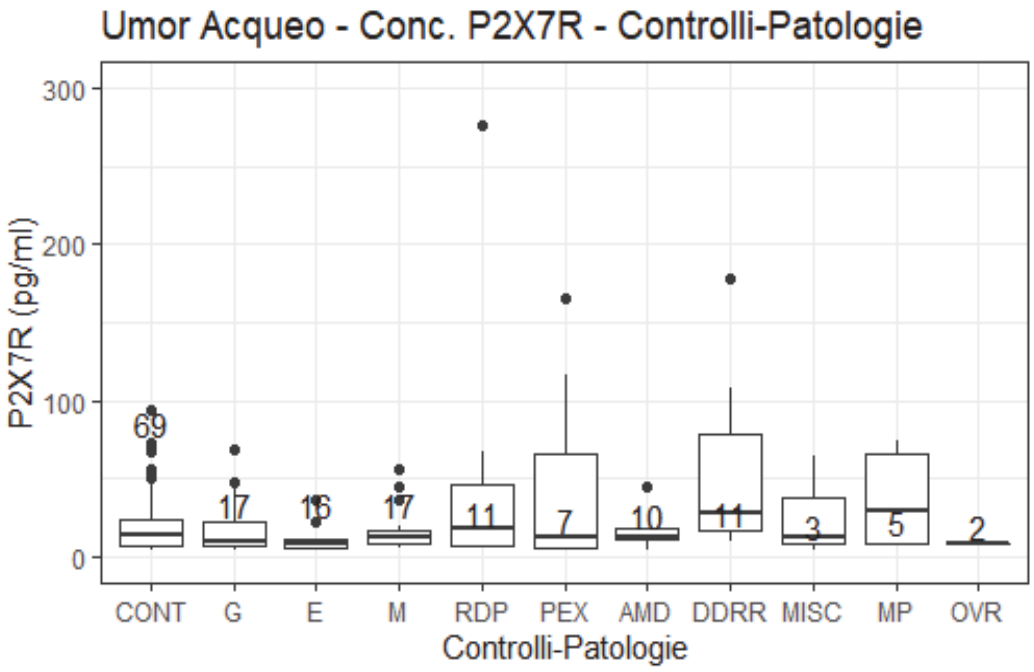

Figure 27. Box-plot of P2X7r concentration values (pg/ml) found in the Control (CONT) and disease groups in acqueous humour

Table 9. Percentiles of the distribution of P2X7r values (pg/ml) detected in aqueous humour samples

Group definition	N of pz	media	0%	10%	25%	50%	75%	100%
CONT	69	21,35	3,9	5,25	7,31	13,4	23,77	93,88
G	17	18,37	4,22	4,74	6,14	9,32	21,78	67,91
M	17	17,19	5,93	7,3	8,34	11,7	16,26	55,92
E	16	11,55	3,9	3,9	5,59	7,38	11,37	36,69
RDP	11	47,01	5,25	5,93	7,31	17,99	46,37	277,05
DDRR	11	53,4	10,06	12,04	16,63	27,05	78,23	178,69
AMD	10	17,67	3,9	3,95	10,87	12,12	17,58	44,68
PEX	7	46,08	3,9	4,71	5,25	12,81	65,08	165,21
MP	5	37,12	7,97	8,24	8,64	29,05	65,86	74,09
MISC	3	26,5	3,56	5,26	7,8	12,04	37,97	63,9
OVR	2	8,07	7,31	7,46	7,69	8,07	8,45	8,83

From the graph in Figure 17, it is evident that for each group, the distribution of P2X7r values is asymmetrical towards high concentration values. In 8 of the 11 groups shown in Figure 17, outliers are evident (dots indicate the outliers). The control group (CONT) shows outliers of values approximately equal to and above the 90% percentile (53 pg/ml) shown in Table 9. The highest value outliers belong to the DDRR, PEX and RDP categories and are well above the maximum value of CONT (94 pg/ml). The graph and the values in Table 9 show that the 75 per centile of the DDRR, PEX and RDP categories have values greater than the 3rd quartile of CONT (24 pg/ml), indicating that, even with a limited number of observations, the P2X7r concentration for these diseases (108, 65 and 46 pg/ml respectively) tends to be greater than the receptor concentration values in the control group. Other pathologies such as Macular Pucker, AMD and the pathologies enclosed in the MISC category show values that are 75% higher than the control group, while other pathologies such as myopia (M) and glaucoma (G) the 3rd quartile (75%) have values similar to or lower than the control value. The Kruskal-Wallis Chi-squared on the equality of the medians of the groups listed in Figure 17 and Table 9 (Kruskal-Wallis chi-squared = 18.254, df = 10, p-value = 0.05082) estimates a p-value slightly above the test reliability limit (p=0.05), confirming that the median value of the P2X7r concentration measured in the groups listed in Table 8 is not the same.

Table 10. Kruskal-Wallis chi-squared test result

concentrazione	n	statistic	df	p-value	method	alpha
p2x7r_pg_ml	168	18,3	10	0,0508	Kruskal-Wallis	0,05

Table 11 shows the paired hypothesis testing between controls and each disease group. The Dunn-test between the paired groups allows to control the type of correction to be introduced to account for repeated testing.

We ran the test twice. Firstly, the Dunn-test was run with no correction and the test results indicate a significance ($p < 0.05$) between the P2X7r values found in the endothelial dystrophy group and the rhegmatogenous retinal detachment group compared to the control. Secondly we decided to apply the Bonferroni's correction factor to to counteract the multiple comparisons problem.

Table 11. Dunn-test with no correction

concentrazione	group1	group2	n1	n2	statistic	p	p.adj	p.adj.signif
p2x7r_pg_ml	CONT	G	69	17	-1,0631	0,2877	0,2877	ns
p2x7r_pg_ml	CONT	E	69	16	-2,3297	0,0198	0,0198	*
p2x7r_pg_ml	CONT	M	69	17	-0,1363	0,8916	0,8916	ns
p2x7r_pg_ml	CONT	RDP	69	11	0,6754	0,4994	0,4994	ns
p2x7r_pg_ml	CONT	PEX	69	7	-0,3021	0,7626	0,7626	ns
p2x7r_pg_ml	CONT	AMD	69	10	-0,1228	0,9023	0,9023	ns
p2x7r_pg_ml	CONT	DDRR	69	11	2,5495	0,0108	0,0108	*
p2x7r_pg_ml	CONT	MISC	69	3	-0,2721	0,7856	0,7856	ns
p2x7r_pg_ml	CONT	MP	69	5	1,0179	0,3087	0,3087	ns
p2x7r_pg_ml	CONT	OVR	69	2	-0,9451	0,3446	0,3446	ns

In Table 12, we show the results of the Dunn-test in which we applied Bonferroni's correction factor, which takes into account repeated testing. Following the application of this factor, the probability of the test is greater than 0.05, therefore not significant in the groups analysed

Table 12. Dunn-test with Bonferroni's correction factor

concentrazione	group1	group2	n1	n2	statistic	p	p.adj	p.adj.signif
p2x7r_pg_ml	CONT	G	69	17	-1,0631	0,2877	1	ns
p2x7r_pg_ml	CONT	E	69	16	-2,3297	0,0198	1	ns*

p2x7r_pg_ml	CONT	M	69	17	-0,1363	0,8916	1	ns
p2x7r_pg_ml	CONT	RDP	69	11	0,6754	0,4994	1	ns
p2x7r_pg_ml	CONT	PEX	69	7	-0,3021	0,7626	1	ns
p2x7r_pg_ml	CONT	AMD	69	10	-0,1228	0,9023	1	ns
p2x7r_pg_ml	CONT	DDRR	69	11	2,5495	0,0108	0,5934	ns*
p2x7r_pg_ml	CONT	MISC	69	3	-0,2721	0,7856	1	ns
p2x7r_pg_ml	CONT	MP	69	5	1,0179	0,3087	1	ns
p2x7r_pg_ml	CONT	OVR	69	2	-0,9451	0,3446	1	ns

Acqueous and serum analysis of sP2X7R concentrations

Of 206 patients enrolled for aqueous humour analysis, 34 serum samples were not taken or could not be analysed. Of the 170 samples taken and analysed, only 142 could be correlated with the respective aqueous samples.

Sperman's non-parametric test shows significant correlations (p-value <0.05) for sP2X7r concentration values in aqueous humour and serum in the control group, in the glaucoma and PEX group, as shown in table 13 and in Figure 18..

Table 13. sP2X7r acqueous/serum correlation

gruppo	sample	r	p-value
CONT	61	0,3946	0,0017*
G	14	0,5385	0,0500*
M	14	0,3187	0,2665
E	14	0,3050	0,2890
RDP	9	0,0837	0,8305
DDRR	5	0,4	0,5167
AMD	9	0,2427	0,5292
PEX	7	0,7857	0,048*
MP	5	0,6	0,35
MISC	2	-1	1,00
OVR	2	1	1,00
Tot	142		

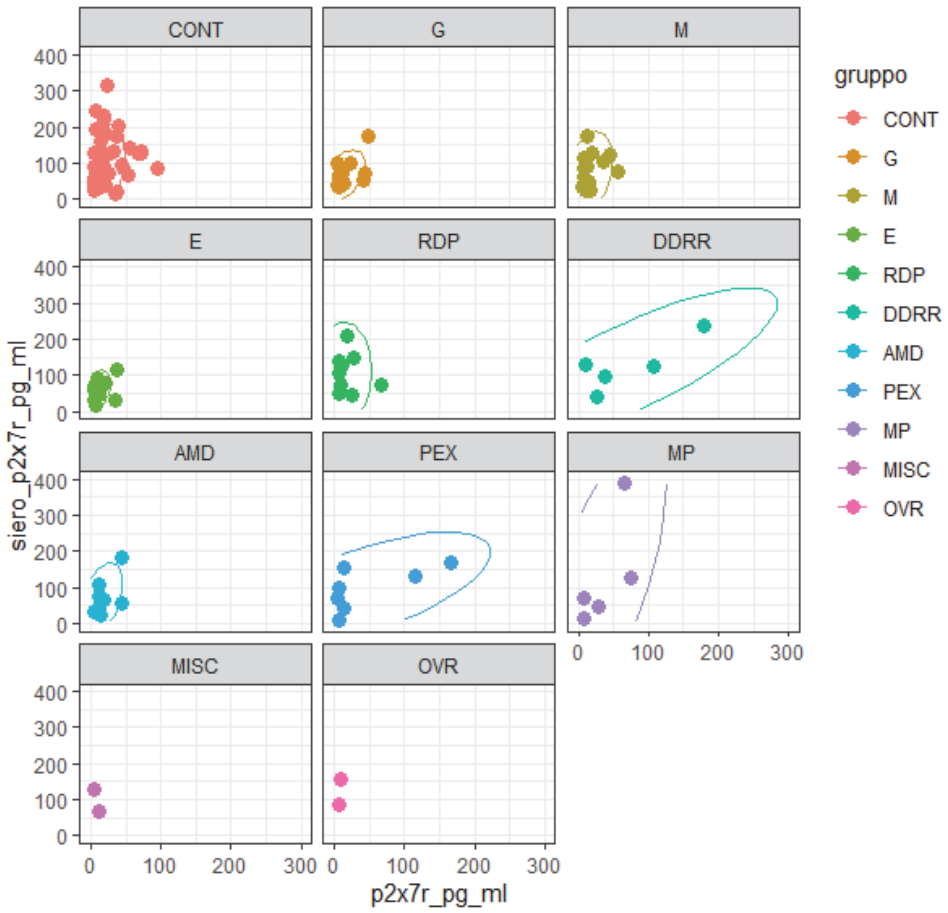

Figure 18.Scatter-plot representation of sP2X7r acqueous/serum correlation

Analysis of sP2X7R concentrations in vitreous humour

The dataset in which the P2X7r concentration values are collected is reproduced in the table in Appendix C. There are a total of 50 cases in this table, and the classification of the data set is the same as that used for the aqueous humour samples. The diagram in Figure 1 shows the P2X7r concentration values related to the volume of vitreous extracted for eachsample (min 0.2ml – max 2ml volume samples). It was decided to represent the individual concentration values by means of a dot plot due to the small size (one or two subjects) of many samples, instead of the box-plot representation used to describe the aqueous humour sample. In the diagram in Figure 19, the segment connecting the maximum and minimum values indicates the presence of at least two values. The category NA represents two samples in which the amount of material taken was not reported in the dataset and since the samples belong to two different subjects, it was considered appropriate to exclude them from the analysis.

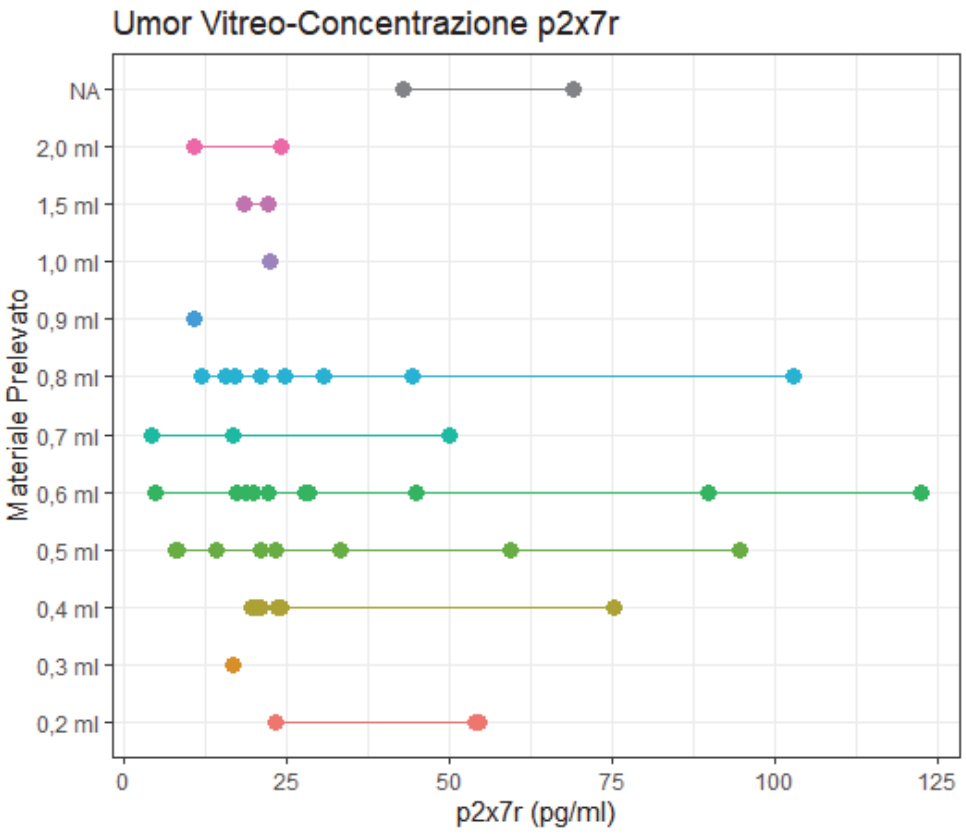

Figure 19. Dot-plot representation of sP2X7r values in vitreous humor in relation to the volume of vitreous extracted

Figure 19 also shows that for many categories of sampled material the P2X7r values are very limited in number. In order to summarise the values of the different categories it was considered appropriate to simplify the percentile representation by summarising in Table 14 the sequences of the categories of sampled material with the minimum (0%), maximum (100%), mean and median (50%) values. The hypothesis test performed for the categories with at least two observations (Kruskal-Wallis chi-squared = 7.0209, df = 10, p-value = 0.7235) supports the initial assumption of equality of the median value in the different groups.

Table 14. Percentiles of the distribution of P2X7 values (pg/ml) detected in the vitreous humour samples

tot_material_sampled	N. of patient	Media	0%	50%	100%
0,2 ml	3	43.90	23.16	54.10	54.45
0,3 ml	1	16.78	16.78	16.78	16.78
0,4 ml	7	29.68	19.71	23.51	75.32
0,5 ml	9	32.80	7.99	22.09	94.74
0,6 ml	11	37.65	4.95	22.13	122.57
0,7 ml	3	23.69	4.22	16.78	50.08
0,8 ml	8	33.51	12.03	22.82	102.76
0,9 ml	2	10.75	10.75	10.75	10.75
1,0 ml	1	22.47	22.47	22.47	22.47
1,5 ml	2	20.23	18.33	20.23	22.13
2,0 ml	2	17.47	10.92	17.47	24.03

The limited number of subjects from whom the vitreous humour sample was taken shows fewer pathologies than observed in Appendix B where aqueous humour samples are collected. Table 15 lists the number of patients in the control (no pathology) categories and the ocular pathologies found in the anamnestic-diagnostic (DDRR – rhegmatogenous retinal detachment; RDP – proliferative diabetic retinopathy; MISC- miscellaneous: subluxed IOL (intraocular lens), cortical lens residues, intraocular foreign body).

Table 15. Groups characteristics: description of the different groups, number of patients enrolled and sampled in each group, percentage of total.

Group definition	N. of samples	%	Details
CONT	19	0,396	assenza di patologie
DDRR	22	0,458	distacco di retina regmatogeno
RDP	4	0,083	retinopatia diabetica proliferante
MISC	3	0,062	miscellanea di patologie con attivazione infiammatoria
Total	48	1	

The blox-plox diagram in Figure 20 shows that the distribution of receptor concentration values in the control group (CONT) have a lower median value and a limited dispersion. In Table 16 the median (50%) is 20 pg/ml and the interquartile range at IQR = 75%-25% = 21.8 pg/ml. The different pathology groups have a greater dispersion and a slightly higher median in DDRR and MISC; in the RDP group median and dispersion are much higher than in the control group.

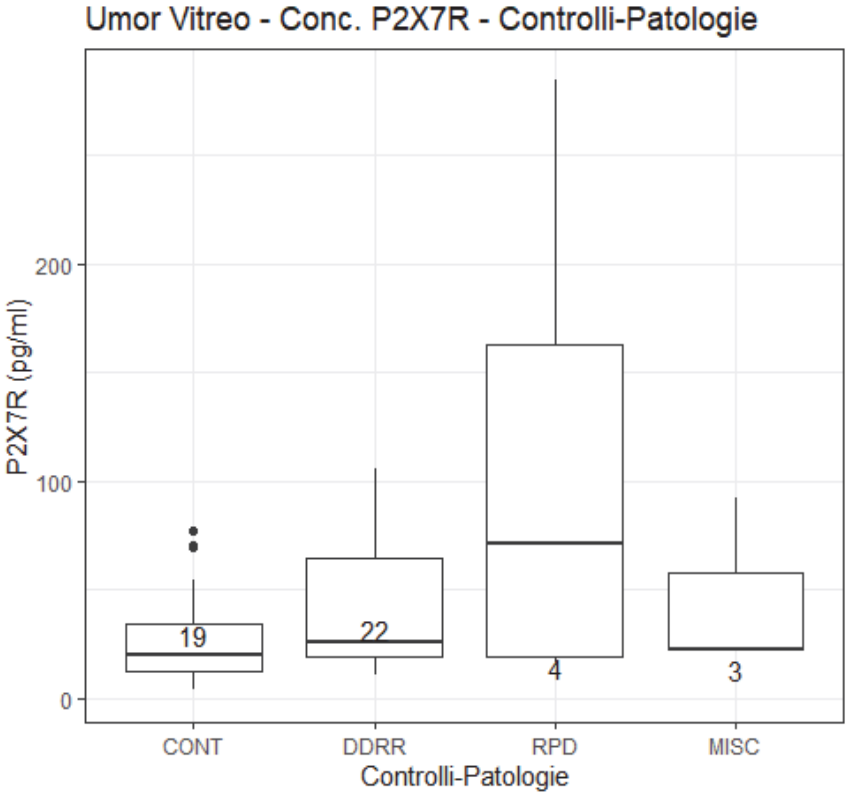

Figure 20. Blox-plot of the P2X7r values distribution detected in healthy patients (CONT) and the pathology groups. Values superimposed on the box-plot indicate sample size.

Table 16. Percentiles of the distribution of P2X7r values (pg/ml) detected in vitreous humour samples

gruppo	soggetti	media	0%	10%	25%	50%	75%	100%
CONT	19	28,02	4,22	6,84	12,73	20,23	34,53	76,92
DDRR	22	42,35	10,75	17,31	19,23	25,93	64,17	105,28
RDP	4	110,91	16,95	17,73	18,91	71,07	163,07	284,57
MISC	3	45,65	22,13	22,2	22,3	22,47	57,41	92,34

The non-parametric hypothesis test performed with the Kruskal-Wallis Test on the equality of the median of the groups in Figure 20 (Kruskal-Wallis chi-squared = 4.6481, df = 3, p-value = 0.1995) does not allow the initial hypothesis to be rejected with probability p-value

= 0.1999 (Talbe 17). The test result therefore does not allow the assertion that there is a significant difference between the P2X7r content in the vitreous of healthy patients and patients with the studied eye diseases. The difference between the sample size with healthy subjects (CONT) and subjects with DDRR (Regmatogenous Retinal Detachment) - 19 and 22 cases, respectively - and the size of the RDP (4 subjects) and MISC (3 subjects) groups suggested us to use Dunn's Test to perform the pairwise comparison of the groups shown in Table 16.

Table 17. Kruskal-Wallis chi-squared test result

concentrazione	n	statistic	df	p	method
p2x7r_pg_ml	48	4,648084	3	0,1991	Kruskal-Wallis

Table 18 shows the result of the Dunn-Test between the control group (CONT) and the pathology and between the pathologies: the p-value obtained in the presence of the Bonferroni correction (p.adj.signif) proves that the Test is non-significant for any pair of groups.

Table 18. Dunn-test results without and with Bonferroni's correction

concetrazione	gruppo1	gruppo2	n1	n2	statistic	p[(1)]	p.adj[(2)]	p.adj.signif[(3)]
p2x7r_pg_ml	CONT	DDRR	19	22	1.8648	0.0622	0.3732	ns
p2x7r_pg_ml	CONT	RDP	19	4	1.4010	0.1612	0.9672	ns
p2x7r_pg_ml	CONT	MISC	19	3	1.1831	0.2368	1	ns
p2x7r_pg_ml	DDRR	RDP	22	4	0.3435	0.7312	1	ns
p2x7r_pg_ml	DDRR	MISC	22	3	0.2453	0.8062	1	ns
p2x7r_pg_ml	RDP	MISC	4	3	-0.0468	0.9627	1	ns

---

(1) p-value of the pairwise test without correction factor
(2) p-value of the pairwise test with Bonferroni correction factor
(3) degree of significance of the test in the presence of correction (ns, <0.1, <0.05, <0.01)

Vitreous and serum analysis of sP2X7R concentrations

Sperman's non-parametric test shows no significant correlations (p-value <0.05) for P2X7r concentration values in vitreous humour and plasma serum, Table 19 and Figure 21.

Table 19. sP2X7r viteou/serum correlation

gruppo	sample	r	pvalue
CONT	14	0,0857	0,7732
DDRR	18	0,2714	0,2749
RPD	3	-0,5	1
MISC	3	0,5	1

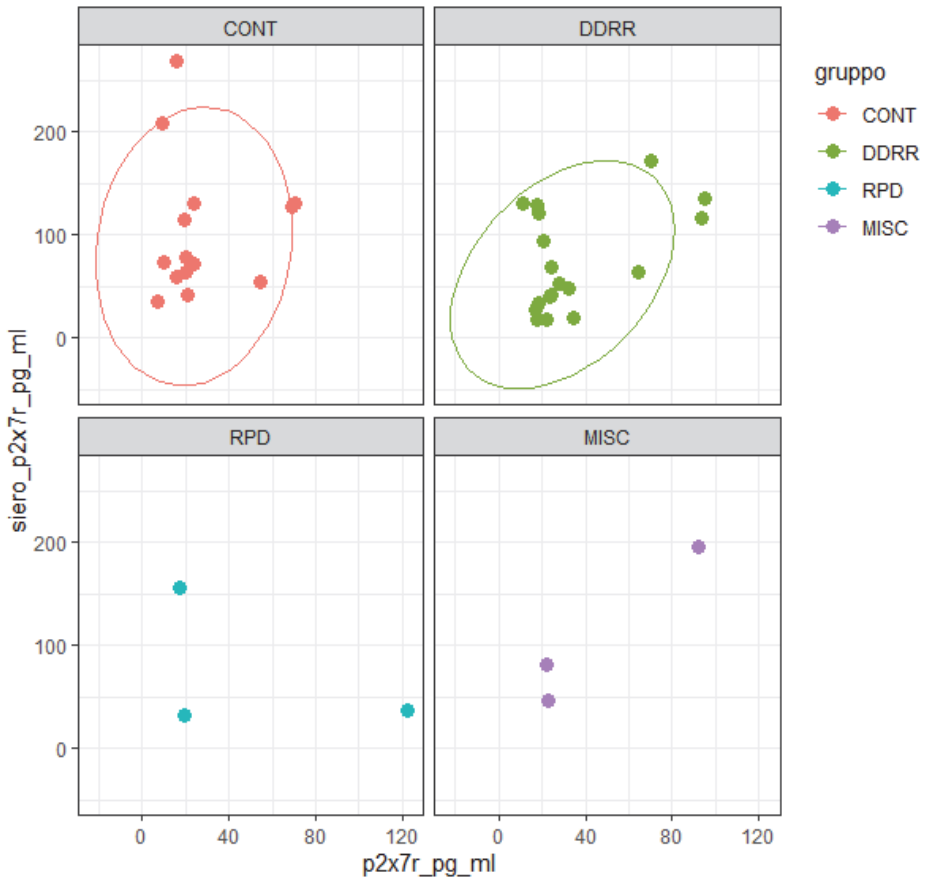

Figure 21. Scatter-plot representation of sP2X7r viterous/serum correlation

CHAPTER 6: DISCUSSION AND CONCLUSIONS

This study provided a fair amount of data on the presence of the soluble form of the P2X7 receptor (sP2X7R) in aqueous humour and vitreous humour and its involvement in inflammatory eye disease.

Analysis of sP2X7R concentrations was only possible in 168 samples compared to the 206 aqueous samples initially collected due to the small amount of biological fluid (<0.05ml) that could sometimes be taken from the anterior chamber of the eye, in order to ensure the subsequent planned surgery could be performed safely for the patient. A further obstacle encountered during the study was the relatively low number of vitrectomy procedures performed on patients meeting the inclusion criteria, which allowed only 50 samples to be collected. Finally, limitations also included the number of patients who denied their consent, but above all the shutdown of surgical turnover related to the COVID-19 pandemic, with a total restriction of surgeries scheduled in the period February - September 2020 and occasional lockdown periods between February 2021-February 2022.

- Check for the presence of the soluble form of the P2X7 receptor (sP2X7R) in aqueous humour and vitreous humour.

In this study, the soluble form of the P2X7 receptor was identified for the first time in aqueous humour and vitreous humour and was measurable using a specific ELISA kit.

The range of sP2X7R concentrations in the aqueous humour samples from the control group was 3.89 to 93.87 pg/ml; in the aqueous humour samples from the pathological groups the concentrations ranged from 3.55 to 277.04 pg/ml. In the vitreous humour, the range of sP2X7R concentrations in the control group was 4.21-76.92 pg/ml and in the group of cases with pathological conditions the range of concentrations was 28.52-284.57 pg/ml. Within the rhegmatogenous retinal detachment group, the range was 28.52-105.28 pg/ml. Within the proliferative diabetic retinopathy group, the range was 6.94 – 284.57 pg/ml.

From the data collected and considering that the sensitivity limit of the kit used with regard to sP2X7R concentrations is 7pg/ml, it is possible to state that the soluble form of the P2X7 receptor (sP2X7R) is released into ocular fluids both in the presence of ocular pathogenic inflammatory diseases and in their absence, but with different amount. In addition, concentrations of the soluble form of this receptor are measurable

by the ELISA kit used, defining a scientific and repeatable way of assessing concentrations of this analyte.

By performing the Kruskal-Wallis test on the sP2X7r concentration values (expressed in pg/ml) detected in the aqueous and vitreous humour samples in relation to the relative amount of material collected, we also showed that the median value of the detected concentration of sP2X7r does not depend on the amount of material collected in the sample, the difference in the median not being significant. This is especially important in aqueous samples, where sampling is limited by the small amount of aqueous that can be taken from the anterior chamber, so that the following steps of the surgery can then be carried out safely.

Further studies are needed to find the cellular source of the soluble form of this receptor, bearing in mind that the P2X7 receptor has been found on the membrane of many cells in the tissues of the eyeball and ocular adnexa, and some of them, such as corneal epithelial cells, retinal Müller cells, cells of the retinal pigment epithelium and photoreceptors, actively participate in ocular inflammatory processes [85]. In the search for sources, we should also build on the results of the study conducted at the University of Ferrara, which identified peripheral blood mononuclear cells (PBMCs) isolated from peripheral blood as a possible source of the plasma-soluble form of the receptor. PBMCs isolated from healthy subjects release sP2X7R into the culture medium after stimulation with BzATP [2',3'-O-(4benzoylbenzoyl)-ATP], an ATP analogue, and to a greater extent after pre-stimulation with LPS, simulating an inflammatory condition on an infectious basis in vitro. Furthermore, plasma sP2X7R is present to a large extent associated with microvesicles/microparticles (MVs/MPs), i.e. heterogeneous populations of particles of different sizes and cellular origins [84].

- <u>Compare sP2X7R levels in healthy conditions and in the presence of different ocular pathological conditions.</u>

In the second part of the study, a statistical analysis of the sP2X7R concentration values was carried out, comparing each individual group of patients with the ocular disease conditions under investigation with the control group for aqueous humour and vitreous humour.

The Kruskal-Wallis Chi-squared on the equality of the medians of the groups, both control and pathology groups of the acqueous samples, (Kruskal-Wallis chi-squared = 18.254, df = 10, p-value = 0.05082) estimates a p-value slightly above the test reliability

limit (p=0.05), confirming that the median value of the sP2X7r concentration measured in the pathology groups, when all the data are considered together, is significantly different from the control group. Despite the finding of high maximum concentrations of P2X7r in its soluble form in the disease groups, analysing each pathology group compared to the control group, statistical analysis using Dunn's Test to perform the pairwise comparison of the groups with the Bonferroni's correction factor, failed to confirm a statistically significant difference. It is interesting to note that by not applying Bonferroni's correction factor to the statistical analysis, the concentrations of the soluble P2X7 receptor in the rhegmatogenous retinal detachment and endothelial dystrophy groups were significantly different (p=0.01 in both groups). This is probably due to the fact that the Dunn Test takes into account the representativeness of the sample for each group. In fact, the sample size reflects on both the median and the sample dispersion. It should be noted that in our analysis, the control group consists of 69 aqueous samples, while the pathological groups have a range of 2 (i.e. retinal vascular occlusion) to 17 (i.e. glaucoma and myopia) aqueous samples.

The non-parametric hypothesis test performed with the Kruskal-Wallis Test on the equality of the median of the groups, both control and pathology groups of the vitreous samples (Kruskal-Wallis chi-squared = 4.6481, df = 3, p-value = 0.1995) does not allow the initial hypothesis to be rejected with probability p-value = 0.1999 (Table 17). The test result therefore does not allow the assertion that there is a significant difference between the P2X7r concentration in the vitreous of healthy patients and patients with the studied eye diseases. The difference between the sample size with healthy subjects (CONT) and subjects with DDRR (Regmatogenous Retinal Detachment) - 19 and 22 cases, respectively - and the size of the RDP (proliferative diabetic retinopathy - 4 subjects) and miscellaneous (3 subjects) groups suggested us to use Dunn's Test to perform the pairwise comparison of the groups.

The reason for the lack of significance in these analyses is probably due to the paucity of samples collected during the time available for the study. A clarification is however necessary: the overall amount of samples taken was relevant, nevertheless when stratified by singular diseases an under-reporting situation occurs, which could explain the test's drop in significance.

Other possible reasons of the loss pf samples to be taken into account were: the impossibility of analysing some of the aqueous humour samples (loss of 38 samples out of the total of 206) due to the fact that the amount of aqueous humour that could be taken from the anterior chamber of the eye did not reach the minimum necessary for analysis using the ELISA kit (minimum sample quantity 0.05 ml); the limited number of vitrectomy operations carried out on patients compatible with the inclusion criteria during the data collection period; finally, the selected patients who refused to give consent. From this we can deduce that, in order to obtain reliable and statistically significant results, it would be necessary to continue collecting samples in order to enlarge the above-mentioned single pathology groups.

Although no satistically significant difference emerged, it is interesting to note that sP2X7r concentration values are elevated in the vitreous humor of proliferating diabetic retinopathy patients. A great deal of evidence from in vitro studies using cell cultures and in vivo studies using mouse models of diabetes has revealed an important role for P2X7R in the pathogenesis of diabetic retinopathy, one of the main microangiopathic complications of diabetes mellitus. Exposure of pericytes to high concentrations of glucose induces the activation of a P2X7Rmediated signalling pathway that promotes the acquisition by these cells of an inflammatory phenotype, as evidenced by the secretion of TNF-α and IL-1β. In the same study that demonstrated this phenomenon, it was also found that hyperglycaemia-induced damage in retinal pericytes leads to cell lysis, accompanied by the release of ATP into the extracellular environment, which in turn binds P2X7R on neighbouring cells, activating the inflammasome and taking on the function of an inflammatory damage signalling device via an autocrinoparacrine mechanism [122]. Moreover, P2X7R activation is a powerful trigger for VEGF release. Indeed, the expression of the NLRP3 inflammasome, the activation of which can occur through P2X7R stimulation, is increased in the vitreous fibrovascular membrane of patients with diabetic retinopathy and dysregulation of NLRP3 in hyperglycaemic transgenic mice leads to vascular *leakeage* and retinal neovascularisation [120]. These results support the hypothesis that the P2X7 receptor is a key factor in the onset of diabetic retinopathy.

It would therefore be interesting to further expand the data collection and include both diabetic patients without ocular complications and patients with diabetic retinopathy in

the analysis, in order to highlight possible different level of P2X7r expression in the different disease's stage.

- Compare the levels of sP2X7R in aqueous humour and vitreous humour with those in serum.

This comparison was conducted in an attempt to compare the concetration of the P2X7r receptor in its aqueous or vitreous soluble form and in serum. However, no statistically significant correlation between local and systemic concentration was found in the analysis. This confirms that the eye is a site of immunological privilege.

In conclusion, it is possible to extrapolate from this study intersting data that reflect a local and time-limited reality, but which could lay the foundations for further investigations. The presence of the soluble form of the P2X7 receptor in aqueous humour and vitreous humour was tested and confirmed, and the ELISA kit used proved to be a reliable tool. Due to the limited number of samples tested, it cannot be said that sP2X7R is a marker of ocular inflammation in general, but in our opinion still remain a field that deserves a deeper investigation.

Bibliography

[1] M. J. L. Bours, P. C. Dagnelie, A. L. W. A. Giuliani, and F. Di Virgilio, "P2 Receptors and Extracellular ATP: A Novel Homeostatic Pathway in Inflammation," *Frontiers in bioscience (Scholar edition),* vol. 3, p. 1443-1456, 2011.

[2] F. Di Virgilio, 'The P2Z purinoceptor: an intriguing role in immunity, inflammation and cell death,' *Immunology today,* vol. 16, no. 11, p. 524-528, 1995.

[3] F. Di Virgilio, 'P2X Receptors and Inflammation,' *Current medicinal chemistry,* vol.
22, no. 7, p. 866-877, 2015.

[4] A. Surprenant and R. A. North, "Signaling at purinergic P2X receptors," *Annual review of physiology,* vol. 71, p. 333-359, 2009.

[5] F. Di Virgilio, D. Dal Ben, A. C. Sarti, A. L. Giuliani, and S. Falzoni, "The P2X7 Receptor in Infection and Inflammation," *Immunity,* vol. 47, no. 1, pp. 15-31, 2017.

[6] E. Orioli, E. De Marchi, A. L. Giuliani and E. Adinolfi, "P2X7 Receptor Orchestrates Multiple Signalling Pathways Triggering Inflammation, Autophagy and
Metabolic/Trophic Responses," *Current medicinal chemistry,* vol. 24, no. 21, pp. 22612275, 2017.

[7] K. Yoshida, M. Ito, and I. Matsuoka, "P2X7 receptor antagonist activity of the antiallergic agent oxatomide," *European journal of pharmacology,* vol. 767, pp. 41-51, 2015.

[8] É. M. Salles, M. N. Menezes, R. Siqueira, H. Borges da Silva, E. P. Amaral, S. I. Castillo-Méndez, I. Cunha, A. Cassado, F. S. Vieira, D. N. Olivieri, C. E. Tadokoro, J. M. Alvarez, R. Coutinho-Silva and M. R. D'Império-Lima, "P2X7 Receptor Drives Th1 Cell Differentiation and Controls the Follicular Helper T Cell Population to Protect Against Plasmodium Chabaudi Malaria," *PLoS pathogens,* vol. 13, no. 8, p. e1006595, 2017.

[9] A. B. Mackenzie, M. T. Young, E. Adinolfi, and A. Surprenant, "Pseudoapoptosis Induced by Brief Activation of ATP-gated P2X7 Receptors," *The Journal of biological chemistry,* vol. 280, no. 40, p. 33968-33976, 2005.

[10] D. Yang, Y. He, R. Munoz-Planillo, Q. Liu, and G. Nunez, " Caspase-11 requires the pannexin-1 channel and the purinergic P2X7 pore to mediate pyroptosis and endotoxic shock," *Immunity,* vol. 43, no. 5, p. 923-932, 2015.

[11] F. Di Virgilio and E. Adinolfi, "Extracellular purines, purinergic receptors and tumor growth," *Oncogene,* vol. 36, no. 3, p. 293-303, 2017.

[12] F. Di Virgilio, S. Falzoni, A. L. Giuliani, and E. Adinolfi, "P2 receptors in cancer progression and metastatic spreading," *Current opinion in pharmacology,* vol. 29, pp. 17-25, 2016.

[13] E. Adinolfi, M. G. Callegari, D. Ferrari, C. Bolognesi, M. Minelli, M. R. Wieckowski, P. Pinton, R. Rizzuto, and F. Di Virgilio, "Basal activation of the P2X7 ATP receptor elevates mitochondrial calcium and potential, increases cellular ATP levels, and promotes serum-independent growth," *Molecular biology of the cell,* vol. 16, no. 7, p. 3260-3272, 2005.

[14] H. Borges da Silva, L. Beura, H. Wang, E. A. Hanse, R. Gore, M. C. Scott, D. A. Walsh, K. E. Block, R. Fonseca, Y. Yan, K. L. Hippen, B. R. Blazar, D. Masopust, A. Kelekar, L. Vulchanova, K. A. Hogquist, and S. C. Jameson, "The purinergic receptor P2RX7 directs metabolic fitness of long-lived memory CD8+ T cells," *Nature,* vol. 559, no. 7713, pp. 264-268, 2018.

[15] V. Kumar, A. K. Abbas and J. C. Aster, Robbins and Cotran. The pathological basis of diseases., Edra, 2017.

[16] O. Takeuchi and S. Akira, "Pattern recognition receptors and inflammation," *Cell,* vol. 140, no. 6, p. 805-820, 2010.

[17] E. Adinolfi, A. L. Giuliani, E. De Marchi, A. Pegoraro, E. Orioli, and F. Di Virgilio, "The P2X7 receptor: A main player in inflammation," *Biochemical pharmacology,* vol. 151, p. 234-244, 2018.

[18] M. P. Abbracchio, G. Burnstock, A. Verkhratsky, and H. Zimmermann, "Purinergic Signalling in the Nervous System: An Overview," *Trends in neuroscience,* vol. 32, no. 1, p. 19-29, 2009.

[19] C. Oury, E. Toth-Zsamboki, J. Vermylen and M. F. & Hoylaerts, "The platelet ATP and ADP receptors," *Current pharmaceutical design,* vol. 12, no. 7, p. 859-875, 2006.

[20] G. Burnstock and A. Verkhratsky, 'Evolutionary origins of the purinergic signalling system,' *Acta physiologica (Oxford, England),* vol. 195, no. 4, p. 415-447, 2009.

[21] E. De Marchi, E. Orioli, A. Pegoraro, E. Adinolfi, and F. Di Virgilio, "Detection of Extracellular ATP in the Tumor Microenvironment, Using the pmeLUC Biosensor," *Methods in molecular biology (Clifton, N. J.),* vol. 2041, p. 183-195, 2020.

[22] F. Di Virgilio, A. C. Sarti, S. Falzoni, E. De Marchi, and E. Adinolfi, "Extracellular ATP and P2 purinergic signalling in the tumour microenvironment," *Nature reviews. Cancer,* vol. 18, no. 10, p. 601-618, 2018.

[23] P. Pellegatti, S. Falzoni, P. Pinton, R. Rizzuto and F. Di Virgilio, 'A Novel Recombinant Plasma Membrane-targeted Luciferase Reveals a New Pathway for ATP Secretion,' *Molecular biology of the cell,* vol. 16, no. 8, p. 3659-3665, 2005.

[24] P. Pellegatti, L. Raffaghello, G. Bianchi, F. Piccardi, V. Pistoia, and F. Di Virgilio, "Increased level of extracellular ATP at tumor sites: in vivo imaging with plasma membrane luciferase," *PloS one,* vol. 3, no. 7, p. e2599, 2008.

[25] F. Di Virgilio, A. C. Sarti, and R. Coutinho-Silva, "Purinergic signaling, DAMPs, and inflammation," *American journal of physiology. Cell physiology,* vol. 318, no. 5, p. C832-C835, 2020.

[26] G. G. Yegutkin, "Enzymes involved in metabolism of extracellular nucleotides and nucleosides: functional implications and measurement of activities," *Critical reviews in biochemistry and molecular biology,* vol. 49, no. 6, p. 473-497, 2014.

[27] A. Ohta and M. Sitkovsky, " Role of G-protein-coupled adenosine receptors in downregulation of inflammation and protection from tissue damage," *Nature,* vol. 414, no. 6866, p. 916-920, 2001.

[28] A. L. Giuliani, A. C. Sarti, and F. Di Virgilio, "Extracellular nucleotides and nucleosides as signalling molecules," *Immunology letters,* vol. 205, p. 16-24, 2019.

[29] E. R. Lazarowski, 'Vesicular and conductive mechanisms of nucleotide release,' *Purinergic signalling,* vol. 8, no. 3, p. 359-373, 2012.

[30] L. Perruzza, G. Gargari, M. Proietti, B. Fosso, A. M. D'Erchia, C. E. Faliti, T. Rezzonico-Jost, D. Scribano, L. Mauri, D. Colombo, G. Pellegrini, A. Moregola, C.
Mooser, G. Pesole, M. Nicoletti, G. D. Norata, M. B. Geuking and K. D. McCoy, "T Follicular Helper Cells Promote a Beneficial Gut Ecosystem for Host Metabolic Homeostasis by Sensing Microbiota-Derived Extracellular ATP," *Cell reports,* vol. 18, no. 11, p. 2566-2575, 2017.

[31] D. Ferrari, P. Chiozzi, S. Falzoni, S. Hanau and F. Di Virgilio, 'Purinergic modulation of interleukin-1 beta release from microglial cells stimulated with bacterial endotoxin,' *The Journal of experimental medicine,* vol. 185, no. 3, p. 579-582, 1997.

[32] M. M. Chaves, C. Marques-da-Silva, A. P. T. Monteiro, C. Canetti, and R. CoutinhoSilva, "Leukotriene B4 Modulates P2X7 Receptor-Mediated Leishmania amazonensis Elimination in Murine Macrophages," *The Journal of Immunology,* vol. 192, p. 4765- 4773, 2014.

[33] S. Ahmad, A. Ahmad and C. W. White, 'Purinergic signaling and kinase activation for survival in pulmonary oxidative stress and disease,' *Free Radical Biology and Medicine,* vol. 41, p. 29-40, 2006.

[34] I. R. Orriss, G. E. Knight, J. C. Utting, S. E. B. Taylor, G. Burnstock, and T. R. Arnett, "Hypoxia stimulates vesicular ATP release from rat osteoblasts," *Journal of cellular physiology,* vol. 220, p. 155-162, 2009.

[35] J. Linden, F. Koch-Nolte, and G. Dahl, "Purine release, metabolism, and signaling in the inflammatory response," *Annual review of immunology,* vol. 37, p. 325-347, 2019.

[36] Z. Hou and J. Cao, "Comparative study of the P2X gene family in animals and plants," *Purinergic signalling,* vol. 12, p. 269-281, 2016.

[37] S. E. Cheng, I. T. Lee, C. C. Lin, W. L. Wu, L. D. Hsiao, and C. M. Yang, "ATP mediates NADPH oxidase/ROS generation and COX-2/PGE2 expression in A549 cells: role of P2 receptor-dependent STAT3 activation," *PloS one,* vol. 8, 2013.

[38] C. Cekic and J. Linden, "Purinergic regulation of the immune system," *Nature Reviews Immunology,* vol. 16, p. 177, 2016.

[39] L. E. B. Savio, P. de Andrade Mello, C. G. da Silva, and R. Coutinho-Silva, "The P2X7 receptor in inflammatory diseases: angel or demon?," *Frontiers in pharmacology,* vol. 9, p. 52, 2018.

[40] G. Burnstock, 'Physiology and pathophysiology of purinergic neurotransmission,' *Physiological reviews,* vol. 87, p. 659-797, 2007.

[41] G. Burnstock, 'Purine and pyrimidine receptors,' *Cellular and molecular life sciences,* vol. 64, p. 1471, 2007.

[42] R. A. North, "P2X receptors," *Philosophical Transactions of the Royal Society B: Biological Sciences,* vol. 371, p. 20150427, 2016.

[43] P. Abramowski, C. Ogrodowczyk, R. Martin, and O. Pongs, "A truncation variant of the cation channel P2RX5 is upregulated during T cell activation," *PloS one,* vol. 9, p. e104692, 2014.

[44] W. J. Norde, I. M. Overes, F. Maas, H. Fredrix, J. C. M. Vos, M. G. D. Kester, R. van der Voort, I. Jedema, J. F. Falkenburg, A. V. Schattenberg et al, "Myeloid leukemic progenitor cells can be specifically targeted by minor histocompatibility antigen LRH-1-reactive cytotoxic T cells," *Blood, The Journal of the American Society of Hematology,* vol. 113, p. 2312-2323, 2009.

[45] T. Woehrle, L. Yip, A. Elkhal, Y. Sumi, Y. Chen, Y. Yao, P. A. Insel and W. G. Junger, "Pannexin-1 hemichannel-mediated ATP release together with P2X1 and P2X4 receptors regulate T-cell activation at the immune synapse," *Blood, The Journal of the American Society of Hematology,* vol. 116, p. 3475-3484, 2010.

[46] M. Idzko, D. Ferrari, and H. K. Eltzschig, "Nucleotide signalling during inflammation," *Nature,* vol. 509, p. 310-317, 2014.

[47] M. R. Thomas and R. F. Storey, "Effect of P2Y12 inhibitors on inflammation and immunity," *Thrombosis and haemostasis,* vol. 114, p. 490-497, 2015.

[48] F. Di Virgilio, L. H. Jiang, S. Roger, S. Falzoni, A. C. Sarti, V. Vultaggio-Poma, P. Chiozzi, and E. Adinolfi, "Structure, function and techniques of investigation of the P2X7 receptor (P2X7R) in mammalian cells," *Tumor Immunology and Immunotherapy- Molecular Methods,* p. 115, 2019.

[49] R. A. North and A. Surprenant, 'Pharmacology of cloned P2X receptors,' *Annual review of pharmacology and toxicology,* vol. 40, p. 563-580, 2000.

[50] A. Surprenant, F. Rassendren, E. Kawashima, R. A. North, and G. Buell, "The cytolytic P2Z receptor for extracellular ATP identified as a P2X receptor (P2X7)," *Science,* vol. 272, p. 735-738, 1996.

[51] F. Di Virgilio, G. Schmalzing, and F. Markwardt, "The elusive P2X7 macropore," *Trends in cell biology,* vol. 28, p. 392-404, 2018.

[52] M. Harkat, L. Peverini, A. H. Cerdan, K. Dunning, J. Beudez, A. Martz, N. Calimet, A. Specht, M. Cecchini, T. Chataigneau, and others, "On the permeation of large organic cations through the pore of ATP-gated P2X receptors," *Proceedings of the National Academy of Sciences,* vol. 114, p. E3786-E3795, 2017.

[53] G. N. Buell, F. Talabot, A. Gos, J. Lorenz, E. Lai, M. A. Morris and S. E. Antonarakis, "Gene structure and chromosomal localization of the human P2X7 receptor. ," *Receptors & channels,* vol. 5, p. 347-354, 1998.

[54] R. Sluyter, "The P2X7 receptor," in *Protein Reviews*, Springer, 2017, p. 17-53.

[55] B. Cheewatrakoolpong, H. Gilchrest, J. C. Anthes and S. Greenfeder, 'Identification and characterization of splice variants of the human P2X7 ATP channel,' *Biochemical and biophysical research communications,* vol. 332, p. 17-27, 2005.

[56] M. Carluccio, M. Zuccarini, S. Ziberi, P. Giuliani, C. Morabito, M. A. Mariggiò, M. T. Lonardo, E. Adinolfi, E. Orioli, P. Di Iorio, and others, "Involvement of P2X7 receptors in the osteogenic differentiation of mesenchymal stromal/stem cells derived from human subcutaneous adipose tissue," *Stem Cell Reviews and Reports,* vol. 15, p. 574- 589, 2019.

[57] E. Adinolfi, M. Cirillo, R. Woltersdorf, S. Falzoni, P. Chiozzi, P. Pellegatti, M. G. Callegari, D. Sandona, F. Markwardt, G. Schmalzing and others, "Trophic activity of a naturally occurring truncated isoform of the P2X7 receptor," *The FASEB Journal,* vol. 24, p. 3393-3404, 2010.

[58] T. Kawate, J. C. Michel, W. T. Birdsong, and E. Gouaux, "Crystal structure of the ATPgated P2X 4 ion channel in the closed state," *Nature,* vol. 460, p. 592-598, 2009.

[59] A. Karasawa and T. Kawate, "Structural basis for subtype-specific inhibition of the P2X7 receptor," *elife,* vol. 5, p. e22153, 2016.

[60] S. E. Mansoor, W. Lü, W. Oosterheert, M. Shekhar, E. Tajkhorshid, and E. Gouaux, "Xray structures define human P2X 3 receptor gating cycle and antagonist action," *Nature,* vol. 538, p. 66-71, 2016.

[61] M. Hattori and E. Gouaux, "Molecular mechanism of ATP binding and ion channel activation in P2X receptors," *Nature,* vol. 485, p. 207-212, 2012.

[62] R. A. North, 'Molecular physiology of P2X receptors,' *Physiological reviews,* vol. 82, p. 1013-1067, 2002.

[63] M. Munerati, R. Cortesi, D. Ferrari, F. Di Virgilio and C. Nastruzzi, 'Macrophages loaded with doxorubicin by ATP-mediated permeabilization: potential carriers for antitumor therapy,' *Biochimica et Biophysica Acta (BBA)-Molecular Cell Research,* vol. 1224, p. 269-276, 1994.

[64] D. Ferrari, C. Pizzirani, E. Adinolfi, R. M. Lemoli, A. Curti, M. Idzko, E. Panther, and F. Di Virgilio, "The P2X7 receptor: a key player in IL-1 processing and release," *The Journal of Immunology,* vol. 176, p. 3877-3883, 2006.

[65] F. Martinon, K. Burns and J. Tschopp, 'The inflammasome: a molecular platform triggering activation of inflammatory caspases and processing of proIL-β,' *Molecular cell,* vol. 10, p. 417-426, 2002.

[66] J. S. Ainscough, G. F. Gerberick, M. Zahedi-Nejad, G. Lopez-Castejon, D. Brough, I. Kimber, and R. J. Dearman, "Dendritic cell IL-1α and IL-1β are polyubiquitinated and degraded by the proteasome," *Journal of Biological Chemistry,* vol. 289, p. 35582- 35592, 2014.

[67] S. Benko, D. J. Philpott and S. E. Girardin, 'The microbial and danger signals that activate Nod-like receptors,' *Cytokine,* vol. 43, p. 368-373, 2008.

[68] N. Kelley, D. Jeltema, Y. Duan, and Y. He, "The NLRP3 inflammasome: an overview of mechanisms of activation and regulation," *International journal of molecular sciences,* vol. 20, p. 3328, 2019.

[69] R. Muñoz-Planillo, P. Kuffa, G. Martínez-Colón, B. L. Smith, T. M. Rajendiran, and G. Núñez, "K+ efflux is the common trigger of NLRP3 inflammasome activation by bacterial toxins and particulate matter," *Immunity,* vol. 38, p. 1142-1153, 2013.

[70] Y. He, M. Y. Zeng, D. Yang, B. Motro, and G. Núñez, "NEK7 is an essential mediator of NLRP3 activation downstream of potassium efflux," *Nature,* vol. 530, p. 354-357, 2016.

[71] C. Pizzirani, D. Ferrari, P. Chiozzi, E. Adinolfi, D. Sandona, E. Savaglio, and F. Di Virgilio, "Stimulation of P2 receptors causes release of IL-1β-loaded microvesicles from human dendritic cells," *Blood,* vol. 109, p. 3856-3864, 2007.

[72] Y. Qu, L. Franchi, G. Nunez, and G. R. Dubyak, "Nonclassical IL-1β secretion stimulated by P2X7 receptors is dependent on inflammasome activation and

correlated with exosome release in murine macrophages," *The Journal of Immunology,* vol. 179, p. 1913-1925, 2007.

[73] M. M. Gaidt, T. S. Ebert, D. Chauhan, T. Schmidt, J. L. Schmid-Burgk, F. Rapino, A.
A. B. Robertson, M. A. Cooper, T. Graf, and V. Hornung, "Human monocytes engage an alternative inflammasome pathway," *Immunity,* vol. 44, p. 833-846, 2016.

[74] Y. Liu, Y. Xiao, and Z. Li, "P2X7 receptor positively regulates MyD88-dependent NF-κB activation," *Cytokine,* vol. 55, p. 229-236, 2011.

[75] M. Barberà-Cremades, A. Baroja-Mazo, A. I. Gomez, F. Machado, F. Di Virgilio, and P. Pelegrın, "P2X7 receptoŕ-stimulation causes fever via PGE2 and IL-1β release," *The FASEB Journal,* vol. 26, p. 2951-2962, 2012.

[76] B. F. King, "Novel P2X7 receptor antagonists ease the pain," *British journal of pharmacology,* vol. 151, p. 565-567, 2007.

[77] D. Ferrari, C. Stroh, and K. Schulze-Osthoff, "P2X7/P2Z purinoreceptor-mediated activation of transcription factor NFAT in microglial cells," *Journal of Biological Chemistry,* vol. 274, p. 13205-13210, 1999.

[78] E. Adinolfi, L. Raffaghello, A. L. Giuliani, L. Cavazzini, M. Capece, P. Chiozzi, G. Bianchi, G. Kroemer, V. Pistoia, and F. Di Virgilio, "Expression of P2X7 receptor increases in vivo tumor growth," *Cancer research,* vol. 72, p. 2957-2969, 2012.

[79] T. Gicquel, S. Robert, P. Loyer, T. Victoni, A. Bodin, C. Ribault, F. Gleonnec, I. Couillin, E. Boichot and V. Lagente, "IL-1β production is dependent on the activation of purinergic receptors and NLRP3 pathway in human macrophages," *The FASEB Journal,* vol. 29, p. 4162-4173, 2015.

[80] L. M. Hill, M. L. Gavala, L. Y. Lenertz and P. J. Bertics, "Extracellular ATP may contribute to tissue repair by rapidly stimulating purinergic receptor X7-dependent vascular endothelial growth factor release from primary human monocytes," *The Journal of Immunology,* vol. 185, p. 3028-3034, 2010.

[81] G. R. Dubyak, "P2X7 receptor regulation of non-classical secretion from immune effector cells," *Cellular microbiology,* vol. 14, p. 1697-1706, 2012.

[82] D. Wallach, T.-B. Kang, C. P. Dillon, and D. R. Green, "Programmed necrosis in inflammation: Toward identification of the effector molecules," *Science,* vol. 352, p. aaf2154, 2016.

[83] D. Ferrari, M. Los, M. K. A. Bauer, P. Vandenabeele, S. Wesselborg and K. SchulzeOsthoff, "P2Z purinoreceptor ligation induces activation of caspases with distinct roles in apoptotic and necrotic alterations of cell death," *FEBS letters,* vol. 447, p. 71-75, 1999.

[84] A. L. Giuliani, M. Berchan, J. M. Sanz, A. Passaro, S. Pizzicotti, V. Vultaggio Poma, A. C. Sarti, and F. Di Virgilio, "The P2X7 Receptor Is Shed Into Circulation: Correlation With C-Reactive Protein Levels," *Frontiers in immunology,* vol. 10, p. 793, 2019.

[85] M. Dutot, E. Olivier, A. Wakx, and P. Rat, "The role of the P2X7 receptor in ocular stresses: A potential therapeutic target," *Vision,* vol. 1, p. 14, 2017.

[86] ClinicalTrials.gov, "Antidepressant Trial With P2X7 Antagonist JNJ-54175446 (ATP)," U.S. National Library of Medicine, 2019. [Online]. Available: https://www.clinicaltrials.gov/ct2/show/NCT04116606?term=p2x7&draw=2&rank=2.
[Consulted on 16 June 2020].

[87] ClinicalTrials.gov, "A Positron Emission Tomography (PET) Study to Investigate P2X7 Receptor Occupancy by JNJ-55308942 Using [18F]-JNJ-64413739," U.S.
National Library of Medicine, 2018. [Online]. Available: https://www.clinicaltrials.gov/ct2/show/NCT03437590?term=p2x7&draw=2&rank=7. [Consulted on 16 June 2020].

[88] ClinicalTrials.gov, "A Study to Investigate P2X7 Receptor Occupancy by JNJ54175446 With the Newly Developed P2X7 Receptor Positron Emission Tomography (PET) Tracer 18F-JNJ-64413739," U. S. National Library of Medicine, 2017. [Online].
Available:
https://www.clinicaltrials.gov/ct2/show/NCT03088644?term=p2x7&draw=2&rank=8. [Consulted on 16 June 2020].

[89] ClinicalTrials.gov, "P2X7 Receptor, Inflammation and Neurodegenerative Diseases (NeuroInfiam)," U.S. National Library of Medicine, 2019. [Online]. Available:
https://www.clinicaltrials.gov/ct2/show/NCT03918616?term=p2x7&draw=2&rank=4. [Accessed June 16, 2020].

[90] T. Pauloin, M. Dutot, H. Liang, E. Chavinier, J.-M. Warnet and P. Rat, "Corneal protection with high-molecular-weight hyaluronan against in vitro and in vivo sodium lauryl sulfate-induced toxic effects," *Cornea,* vol. 28, p. 1032-1041, 2009.

[91] T. Pauloin, M. Dutot, J.-M. Warnet and P. Rat, "In vitro modulation of preservative toxicity: high molecular weight hyaluronan decreases apoptosis and oxidative stress induced by benzalkonium chloride," *European Journal of Pharmaceutical Sciences,* vol. 34, p. 263-273, 2008.

[92] A. Wakx, M. Dutot, F. Massicot, F. Mascarelli, G. A. Limb and P. Rat, 'Amyloid β peptide induces apoptosis through P2X7 cell death receptor in retinal cells: modulation
by marine omega-3 fatty acids DHA and EPA," *Applied biochemistry and biotechnology,* vol. 178, p. 368-381, 2016.

[93] A. Bhattacharya, B. Lord, J.-S. Grigoleit, Y. He, I. Fraser, S. N. Campbell, N. Taylor,
L. Aluisio, J. C. O'Connor, M. Papp and others, "Neuropsychopharmacology of JNJ55308942: evaluation of a clinical candidate targeting P2X7 ion channels in animal models of neuroinflammation and anhedonia," *Neuropsychopharmacology,* vol. 43, p. 2586-2596, 2018.

[94] E. L. Fletcher, A. Y. Wang, A. I. Jobling, M. V. Rutar, U. Greferath, B. Gu and K. A. Vessey, "Targeting P2X7 receptors as a means for treating retinal disease," *Drug discovery today,* 2019.

[95] W. Danquah, C. Meyer-Schwesinger, B. Rissiek, C. Pinto, A. Serracant-Prat, M. Amadi, D. Iacenda, J.-H. Knop, A. Hammel, P. Bergmann, and others, "Nanobodies that block gating of the P2X7 ion channel ameliorate inflammation," *Science translational medicine,* vol. 8, p. 366ra162-366ra162, 2016.

[96] "Global report on diabetes," World Health Organization, 2016. [Online]. Available: https://www.who.int/diabetes/global-report/en/. [Accessed June 3, 2020].

[97] L. Guariguata, D. R. Whiting, I. Hambleton, J. Beagley, U. Linnenkamp, and J. E. Shaw, "Global estimates of diabetes prevalence for 2013 and projections for 2035," *Diabetes research and clinical practice,* vol. 103, p. 137-149, 2014.

[98] G. A. Lutty, "Effects of diabetes on the eye," *Investigative ophthalmology & visual science,* vol. 54, p. ORSF81-ORSF87, 2013.

[99] S. Priyadarsini, A. Whelchel, S. Nicholas, R. Sharif, K. Riaz, and D. Karamichos, "Diabetic keratopathy: Insights and challenges," *Survey of Ophthalmology,* 2020.

[100] J. Kim, C.-S. Kim, E. Sohn, I.-H. Jeong, H. Kim, and J. S. Kim, "Involvement of advanced glycation end products, oxidative stress and nuclear factor-kappaB in the development of diabetic keratopathy," *Graefe's Archive for Clinical and Experimental Ophthalmology,* vol. 249, p. 529-536, 2011.

[101] C. Mankus, C. Rich, M. Minns, and V. Trinkaus-Randall, "Corneal epithelium expresses a variant of P2X7 receptor in health and disease," *PLoS One,* vol. 6, 2011.

[102] K. Kneer, M. B. Green, J. Meyer, C. B. Rich, M. S. Minns, and V. Trinkaus-Randall, "High fat diet induces pre-type 2 diabetes with regional changes in corneal sensory nerves and altered P2X7 expression and localization," *Experimental eye research,* vol. 175, p. 44-55, 2018.

[103] X. Zhang, J. B. Saaddine, C.-F. Chou, M. F. Cotch, Y. J. Cheng, L. S. Geiss, E. W. Gregg, A. L. Albright, B. E. K. Klein, and R. Klein, "Prevalence of diabetic retinopathy in the United States, 2005-2008," *Jama,* vol. 304, p. 649-656, 2010.

[104] C. P. Wilkinson, F. L. Ferris III, R. E. Klein, P. P. Lee, C. D. Agardh, M. Davis, D. Dills, A. Kampik, R. Pararajasegaram, J. T. Verdaguer and others, "Proposed international clinical diabetic retinopathy and diabetic macular edema disease severity scales," *Ophthalmology,* vol. 110, p. 1677-1682, 2003.

[105] C. Olvera-Montaño, J. A. Castellanos-González, J. Navarro-Partida, E. G. CardonaMuñoz, A. K. López-Contreras, L. M. Roman-Pintos, R. R. Robles-Rivera and A. D. Rodrıgueź-Carrizalez , "Oxidative Stress as the Main Target in Diabetic Retinopathy Pathophysiology," *Journal of diabetes research,* vol. 2019, 2019.

[106] M.-Y. Wu, G.-T. Yiang, T.-T. Lai and C.-J. Li, "The oxidative stress and mitochondrial dysfunction during the pathogenesis of diabetic retinopathy," *Oxidative medicine and cellular longevity,* vol. 2018, 2018.

[107] M. C. Potilinski, V. Lorenc, S. Perisset, and J. E. Gallo, "Mechanisms behind Retinal Ganglion Cell Loss in Diabetes and Therapeutic Approach," *International Journal of Molecular Sciences,* vol. 21, p. 2351, 2020.

[108] R. Simó, A. W. Stitt and T. W. Gardner, 'Neurodegeneration in diabetic retinopathy: does it really matter?," *Diabetologia,* vol. 61, p. 1902-1912, 2018.

[109] A. Bringmann and P. Wiedemann, 'Müller glial cells in retinal disease,' *Ophthalmologica,* vol. 227, p. 1-19, 2012.

[110] S. Vujosevic, A. Micera, S. Bini, M. Berton, G. Esposito, and E. Midena, "Aqueous humor biomarkers of Müller cell activation in diabetic eyes," *Investigative ophthalmology & visual science,* vol. 56, p. 3913-3918, 2015.

[111] M. Mesquida, F. Drawnel, and S. Fauser, "The role of inflammation in diabetic eye disease," in *Seminars in immunopathology*, 2019.

[112] A. S. Al-Kharashi, "Role of oxidative stress, inflammation, hypoxia and angiogenesis in the development of diabetic retinopathy," *Saudi journal of ophthalmology,* vol. 32, p. 318-323, 2018.

[113] A. Rübsam, S. Parikh, and P. E. Fort, "Role of inflammation in diabetic retinopathy," *International journal of molecular sciences,* vol. 19, p. 942, 2018.

[114] C. Altmann and M. H. Schmidt, 'The role of microglia in diabetic retinopathy: inflammation, microvasculature defects and neurodegeneration," *International journal of molecular sciences,* vol. 19, p. 110, 2018.

[115] F. S. Sorrentino, M. Allkabes, G. Salsini, C. Bonifazzi, and P. Perri, "The Importance of Glial Cells in the Homeostasis of the Retinal Microenvironment and Their Pivotal Role in the Course of Diabetic Retinopathy," *Life sciences,* vol. 162, p. 54-59, 2016.

[116] S. Vujosevic and R. Simó, "Local and systemic inflammatory biomarkers of diabetic retinopathy: an integrative approach," *Investigative ophthalmology & visual science,* vol. 58, p. BIO68-BIO75, 2017.

[117] J. V. Busik, S. Mohr, and M. B. Grant, "Hyperglycemia-induced reactive oxygen species toxicity to endothelial cells is dependent on paracrine mediators," *Diabetes,* vol. 57, p. 1952-1965, 2008.

[118] S. Pavlou, J. Augustine, R. Cunning, K. Harkin, A. W. Stitt, H. Xu, and M. Chen, "Attenuating Diabetic Vascular and Neuronal Defects by Targeting P2rx7," *International journal of molecular sciences,* vol. 20, p. 2101, 2019.

[119] J.-A. C. Portillo, Y. L. Corcino, Y. Miao, J. Tang, N. Sheibani, T. S. Kern, G. R. Dubyak, and C. S. Subauste, "CD40 in retinal Müller cells induces P2X7-dependent cytokine expression in macrophages/microglia in diabetic mice and development of early experimental diabetic retinopathy," *Diabetes,* vol. 66, p. 483-493, 2017.

[120] S. S. Chaurasia, R. R. Lim, B. H. Parikh, Y. S. Wey, B. B. Tun, T. Y. Wong, C. D. Luu, R. Agrawal, A. Ghosh, A. Mortellaro and others, "The NLRP3 inflammasome may contribute to pathologic neovascularization in the advanced stages of diabetic retinopathy," *Scientific reports,* vol. 8, p. 1-15, 2018.

[121] C. Clapp, N. Diaz-Lezama, E. Adan-Castro, G. Ramirez-Hernandez, B. MorenoCarranza, A. C. Sarti, S. Falzoni, A. Solini, and F. Di Virgilio, "Pharmacological blockade of the P2X7 receptor reverses retinal damage in a rat model of type 1 diabetes," *Acta diabetologica,* vol. 56, p. 1031-1036, 2019.

[122] C. B. M. Platania, G. Giurdanella, L. Di Paola, G. M. Leggio, F. Drago, S. Salomone, and C. Bucolo, "P2X7 receptor antagonism: implications in diabetic retinopathy," *Biochemical pharmacology,* vol. 138, p. 130-139, 2017.

[123] T. Sugiyama, M. Kobayashi, H. Kawamura, Q. Li and D. G. Puro, "Enhancement of P2X7-induced pore formation and apoptosis: an early effect of diabetes on the retinal microvasculature," *Investigative ophthalmology & visual science,* vol. 45, p. 1026- 1032, 2004.

[124] M. Shibata, E. Ishizaki, T. Zhang, M. Fukumoto, A. Barajas-Espinosa, T. Li, and D. G. Puro, "Purinergic vasotoxicity: Role of the pore/oxidant/KATP channel/Ca2+ pathway in P2X7-induced cell death in retinal capillaries," *Vision,* vol. 2, p. 25, 2018.

[125] P. Mitchell, G. Liew, B. Gopinath, and T. Y. Wong, "Age-related macular degeneration," *The Lancet,* vol. 392, p. 1147-1159, 2018.

[126] "Maculopathies. When the problem is in the centre of the retina," SOI-Società Oftalmologica Italiana, [Online]. Available: https://www.sedesoi.com/patologie20.php. [Accessed 3 June 2020].

[127] W. M. Al-Zamil and S. A. Yassin, "Recent developments in age-related macular degeneration: a review," *Clinical interventions in aging,* vol. 12, p. 1313, 2017.

[128] M. Chen and H. Xu, "Parainflammation, chronic inflammation, and age-related macular degeneration," *Journal of leukocyte biology,* vol. 98, p. 713-725, 2015.

[129] C. E. Gallenga, F. Parmeggiani, C. Costagliola, A. Sebastiani, and P. E. Gallenga, "Inflammaging: should this term be suitable for age-related macular degeneration too?," *Inflammation Research,* vol. 63, p. 105-107, 2014.

[130] T. J. Heesterbeek, L. Lorés-Motta, C. B. Hoyng, Y. T. E. Lechanteur, and A. I. den Hollander, "Risk factors for progression of age-related macular degeneration," *Ophthalmic and Physiological Optics,* vol. 40, p. 140-170, 2020.

[131] T. Sepp, J. C. Khan, D. A. Thurlby, H. Shahid, D. G. Clayton, A. T. Moore, A. C. Bird, and J. R. W. Yates, "Complement factor H variant Y402H is a major risk determinant for geographic atrophy and choroidal neovascularization in smokers and nonsmokers," *Investigative ophthalmology & visual science,* vol. 47, p. 536-540, 2006.

[132] B. Liu, L. Wei, C. Meyerle, J. Tuo, H. N. Sen, Z. Li, S. Chakrabarty, E. Agron, C.-C. Chan, M. L. Klein and others, "Complement component C5a promotes expression of IL22 and IL-17 from human T cells and its implication in age-related macular degeneration," *Journal of translational medicine,* vol. 9, p. 111, 2011.

[133] J. M. Skeie, J. H. Fingert, S. R. Russell, E. M. Stone, and R. F. Mullins, "Complement component C5a activates ICAM-1 expression on human choroidal endothelial cells," *Investigative ophthalmology & visual science,* vol. 51, p. 5336-5342, 2010.

[134] Y. Chen, M. Zhong, L. Liang, F. Gu, and H. Peng, "Interleukin-17 induces angiogenesis in human choroidal endothelial cells in vitro," *Investigative ophthalmology & visual science,* vol. 55, p. 6968-6975, 2014.

[135] A. Kauppinen, J. J. Paterno, J. Blasiak, A. Salminen, and K. Kaarniranta, "Inflammation and its role in age-related macular degeneration," *Cellular and Molecular Life Sciences,* vol. 73, p. 1765-1786, 2016.

[136] S. Abokyi, C.-H. To, T. T. Lam and D. Y. Tse, "Central Role of Oxidative Stress in Age-Related Macular Degeneration: Evidence from a Review of the Molecular Mechanisms and Animal Models," *Oxidative Medicine and Cellular Longevity,* vol. 2020, 2020.

[137] E. B Domènech and G. Marfany, "The Relevance of Oxidative Stress in the Pathogenesis and Therapy of Retinal Dystrophies," *Antioxidants,* vol. 9, p. 347, 2020.

[138] A. Kijlstra, Y. Tian, E. R. Kelly and T. J. M. Berendschot, 'Lutein: more than just a filter for blue light,' *Progress in retinal and eye research,* vol. 31, p. 303-315, 2012.

[139] F. Parmeggiani, M. R. Romano, C. Costagliola, F. Semeraro, C. Incorvaia, S. D'Angelo, P. Perri, P. De Palma, K. De Nadai and A. Sebastiani, 'Mechanism of inflammation in age-related macular degeneration,' *Mediators of inflammation,* vol. 2012, 2012.

[140] X. Cao, D. Shen, M. M. Patel, J. Tuo, T. M. Johnson, T. W. Olsen, and C.-C. Chan, "Macrophage polarization in the maculae of age-related macular degeneration: A pilot study," *Pathology international,* vol. 61, p. 528-535, 2011.

[141] C. Faber, A. Singh, M. K. Falk, H. B. Juel, T. L. Sørensen, and M. H. Nissen, "Agerelated macular degeneration is associated with increased proportion of CD56+ T cells in peripheral blood," *Ophthalmology,* vol. 120, p. 2310-2316, 2013.

[142] K. Nassar, S. Grisanti, E. Elfar, J. Lüke, M. Lüke, and S. Grisanti, "Serum cytokines as biomarkers for age-related macular degeneration," *Graefe's Archive for Clinical and Experimental Ophthalmology,* vol. 253, p. 699-704, 2015.

[143] J. E. Knickelbein, C.-C. Chan, H. N. Sen, F. L. Ferris, and R. B. Nussenblatt, "Inflammatory mechanisms of age-related macular degeneration," *International ophthalmology clinics,* vol. 55, p. 63, 2015.

[144] R. T. Liu, J. Gao, S. Cao, N. Sandhu, J. Z. Cui, C. L. Chou, E. Fang, and J. A. Matsubara, "Inflammatory mediators induced by amyloid-beta in the retina and RPE in vivo: implications for inflammasome activation in age-related macular degeneration," *Investigative ophthalmology & visual science,* vol. 54, p. 2225-2237, 2013.

[145] Y. Liao, H. Zhang, D. He, Y. Wang, B. Cai, J. Chen, J. Ma, Z. Liu, and Y. Wu, "Retinal Pigment Epithelium Cell Death Is Associated With NLRP3 Inflammasome Activation by All-trans Retinal," *Investigative ophthalmology & visual science,* vol. 60, p. 3034- 3045, 2019.

[146] O. A. Anderson, A. Finkelstein, and D. T. Shima, "A2E induces IL-1ss production in retinal pigment epithelial cells via the NLRP3 inflammasome," *PloS one,* vol. 8, 2013.

[147] C. Brandstetter, L. K. M. Mohr, E. Latz, F. G. Holz, and T. U. Krohne, "Light induces NLRP3 inflammasome activation in retinal pigment epithelial cells via lipofuscinmediated photooxidative damage," *Journal of Molecular Medicine,* vol. 93, p. 905- 916, 2015.

[148] A. Kauppinen, H. Niskanen, T. Suuronen, K. Kinnunen, A. Salminen, and K. Kaarniranta, "Oxidative stress activates NLRP3 inflammasomes in ARPE-19 cells-implications for age-related macular degeneration (AMD)," *Immunology letters,* vol. 147, p. 29-33, 2012.

[149] E. Korhonen, N. Piippo, M. Hytti, J. M. T. Hyttinen, K. Kaarniranta and A. Kauppinen,
"Only IL-1β release is inflammasome-dependent upon ultraviolet B irradiation although IL-18 is also secreted," *The FASEB Journal,* vol. 34, p. 6437-6448, 2020.

[150] Y. Kim, V. Tarallo, N. Kerur, T. Yasuma, B. D. Gelfand, A. Bastos-Carvalho, Y. Hirano, R. Yasuma, T. Mizutani, B. J. Fowler, and others, "DICER1/Alu RNA dysmetabolism induces Caspase-8-mediated cell death in age-related macular degeneration," *Proceedings of the National Academy of Sciences,* vol. 111, p. 16082- 16087, 2014.

[151] N. Kerur, Y. Hirano, V. Tarallo, B. J. Fowler, A. Bastos-Carvalho, T. Yasuma, R. Yasuma, Y. Kim, D. R. Hinton, C. J. Kirschning et al, "TLR-independent and P2X7-dependent signaling mediate Alu RNA-induced NLRP3 inflammasome activation in geographic atrophy," *Investigative ophthalmology & visual science,* vol. 54, p. 7395-7401, 2013.

[152] J. Gao, J. Z. Cui, E. To, S. Cao, and J. A. Matsubara, "Evidence for the activation of pyroptotic and apoptotic pathways in RPE cells associated with NLRP3 inflammasome in the rodent eye," *Journal of neuroinflammation,* vol. 15, p. 15, 2018.

[153] L. Wang, S. Schmidt, P. P. Larsen, J. H. Meyer, W. R. Roush, E. Latz, F. G. Holz and T.
U. Krohne, "Efficacy of novel selective NLRP3 inhibitors in human and murine retinal pigment epithelial cells," *Journal of Molecular Medicine,* vol. 97, p. 523-532, 2019.

[154] T. Noguchi, K. Ishii, H. Fukutomi, I. Naguro, A. Matsuzawa, K. Takeda, and H. Ichijo, "Requirement of reactive oxygen species-dependent activation of ASK1-p38 MAPK pathway for extracellular ATP-induced apoptosis in macrophage," *Journal of Biological Chemistry,* vol. 283, p. 7657-7665, 2008.

[155] S. Guha, G. C. Baltazar, E. E. Coffey, L.-A. Tu, J. C. Lim, J. M. Beckel, S. Patel, T.
Eysteinsson, W. Lu, A. O'Brien-Jenkins and others, 'Lysosomal alkalinization, lipid oxidation, and reduced phagosome clearance triggered by activation of the P2X7 receptor," *The FASEB Journal,* vol. 27, p. 4500-4509, 2013.

[156] D. Yang, S. G. Elner, A. J. Clark, B. A. Hughes, H. R. Petty, and V. M. Elner, "Activation of P2X receptors induces apoptosis in human retinal pigment epithelium,"
Investigative ophthalmology & visual science, vol. 52, p. 1522-1530, 2011.

[157] B. J. Fowler, B. D. Gelfand, Y. Kim, N. Kerur, V. Tarallo, Y. Hirano, S. Amarnath, D. H. Fowler, M. Radwan, M. T. Young and others, "Nucleoside reverse transcriptase inhibitors possess intrinsic anti-inflammatory activity," *Science,* vol. 346, p. 1000- 1003, 2014.

[158] T. Mizutani, B. J. Fowler, Y. Kim, R. Yasuma, L. A. Krueger, B. D. Gelfand, and J. Ambati, "Nucleoside reverse transcriptase inhibitors suppress laser-induced choroidal neovascularization in mice," *Investigative ophthalmology & visual science,* vol. 56, p. 7122-7129, 2015.

[159] S. Notomi, T. Hisatomi, Y. Murakami, H. Terasaki, S. Sonoda, R. Asato, A. Takeda, Y. Ikeda, H. Enaida, T. Sakamoto and others, "Dynamic increase in extracellular ATP accelerates photoreceptor cell apoptosis via ligation of P2RX7 in subretinal hemorrhage," *PloS one,* vol. 8, 2013.

[160] D. Yang, "Targeting the P2X7 receptor in age-related macular degeneration," *Vision,* vol. 1, p. 11, 2017.

[161] E. Olivier, M. Dutot, A. Regazzetti, T. Leguillier, D. Dargere, N. Auzeil, O. Laprévote, and P. Rat, "P2X7-pannexin-1 and amyloid β-induced oxysterol input in human retinal cells: Role in age-related macular degeneration?," *Biochimie,* vol. 127, p. 70-78, 2016.

[162] B. J. Gu, P. N. Baird, K. A. Vessey, K. K. Skarratt, E. L. Fletcher, S. J. Fuller, A. J. Richardson, R. H. Guymer, and J. S. Wiley, "A rare functional haplotype of the P2RX4 and P2RX7 genes leads to loss of innate phagocytosis and confers increased risk of age-related macular degeneration," *The FASEB Journal,* vol. 27, p. 1479-1487, 2013.

[163] K. A. Vessey, B. J. Gu, A. I. Jobling, J. A. Phipps, U. Greferath, M. X. Tran, M. A. Dixon, P. N. Baird, R. H. Guymer, J. S. Wiley, and others, "Loss of function of P2X7 receptor scavenger activity in aging mice: a novel model for investigating the early pathogenesis of age-related macular degeneration," *The American journal of pathology,* vol. 187, p. 1670-1685, 2017.

[164] Y.-C. Tham, X. Li, T. Y. Wong, H. A. Quigley, T. Aung and C.-Y. Cheng, "Global prevalence of glaucoma and projections of glaucoma burden through 2040: a systematic review and meta-analysis," *Ophthalmology,* vol. 121, p. 2081-2090, 2014.

[165] D. Križaj, "What is glaucoma?," *Webvision: The Organization of the Retina and Visual System [Internet],* 2019.

[166] J. Kanski and B. Bowling, Kanski's Clinical Ophthalmology. A systematic approach, VIII ed, Elsevier, 2016.

[167] A. J. Baneke, K. S. Lim, and M. Stanford, "The pathogenesis of raised intraocular pressure in uveitis," *Current eye research,* vol. 41, p. 137-149, 2016.

[168] I. Soto and G. R. Howell, "The complex role of neuroinflammation in glaucoma," *Cold Spring Harbor perspectives in medicine,* vol. 4, p. a017269, 2014.

[169] K. Evangelho, M. Mogilevskaya, M. Losada-Barragan, and J. K. Vargas-Sanchez, "Pathophysiology of primary open-angle glaucoma from a

neuroinflammatory and neurotoxicity perspective: a review of the literature," *International ophthalmology,* vol. 39, p. 259-271, 2019.

[170] R. Vohra, J. C. Tsai, and M. Kolko, "The role of inflammation in the pathogenesis of glaucoma," *Survey of ophthalmology,* vol. 58, p. 311-320, 2013.

[171] G. Tezel, 'Oxidative stress in glaucomatous neurodegeneration: mechanisms and consequences,' *Progress in retinal and eye research,* vol. 25, p. 490-513, 2006.

[172] M. Aslan, S. Dogan and E. Kucuksayan, "Oxidative stress and potential applications of free radical scavengers in glaucoma," *Redox Report,* vol. 18, p. 76-87, 2013.

[173] P. A. Williams, N. Marsh-Armstrong, G. R. Howell, A. Bosco, J. Danias, J. Simon, A. Di Polo, M. H. Kuehn, S. Przedborski, M. Raff and others, "Neuroinflammation in glaucoma: a new opportunity," *Experimental eye research,* vol. 157, p. 20-27, 2017.

[174] L. P. Xue, J. Lu, Q. Cao, S. Hu, P. Ding, and E.-A. Ling, "Müller glial cells express nestin coupled with glial fibrillary acidic protein in experimentally induced glaucoma in the rat retina," *Neuroscience,* vol. 139, p. 723-732, 2006.

[175] N. M. Kerr, C. S. Johnson, C. R. Green and H. V. Danesh-Meyer, "Gap junction protein connexin43 (GJA1) in the human glaucomatous optic nerve head and retina," *Journal of Clinical Neuroscience,* vol. 18, p. 102-108, 2011.

[176] M. R. Hernandez, "The optic nerve head in glaucoma: role of astrocytes in tissue remodeling," *Progress in retinal and eye research,* vol. 19, p. 297-321, 2000.

[177] M.-N. Delyfer, V. Forster, N. Neveux, S. Picaud, T. Léveillard, and J.-A. Sahel, "Evidence for glutamate-mediated excitotoxic mechanisms during photoreceptor degeneration in the rd1 mouse retina," *Molecular vision,* vol. 11, p. 688-696, 2005.

[178] A. Bosco, S. D. Crish, M. R. Steele, C. O. Romero, D. M. Inman, P. J. Horner, D. J. Calkins, and M. L. Vetter, "Early reduction of microglia activation by irradiation in a model of chronic glaucoma," *PloS one,* vol. 7, 2012.

[179] A. Bosco, K. T. Breen, S. R. Anderson, M. R. Steele, D. J. Calkins, and M. L. Vetter, "Glial coverage in the optic nerve expands in proportion to optic axon loss in chronic mouse glaucoma," *Experimental eye research,* vol. 150, p. 34-43, 2016.

[180] S. Mélik Parsadaniantz, A. Réaux-le Goazigo, A. Sapienza, C. Habas and C. Baudouin,
"Glaucoma: A Degenerative Optic Neuropathy Related to Neuroinflammation?," *Cells,* vol. 9, p. 535, 2020.

[181] X. Wei, K.-S. Cho, E. F. Thee, M. J. Jager, and D. F. Chen, "Neuroinflammation and microglia in glaucoma: time for a paradigm shift," *Journal of neuroscience research,* vol. 97, p. 70-76, 2019.

[182] G. R. Howell, I. Soto, X. Zhu, M. Ryan, D. G. Macalinao, G. L. Sousa, L. B. Caddle, K. H. MacNicoll, J. M. Barbay, V. Porciatti and others, "Radiation treatment inhibits monocyte entry into the optic nerve head and prevents neuronal damage in a mouse model of glaucoma," *The Journal of clinical investigation,* vol. 122, p. 1246-1261, 2012.

[183] K. Midwood, S. Sacre, A. M. Piccinini, J. Inglis, A. Trebaul, E. Chan, S. Drexler, N. Sofat, M. Kashiwagi, G. Orend and others, "Tenascin-C is an endogenous activator of Toll-like receptor 4 that is essential for maintaining inflammation in arthritic joint disease," *Nature medicine,* vol. 15, p. 774, 2009.

[184] C. Luo, X. Yang, A. D. Kain, D. W. Powell, M. H. Kuehn, and G. Tezel, "Glaucomatous tissue stress and the regulation of immune response through glial Toll-like receptor signaling," *Investigative ophthalmology & visual science,* vol. 51, p. 5697-5707, 2010.

[185] G. Tezel, X. Yang, C. Luo, J. Cai and D. W. Powell, "An astrocyte-specific proteomic approach toInflammatory responses in experimental rat glaucoma," *Investigative ophthalmology & visual science,* vol. 53, p. 4220-4233, 2012.

[186] S. K. Dubey, J. F. Hejtmancik, S. R. Krishnadas, R. Sharmila, A. Haripriya, and P. Sundaresan, "Evaluation of genetic polymorphisms in clusterin and tumor necrosis factor-alpha genes in South Indian individuals with pseudoexfoliation syndrome," *Current eye research,* vol. 40, p. 1218-1224, 2015.

[187] T. Nakazawa, C. Nakazawa, A. Matsubara, K. Noda, T. Hisatomi, H. She, N. Michaud, A. Hafezi-Moghadam, J. W. Miller, and L. I. Benowitz, "Tumor necrosis factor-α mediates oligodendrocyte death and delayed retinal ganglion cell loss in a mouse model of glaucoma," *Journal of Neuroscience,* vol. 26, p. 12633-12641, 2006.

[188] B. Burgos-Blasco, B. Vidal-Villegas, F. Saenz-Frances, L. Morales-Fernandez, L. Perucho-Gonzalez, J. Garcia-Feijoo, and J. M. Martinez-de-la-Casa, "Tear and aqueous humour cytokine profile in primary open-angle glaucoma," *Acta Ophthalmologica,* 2020.

[189] L. Dong, Y. Hu, L. Zhou and X. Cheng, "P2X7 receptor antagonist protects retinal ganglion cells by inhibiting microglial activation in a rat chronic ocular hypertension model," *Molecular medicine reports,* vol. 17, p. 2289-2296, 2018.

[190] Y. Zhang, Y. Xu, Q. Sun, S. Xue, H. Guan, and M. Ji, "Activation of P2X7R-NLRP3 pathway in Retinal microglia contribute to Retinal Ganglion Cells death in chronic ocular hypertension (COH)," *Experimental eye research,* vol. 188, p. 107771, 2019.

[191] W. Lu, F. Albalawi, J. M. Beckel, J. C. Lim, A. M. Laties, and C. H. Mitchell, "The P2X7 receptor links mechanical strain to cytokine IL-6 up-regulation and release in neurons and astrocytes," *Journal of neurochemistry,* vol. 141, p. 436-448, 2017.

[192] M. J. P. de Lara, M. Avilés-Trigueros, A. Guzmán-Aránguez, F. J. Valiente-Soriano, P. de la Villa, M. Vidal-Sanz, and J. Pintor, "Potential role of P2X7 receptor in neurodegenerative processes in a murine model of glaucoma," *Brain research bulletin,* vol. 150, p. 61-74, 2019.

[193] K. Sakamoto, K. Endo, T. Suzuki, K. Fujimura, Y. Kurauchi, A. Mori, T. Nakahara and K. Ishii, "P2X7 receptor antagonists protect against N-methyl-D-aspartic acid-induced neuronal injury in the rat retina," *European journal of pharmacology,* vol. 756, p. 52- 58, 2015.

[194] A. G. P. Konstas and A. Ringvold, "Epidemiology of exfoliation syndrome," *Journal of glaucoma,* vol. 27, p. S4-S11, 2018.

[195] M. Zenkel and U. Schlötzer-Schrehardt, "The composition of exfoliation material and the cells involved in its production," *Journal of glaucoma,* vol. 23, p. S12-S14, 2014.

[196] R. Ritch and U. Schlötzer-Schrehardt, 'Exfoliation syndrome,' *Survey of ophthalmology,* vol. 45, p. 265-315, 2001.

[197] R. Ritch, "Ocular Findings in Exfoliation Syndrome," *Journal of glaucoma,* vol. 27, p. S67-S71, 2018.

[198] R. Ritch, 'The management of exfoliative glaucoma,' *Progress in brain research,* vol. 173, p. 211-224, 2008.

[199] J. Gottanka, C. Flügel-Koch, P. Martus, D. H. Johnson and E. Lütjen-Drecoll, "Correlation of pseudoexfoliative material and optic nerve damage in pseudoexfoliation syndrome," *Investigative ophthalmology & visual science,* vol. 38, p. 2435-2446, 1997.

[200] M. C. Leske, A. Heijl, L. Hyman, B. Bengtsson, L. Dong, Z. Yang, E. M. G. T. Group and others, "Predictors of long-term progression in the early manifest glaucoma trial," *Ophthalmology,* vol. 114, p. 1965-1972, 2007.

[201] A. Heijl, B. Bengtsson, L. Hyman, M. C. Leske, E. M. G. T. Group and others, 'Natural history of open-angle glaucoma,' *Ophthalmology,* vol. 116, p. 2271-2276, 2009.

[202] L. Hyman, A. Heijl, M. C. Leske, B. Bengtsson, and Z. Yang, "Natural history of intraocular pressure in the early manifest glaucoma trial: a 6-year follow-up," *Archives of ophthalmology,* vol. 128, p. 601-607, 2010.

[203] R. Ritch, "Ocular and systemic manifestations of exfoliation syndrome," *Journal of glaucoma,* vol. 23, p. S1-S8, 2014.

[204] R. E. Davis and J. S. Schuman, *Pseudoexfoliation syndrome: don't brush it off,* BMJ Publishing Group Ltd, 2013.

[205] G. L. Kanthan, P. Mitchell, G. Burlutsky, E. Rochtchina and J. J. Wang, "Pseudoexfoliation syndrome and the long-term incidence of cataract and cataract surgery: the blue mountains eye study," *American journal of ophthalmology,* vol. 155, p. 83-88, 2013.

[206] E. Anastasopoulos, P. Founti, and F. Topouzis, "Update on pseudoexfoliation syndrome pathogenesis and associations with intraocular pressure, glaucoma and systemic diseases," *Current opinion in ophthalmology,* vol. 26, p. 82-89, 2015.

[207] W. Wang, M. He, M. Zhou, and X. Zhang, "Ocular pseudoexfoliation syndrome and vascular disease: a systematic review and meta-analysis," *PloS one,* vol. 9, 2014.

[208] J. Djordjevic-Jocic, P. Jovanovic, M. Bozic, A. Tasic, and Z. Rancic, "Prevalence and early detection of abdominal aortic aneurysm in pseudoexfoliation syndrome and pseudoexfoliation glaucoma," *Current eye research,* vol. 37, p. 617-623, 2012.

[209] M. R. Praveen, S. K. Shah, A. R. Vasavada, R. P. Diwan, S. M. Shah, B. R. Zumkhawala, and R. Thomas, "Pseudoexfoliation as a risk factor for peripheral vascular disease: a case-control study," *Eye,* vol. 25, p. 174-179, 2011.

[210] K. A. Gonen, T. Gonen, and B. Gumus, "Renal artery stenosis and abdominal aorta aneurysm in patients with pseudoexfoliation syndrome," *Eye,* vol. 27, p. 735-741, 2013.

[211] T. Cumurcu, F. Dorak, B. E. Cumurcu, L. G. Erbay and E. Ozsoy, "Is there any relation between pseudoexfoliation syndrome and Alzheimer's type dementia?," in *Seminars in ophthalmology*, 2013.

[212] S. Yazdani, A. Tousi, M. Pakravan, and A.-R. Faghihi, "Sensorineural hearing loss in pseudoexfoliation syndrome," *Ophthalmology,* vol. 115, p. 425-429, 2008.

[213] S. E. Gökce and M. I. Gökce, "Relationship between pseudoexfoliation syndrome and erectile dysfunction: a possible cause of endothelial dysfunction for development of erectile dysfunction," *International braz j urol,* vol. 41, p. 547-551, 2015.

[214] B. M. Wirostko, K. Curtin, R. Ritch, S. Thomas, K. Allen-Brady, K. R. Smith, G. S. Hageman, and R. R. Allingham, "Risk for exfoliation syndrome in women with pelvic organ prolapse: a Utah Project on Exfoliation Syndrome (UPEXS) study," *JAMA ophthalmology,* vol. 134, p. 1255-1262, 2016.

[215] G. Thorleifsson, K. P. Magnusson, P. Sulem, G. B. Walters, D. F. Gudbjartsson, H.
Stefansson, T. Jonsson, A. Jonasdottir, G. Stefansdottir and others,

"Common sequence variants in the LOXL1 gene confer susceptibility to glaucoma exfoliation," *Science,* vol. 317, p. 1397-1400, 2007.

[216] T. T. Khan, G. Li, I. D. Navarro, R. D. Kastury, C. J. Zeil, T. M. Semchyshyn, F. J. Moya, D. L. Epstein, P. Gonzalez, and P. Challa, "LOXL1 expression in lens capsule tissue specimens from individuals with pseudoexfoliation syndrome and glaucoma," *Molecular vision,* vol. 16, p. 2236, 2010.

[217] M. Ghaffari Sharaf, K. F. Damji, and L. D. Unsworth, "Recent advances in risk factors associated with ocular exfoliation syndrome," *Acta ophthalmologica,* vol. 98, p. 113- 120, 2020.

[218] U. Schlötzer-Schrehardt, M. Zenkel, M. Küchle, L. Y. Sakai and G. O. H. Naumann,
"Role of transforming growth factor-β1 and its latent form binding protein in pseudoexfoliation syndrome," *Experimental eye research,* vol. 73, p. 765-780, 2001.

[219] U. Schlötzer-Schrehardt, J. Lommatzsch, M. Küchle, A. G. P. Konstas, and G. O. H. Naumann, "Matrix metalloproteinases and their inhibitors in aqueous humor of patients with pseudoexfoliation syndrome/glaucoma and primary open-angle glaucoma," *Investigative ophthalmology & visual science,* vol. 44, p. 1117-1125, 2003.

[220] J. H. Kang, S. J. Loomis, J. L. Wiggs, W. C. Willett, and L. R. Pasquale, "A prospective study of folate, vitamin B6, and vitamin B12 intake in relation to exfoliation glaucoma or suspected exfoliation glaucoma," *JAMA ophthalmology,* vol. 132, p. 549-559, 2014.

[221] A. Want, S. R. Gillespie, Z. Wang, R. Gordon, C. Iomini, R. Ritch, J. M. Wolosin, and A. M. Bernstein, "Autophagy and mitochondrial dysfunction in tenon fibroblasts from exfoliation glaucoma patients," *PloS one,* vol. 11, 2016.

[222] Y. A. Yaz, N. Yıldırım, Y. Yaz, N. Tekin, M. İnal, and F. M. Şahin, "Role of oxidative stress in pseudoexfoliation syndrome and pseudoexfoliation glaucoma," *Turkish journal of ophthalmology,* vol. 49, p. 61, 2019.

[223] S. Romeo Villadóniga, E. Rodrıguez Garćıa , O. Sagastágoia Epelde, M. D. Álvarez Dıaz, D. Pedrol, and J. Carleś , "Effects of Oral Supplementation with Docosahexaenoic Acid (DHA) plus Antioxidants in Pseudoexfoliative Glaucoma: A 6-Month OpenLabel Randomized Trial," *Journal of ophthalmology,* vol. 2018, 2018.

[224] T. S. Sarenac Vulovic, S. M. Pavlovic, and N. S. Zdravkovic, "Proinflammatory cytokines induce XFG development," *Ocular immunology and inflammation,* vol. 24, p. 671- 677, 2016.

[225] Z. Yildirim, F. Yildirim, N. I. Uçgun and A. Sepici-Dinçel, "The role of the cytokines in the pathogenesis of pseudoexfoliation syndrome," *International journal of ophthalmology,* vol. 6, p. 50, 2013.

[226] T. Sarenac Vulovic, S. Pavlovic, M. Lutovac, V. Zdravkovic, S. Sreckovic and N.
Zdravkovic, 'Regulatory cytokines prescribe the outcome of the inflammation in the
process of pseudoexfoliation production," *Journal of the Chinese Medical Association,* vol. 82, p. 935-940, 2019.

[227] T. Gonen, S. Guzel, and K. H. Keskinbora, "YKL-40 is a local marker for inflammation in patients with pseudoexfoliation syndrome," *Eye,* vol. 33, p. 772-776, 2019.

[228] M. Borazan, A. Karalezli, C. Kucukerdonmez, N. Bayraktar, S. Kulaksizoglu, A. Akman and Y. A. Akova, "Aqueous humor and plasma levels of vascular endothelial growth factor and nitric oxide in patients with pseudoexfoliation syndrome and pseudoexfoliation glaucoma," *Journal of glaucoma,* vol. 19, p. 207-211, 2010.

[229] S. C. Koukoula, A. Katsanos, I. K. Tentes, G. Labiris, and V. P. Kozobolis, "Retrobulbar hemodynamics and aqueous humor levels of endothelin-1 in exfoliation syndrome and exfoliation glaucoma," *Clinical ophthalmology (Auckland, NZ),* vol. 12, p. 1199, 2018.

[230] P. Gain, R. Jullienne, Z. He, M. Aldossary, S. Acquart, F. Cognasse, and G. Thuret, "Global survey of corneal transplantation and eye banking," *JAMA ophthalmology,* vol. 134, p. 167-173, 2016.

[231] J. A. Bonanno, 'Identity and regulation of ion transport mechanisms in the corneal endothelium,' *Progress in retinal and eye research,* vol. 22, p. 69-94, 2003.

[232] A. O. Eghrari, S. A. Riazuddin, and J. D. Gottsch, "Fuchs corneal dystrophy," in *Progress in molecular biology and translational science,* vol. 134, Elsevier, 2015, p. 79-97.

[233] M. Matthaei, A. Hribek, T. Clahsen, B. Bachmann, C. Cursiefen, and A. S. Jun, "Fuchs endothelial corneal dystrophy: Clinical, genetic, pathophysiologic, and therapeutic aspects," *Annual review of vision science,* vol. 5, p. 151-175, 2019.

[234] J. Zhang, C. N. J. McGhee and D. V. Patel, "The molecular basis of fuchs' endothelial corneal dystrophy," *Molecular diagnosis & therapy,* vol. 23, p. 97-112, 2019.

[235] X. Zhang, R. P. Igo, J. Fondran, V. V. Mootha, M. Oliva, K. Hammersmith, A. Sugar, J. H. Lass, and S. K. Iyengar, "Association of smoking and other risk factors with Fuchs' endothelial corneal dystrophy severity and corneal thickness," *Investigative ophthalmology & visual science,* vol. 54, p. 5829-5835, 2013.

[236] U. V. Jurkunas, "Fuchs endothelial corneal dystrophy through the prism of oxidative stress," *Cornea,* vol. 37, p. S50-S54, 2018.

[237] M. Matthaei, H. Meng, A. K. Meeker, C. G. Eberhart and A. S. Jun, "Endothelial Cdkn1a
(p21) overexpression and accelerated senescence in a mouse model of Fuchs endothelial corneal dystrophy," *Investigative ophthalmology & visual science,* vol. 53, p. 6718-6727, 2012.

[238] U. V. Jurkunas, M. S. Bitar, T. Funaki, and B. Azizi, "Evidence of oxidative stress in the pathogenesis of fuchs endothelial corneal dystrophy," *The American journal of pathology,* vol. 177, p. 2278-2289, 2010.

[239] G. G. Nanda and D. P. Alone, "Current understanding of the pathogenesis of Fuchs' endothelial corneal dystrophy," *Molecular vision,* vol. 25, p. 295, 2019.

[240] B. Azizi, A. Ziaei, T. Fuchsluger, T. Schmedt, Y. Chen, and U. V. Jurkunas, "p53regulated increase in oxidative-stress-induced apoptosis in Fuchs endothelial corneal dystrophy: a native tissue model," *Investigative ophthalmology & visual science,* vol. 52, p. 9291-9297, 2011.

[241] M. Nita and A. Grzybowski, "The role of the reactive oxygen species and oxidative stress in the pathomechanism of age-related ocular diseases and other pathologies of the anterior and posterior eye segments in adults," *Oxidative Medicine and Cellular Longevity,* vol. 2016, 2016.

[242] N. Okumura, K. Hashimoto, M. Kitahara, H. Okuda, E. Ueda, K. Watanabe, M. Nakahara, T. Sato, S. Kinoshita, T. Tourtas and others, "Activation of TGF-β signaling induces cell death via the unfolded protein response in Fuchs endothelial corneal dystrophy," *Scientific reports,* vol. 7, p. 1-12, 2017.

[243] S. O. Tone, V. Kocaba, M. Böhm, A. Wylegala, T. L. White, and U. V. Jurkunas, "Fuchs endothelial corneal dystrophy: The vicious cycle of fuchs pathogenesis," *Progress in Retinal and Eye Research,* p. 100863, 2020.

[244] N. J. S. London, S. R. Rathinam, and E. T. Cunningham, "The epidemiology of uveitis in developing countries," *International Ophthalmology Clinics,* vol. 50, p. 1-17, 2010.

[245] A. D. Dick, N. Tundia, R. Sorg, C. Zhao, J. Chao, A. Joshi, and M. Skup, "Risk of ocular complications in patients with noninfectious intermediate uveitis, posterior uveitis, or panuveitis," *Ophthalmology,* vol. 123, p. 655-662, 2016.

[246] D. A. Jabs, R. B. Nussenblatt, J. T. Rosenbaum, Standardization of Uveitis Nomenclature (SUN) Working Group and others, "Standardization of uveitis nomenclature for reporting clinical data. Results of the First International Workshop," *American journal of ophthalmology,* vol. 140, p. 509-516, 2005.

[247] N. D. Heuss, U. Lehmann, C. C. Norbury, S. W. McPherson, and D. S. Gregerson, "Local activation of dendritic cells alters the pathogenesis of autoimmune disease in the retina," *The Journal of Immunology,* vol. 188, p. 1191-1200, 2012.

[248] A. S. Postole, A. B. Knoll, G. U. Auffarth, and F. Mackensen, "In vivo confocal microscopy of inflammatory cells in the corneal subbasal nerve plexus in patients with different subtypes of anterior uveitis," *British Journal of Ophthalmology,* vol. 100, p. 1551-1556, 2016.

[249] J. H. Chang, P. McCluskey and D. Wakefield, "Expression of toll-like receptor 4 and its associated lipopolysaccharide receptor complex by resident antigen-presenting cells in the human uvea," *Investigative ophthalmology & visual science,* vol. 45, p. 1871- 1878, 2004.

[250] W. Lin, T. Liu, B. Wang, and H. Bi, "The role of ocular dendritic cells in uveitis," *Immunology letters,* 2019.

[251] J. E. Weinstein and K. L. Pepple, "Cytokines in uveitis," *Current opinion in ophthalmology,* vol. 29, p. 267-274, 2018.

[252] B. J. E. Raveney, D. A. Copland, A. D. Dick, and L. B. Nicholson, "TNFR1-dependent regulation of myeloid cell function in experimental autoimmune uveoretinitis," *The Journal of Immunology,* vol. 183, p. 2321-2329, 2009.

[253] "Humira, adalimumab," EMA- European Medicines Agency, [Online]. Available: https://www.ema.europa.eu/en/medicines/human/EPAR/humira. [Consulted on 3 June 2020].

[254] T. Yoshimura, K.-H. Sonoda, N. Ohguro, Y. Ohsugi, T. Ishibashi, D. J. Cua, T. Kobayashi, H. Yoshida, and A. Yoshimura, "Involvement of Th17 cells and the effect of anti-IL-6 therapy in autoimmune uveitis," *Rheumatology,* vol. 48, p. 347-354, 2009.

[255] J. Tode, E. Richert, S. Koinzer, A. Klettner, U. Pickhinke, C. Garbers, S. Rose-John, B. Nölle, and J. Roider, "Intravitreal injection of anti-Interleukin (IL)-6 antibody attenuates experimental autoimmune uveitis in mice," *Cytokine,* vol. 96, p. 8-15, 2017.

[256] S. Karkhur, M. Hasanreisoglu, E. Vigil, M. S. Halim, M. Hassan, C. Plaza, N. V. Nguyen, R. Afridi, A. T. Tran, D. V. Do and others, "Interleukin-6 inhibition in the management of non-infectious uveitis and beyond," *Journal of ophthalmic inflammation and infection,* vol. 9, p. 17, 2019.

[257] K. G.-J. Ooi, G. Galatowicz, V. L. Calder, and S. L. Lightman, "Cytokines and chemokines in uveitis-Is there a correlation with clinical phenotype?," *Clinical medicine & research,* vol. 4, p. 294-309, 2006.

[258] A. D. Dick, 'Immune mechanisms of uveitis: insights into disease pathogenesis and treatment,' *International ophthalmology clinics,* vol. 40, p. 1-18, 2000.

[259] M. Inoue and K. Kadonosono, "Macular diseases: epiretinal membrane," in *Microincision Vitrectomy Surgery*, vol. 54, Karger Publishers, 2014, p. 159-163.

[260] M. Joshi, S. Agrawal and J. B. Christoforidis, "Inflammatory mechanisms of idiopathic epiretinal membrane formation," *Mediators of inflammation,* vol. 2013, 2013.

[261] S. Myojin, T. Yoshimura, S. Yoshida, A. Takeda, Y. Murakami, Y. Kawano, Y. Oshima, T. Ishibashi, and K.-H. Sonoda, "Gene expression analysis of the irrigation solution samples collected during vitrectomy for idiopathic epiretinal membrane," *PloS one,* vol. 11, 2016.

[262] C. Harada, T. Harada, Y. Mitamura, H. M. Quah, K. Ohtsuka, S. Kotake, S. Ohno, K. Wada, S. Takeuchi, and K. Tanaka, "Diverse NF-kappaB expression in epiretinal membranes after human diabetic retinopathy and proliferative vitreoretinopathy," *Mol Vis,* vol. 10, p. 31-36, 2004.

[263] R. I. Kohno, Y. Hata, S. Kawahara, T. Kita, R. Arita, Y. Mochizuki, L. P. Aiello, and T. Ishibashi, "Possible contribution of hyalocytes to idiopathic epiretinal membrane formation and its contraction," *British Journal of Ophthalmology,* vol. 93, p. 1020- 1026, 2009.

[264] D. J. Kauffmann, J. C. Van Meurs, D. A. Mertens, E. Peperkamp, C. Master, and M. E. Gerritsen, "Cytokines in vitreous humor: interleukin-6 is elevated in proliferative vitreoretinopathy," *Investigative ophthalmology & visual science,* vol. 35, p. 900-906, 1994.

[265] S. J. Burke, D. Lu, T. E. Sparer, T. Masi, M. R. Goff, M. D. Karlstad and J. J. Collier,
"NF-κB and STAT1 control CXCL1 and CXCL2 gene transcription," *American Journal of Physiology-Endocrinology and Metabolism,* vol. 306, p. E131-E149, 2014.

ID	DoB	Età	SESSO	OCCHIO	INTERVENTO	DATA INTERVENTO	MATERIALE PRELEVATO	TOT materiale prelevato	num di campioni	PATOLOGIA PRINCIPALE	ALTRE PATO OCULARI	PATO SISTEMICHE	P2X7r pg/ml	II analisi [P2X7r]	medie
A1	02/12/54	64	M	OD	FACO+IOL	27/03/19	Acqueo	0,1 ml	2 (x 0,05 ml)	Cataratta corticonucleare	/	Diabete NID, ipercolesterolemia			
A2	18/08/44	74	M	OD	FACO+IOL	27/03/19	Acqueo	0,1 ml	2 (x 0,05 ml)	Cataratta corticonucleare	/	Epatite (HBV/HCV?), tifo, ipert.art., IPB			
A3	13/12/60	58	M	OS	FACO+IOL	27/03/19	Acqueo	0,05 ml	1 (x 0,05 ml)	Cataratta sottocapsulare posteriore	Ciclite eterocromica di Fuchs	/			
A4	02/09/42	76	M	OS	ICCE+FS+VVPP	28/03/19	Acqueo	0,2 ml	2 (x 0,1 ml)	Sublussazione cristallino	OS PEX, iridofacodonesi, scarsa midriasi, ipertono; OD ambliopia	BPCO, OSAS in CPAP, bioprotesi aortica, cardiopatia ischemica cronica, NSTEMI 2005 PTC+BMS, NSTEMI 2012 PTCA+DES, PTCA+stent ramo circonflesso medio-distale, ipert.art., IPB, IRC IIIA, iperuricemia			
A5	22/02/63	56	M	OS	FACO+IOL	02/04/19	Acqueo	0,2 ml	2 (x 0,1 ml)	Cataratta corticonucleare e sottocapsulare posteriore	scarsa midriasi	ipert. art., tp ASA	20,11826		
A6	18/10/63	55	M	OS	Rimozione PDMS	02/04/19	Acqueo	0,2 ml	2 (x 0,1 ml)	Esiti di DDR, PDMS pesante dalla CV	Pseudofachia		23,40733		
A7	06/09/51	67	M	OS	Vitrectomia	03/04/19	Acqueo	0,2 ml	2 (x 0,1 ml)	Emovitreo in retinopatia diabetica	retinopatia diabetica, trazione vitreo-retinica inferiore, impianto Desametasone ivt in OO nel 2017, FACO+IOL+VVPP+PEELING MER+TAIOFTAL in OD 5/2018 in OS 12/2018, tp Combigan coll OO 2 vv/die	diabete ID, ipert.art., ritenzione urinaria, IPB in tp Omnic, tp ASA			
A8	20/09/45	73	F	OS	FACO+IOL	04/04/19	Acqueo	0,05 ml	1 (x 0,05 ml)	Cataratta nucleare	Glaucoma oo, tp Cosopt coll	ipert.art.	4,562467		
A9	27/06/30	88	F	OS	FACO+IOL	04/04/19	Acqueo	0,1 ml	2 (x 0,05 ml)	Cataratta ambroide	PEX OO, scarsa midriasi, iridotomie OO	ipert.art., tremore senile			
A10	09/01/38	81	F	OD	FACO+IOL	04/04/19	Acqueo	0,05 ml	1 (x 0,05 ml)	Cataratta corticonucleare	guttae endoteliali e scarsa conta endoteliale	ipert.art., FA in tp coumadin	6,12129		

ID	DoB	Età	SESSO	OCCHIO	INTERVENTO	DATA INTERVENTO	MATERIALE PRELEVATO	TOT materiale prelevato	num di campioni	PATOLOGIA PRINCIPALE	ALTRE PATO OCULARI	PATO SISTEMICHE	P2X7r pg/ml	II analisi [P2X7r]	medie
A11	09/12/46	72	M	OS	FACO+IOL	04/04/19	Acqueo	0,05 ml	1 (x 0,05 ml)	Cataratta nucleare	Trabeculectomia OO (circa 30 aa fa), glaucoma OO, non tp antiglaucomatosa in atto	fumatore, iperuricemia in tp	4,855588		
A12	05/09/45	73	M	OD	FACO+IOL+VVPP+	04/04/19	Acqueo	0,2 ml	2 (x 0,1 ml)	Cataratta+pucker maculare	retinopatia diabetica, pregresso intervento FACO+IOL+VVPP+PEELING MER in OS 9/2018	DMID, pregresso IMA (2014) PTCA+STENT, TEA carotide dx, ipert.art., tp ASA, BPCO di grado moderato			
A13	22/04/39	80	F	OS	FACO+IOL	10/04/19	Acqueo	0,05 ml	1 (x 0,05 ml)	Cataratta nucleare	pregressa uveite OD, qualche gutta endoteliale, cornea verticillata da amiodarone	pacemaker, ipert.art., FA con bradi-tachicardia in tp Eliquis (NAO), artrite reumatoide			
A14	21/12/72	46	F	OD	FACO+IOL	11/04/19	Acqueo	0,1 ml	2 (x 0,05 ml)	Cataratta nucleare	miopia elevata(-20 D), monocola funzionale per ambliopia OS, in OD esiti di trattamento laser periferia inferiore	/	9,765372		
A15	01/11/37	82	F	OD	FACO+IOL	11/04/19	Acqueo	0,05 ml	1 (x 0,05 ml)	Cataratta nucleare	distrofia maculare	FA in tp TAO (coumadin), ipert.art., pregresso CA mammario asportato e in tp Tamoxifene	3,950411		
A16	08/07/44	74	F	OS	FACO+IOL	11/04/19	Acqueo	0,1 ml	2 (x 0,05 ml)	Cataratta nucleare	Monocola funzionale (ambliopia OD),	ipotiroidismo in tp, fumatrice	6,054463		
A17	05/05/30	88	F	OS	FACO+IOL	11/04/19	Acqueo	0,1 ml	2 (x 0,05 ml)	Cataratta corticonucleare e sottocapsulare posteriore	/	ipert.art., FA in tp NAO (Apixaban), decadimento cognitivo,ermia gastro-iatale	6,9523		
A18	21/07/40	79	M	OD	FACO+IOL	10/09/19	Acqueo	0,05 ml	1(x 0,05 ml)	Cataratta in PEX	PEX, scarsa midriasi	DMID, ipert. Art., tp ASA	6,12129	324,2988	165,21
A19	03/01/31	88	F	OD	Vitrectomia	10/09/19	Acqueo	0,05 ml	1(x 0,05 ml)	IOL sub lussata	PEX, scarsa midriasi		5,661329	226,4818	116,0716
A20	01/12/47	71	F	OD	FACO+IOL	10/09/19	Acqueo	0,05 ml	1(x 0,05 ml)	Cataratta	media midriasi	ipert.art. tp ASA HCV+	49,95423		

ID	DoB	Età	SESSO	OCCHIO	INTERVENTO	DATA INTERVENTO	MATERIALE PRELEVATO	TOT materiale prelevato	num di campioni	PATOLOGIA PRINCIPALE	ALTRE PATO OCULARI	PATO SISTEMICHE	P2X7r pg/ml	II analisi [P2X7r]	medie
A21	27/03/40	69	M	OD	FACO+IOL	10/09/19	Acqueo	0,05 ml	1(x 0,05 ml)	Cataratta in glaucoma+ EMD	EMD, glaucoma	DMID, tp ASA	277,04715		
A22	13/04/37	82	M	OS	FACO+IOL	26/09/19	Acqueo	0,05 ml	1(x 0,05 ml)	Cataratta		DMID pregresso IMA, BPCO, tp ASA	7,52952		
A23	23/01/39	80	F	OD	FACO+IOL	26/09/19	Acqueo	0,05 ml	1(x 0,05 ml)	Cataratta	PEX, Atrofia orletto pupillare				
A24	07/08/41	78	F	OS	FACO+IOL	26/09/19	Acqueo	0,05 ml	1(x 0,05 ml)	Cataratta	miopia, conta endoteliale<2000, monocolo funzionale	FA in NAO	4,216871	20,70853	12,4627
A25	06/08/53	66	M	OS	FACO+IOL	26/09/19	Acqueo	0,05 ml	1(x 0,05 ml)	Cataratta			8,339797	9,834711	9,09
A26	06/05/48	71	M	OD	FACO+IOL	26/09/19	Acqueo	0,05 ml	1(x 0,05 ml)	Cataratta		plavix (tp ASA), ipert. Art.	14,19096		
A27	25/12/37	81	F	OD	FACO+IOL	02/10/19	Acqueo	0,05 ml	1(x 0,05 ml)	Cataratta	Esiti di MBL OD		63,90051		
A28	20/12/31	87	F	OS	FACO+IOL	02/10/19	Acqueo	0,05 ml	1(x 0,05 ml)	Cataratta		HBV+, pm in coumadin	7,3085		
A29	15/10/46	73	M	OD	Vitrectomia	15/10/19	Acqueo	0,05 ml	1(x 0,05 ml)	Foro maculare			7,685823	129,0907	68,38826
A30	13/02/74	45	M	OS	Vitrectomia	15/10/19	Acqueo	0,05 ml	1(x 0,05 ml)	Distacco di retina	DDR/cataratta		81,72063	122,3045	102,0126
A31	11/08/52	67	M	OS	FACO+IOL	06/11/19	Acqueo	0,05 ml	1(x 0,05 ml)	Cataratta	OVP, Ozurdex		8,833663		
A32	19/05/39	80	M	OS	FACO+IOL	06/11/19	Acqueo	0,05 ml	1(x 0,05 ml)	Cataratta	miopia elevata		36,77348		
A33	07/12/37	81	M	OD	FACO+IOL	20/11/19	Acqueo	0,05 ml	1(x 0,05 ml)	Cataratta		DMID, ipert. Art., tp ASA	5,219639		
A34	12/08/50	69	F	OD	FACO+IOL	20/11/19	Acqueo	0,05 ml	1(x 0,05 ml)	Cataratta		DMID + oha, tp asa	36,84541		
A35	23/07/37	82	M	OS	FACO+IOL	26/11/19	Acqueo	0,05 ml	1(x 0,05 ml)	Cataratta		DMID, tp asa, tp ominic per IPB			
A36	22/11/47	72	M	OD	FACO+IOL	26/11/19	Acqueo	0,05 ml	1(x 0,05 ml)	Cataratta	PEX, scarsa midriasi				
A37	23/10/40	79	M	OS	FACO+IOL	27/11/19	Acqueo	0,05 ml	1(x 0,05 ml)	Cataratta		DMNID, preg ima(ptca+stent), ipta, tp NAO, Ateromasia tsa	38,99443		
A38	26/10/36	83	M	OS	FACO+IOL	27/11/19	Acqueo	0,05 ml	1(x 0,05 ml)	Cataratta	iridotomia, guttae in OD, media midriasi	PM, tp NAO, ipta			
A39	11/07/41	78	M	OD	FACO+IOL	27/11/19	Acqueo	0,05 ml	1(x 0,05 ml)	Cataratta		pregr tia, pregr ima, ipta, tp asa, cardiopatia ischemica, tp alfa litico	13,24029	19,05258	16,14644
A40	18/04/45	74	F	OD	FACO+IOL	27/11/19	Acqueo	0,05 ml	1(x 0,05 ml)	Cataratta		ipta	10,68009	15,81643	13,24826
A41	27/03/36	83	M	OD	FACO+IOL	28/11/19	Acqueo	0,05 ml	1(x 0,05 ml)	Cataratta			52,75389		
A42	01/12/44	74	M	OD	FACO+IOL	28/11/19	Acqueo	0,05 ml	1(x 0,05 ml)	Cataratta		DMID, Coumadin, sost valv aortica, Ipta, cardura	37,35612		

ID	DoB	Età	SESSO	OCCHIO	INTERVENTO	DATA INTERVENTO	MATERIALE PRELEVATO	TOT materiale prelevato	num di campioni	PATOLOGIA PRINCIPALE	ALTRE PATO OCULARI	PATO SISTEMICHE	P2X7r pg/ml	II analisi [P2X7r]	medie
A43	29/08/34	85	F	OD	FACO+IOL	28/11/19	Acqueo	0,05 ml	1(x 0,05 ml)	Cataratta	Glaucoma, monocola, pregressa trabeculectomia	DMID	9,18481	3,093247	6,139029
A44	21/06/43	76	M	OS	FACO+IOL	28/11/19	Acqueo	0,05 ml	1(x 0,05 ml)	Cataratta		IPTA	25,06091		
A45	12/09/36	83	F	OS	FACO	03/12/19	Acqueo	0,05 ml	1(x0,05 ml)	Cataratta	Cataratta in dmle os	tp asa allergia penicilline	44,36212		
A46	18/05/38	81	F	OD	FACO+IOL	04/12/19	Acqueo	0,05 ml	1(x0,05 ml)	Cataratta	Distrofia endoteliale di Fuchs		11,38823		
A47	11/09/78	41	M	OS	FACO+IOL	05/12/19	Acqueo	0,05 ml	1(x0,05 ml)	Cataratta totale			23,7706		
A48	20/05/35	84	M	OD	FACO+IOL	05/12/19	Acqueo	0,05 ml	1(x0,05 ml)	Cataratta	PEX, ca ipoprofonda				
A49	07/03/42	77	F	OS	FACO+IOL	05/12/19	Acqueo	0,05 ml	1(x0,05 ml)	Cataratta	ca ipoprofonda, scarsa midriasi	tp asa			
A50	25/12/38	80	F	OD	FACO+IOL	10/12/19	Acqueo	0,05 ml	1(x0,05 ml)	Cataratta	DMLE e glaucoma od		13,09409	16,84752	14,97081
A51	04/10/40	79	F	OS	FACO+IOL	10/12/19	Acqueo	0,05 ml	1(x0,05 ml)	Cataratta		ipt art, esiti mastectomia	35,72396	32,01065	33,86731
A52	11/06/54	65	F	OS	FACO+IOL	09/01/20	Acqueo	0,05 ml	1(x0,05 ml)	Cataratta	Retinopatia diabetica, media midriasi	DMID, favismo			
A53	17/06/50	69	M	OD	FACO+IOL	22/01/20	Acqueo	0,05 mL	1(x0,05 ml)	Cataratta nucleare densa	PEX, distrofia maculare, scarsa midriasi	tp clopidogrel			
A54	23/09/31	88	F	OS	FACO+IOL	22/01/20	Acqueo	0,05 mL	1(x0,05 ml)	Cataratta nucleare densa con riflessi ambroidi	distrofia maculare, angiosclerosi	DMNID			
A55	08/08/46	73	F	OD	FACO+IOL	24/01/20	Acqueo	0,05 mL	1(x0,05 ml)	Cataratta corticonucleare densa evoluta	Glaucoma, angiosclerosi,iridotomia	DMNID ipert. Arta. PM, clopidogrel			
A56	14/11/65	54	F	OD	FACO+IOL	24/01/20	Acqueo	0,05 mL	1(x0,05 ml)	Cataratta nucleare e sottocapsulare posteriore			46,45323233		
A57	28/04/41	78	F	OS	FACO+IOL	24/01/20	Acqueo	0,05 mL	1(x0,05 ml)	Cataratta corticonucleare	atrofia orletto, angiosclerosi		31,81802442		
A58	12/10/37	82	F	OS	FACO+IOL	28/01/20	Acqueo	0,05 mL	1(x0,05 ml)	Cataratta corticonucleare	distrofia maculare oo, angiosclerosi				
A59	27/07/58	61	F	OD	FACO+IOL	28/01/20	Acqueo	0,05 mL	1(x0,05 ml)	Cataratta nucleare	Glaucoma oo , miope elevata, corioretinosi miopica		40,15172506		
A60	08/03/42	77	M	OS	FACO+IOL	30/01/20	Acqueo	0,05 mL	1(x0,05 ml)	Cataratta corticonucleare sottocapsulare posteriore	monocolo	DMNID	72,36782492		
A61	18/07/48	71	M	OS	FACO+IOL	30/01/20	Acqueo	0,05 mL	1(x0,05 ml)	Cataratta nucleare posteriore	Retinopatia diabetica, ipermetrope	ipert. art., tp ASA	67,2295357		
A62	17/07/40	79	F	OD	FACO+IOL	31/01/20	Acqueo	0,05 mL	1(x0,05 ml)	Cataratta corticonucleare	iridotomia OO	ipert	44,41988866		
A63	17/06/44	75	M	OS	FACO+IOL	31/01/20	Acqueo	0,05 mL	1(x0,05 ml)	Cataratta nucleare	angiosclerosi		70,99646881		

ID	DoB	Età	SESSO	OCCHIO	INTERVENTO	DATA INTERVENTO	MATERIALE PRELEVATO	TOT materiale prelevato	num di campioni	PATOLOGIA PRINCIPALE	ALTRE PATO OCULARI	PATO SISTEMICHE	P2X7r pg/ml	II analisi [P2X7r]	medie
A64	03/03/58	61	F	OS	FACO+IOL	04/02/20	Acqueo	0,05 mL	1(x0,05 ml)	Cataratta nucleare e sottocapsulare posteriore	Glaucoma (tp Saflutan, Qualid ofta, Droptimol),Retinopatia diabetica, Edema maculare diabetico (tp con ivt)	DMNID			
A65	22/04/47	72	F	OS	FACO+IOL	04/02/20	Acqueo	0,05 mL	1(x0,05 ml)	Cataratta corticonucleare	DMLE, Glaucoma in tp con Saflutan e timololo	ipta, cardioasa			
A66	13/07/56	63	M	OD	FACO+IOL	05/02/20	Acqueo	0,05 mL	1(x0,05 ml)	Cataratta corticonucleare	Cheratouveite erpetica recidivante,conta < 2000	DMNID, tp asa			
A67	12/02/39	80	F	OS	FACO+IOL	05/02/20	Acqueo	0,05 mL	1(x0,05 ml)	Cataratta nucleare e posteriore	PEX				
A68	17/10/56	63	M	OS	Vitrectomia	18/02/20	Acqueo	0,05 mL	1(x0,05 ml)	PDMS	esiti di DDR		178,6917		
A69	02/10/54	65	F	OS	FACO+IOL	18/02/20	Acqueo	0,05 mL	1(x0,05 ml)	Cataratta corticonucleare		tp asa	14,41937		
A70	15/04/45	74	F	OS	FACO+IOL	18/02/20	Acqueo	0,05 mL	1(x0,05 ml)	Cataratta corticonucleare	guttae	DMNID, tp asa, ipert. art.			
A71	19/02/61	58	F	OS	FACO+IOL	21/02/20	Acqueo	0,05 mL	1(x0,05 ml)	Cataratta sottocapsulare posteriore	miopia		13,3992		
A72	14/01/43	77	M	OS	FACO+IOL	21/02/20	Acqueo	0,05 mL	1(x0,05 ml)	Cataratta nucleare	scarsa midriasi, angiosclerosi	DMNID, ipert. art., tea carotidea, ptca+stent, tp asa	15,43996		
A73	27/06/45	74	F	OS	FACO+IOL	21/02/20	Acqueo	0,05 mL	1(x0,05 ml)	Cataratta nucleare e sottocapsulare posteriore	Monocola (ambiopia OD), angiosclerosi		16,8014		
A74	22/02/35	84	M	OD	FACO+IOL	21/02/20	Acqueo	0,05 mL	1(x0,05 ml)	Cataratta corticonucleare e sottocapsulare posteriore	angiosclerosi, scarsa midriasi	tp omnic	14,75952		
A75	25/03/42	77	M	OS	FACO+IOL	25/02/20	Acqueo	0,05 mL	1(x0,05 ml)	Cataratta		DMNID, tp omnic	13,3992		
A76	26/06/38	82	F	OD	FACO+IOL	23/09/20	Acqueo	0,05 mL	1(x0,05 ml)	Cataratta		DMNID - non RD, ipert.art	70,22121939		
A77	19/04/48	72	F	OD	FACO+IOL	23/09/20	Acqueo	0,05 mL	1(x0,05 ml)	Cataratta complicata totale	RD trattata con PRP	DMID, tp ASA	65,8612996		
A78	30/04/05	73	M	OS	FACO+IOL	23/09/20	Acqueo	0,05 mL	1(x0,05 ml)	Cataratta	iniziale pucker maculare	/	35,96707084		
A79	17/12/55	64	M	OD	Rimozione PDMS	23/09/20	Acqueo	0,5 mL	2(x0,2 ml) + 1(x0,1 ml	PDMS in CV	esiti di DDR	poliallergie (FANS), ipert.art.	9,887455351	205,9245015	107,906
A80	03/01/47	73	M	OS	FACO+IOL	24/09/20	Acqueo	0,05 mL	1(x0,05 ml)	Cataratta		DMNID, tp OMNIC, ipert.art			
A81	11/09/47	73	F	OS	VVP+peeling MER	24/09/20	Acqueo	0,05 mL	1(x0,05 ml)	Cataratta+pucker maculare	pucker maculare	MBL tratto con adrotp in OD			
A82	04/12/49	77	F	OS	FACO+IOL	29/09/20	Acqueo	0,05 mL	1(x0,05 ml)	Cataratta	Non RD	DMNID	66,545314		
A83	11/12/51	68	M	OD	FACO+IOL	29/09/20	Acqueo	0,05 mL	1(x0,05 ml)	Cataratta	RDNP ed EMD, scarsa conta endoteliale	DMID, ipert. art, ipertrofia ventr sn			

ID	DoB	Età	SESSO	OCCHIO	INTERVENTO	DATA INTERVENTO	MATERIALE PRELEVATO	TOT materiale prelevato	num di campioni	PATOLOGIA PRINCIPALE	ALTRE PATO OCULARI	PATO SISTEMICHE	P2X7r pg/ml	II analisi [P2X7r]	medie
A84	22/05/55	65	F	OS	FACO+IOL	29/09/20	Acqueo	0,1 ml	1 (x 0,1 ml)	Cataratta	RDNP, non EMD, pregressa IVT Ozurdex	DMNID	26,87295848		
A85	06/04/46	74	M	OS	VVP+peeling MER	29/09/20	Acqueo	0,1 ml	1 (x 0,1 ml)	Pucker maculare OS	Pseudofachia	Ipert. art, tp Clopidogrel	74,09103186		
A86	18/05/59	61	F	OS	VVP x DDR totale	01/10/20	Acqueo	0,1 ml	1 (x 0,1 ml)	DDR totale	Pseudofachia		54,44646638		
A87	04/08/49	71	F	OS	VVP+peeling MER	06/10/20	Acqueo	0,2 ml	2 (x 0,1 ml)	Pucker maculare	Pseudofachia	/	29,04564537		
A88	15/07/48	72	F	OD	FACO+IOL	06/10/20	Acqueo	0,05 mL	1(x0,05 ml)	Cataratta corticonucleare	/	ipert.art, diabete NID			
A89	08/05/40	80	F	OS	FACO+IOL	08/10/20	Acqueo			Cataratta corticonucleare	/	ipert.art, diabete NID, ateromasia TSA	93,87692683		
A90	06/08/46	74	F	OD	FACO+IOL	08/10/20	Acqueo			Cataratta corticonucleare	cornea guttata (Fuchs)	tp ASA	48,51044508	24,85692889	36,68369
A91	29/03/33	87	M	OD	FACO+IOL	09/10/20	Acqueo	0,05 ml	1 (x 0,05 ml)	Cataratta corticonucleare avanzata	/	Diabete NID, ipert.art, 2 IMA, cardiopatia ischemica, ateromasia TSA			
A92	02/10/35	85	M	OS	FACO+IOL	09/10/20	Acqueo	0,05 ml	1 (x 0,05 ml)	Cataratta corticonucleare	/	diabete NID, tpASA	21,43574221		
A93	13/03/40	80	M	OD	FACO+IOL	15/10/20	Acqueo	0,1 ml	1 (x 0,1 ml)	Cataratta corticonucleare	Glaucoma, scarsa midriasi	Diabete NID, ipert.art., IPB in tp, tp coumadin	47,80980376		
A94	27/08/38	82	F	OD	FACO+IOL	15/10/20	Acqueo	0,05 ml	1 (x 0,05 ml)	Cataratta corticonucleare	glaucoma	tp ASA			
A95	19/03/43	77	M	OS	FACO+IOL	15/10/20	Acqueo			Cataratta corticonucleare	/	tp ASA			
A96					FACO+IOL		Acqueo			Cataratta corticonucleare					
A97					FACO+IOL		Acqueo			Cataratta corticonucleare					
A98	05/05/48	72	F	OD	FACO+IOL	20/10/20	Acqueo	0,15 ml	1 (x 0,15 ml)	Cataratta corticonucleare	Distacco di retina operato contestualmente	/	10,05946948		
A99	27/08/35	85	M	OD	FACO+IOL	27/10/20	Acqueo	0,1 ml	1 (x 0,1 ml)	Cataratta corticonucleare	glaucoma, scarsa midriasi	diabete ID, IPB in tp alfalitici, BPCO	67,91396488		
A100	21/08/50	70	F	OS	FACO+IOL	09/10/20	Acqueo	0,05 ml	1 (x 0,05 ml)	Cataratta corticonucleare	/	diabete ID, ipert.art., lieve irc	55,28544387		
A101	22/05/39	81	M	OD	FACO+IOL	09/10/20	Acqueo	0,1 ml	1 (x 0,1 ml)	Cataratta corticonucleare	CNV peripapillare	ipert.art., IPB in tp alfalitici, sndr depressiva	44,67624498		
A102	07/08/53	67	M	OS	FACO+IOL	03/11/20	Acqueo	0,1 ml	1 (x 0,1 ml)	Cataratta corticonucleare	pucker maculare operato contestualmente	allergia tachipirina, ipert. art. tp ASA	7,965342		
A103	07/09/47	73	M	OD	FACO+IOL	05/11/20	Acqueo	0,05 ml	1 (x 0,05 ml)	Cataratta bianca	glaucoma	/	7,62612		
A104	12/07/42	78	F	OS	FACO+IOL	05/11/20	Acqueo	0,05 ml	1 (x 0,05 ml)	Cataratta corticonucleare	pucker maculare non operato	/	8,643926		
A105	02/02/52	68	F	OD	FACO+IOL	05/11/20	Acqueo	0,2 ml	1 (x 0,2 ml)	Cataratta corticonucleare	miopia elevata	/	97,42522914	14,41937	55,9223

ID	DoB	Età	SESSO	OCCHIO	INTERVENTO	DATA INTERVENTO	MATERIALE PRELEVATO	TOT materiale prelevato	num di campioni	PATOLOGIA PRINCIPALE	ALTRE PATO OCULARI	PATO SISTEMICHE	P2X7r pg/ml	II analisi [P2X7r]	medie
A106	07/02/61	59	M	OS	FACO+IOL	10/11/20	Acqueo	0,1 ml	1 (x 0,1 ml)	Cataratta corticonucleare	retinopatia diabetica con edema maculare	diabete NID, tp ASA	5,930702		
A107	10/12/31	89	M	OS	FACO+IOL	10/12/20	Acqueo	0,05 ml	1 (x 0,05 ml)	Cataratta corticonucleare	/	Diabete ID, tp ASA, ipert.art., pucker maculare			
A108	09/09/46	74	F	OS	FACO+IOL	10/12/20	Acqueo	0,1 ml	1 (x 0,1 ml)	Cataratta corticonucleare	glaucoma	ipert.art., sndr ansiosa	10,68079		
A109	18/05/29	91	M	OS	FACO+IOL	10/12/20	Acqueo	0,1 ml	1 (x 0,1 ml)	Cataratta corticonucleare	DMLE essudativa trattata con IVT antiVEGF	tp ASA	24,1853117	12,71932	18,45232
A110	16/02/89	31	F	OS	FACO+IOL	10/12/20	Acqueo	0,1 ml	1 (x 0,1 ml)	Cataratta corticonucleare	retinopatia diabetica proliferante, laser trattamento PRP, edema maculare diabetico in tp IVT Ozurdex	Diabete ID	12,03962		
A111			M	OD	FACO+IOL	17/12/20	Acqueo	0,05 ml	1 (x 0,05 ml)	Cataratta corticonucleare	racidiva di DDR		41,03500642	13,05924	27,04712
A112	14/09/62	58	F	OD	FACO+IOL	28/12/20	Acqueo	NON PRELEVATO	NON PRELEVATO	Glaucoma acuto facomorfico	sinechie iridolenticolari, glaukom fleken, ipertono	/			
A113	30/05/30	90	F	OS	FACO+IOL	05/01/21	Acqueo	0,05 ml	1 (x 0,05 ml)	Cataratta corticonucleare	cornea verticillata per cordarone	tp cordarone, ipert.art	12,03962		
A114	20/12/40	80	F	OD	FACO+IOL	05/01/21	Acqueo	0,05 ml	1 (x 0,05 ml)	Cataratta corticonucleare	DMLE essudativa trattata con IVT antiVEGF	ipert.art.	10,68079		
A115	12/05/75	45	F	OS	FACO+IOL	05/01/21	Acqueo	0,1 ml	1 (x 0,1 ml)	Cataratta corticonucleare	miopia elevata	/	79,23717027	8,983288	44,11023
A116	29/01/68	53	F	OS	FACO+IOL	05/01/21	Acqueo	0,2 ml	2 (x 0,1 ml)	Cataratta corticonucleare	DDR operato contestualmente		66,35683671	10,68079	38,51881
A117	08/05/54	66	F	OD	FACO+IOL	07/01/21	Acqueo	0,05 ml	1 (x 0,05 ml)	Cataratta corticonucleare con riflessi ambroidi	retinopatia diabetica, laser trattamento PRPR, edema maculare diabetico in tp IVT, glaucoma	diabete ID	5,930702		
A118	08/03/59	61	M	OS	FACO+IOL	07/01/21	Acqueo	0,05 ml	1 (x 0,05 ml)	Cataratta corticonucleare	scarsa midriasi	diabete ID,ipert.art., tp ASA, stent cardiaci	14,88014		
A119	27/03/40	80	F	OS	FACO+IOL	07/01/21	Acqueo	0,05 ml	1 (x 0,05 ml)	Cataratta corticonucleare	DMLE essudativa trattata con IVT antiVEGF	HBV+	12,12446		
A120	10/11/46	74	M	OS	FACO+IOL	12/01/21	Acqueo	0,1 ml	1 (x 0,1 ml)	Cataratta corticonucleare	/	tp ASA	9,700651		

ID	DoB	Età	SESSO	OCCHIO	INTERVENTO	DATA INTERVENTO	MATERIALE PRELEVATO	TOT materiale prelevato	num di campioni	PATOLOGIA PRINCIPALE	ALTRE PATO OCULARI	PATO SISTEMICHE	P2X7r pg/ml	II analisi [P2X7r]	medie
A121	06/05/41	79	M	OS	FACO+IOL	12/01/21	Acqueo	0,05 ml	1 (x 0,05 ml)	Cataratta corticonucleare	guttae endoteliali (Fuchs), iridofacodonesi	ipert.art.	10,05947		
A122	09/05/54	66	F	OS	FACO+IOL	14/01/21	Acqueo	0,05 ml	1 (x 0,05 ml)	Cataratta corticonucleare	miopia elevata	/	16,25899		
A123	16/09/52	68	M	OS	FACO+IOL	14/01/21	Acqueo			Cataratta corticonucleare	edema maculare diabetico, retinopatia diabetica, glaucoma, scarsa midriasi	pregresso TIA, diabete	24,54638	11,43596	17,99117
A124	07/11/52	68	M	OS	FACO+IOL	19/01/21	Acqueo	0,2 ml	2 (x 0,1 ml)	Cataratta corticonucleare	scarsa midriasi	Diabete NID, ipert.art			
A125	21/01/48	72	F	OS	FACO+IOL	19/01/21	Acqueo	0,1 ml	1 (x 0,1 ml)	Cataratta corticonucleare	miopia elevata	ipert.art., ateromasia TSA	8,339797		
A126	17/02/57	63	M	OS	FACO+IOL	21/01/21	Acqueo	0,1 ml	1 (x 0,1 ml)	Cataratta corticonucleare	miopia elevata, (pregresso DDR in occhio controlaterale)	/	8,339797		
A127	25/04/38	82	M	OS	FACO+IOL	26/01/21	Acqueo	0,05 ml	1 (x 0,05 ml)	Cataratta corticonucleare	scarsa midriasi	Diabete NID, ipert.art.	18,32855		
A128	09/03/37	83	M	OS	FACO+IOL	26/01/21	Acqueo	0,05 ml	1 (x 0,05 ml)	Cataratta corticonucleare	PEX, scarsa midriasi	ipert.art. IPB in tp Alfuzosina, tp ASA	12,81312		
A129	20/08/56	64	F	OS	FACO+IOL	02/02/21	Acqueo	0,3 ml	2 (x 0,15 ml)	Cataratta corticonucleare	miopia elevata	/	31,47132654	7,652225	19,56178
A130	22/04/46	74	F	OS	FACO+IOL	02/02/21	Acqueo	0,1 ml	1 (x 0,1 ml)	Cataratta corticonucleare	bassa conta endoteliale	Diabete, ipert.art, tp ASA	8,683647		
A131	27/09/54	66	M	OS	FACO+IOL	02/02/21	Acqueo	0,05 ml	1 (x 0,05 ml)	Cataratta corticonucleare	glaucoma, scarsa midriasi	IPB in tp amsulosina, ipert.art., tp ASA, bypass AC	21,7812		
A132	17/03/47	73	M	OS	FACO+IOL	04/02/21	Acqueo	0,05 ml	1 (x 0,05 ml)	Cataratta corticonucleare	non retinopatia diabetica	diabete ID, ossigenoterapia	19,7091		
A133	26/06/36	84	M	OD	FACO+IOL	04/02/21	Acqueo	0,1 ml	1 (x 0,1 ml)	Cataratta corticonucleare	glaucoma, DMLE (essudativa?), non segni di retinopatia diabetica	Diabete ID	4,216871		
A134	27/03/33	87	M	OS	FACO+IOL	09/02/21	Acqueo	0,1 ml	1 (x 0,1 ml)	Cataratta corticonucleare	DMLE essudativa trattata con IVT antiVEGF	diabete NID, ipert.art., FA, tp Eliquis, scompenso cardiaco	11,43596		
A135	28/06/37	83	F	OS	FACO+IOL	09/02/21	Acqueo	0,1 ml	1 (x 0,1 ml)	Cataratta corticonucleare	glaucoma, tp ipotonizzante topica, pregresse iridotomie	ipert.art., FA in tp	43,97969		
A136	30/09/37	83	F	OD	FACO+IOL	09/02/21	Acqueo	0,05 ml	1 (x 0,05 ml)	Cataratta corticonucleare	DMLE essudativa trattata con IVT antiVEGF	ipert.art.	12,12446		
A137	05/10/46	74	M	OS	FACO+IOL	16/02/21	Acqueo	0,15 ml	1 (x 0,1 ml) + 1(x 0,05	Cataratta corticonucleare	scarsa midriasi	Diabete NID	11,09177		

ID	DoB	Età	SESSO	OCCHIO	INTERVENTO	DATA INTERVENTO	MATERIALE PRELEVATO	TOT materiale prelevato	num di campioni	PATOLOGIA PRINCIPALE	ALTRE PATO OCULARI	PATO SISTEMICHE	P2X7r pg/ml	II analisi [P2X7r]	medie
A138	28/11/35	85	M	OS	FACO+IOL	16/02/21	Acqueo	0,05 ml	1 (x 0,05 ml)	Cataratta corticonucleare	PEX, glaucoma, DMLE	/	5,247038		
A139	06/06/54	66	F	OD	FACO+IOL	16/02/21	Acqueo	0,1 ml	1 (x 0,1 ml)	Cataratta corticonucleare	miopia elevata	/	7,3085		
A140					FACO+IOL		Acqueo			Cataratta corticonucleare					
A141	08/08/34	86	M	OS	FACO+IOL	23/02/21	Acqueo	0,25 ml	1 (x0,1 ml) + 1 (x 0,15	Cataratta corticonucleare	esiti di occlusione venosa centrale della retina	Diabete NID, IRC	7,3085		
A142	07/05/49	71	F	OS	FACO+IOL	23/02/21	Acqueo	0,2 ml	2 (x 0,1 ml)	Cataratta corticonucleare	edema maculare diabetico in tp Ozurdex IVT	diabete ID, PTCA cardiaco	9,371472	7,99599	8,683731
A143	01/11/39	82	M	OD	FACO+IOL	10/02/22	Acqueo			Cataratta corticonucleare	/	tp ASA	7,965342566		
A144	09/11/35	86	M	OS	FACO+IOL	10/02/22	Acqueo	0,05 ml	1 (x 0,05 ml)	Cataratta corticonucleare	scarsa midriasi, bassa conta endoteliale	ipert.art., tp Eliquis	11,36011169		
A145	05/09/40	81	F	OS	FACO+IOL	10/02/22	Acqueo	0,1 ml	1 (x 0,1 ml)	Cataratta corticonucleare	/	/	8,643926015		
A146	01/02/42	80	F	OD	FACO+IOL	10/02/22	Acqueo	0,05 ml	1 (x 0,05 ml)	Cataratta corticonucleare	scarsa midriasi	ipert.art.	19,52652957		
A147	05/01/47	75	M	OS	FACO+IOL	10/02/22	Acqueo	0,05 ml	1 (x 0,05 ml)	Cataratta corticonucleare	miopia elevata	tp clopidogrel, IPB in tp Omnic	11,36011169		
A148	24/09/47	74	M	OD	FACO+IOL	10/02/22	Acqueo	0,05 ml	1 (x 0,05 ml)	Cataratta corticonucleare	/	/	16,80140367		
A149	20/10/53	68	F	OD	FACO+IOL	10/02/22	Acqueo	0,2 ml	2 (x 0,1 ml)	Cataratta corticonucleare	miopia elevata, glaucoma	/	11,69984354		
A150	23/04/48	73	M	OD	FACO+IOL	10/02/22	Acqueo	0,2 ml	2 (x 0,1 ml)	Cataratta corticonucleare	bassa conta endoteliale	ipert.art., tp Xarelto, FA	21,91347513		
A151	15/06/44	77	F	OD	FACO+IOL	10/02/22	Acqueo	0,2 ml	1 (x 0,2 ml)	Cataratta corticonucleare	/	ipert.art.	5,252856109		
A152	03/08/57	64	M	OD	FACO+IOL	10/02/22	Acqueo	0,6 ml	1 (x 0,6 ml)	Cataratta corticonucleare	pregresso DDR, olio di silicone in CV asportato contestualmente	/	13,39919966		
A153	17/01/38	84	M	OD	FACO+IOL	11/02/22	Acqueo	0,05 ml	1 (x 0,05 ml)	Cataratta corticonucleare evoluta ambroide	bassa conta endoteliale	CA orofaringeo, tp ASA	35,94062917		
A154	13/06/35	86	F	OD	FACO+IOL	11/02/22	Acqueo	0,15 ml	1 (x 0,15 ml)	Cataratta corticonucleare evoluta	/	pacemaker	21,23125594		
A155	14/06/40	81	M	OS	FACO+IOL	11/02/22	Acqueo	0,1 ml	1 (x 0,1 ml)	Cataratta corticonucleare	scarsa midriasi	diabete NID, IPB in tp Omnic, ipert.art.	6,608730172		
A156	23/01/38	84	F	OD	FACO+IOL	11/02/22	Acqueo	0,1 ml	1 (x 0,1 ml)	Cataratta corticonucleare evoluta		diabete NID; tp ASA	10,68078718		
A157	02/03/44	77	F	OD	FACO+IOL	15/02/22	Acqueo	0,1 ml	1 (x 0,1 ml)	Cataratta corticonucleare	PEX, glaucoma, esiti di occlusione venosa retinica	favismo, sndr ansionsa in tp xanax	3,897719173		
A158	24/04/50	71	M	OD	FACO+IOL	15/02/22	Acqueo	0,1 ml	1 (x 0,1 ml)	Cataratta corticonucleare	retinopatia diabetica con edema maculare in tp Ozurdex IVT, trattamento laser PRP	ipert.art, pregressa PCA, tp Xarelto	5,252856109		

ID	DoB	Età	SESSO	OCCHIO	INTERVENTO	DATA INTERVENTO	MATERIALE PRELEVATO	TOT materiale prelevato	num di campioni	PATOLOGIA PRINCIPALE	ALTRE PATO OCULARI	PATO SISTEMICHE	P2X7r pg/ml	II analisi [P2X7r]	medie
A159	30/04/37	84	F	OD	FACO+IOL	16/02/22	Acqueo	0,1 ml	1 (x 0,1 ml)	Cataratta corticonucleare	retinopatia diabetica	diabete ID, ipert.art,cardiopatia ischemica, bypass AC, tp ASA e inhixa	24,30272402		
A160	11/08/39	82	M	OD	FACO+IOL	16/02/22	Acqueo	0,1 ml	1 (x 0,1 ml)	Cataratta corticonucleare	glaucoma, bassa conta endoteliale	diabete NID, ipert.art., FA, tp pradaxa	12,03962183		
A161	10/03/38	83	F	OD	FACO+IOL	16/02/22	Acqueo	0,1 ml	1 (x 0,1 ml)	Cataratta corticonucleare	bassa conta endoteliale	ipert.art., embolia polmonare, TVP, tp xarelto, sndr depressiva in tp	3,897719173		
A162	05/11/39	82	F	OD	FACO+IOL	17/02/22	Acqueo	0,2 ml	2 (x 0,1 ml)	Cataratta corticonucleare		ipert.art.	5,930700924		
A163	12/11/48	73	F	OD	FACO+IOL	17/02/22	Acqueo	0,2 ml	2 (x 0,1 ml)	Cataratta corticonucleare	scarsa conta endoteliale	ipert.art.	4,575195575		
A164	07/02/47	75	M	OS	FACO+IOL	17/02/22	Acqueo	0,2 ml	2 (x 0,1 ml)	Cataratta corticonucleare		ipert.art.	8,304611171		
A165	13/01/37	85	M	OS	FACO+IOL	17/02/22	Acqueo	0,05 ml	1 (x 0,05 ml)	Cataratta corticonucleare	glaucoma	ipert.art., tp Xarelto			
A166	16/08/49	72	F	OS	FACO+IOL	17/02/22	Acqueo	0,05 ml	1 (x 0,05 ml)	Cataratta corticonucleare	glaucoma		6,608730172		
A167	30/07/42	79	M	OS	FACO+IOL	17/02/22	Acqueo	0,2 ml	2 (x 0,1 ml)	Cataratta corticonucleare	pterigio	ipert.art., tp Tamsulosina	23,61984606		
A168	06/08/49	72	F	OS	FACO+IOL	17/02/22	Acqueo	0,05 ml	1 (x 0,05 ml)	Cataratta corticonucleare	iridotomia, ca ipoprofonda, pregressa OVBR	ipert.art., tp ASA			
A169	19/11/39	82	M	OD	FACO+IOL	23/02/22	Acqueo	0,1 ml	1 (x 0,1 ml)	Cataratta corticonucleare evoluta	scarsa conta endoteliale		5,930700924		
A170	23/11/73	78	F	OD	FACO+IOL	23/02/22	Acqueo	0,1 ml	1 (x 0,1 ml)	Cataratta corticonucleare	scarsa conta endoteliale	ipert. arteriosa in tp	3,897719173		
A171	20/12/42	79	M	OS	FACO+IOL	23/02/22	Acqueo	0,05 ml	1 (x 0,05 ml)	Cataratta corticonucleare	/	ipert. arteriosa in tp, tp Asa	5,930700924		
A172	26/11/62	59	M	OD	FACO+IOL	23/02/22	Acqueo	0,05 ml	1 (x 0,05 ml)	Cataratta corticonucleare	/	/	5,930700924		
A173	16/07/66	55	M	OS	FACO+IOL	23/02/22	Acqueo			Cataratta corticonucleare	scarsa midriasi, ambliopia relativa in OS	/	3,897719173		
A174	25/01/39	83	F	OD	FACO+IOL	24/02/22	Acqueo	0,1 ml	1 (x 0,1 ml)	Cataratta corticonucleare	ipotalamia, iridotomia	/	4,575195575		
A175	07/03/51	70	F	OS	FACO+IOL	24/02/22	Acqueo	0,2 ml	2 (x 0,1 ml)	Cataratta corticonucleare	/	/	5,591755472		
A176	27/10/52	69	F	OD	FACO+IOL	24/02/22	Acqueo			Cataratta corticonucleare	intervento per strabismo OD	/	6,608730172		
A177	25/04/58	63	F	OS	FACO+IOL	24/02/22	Acqueo	0,1 ml	1 (x 0,1 ml)	Cataratta corticonucleare	/	/	4,914002816		
A178	01/02/46	76	M	OD	FACO+IOL	24/02/22	Acqueo	0,05 ml	1 (x 0,05 ml)	Cataratta corticonucleare	/	/			
A179	03/05/59	62	F	OS	FACO+IOL	01/03/22	Acqueo	0,1 ml	1 (x 0,1 ml)	Cataratta corticonucleare	Miopia elevata, corioretinosi miopica	allergia ASA	5,930700924		

ID	DoB	Età	SESSO	OCCHIO	INTERVENTO	DATA INTERVENTO	MATERIALE PRELEVATO	TOT materiale prelevato	num di campioni	PATOLOGIA PRINCIPALE	ALTRE PATO OCULARI	PATO SISTEMICHE	P2X7r pg/ml	II analisi [P2X7r]	medie
A180	09/03/39	82	F	OD	FACO+IOL	01/03/22	Acqueo	0,05 ml	1 (x 0,05 ml)	Cataratta corticonucleare	glaucoma, tp AZARGA e GANFORT; distrofia EPR maculare	Diabete ID, tp ASA, ipert.art, vasculopatia AAII			
A181	24/10/41	80	M	OD	FACO+IOL	01/03/22	Acqueo	0,1 ml	1 (x 0,1 ml)	Cataratta corticonucleare	leucomi corneali	tp TAMSULOSIN, tp ASA, ipert.art, pregressi PCA	3,897719173		
A182	10/03/54	67	M	OD	FACO+IOL	01/03/22	Acqueo	0,1 ml	1 (x 0,1 ml)	Cataratta corticonucleare	/	ipert.art, asma	5,252856109		
A183	03/03/38	83	F	OD	FACO+IOL	01/03/22	Acqueo			Cataratta corticonucleare	/	tp ASA	8,643926015		
A184	20/07/41	80	M	OS	FACO+IOL	03/03/22	Acqueo	0,05 ml	1 (x 0,05 ml)	Cataratta corticonucleare	pterigio, iridotomia per ca ipoprofonda, bassa conta endoteliale	ipert.art, ateromasia TSA	12,03962183		
A185	31/05/58	63	F	OD	FACO+IOL	03/03/22	Acqueo	0,05 ml	1 (x 0,05 ml)	Cataratta corticonucleare	/	ipert.art, alleriga ASA	5,252856109		
A186	24/05/33	88	M	OD	FACO+IOL	03/03/22	Acqueo	0,05 ml	1 (x 0,05 ml)	Cataratta corticonucleare	/	ipert.art., FA, tp coumadin, tp terazosina	10,00164817		
A187	22/02/46	76	F	OD	FACO+IOL	03/03/22	Acqueo	0,1 ml	1 (x 0,1 ml)	Cataratta corticonucleare	glaucoma in tp Cosopt e Acamba coll, bassa conta endoteliale, distrofia epr maculare	ipert.art, tp ASA, exfumatore,	13,39919966		
A188	19/01/45	77	M	OD	FACO+IOL	08/03/22	Acqueo	0,05 ml	1 (x 0,05 ml)	Cataratta corticonucleare	distrofia Fuchs (guttae endoteliali e bassa conta), scarsa midriasi	tp TAMSULOSIN, tp ASA	3,897719173		
A189	13/03/54	67	F	OD	FACO+IOL	08/03/22	Acqueo	0,05 ml	1 (x 0,05 ml)	Cataratta corticonucleare	guttae endoteliali, sinechie iridolenticolari, distrofia maculare	ipert.art.	8,643926015		
A190	22/01/44	78	M	OS	FACO+IOL	08/03/22	Acqueo	0,2 ml	2 (x 0,1 ml)	Cataratta corticonucleare	scarsa midriasi	tp Silodyx, tp ASA	10,00164817		
A191	24/06/42	79	F	OD	FACO+IOL	08/03/22	Acqueo	0,05 ml	1 (x 0,05 ml)	Cataratta corticonucleare	/	Diabete iD, ipert.art, FA in NAO	7,286944002		
A192	18/09/43	78	F	OS	FACO+IOL	08/03/22	Acqueo	0,1 ml	1 (x 0,1 ml)	Cataratta corticonucleare	distrofia Fuchs (guttae endoteliali e bassa conta)	ipert. art, allergia chinoloni, pregresso H.Zoster emivolto dx	5,930700924		
A193	21/05/48	73	M	OS	FACO+IOL	09/03/22	Acqueo	0,05 ml	1 (x 0,05 ml)	Cataratta corticonucleare	glaucoma, scarsa midriasi	/	9,3226945		
A194	19/01/48	74	M	OS	FACO+IOL	09/03/22	Acqueo	0,05 ml	1 (x 0,05 ml)	Cataratta corticonucleare	miopia elevata	ipert.art.	7,286944002		
A195	15/12/43	78	F	OD	FACO+IOL	09/03/22	Acqueo	0,15 ml	1 (x 0,15 ml)	Cataratta corticonucleare	glaucoma	diabete NID, tp ASA	6,269692484		
A196	29/04/69	52	M	OD	FACO+IOL	09/03/22	Acqueo	0,2 ml	2 (x 0,1 ml)	Cataratta corticonucleare densa	pregressa uveite	tp anticoagulante orale	3,559049975		

ID	DoB	Età	SESSO	OCCHIO	INTERVENTO	DATA INTERVENTO	MATERIALE PRELEVATO	TOT materiale prelevato	num di campioni	PATOLOGIA PRINCIPALE	ALTRE PATO OCULARI	PATO SISTEMICHE	P2X7r pg/ml	II analisi [P2X7r]	medie
A197	26/11/38	83	F	OS	FACO+IOL	15/03/22	Acqueo	0,1 ml	1 (x 0,1 ml)	Cataratta corticonucleare	/	ipert. art., pregresse trombosi, embolie, aneurisma cerebrale, scompenso cardiaco, tp eliquis (NAO), pacemaker	11,02042624		
A198	07/06/51	70	F	OD	FACO+IOL	15/03/22	Acqueo	0,05 ml	1 (x 0,05 ml)	Cataratta corticonucleare	guttae endotelieli e bassa conta (Fuchs?)	fumatore, ipert. art.	5,930700924		
A199	08/01/59	63	F	OD	FACO+IOL	15/03/22	Acqueo	0,2 ml	2 (x 0,1 ml)	Cataratta corticonucleare	distrofia EPR maculare	/	3,897719173		
A200	19/12/46	75	F	OS	FACO+IOL	15/03/22	Acqueo	0,2 ml	2 (x 0,1 ml)	Cataratta corticonucleare	glaucoma tp Azarga, drusen maculari	ipert.art., FA in tp Xarelto (NAO), ex fumatore, microcitemia	4,914002816		
A201	18/01/41	81	M	OD	FACO+IOL	15/03/22	Acqueo	0,3 ml	2 (x 0,15 ml)	Cataratta corticonucleare	diplopia verticale (paresi muscolare)	tachiFA in tp Lixiana (NAO), ipert.art., bronchite cronica	8,983287119		
A202	07/06/44	77	M	OD	FACO+IOL	17/03/22	Acqueo	0,05 ml	1 (x 0,05 ml)	Cataratta corticonucleare	PEX	ipert.art, diabete NID	14,07926765		
A203	01/12/63	58	F	OS	FACO+IOL	24/03/22	Acqueo	0,2 ml	2 (x 0,1 ml)	Cataratta corticonucleare	/	sndr depressiva in tp sertralina	8,983287119		
A204	09/04/48	73	M	OD	FACO+IOL	24/03/22	Acqueo	0,05 ml	1 (x 0,05 ml)	Cataratta corticonucleare	pterigio OD	innesto aortico, ateromasia iliaca, Ca polmonare, tp ASA			
A205	22/08/52	69	M	OS	FACO+IOL	24/03/22	Acqueo	0,1 ml	1 (x 0,1 ml)	Cataratta corticonucleare	/	ipert.art., pregresso IMA, tp ASA	14,75952189		
A206	04/07/60	61	F	OS	FACO+IOL	24/03/22	Acqueo	0,2 ml	1 (x 0,2 ml)	Cataratta corticonucleare	Miopia elevata, corioretinosi miopica	/	15,09971891		
A207	24/07/45	76	F	OD	FACO+IOL	06/04/22	Acqueo	0,05 ml	1 (x 0,05 ml)	Cataratta corticonucleare	PEX	/	5,252856109		
A208	20/11/53	68	F	OS	FACO+IOL	06/04/22	Acqueo	0,15 ml	1 (x 0,15 ml)	Cataratta corticonucleare	miopia elevata, scarsa conta endoteliale	/	8,643926015		
A209	18/08/58	63	M	OD	FACO+IOL	26/04/22	Acqueo	0,05 ml	1 (x 0,05 ml)	Cataratta corticonucleare	distacco di retina operato contestualmente	/	12,03962183		
A210	21/01/40	82	F	OS	FACO+IOL	06/05/22	Acqueo	0,1 ml	1(x 0,1 ml)	cataratta nucleare	distacco di retina operato contestualmente, bassa conta endoteliale	splenectomia, stato ansioso	19,86738103		

NUM	ID	CONTROLL	DoB	Età	SESSO	OCCHIO	PATOLOGIA PRINCIPALE	ALTRE PATO OCULARI	PATO SISTEMICHE	[P2X7r] pg/ml	SIERO[P2X7r] pg/ml
C1	A1	Controllo	02/12/54	64	M	OD	Cataratta corticonucleare	/	Diabete NID, ipercolesterolemia		
C2	A2	Controllo	18/08/44	74	M	OD	Cataratta corticonucleare	/	Epatite (HBV/HCV?), tifo, ipert.art., IPB		
C3	A5	Controllo	22/02/63	56	M	OS	Cataratta corticonucleare e sottocapsulare posteriore	scarsa midriasi	ipert. art., tp ASA	20,11826	
C4	A16	Controllo	08/07/44	74	F	OS	Cataratta corticonucleare e sottocapsulare posteriore	Monocola funzionale (ambliopia OD),	ipotiroidismo in tp, fumatrice	6,054463	

NUM	ID	CONTROLL	DoB	Età	SESSO	OCCHIO	PATOLOGIA PRINCIPALE	ALTRE PATO OCULARI	PATO SISTEMICHE	[P2X7r] pg/ml	SIERO[P2X7r] pg/ml
C5	A17	Controllo	05/05/30	88	F	OS	Cataratta corticonucleare e sottocapsulare posteriore	/	ipert.art., FA in tp NAO (Apixaban), decadimento cognitivo,ermia gastro-iatale	6,9523	192,8109879
C6	A20	Controllo	01/12/47	71	F	OD	Cataratta	media midriasi	ipert.art. tp ASA HCV+	49,95423	
C7	A22	Controllo	13/04/37	82	M	OS	Cataratta	/	DMID pregresso IMA, BPCO, tp ASA	7,52952	244,6419
C8	A25	Controllo	06/08/53	66	M	OS	Cataratta	/	/	9,09	40,26004
C9	A26	Controllo	06/05/48	71	M	OD	Cataratta	/	plavix (tp ASA), ipert. Art.	14,19096	67,095005
C10	A28	Controllo	20/12/31	87	F	OS	Cataratta	/	HBV+, pm in coumadin	7,3085	
C11	A29	Controllo	15/10/46	73	M	OD	Foro maculare	/	/	68,38826	
C12	A33	Controllo	07/12/37	81	M	OD	Cataratta		DMID, ipert. Art., tp ASA	5,219639	89,224905

NUM	ID	CONTROLL	DoB	Età	SESSO	OCCHIO	PATOLOGIA PRINCIPALE	ALTRE PATO OCULARI	PATO SISTEMICHE	[P2X7r] pg/ml	SIERO[P2X7r] pg/ml
C13	A34	Controllo	12/08/50	69	F	OD	Cataratta		DMID + oha, tp asa	36,84541	173,8561
C14	A35	Controllo	23/07/37	82	M	OS	Cataratta		DMID, tp asa, tp ominic per IPB		126,65744
C15	A37	Controllo	23/10/40	79	M	OS	Cataratta		DMNID, preg ima(ptca+stent), ipta, tp NAO, Ateromasia tsa	38,99443	201,3628
C16	A38	Controllo	26/10/36	83	M	OS	Cataratta	iridotomia, media midriasi	PM, tp NAO, ipta		123,0683
C17	A39	Controllo	11/07/41	78	M	OD	Cataratta		pregr tia, pregr ima, ipta, tp asa, cardiopatia ischemica, tp alfa litico	16,14644	99,640925
C18	A40	Controllo	18/04/45	74	F	OD	Cataratta		ipta	13,24826	37,22281
C19	A41	Controllo	27/03/36	83	M	OD	Cataratta			52,75389	67,777825

NUM	ID	CONTROLL	DoB	Età	SESSO	OCCHIO	PATOLOGIA PRINCIPALE	ALTRE PATO OCULARI	PATO SISTEMICHE	[P2X7r] pg/ml	SIERO[P2X7r] pg/ml
C20	A42	Controllo	01/12/44	74	M	OD	Cataratta		DMID, Coumadin, sost valv aortica, Ipta, cardura	37,35612	21,74928
C21	A44	Controllo	21/06/43	76	M	OS	Cataratta		IPTA	25,06091	70,06812
C22	A47	Controllo	11/09/78	41	M	OS	Cataratta totale			23,7706	315,20115
C23	A49	Controllo	07/03/42	77	F	OS	Cataratta	ca ipoprofonda, scarsa midriasi	tp asa		40,69356
C24	A51	Controllo	04/10/40	79	F	OS	Cataratta		ipt art, esiti mastectomia	33,8673	15,4414888
C25	A56	Controllo	14/11/65	54	F	OD	Cataratta nucleare e sottocapsulare posteriore			46,45323233	86,841035
C26	A57	Controllo	28/04/41	78	F	OS	Cataratta corticonucleare	atrofia orletto, angiosclerosi		31,81802442	131,291935

NUM	ID	CONTROLL	DoB	Età	SESSO	OCCHIO	PATOLOGIA PRINCIPALE	ALTRE PATO OCULARI	PATO SISTEMICHE	[P2X7r] pg/ml	SIERO[P2X7r] pg/ml
C27	A60	Controllo	08/03/42	77	M	OS	Cataratta corticonucleare sottocapsulare posteriore	monocolo	DMNID	72,36782492	125,84319
C28	A62	Controllo	17/07/40	79	F	OD	Cataratta corticonucleare	iridotomia OO	ipert	44,41988866	93,96401
C29	A63	Controllo	17/06/44	75	M	OS	Cataratta nucleare	angiosclerosi		70,99646881	133,33802
C30	A69	Controllo	02/10/54	65	F	OS	Cataratta corticonucleare		tp asa	14,41937	70,1386
C31	A72	Controllo	14/01/43	77	M	OS	Cataratta nucleare	scarsa midriasi, angiosclerosi	DMNID, ipert. art., tea carotidea, ptca+stent, tp asa	15,43996	196,9584
C32	A73	Controllo	27/06/45	74	F	OS	Cataratta nucleare e sottocapsulare posteriore	Monocola (ambiopia OD), angiosclerosi		16,8014	86,619525

NUM	ID	CONTROLL	DoB	Età	SESSO	OCCHIO	PATOLOGIA PRINCIPALE	ALTRE PATO OCULARI	PATO SISTEMICHE	[P2X7r] pg/ml	SIERO[P2X7r] pg/ml
C33	A74	Controllo	22/02/35	84	M	OD	Cataratta corticonucleare e sottocapsulare posteriore	angiosclerosi, scarsa midriasi	tp omnic	14,75952	162,0301
C34	A75	Controllo	25/03/42	77	M	OS	Cataratta		DMNID, tp omnic	13,3992	96,487025
C35	A76	Controllo	26/06/38	82	F	OD	Cataratta		DMNID - non RD, ipert.art	70,22121939	
C36	A80	Controllo	03/01/47	73	M	OS	Cataratta		DMNID, tp OMNIC, ipert.art		202,7317064
C37	A82	Controllo	04/12/49	77	F	OS	Cataratta		DMNID	66,545314	127,8829993
C38	A88	Controllo	15/07/48	72	F	OD	Cataratta corticonucleare	/	ipert.art, diabete NID		60,61188796
C39	A89	Controllo	08/05/40	80	F	OS	Cataratta corticonucleare	/	ipert.art, diabete NID, ateromasia TSA	93,87692683	85,19055419

NUM	ID	CONTROLL	DoB	Età	SESSO	OCCHIO	PATOLOGIA PRINCIPALE	ALTRE PATO OCULARI	PATO SISTEMICHE	[P2X7r] pg/ml	SIERO[P2X7r] pg/ml
C40	A91	Controllo	29/03/33	87	M	OD	Cataratta corticonucleare avanzata	/	Diabete NID, ipert.art, 2 IMA, cardiopatia ischemica, ateromasia TSA		116,8145664
C41	A92	Controllo	02/10/35	85	M	OS	Cataratta corticonucleare	/	diabete NID, tpASA	21,43574221	177,7122458
C42	A95	Controllo	19/03/43	77	M	OS	Cataratta corticonucleare	/	tp ASA		124,6481097
C43	A100	Controllo	21/08/50	70	F	OS	Cataratta corticonucleare	/	diabete ID, ipert.art., lieve irc	55,28544387	141,6538571
C44	A107	Controllo	10/12/31	89	M	OS	Cataratta corticonucleare	/	Diabete ID, tp ASA, ipert.art., pucker maculare		92,97992774

NUM	ID	CONTROLL	DoB	Età	SESSO	OCCHIO	PATOLOGIA PRINCIPALE	ALTRE PATO OCULARI	PATO SISTEMICHE	[P2X7r] pg/ml	SIERO[P2X7r] pg/ml
C45	A118	Controllo	08/03/59	61	M	OS	Cataratta corticonucleare	scarsa midriasi	diabete ID,ipert.art., tp ASA, stent cardiaci	14,88014	102,3276389
C46	A120	Controllo	10/11/46	74	M	OS	Cataratta corticonucleare	/	tp ASA	9,700651	
C47	A124	Controllo	07/11/52	68	M	OS	Cataratta corticonucleare	scarsa midriasi	Diabete NID, ipert.art		231,1972104
C48	A127	Controllo	25/04/38	82	M	OS	Cataratta corticonucleare	scarsa midriasi	Diabete NID, ipert.art.	18,32855	231,1972104
C49	A132	Controllo	17/03/47	73	M	OS	Cataratta corticonucleare		diabete ID, ossigenoterapia	19,7091	220,5972652
C50	A137	Controllo	05/10/46	74	M	OS	Cataratta corticonucleare	scarsa midriasi	Diabete NID	11,09177	98,66647418
C51	A143	Controllo	01/11/39	82	M	OD	Cataratta corticonucleare	/	tp ASA	7,965342566	47,6362994
C52	A145	Controllo	05/09/40	81	F	OS	Cataratta corticonucleare	/	/	8,643926015	
C53	A146	Controllo	01/02/42	80	F	OD	Cataratta corticonucleare	scarsa midriasi	ipert.art.	19,52652957	91,07041798

NUM	ID	CONTROLL	DoB	Età	SESSO	OCCHIO	PATOLOGIA PRINCIPALE	ALTRE PATO OCULARI	PATO SISTEMICHE	[P2X7r] pg/ml	SIERO[P2X7r] pg/ml
C54	A148	Controllo	24/09/47	74	M	OD	Cataratta corticonucleare	/	/	16,80140367	36,88144244
C55	A151	Controllo	15/06/44	77	F	OD	Cataratta corticonucleare	/	ipert.art.	5,252856109	45,27877296
C56	A154	Controllo	13/06/35	86	F	OD	Cataratta corticonucleare evoluta	/	pacemaker	21,23125594	40,57196963
C57	A155	Controllo	14/06/40	81	M	OS	Cataratta corticonucleare	scarsa midriasi	diabete NID, IPB in tp Omnic, ipert.art.	6,608730172	58,27949832
C58	A156	Controllo	23/01/38	84	F	OD	Cataratta corticonucleare evoluta		diabete NID; tp ASA	10,68078718	37,88728245
C59	A162	Controllo	05/11/39	82	F	OD	Cataratta corticonucleare		ipert.art.	5,930700924	52,86638222
C60	A164	Controllo	07/02/47	75	M	OS	Cataratta corticonucleare		ipert.art.	8,304611171	69,83121256
C61	A167	Controllo	30/07/42	79	M	OS	Cataratta corticonucleare	pterigio	ipert.art., tp Tamsulosina	23,61984606	123,5406153

NUM	ID	CONTROLL	DoB	Età	SESSO	OCCHIO	PATOLOGIA PRINCIPALE	ALTRE PATO OCULARI	PATO SISTEMICHE	[P2X7r] pg/ml	SIERO[P2X7r] pg/ml
C62	A168	Controllo	06/08/49	72	F	OS	Cataratta corticonucleare	iridotomia, ca ipoprofonda, pregressa OVBR	ipert.art., tp ASA		70,00159058
C63	A171	Controllo	20/12/42	79	M	OS	Cataratta corticonucleare	/	ipert. arteriosa in tp, tp Asa	5,930700924	46,12043015
C64	A172	Controllo	26/11/62	59	M	OD	Cataratta corticonucleare	/	/	5,930700924	66,59679451
C65	A173	Controllo	16/07/66	55	M	OS	Cataratta corticonucleare	scarsa midriasi, ambliopia relativa in OS	/	3,897719173	45,44707629
C66	A174	Controllo	25/01/39	83	F	OD	Cataratta corticonucleare	ipotalamia, iridotomia	/	4,575195575	88,83299799
C67	A175	Controllo	07/03/51	70	F	OS	Cataratta corticonucleare	/	/	5,591755472	34,53642325
C68	A176	Controllo	27/10/52	69	F	OD	Cataratta corticonucleare	intervento per strabismo OD	/	6,608730172	37,38429998
C69	A177	Controllo	25/04/58	63	F	OS	Cataratta corticonucleare	/	/	4,914002816	23,68417903

NUM	ID	CONTROLL	DoB	Età	SESSO	OCCHIO	PATOLOGIA PRINCIPALE	ALTRE PATO OCULARI	PATO SISTEMICHE	[P2X7r] pg/ml	SIERO[P2X7r] pg/ml
C70	A178	Controllo	01/02/46	76	M	OD	Cataratta corticonucleare	/	/		70,34239037
C71	A181	Controllo	24/10/41	80	M	OD	Cataratta corticonucleare	leucomi corneali	tp TAMSULOSIN, tp ASA, ipert.art, pregressi PCA	3,897719173	59,12661943
C72	A182	Controllo	10/03/54	67	M	OD	Cataratta corticonucleare	/	ipert.art, asma	5,252856109	127,5719207
C73	A183	Controllo	03/03/38	83	F	OD	Cataratta corticonucleare	/	tp ASA	8,643926015	30,52268895
C74	A184	Controllo	20/07/41	80	M	OS	Cataratta corticonucleare	pterigio, iridotomia per ca ipoprofonda, bassa conta endoteliale	ipert.art, ateromasia TSA	12,03962183	131,611646
C75	A185	Controllo	31/05/58	63	F	OD	Cataratta corticonucleare	/	ipert.art, alleriga ASA	5,252856109	36,71385102

NUM	ID	CONTROLL	DoB	Età	SESSO	OCCHIO	PATOLOGIA PRINCIPALE	ALTRE PATO OCULARI	PATO SISTEMICHE	[P2X7r] pg/ml	SIERO[P2X7r] pg/ml
C76	A186	Controllo	24/05/33	88	M	OD	Cataratta corticonucleare	/	ipert.art., FA, tp coumadin, tp terazosina	10,00164817	41,24369881
C77	A190	Controllo	22/01/44	78	M	OS	Cataratta corticonucleare	scarsa midriasi	tp Silodyx, tp ASA	10,00164817	63,14354774
C78	A191	Controllo	24/06/42	79	F	OD	Cataratta corticonucleare	/	Diabete iD, ipert.art, FA in NAO	7,286944002	86,76603567
C79	A197	Controllo	26/11/38	83	F	OS	Cataratta corticonucleare	/	ipert. art., pregresse trombosi, embolie, aneurisma cerebrale, scompenso cardiaco, tp eliquis (NAO), pacemaker	11,02042624	56,72059158

NUM	ID	CONTROLL	DoB	Età	SESSO	OCCHIO	PATOLOGIA PRINCIPALE	ALTRE PATO OCULARI	PATO SISTEMICHE	[P2X7r] pg/ml	SIERO[P2X7r] pg/ml
C80	A201	Controllo	18/01/41	81	M	OD	Cataratta corticonucleare	diplopia verticale (paresi muscolare)	tachiFA in tp Lixiana (NAO), ipert.art., bronchite cronica	8,983287119	118,0789499
C81	A203	Controllo	01/12/63	58	F	OS	Cataratta corticonucleare	/	sndr depressiva in tp sertralina	8,983287119	71,72047674
C82	A204	Controllo	09/04/48	73	M	OD	Cataratta corticonucleare	pterigio OD	innesto aortico, ateromasia iliaca, Ca polmonare, tp ASA		73,15141275
C83	A205	Controllo	22/08/52	69	M	OS	Cataratta corticonucleare	/	ipert.art., pregresso IMA, tp ASA	14,75952189	111,584003

NUM	ID	CONTROLL	DoB	Età	SESSO	OCCHIO	PATOLOGIA PRINCIPALE	ALTRE PATO OCULARI	PATO SISTEMICHE	[P2X7r] pg/ml	SIERO[P2X7r] pg/ml
P1	A4	PEX	02/09/42	76	M	OS	Sublussazione cristallino	PEX, iridofacodonesi, scarsa midriasi, ipertono; OD ambliopia	BPCO, OSAS in CPAP, bioprotesi aortica, cardiopatia ischemica cronica, NSTEMI 2005 PTC+BMS, NSTEMI 2012 PTCA+DES, PTCA+stent ramo circonflesso medio-distale, ipert.art., IPB, IRC IIIA, iperuricemia		
P2	A9	PEX	27/06/30	88	F	OS	Cataratta ambroide	PEX OO, scarsa midriasi, iridotomie OO	ipert.art., tremore senile		

NUM	ID	CONTROLL	DoB	Età	SESSO	OCCHIO	PATOLOGIA PRINCIPALE	ALTRE PATO OCULARI	PATO SISTEMICHE	[P2X7r] pg/ml	SIERO[P2X7r] pg/ml
P3	A18	PEX	21/07/40	79	M	OD	Cataratta in PEX	PEX, scarsa midriasi	DMID, ipert. Art., tp ASA	165,21	166,8218
P4	A19	PEX	03/01/31	88	F	OD	IOL sub lussata	PEX, scarsa midriasi		116,072	131,3557
P5	A23	PEX	23/01/39	80	F	OD	Cataratta	PEX, Atrofia orletto pupillare			129,484
P6	A36	PEX	22/11/47	72	M	OD	Cataratta	PEX, scarsa midriasi			144,0371
P7	A48	PEX	20/05/35	84	M	OD	Cataratta	PEX, ca ipoprofonda			5,721301
P8	A53	PEX	17/06/50	69	M	OD	Cataratta nucleare densa	PEX, distrofia maculare, scarsa midriasi	tp clopidogrel		138,40395
P9	A67	PEX	12/02/39	80	F	OS	Cataratta nucleare e posteriore	PEX			42,89123
P10	A128	PEX	09/03/37	83	M	OS	Cataratta corticonucleare	PEX, scarsa midriasi	ipert.art. IPB in tp Alfuzosina, tp ASA	12,81312	43,46110109

NUM	ID	CONTROLL	DoB	Età	SESSO	OCCHIO	PATOLOGIA PRINCIPALE	ALTRE PATO OCULARI	PATO SISTEMICHE	[P2X7r] pg/ml	SIERO[P2X7r] pg/ml
P11	A138	PEX	28/11/35	85	M	OS	Cataratta corticonucleare	PEX, glaucoma, DMLE	/	5,247038	10,67917749
P12	A157	PEX	02/03/44	77	F	OD	Cataratta corticonucleare	PEX, glaucoma, esiti di occlusione venosa retinica	favismo, sndr ansionsa in tp xanax	3,897719173	68,46871264
P13	A202	PEX	07/06/44	77	M	OD	Cataratta corticonucleare	PEX	ipert.art, diabete NID	14,07926765	155,7753622
P14	A207	PEX	24/07/45	76	F	OD	Cataratta corticonucleare	PEX	/	5,252856109	99,33919378
G1	A8	Glaucoma	20/09/45	73	F	OS	Cataratta nucleare	Glaucoma oo, tp Cosopt coll	ipert.art.	4,562467	
G2	A11	Glaucoma	09/12/46	72	M	OS	Cataratta nucleare	glaucoma OO, non tp antiglaucomatosa in atto, pregressa trabeculectomia OO	fumatore, iperuricemia in tp	4,855588	

NUM	ID	CONTROLL	DoB	Età	SESSO	OCCHIO	PATOLOGIA PRINCIPALE	ALTRE PATO OCULARI	PATO SISTEMICHE	[P2X7r] pg/ml	SIERO[P2X7r] pg/ml
G3	A43	Glaucoma	29/08/34	85	F	OD	Cataratta	Glaucoma, monocola, pregressa trabeculectomia	DMID	6,139029	34,50804
G4	A55	Glaucoma	08/08/46	73	F	OD	Cataratta corticonucleare densa evoluta	Glaucoma, angiosclerosi,iridotomia	DMNID ipert. Arta. PM, clopidogrel		71,47639
G5	A59	Glaucoma	27/07/58	61	F	OD	Cataratta nucleare	Glaucoma oo , miope elevata, corioretinosi miopica		40,15172506	50,983325

NUM	ID	CONTROLL	DoB	Età	SESSO	OCCHIO	PATOLOGIA PRINCIPALE	ALTRE PATO OCULARI	PATO SISTEMICHE	[P2X7r] pg/ml	SIERO[P2X7r] pg/ml
G6	A64	Glaucoma	03/03/58	61	F	OS	Cataratta nucleare e sottocapsulare posteriore	Glaucoma (tp Saflutan, Qualid ofta, Droptimol),Retinopatia diabetica, Edema maculare diabetico (tp con ivt)	DMNID		56,41976
G7	A93	Glaucoma	13/03/40	80	M	OD	Cataratta corticonucleare	Glaucoma, scarsa midriasi	Diabete NID, ipert.art., IPB in tp, tp coumadin	47,80980376	172,338097
G8	A94	Glaucoma	27/08/38	82	F	OD	Cataratta corticonucleare	glaucoma	tp ASA		104,5904291
G9	A99	Glaucoma	27/08/35	85	M	OD	Cataratta corticonucleare	glaucoma, scarsa midriasi	diabete ID, IPB in tp alfalitici, BPCO	67,91396488	976,81983
G10	A103	Glaucoma	07/09/47	73	M	OD	Cataratta bianca	glaucoma	/	7,62612	77,59736381

NUM	ID	CONTROLL	DoB	Età	SESSO	OCCHIO	PATOLOGIA PRINCIPALE	ALTRE PATO OCULARI	PATO SISTEMICHE	[P2X7r] pg/ml	SIERO[P2X7r] pg/ml
G11	A108	Glaucoma	09/09/46	74	F	OS	Cataratta corticonucleare	glaucoma	ipert.art., sndr ansiosa	10,68079	
G12	A131	Glaucoma	27/09/54	66	M	OS	Cataratta corticonucleare	glaucoma, scarsa midriasi	IPB in tp amsulosina, ipert.art., tp ASA, bypass AC	21,7812	100,4965145
G13	A133	Glaucoma	26/06/36	84	M	OD	Cataratta corticonucleare	glaucoma, DMLE (essudativa?), non segni di retinopatia diabetica	Diabete ID	4,216871	41,06545892
G14	A135	Glaucoma	28/06/37	83	F	OS	Cataratta corticonucleare	glaucoma, tp ipotonizzante topica, pregresse iridotomie	ipert.art., FA in tp	43,97969	73,76358179
G15	A160	Glaucoma	11/08/39	82	M	OD	Cataratta corticonucleare	glaucoma, bassa conta endoteliale	diabete NID, ipert.art., FA, tp pradaxa	12,03962183	72,55901215

NUM	ID	CONTROLL	DoB	Età	SESSO	OCCHIO	PATOLOGIA PRINCIPALE	ALTRE PATO OCULARI	PATO SISTEMICHE	[P2X7r] pg/ml	SIERO[P2X7r] pg/ml
G16	A165	Glaucoma	13/01/37	85	M	OS	Cataratta corticonucleare	glaucoma	ipert.art., tp Xarelto		75,11972593
G17	A166	Glaucoma	16/08/49	72	F	OS	Cataratta corticonucleare	glaucoma		6,608730172	52,52854669
G18	A180	Glaucoma	09/03/39	82	F	OD	Cataratta corticonucleare	glaucoma, tp AZARGA e GANFORT; distrofia EPR maculare	Diabete ID, tp ASA, ipert.art, vasculopatia AAII		85,05236432
G19	A187	Glaucoma	22/02/46	76	F	OD	Cataratta corticonucleare	glaucoma in tp Cosopt e Acamba coll, bassa conta endoteliale, distrofia epr maculare	ipert.art, tp ASA, exfumatore,	13,39919966	44,10104274
G20	A193	Glaucoma	21/05/48	73	M	OS	Cataratta corticonucleare	glaucoma, scarsa midriasi	/	9,3226945	54,93791377
G21	A195	Glaucoma	15/12/43	78	F	OD	Cataratta corticonucleare	glaucoma	diabete NID, tp ASA	6,269692484	66,00087178

NUM	ID	CONTROLL	DoB	Età	SESSO	OCCHIO	PATOLOGIA PRINCIPALE	ALTRE PATO OCULARI	PATO SISTEMICHE	[P2X7r] pg/ml	SIERO[P2X7r] pg/ml
G22	A200	Glaucoma	19/12/46	75	F	OS	Cataratta corticonucleare	glaucoma tp Azarga, drusen maculari	ipert.art., FA in tp Xarelto (NAO), ex fumatore, microcitemia	4,914002816	97,54105928
D1	A7	RDP	06/09/51	67	M	OS	Emovitreo in retinopatia diabetica	retinopatia diabetica, trazione vitreo-retinica inferiore, impianto Desametasone ivt in OO nel 2017, FACO+IOL+VVPP +PEELING MER+TAIOFTAL in OD 5/2018 in OS 12/2018, tp Combigan coll OO 2 vv/die	diabete ID, ipert.art., ritenzione urinaria, IPB in tp Omnic, tp ASA		

NUM	ID	CONTROLL	DoB	Età	SESSO	OCCHIO	PATOLOGIA PRINCIPALE	ALTRE PATO OCULARI	PATO SISTEMICHE	[P2X7r] pg/ml	SIERO[P2X7r] pg/ml
D2	A12	RDP	05/09/45	73	M	OD	Cataratta+pucker maculare	retinopatia diabetica, pregresso intervento FACO+IOL+VVPP +PEELING MER in OS 9/2018	DMID, pregresso IMA, PTCA+STENT, TEA carotide dx, ipert.art., tp ASA, BPCO di grado moderato		
D3	A21	RDP	27/03/40	69	M	OD	Cataratta in EMD	EMD, glaucoma	DMID, tp ASA	277,04715	
D4	A52	RDP	11/06/54	65	F	OS	Cataratta	Retinopatia diabetica, media midriasi	DMID, favismo		60,155155
D5	A61	RDP	18/07/48	71	M	OS	Cataratta nucleare posteriore	Retinopatia diabetica, ipermetrope	ipert. art., tp ASA	67,2295357	74,11609
D6	A77	RDP	19/04/48	72	F	OD	Cataratta complicata totale	RD trattata con PRP	DMID, tp ASA	65,8612996	

NUM	ID	CONTROLL	DoB	Età	SESSO	OCCHIO	PATOLOGIA PRINCIPALE	ALTRE PATO OCULARI	PATO SISTEMICHE	[P2X7r] pg/ml	SIERO[P2X7r] pg/ml
D7	A83	RDP	11/12/51	68	M	OD	Cataratta	RDNP ed EMD, scarsa conta endoteliale	DMID, ipert. art, ipertrofia ventr sn		703,6069652
D8	A84	RDP	22/05/55	65	F	OS	Cataratta	RDNP, non EMD, pregressa IVT Ozurdex	DMNID	26,87295848	148,0314036
D9	A106	RDP	07/02/61	59	M	OS	Cataratta corticonucleare	retinopatia diabetica con edema maculare	diabete NID, tp ASA	5,930702	136,9159181
D10	A110	RDP	16/02/89	31	F	OS	Cataratta corticonucleare	retinopatia diabetica proliferante, laser trattamento PRP, edema maculare diabetico in tp IVT Ozurdex	Diabete ID	12,03962	131,7746662

NUM	ID	CONTROLL	DoB	Età	SESSO	OCCHIO	PATOLOGIA PRINCIPALE	ALTRE PATO OCULARI	PATO SISTEMICHE	[P2X7r] pg/ml	SIERO[P2X7r] pg/ml
D11	A117	RDP	08/05/54	66	F	OD	Cataratta corticonucleare con riflessi ambroidi	retinopatia diabetica, laser trattamento PRPR, edema maculare diabetico in tp IVT, glaucoma	diabete ID	5,930702	105,3819275
D12	A123	RDP	16/09/52	68	M	OS	Cataratta corticonucleare	edema maculare diabetico, retinopatia diabetica, glaucoma, scarsa midriasi	pregresso TIA, diabete	17,99117	208,3485156
D13	A142	RDP	07/05/49	71	F	OS	Cataratta corticonucleare	edema maculare diabetico in tp Ozurdex IVT	diabete ID, PTCA cardiaco	8,683731	75,57899579

NUM	ID	CONTROLL	DoB	Età	SESSO	OCCHIO	PATOLOGIA PRINCIPALE	ALTRE PATO OCULARI	PATO SISTEMICHE	[P2X7r] pg/ml	SIERO[P2X7r] pg/ml
D14	A158	RDP	24/04/50	71	M	OD	Cataratta corticonucleare	retinopatia diabetica con edema maculare in tp Ozurdex IVT, trattamento laser PRP	ipert.art, pregressa PCA, tp Xarelto	5,252856109	51,34656941
D15	A159	RDP	30/04/37	84	F	OD	Cataratta corticonucleare	retinopatia diabetica	diabete ID, ipert.art,cardiopatia ischemica, bypass AC, tp ASA e inhixa	24,30272402	46,6255932
R1	A6	DDRR	18/10/63	55	M	OS	Esiti di DDR, PDMS pesante dalla CV	Pseudofachia		23,40733	
R2	A30	DDRR	13/02/74	45	M	OS	Distacco di retina	DDR/cataratta		102,0126	
R3	A68	DDRR	17/10/56	63	M	OS	Esiti di DDR, PDMS pesante dalla CV	PDMS in camera vitrea		178,6917	237,04515

NUM	ID	CONTROLL	DoB	Età	SESSO	OCCHIO	PATOLOGIA PRINCIPALE	ALTRE PATO OCULARI	PATO SISTEMICHE	[P2X7r] pg/ml	SIERO[P2X7r] pg/ml
R4	A86	DDRR	18/05/59	61	F	OS	DDR totale	Pseudofachia		54,44646638	
R5	A79	DDRR	17/12/55	64	M	OD	Esiti di DDR, PDMS pesante dalla CV	PDMS in camera vitrea	poliallergie (FANS), ipert.art.	107,906	126,0338225
R6	A98	DDRR	05/05/48	72	F	OD	Cataratta corticonucleare	Distacco di retina operato contestualmente	/	10,05946948	131,2634
R7	A111	DDRR			M	OD	Cataratta corticonucleare	racidiva di DDR		27,04712	39,86832073
R8	A116	DDRR	29/01/68	53	F	OS	Cataratta corticonucleare	DDR operato contestualmente		38,51881	95,21268258
R9	A152	DDRR	03/08/57	64	M	OD	Cataratta corticonucleare	pregresso DDR, olio di silicone in CV asportato contestualmente		13,39919966	

NUM	ID	CONTROLL	DoB	Età	SESSO	OCCHIO	PATOLOGIA PRINCIPALE	ALTRE PATO OCULARI	PATO SISTEMICHE	[P2X7r] pg/ml	SIERO[P2X7r] pg/ml
R10	A209	DDRR	18/08/58	63	M	OD	Cataratta corticonucleare	distacco di retina operato contestualmente	/	12,03962183	
R11	A210	DDRR	21/01/40	82	F	OS	cataratta nucleare	distacco di retina operato contestualmente, bassa conta endoteliale	splenectomia, stato ansioso	19,86738103	
M1	A14	M	21/12/72	46	F	OD	Cataratta nucleare	miopia elevata(-20 D), monocola funzionale per ambliopia OS, in OD esiti di trattamento laser periferia inferiore	/	9,765372	

NUM	ID	CONTROLL	DoB	Età	SESSO	OCCHIO	PATOLOGIA PRINCIPALE	ALTRE PATO OCULARI	PATO SISTEMICHE	[P2X7r] pg/ml	SIERO[P2X7r] pg/ml
M2	A24	M	07/08/41	78	F	OS	Cataratta	miopia, conta endoteliale<2000, monocolo funzionale	FA in NAO	12,4627	
M3	A32	M	19/05/39	80	M	OS	Cataratta	miopia elevata		36,77348	104,7874
M4	A71	M	19/02/61	58	F	OS	Cataratta sottocapsulare posteriore	miopia		13,3992	174,0952
M5	A105	M	02/02/52	68	F	OD	Cataratta corticonucleare	miopia elevata	/	55,9223	76,58801632
M6	A115	M	12/05/75	45	F	OS	Cataratta corticonucleare	miopia elevata	/	44,11023	123,7715186
M7	A122	M	09/05/54	66	F	OS	Cataratta corticonucleare	miopia elevata	/	16,25899	23,94971233
M8	A125	M	21/01/48	72	F	OS	Cataratta corticonucleare	miopia elevata	ipert.art., ateromasia TSA	8,339797	115,7891959
M9	A126	M	17/02/57	63	M	OS	Cataratta corticonucleare	miopia elevata, (pregresso DDR in occhio controlaterale)	/	8,339797	

NUM	ID	CONTROLL	DoB	Età	SESSO	OCCHIO	PATOLOGIA PRINCIPALE	ALTRE PATO OCULARI	PATO SISTEMICHE	[P2X7r] pg/ml	SIERO[P2X7r] pg/ml
M10	A129	M	20/08/56	64	F	OS	Cataratta corticonucleare	miopia elevata	/	19,56178	127,4626814
M11	A139	M	06/06/54	66	F	OD	Cataratta corticonucleare	miopia elevata	/	7,3085	61,68773255
M12	A147	M	05/01/47	75	M	OS	Cataratta corticonucleare	miopia elevata	tp clopidogrel, IPB in tp Omnic	11,36011169	25,34999077
M13	A149	M	20/10/53	68	F	OD	Cataratta corticonucleare	miopia elevata, glaucoma	/	11,69984354	91,07041798
M14	A179	M	03/05/59	62	F	OS	Cataratta corticonucleare	Miopia elevata, corioretinosi miopica	allergia ASA	5,930700924	35,70859357
M15	A194	M	19/01/48	74	M	OS	Cataratta corticonucleare	miopia elevata	ipert.art.	7,286944002	87,84247722
M16	A206	M	04/07/60	61	F	Cataratta c	Miopia elevata, corioretinosi miopica	/		15,09971891	47,10173421
M17	A208	M	20/11/53	68	F	OS	Cataratta corticonucleare	miopia elevata, scarsa conta endoteliale		8,643926015	42,83266197

NUM	ID	CONTROLL	DoB	Età	SESSO	OCCHIO	PATOLOGIA PRINCIPALE	ALTRE PATO OCULARI	PATO SISTEMICHE	[P2X7r] pg/ml	SIERO[P2X7r] pg/ml
E1	A10	E	09/01/38	81	F	OD	Cataratta corticonucleare	guttae endoteliali e scarsa conta endoteliale	ipert.art., FA in tp coumadin	6,12129	
E2	A46	E	18/05/38	81	F	OD	Cataratta	Distrofia endoteliale di Fuchs		11,38823	45,44748
E3	A70	E	15/04/45	74	F	OS	Cataratta corticonucleare	guttae	DMNID, tp asa, ipert. art.		93,88194
E4	A90	E	06/08/46	74	F	OD	Cataratta corticonucleare	cornea guttata (Fuchs)	tp ASA	36,6869	116,8145664
E5	A121	E	06/05/41	79	M	OS	Cataratta corticonucleare	guttae endoteliali (Fuchs), iridofacodonesi	ipert.art.	10,05947	91,55992107
E6	A130	E	22/04/46	74	F	OS	Cataratta corticonucleare	bassa conta endoteliale	Diabete, ipert.art, tp ASA	8,683647	56,26877526

NUM	ID	CONTROLL	DoB	Età	SESSO	OCCHIO	PATOLOGIA PRINCIPALE	ALTRE PATO OCULARI	PATO SISTEMICHE	[P2X7r] pg/ml	SIERO[P2X7r] pg/ml
E7	A144	E	09/11/35	86	M	OS	Cataratta corticonucleare	scarsa midriasi, bassa conta endoteliale	ipert.art., tp Eliquis	11,36011169	57,60205925
E8	A150	E	23/04/48	73	M	OD	Cataratta corticonucleare	bassa conta endoteliale	ipert.art., tp Xarelto, FA	21,91347513	77,51270702
E9	A153	E	17/01/38	84	M	OD	Cataratta corticonucleare evoluta ambroide	bassa conta endoteliale	CA orofaringeo, tp ASA	35,94062917	32,86306898
E10	A161	E	10/03/38	83	F	OD	Cataratta corticonucleare	bassa conta endoteliale	ipert.art., embolia polmonare, TVP, tp xarelto, sndr depressiva in tp	3,897719173	
E11	A163	E	12/11/48	73	F	OD	Cataratta corticonucleare	scarsa conta endoteliale	ipert.art.	4,575195575	57,43273525
E12	A169	E	19/11/39	82	M	OD	Cataratta corticonucleare evoluta	scarsa conta endoteliale		5,930700924	66,93701261

NUM	ID	CONTROLL	DoB	Età	SESSO	OCCHIO	PATOLOGIA PRINCIPALE	ALTRE PATO OCULARI	PATO SISTEMICHE	[P2X7r] pg/ml	SIERO[P2X7r] pg/ml
E13	A170	E	23/11/73	78	F	OD	Cataratta corticonucleare	scarsa conta endoteliale	ipert. arteriosa in tp	3,897719173	69,3201659
E14	A188	E	19/01/45	77	M	OD	Cataratta corticonucleare	distrofia Fuchs (guttae endoteliali e bassa conta), scarsa midriasi	tp TAMSULOSIN, tp ASA	3,897719173	31,82116011
E15	A189	E	13/03/54	67	F	OD	Cataratta corticonucleare	guttae endoteliali, sinechie iridolenticolari, distrofia maculare	ipert.art.	8,643926015	74,5827634
E16	A192	E	18/09/43	78	F	OS	Cataratta corticonucleare	distrofia Fuchs (guttae endoteliali e bassa conta)	ipert. art, allergia chinoloni, pregresso H.Zoster emivolto dx	5,930700924	19,4180034

NUM	ID	CONTROLL	DoB	Età	SESSO	OCCHIO	PATOLOGIA PRINCIPALE	ALTRE PATO OCULARI	PATO SISTEMICHE	[P2X7r] pg/ml	SIERO[P2X7r] pg/ml
E17	A198	E	07/06/51	70	F	OD	Cataratta corticonucleare	guttae endotelieli e bassa conta (Fuchs?)	fumatore, ipert. art.	5,930700924	69,57484936
Am1	A15	AMD	01/11/37	82	F	OD	Cataratta nucleare	distrofia maculare	FA in tp TAO (coumadin), ipert.art., pregresso CA mammario asportato e in tp Tamoxifene	3,950411	
Am2	A45	AMD	12/09/36	83	F	OS	Cataratta	Cataratta in dmle os	tp asa allergia penicilline	44,36212	55,25615
Am3	A50	AMD	25/12/38	80	F	OD	Cataratta	DMLE e glaucoma od		14,97081	23,418005
Am4	A54	AMD	23/09/31	88	F	OS	Cataratta nucleare densa con riflessi ambroidi	distrofia maculare, angiosclerosi	DMNID		87,472195

NUM	ID	CONTROLL	DoB	Età	SESSO	OCCHIO	PATOLOGIA PRINCIPALE	ALTRE PATO OCULARI	PATO SISTEMICHE	[P2X7r] pg/ml	SIERO[P2X7r] pg/ml
Am5	A58	AMD	12/10/37	82	F	OS	Cataratta corticonucleare	distrofia maculare oo, angiosclerosi			26,45273
Am6	A65	AMD	22/04/47	72	F	OS	Cataratta corticonucleare	DMLE, Glaucoma in tp con Saflutan e timololo	ipta, cardioasa		56,354235
Am7	A101	AMD	22/05/39	81	M	OD	Cataratta corticonucleare	CNV peripapillare	ipert.art., IPB in tp alfalitici, sndr depressiva	44,67624498	184,0546641
Am8	A109	AMD	18/05/29	91	M	OS	Cataratta corticonucleare	DMLE essudativa trattata con IVT antiVEGF	tp ASA	18,45232	64,70232249
Am9	A114	AMD	20/12/40	80	F	OD	Cataratta corticonucleare	DMLE essudativa trattata con IVT antiVEGF	ipert.art.	10,68079	108,8471129

NUM	ID	CONTROLL	DoB	Età	SESSO	OCCHIO	PATOLOGIA PRINCIPALE	ALTRE PATO OCULARI	PATO SISTEMICHE	[P2X7r] pg/ml	SIERO[P2X7r] pg/ml
Am10	A119	AMD	27/03/40	80	F	OS	Cataratta corticonucleare	DMLE essudativa trattata con IVT antiVEGF	HBV+	12,12446	76,58801632
Am11	A134	AMD	27/03/33	87	M	OS	Cataratta corticonucleare	DMLE essudativa trattata con IVT antiVEGF	diabete NID, ipert.art., FA, tp Eliquis, scompenso cardiaco	11,43596	41,06545892
Am12	A136	AMD	30/09/37	83	F	OD	Cataratta corticonucleare	DMLE essudativa trattata con IVT antiVEGF	ipert.art.	12,12446	74,97374029
Am13	A199	AMD	08/01/59	63	F	OD	Cataratta corticonucleare	distrofia EPR maculare	/	3,897719173	31,46635564
Mp1	A78	MP	30/04/05	73	M	OS	Cataratta complicata totale	RD trattata con PRP	DMID, tp ASA	65,8612996	388,4270993
Mp2	A81	MP	11/09/47	73	F	OS	Cataratta+pucker maculare	pucker maculare	MBL tratto con adrotp in OD		188,3480573

NUM	ID	CONTROLL	DoB	Età	SESSO	OCCHIO	PATOLOGIA PRINCIPALE	ALTRE PATO OCULARI	PATO SISTEMICHE	[P2X7r] pg/ml	SIERO[P2X7r] pg/ml
Mp3	A85	MP	06/04/46	74	M	OS	Pucker maculare OS	Pseudofachia	Ipert. art, tp Clopidogrel	74,09103186	126,9581878
Mp4	A87	MP	04/08/49	71	F	OS	Pucker maculare	Pseudofachia	/	29,04564537	47,69610679
Mp5	A102	MP	07/08/53	67	M	OS	Cataratta corticonucleare	pucker maculare operato contestualmente	allergia tachipirina, ipert. art. tp ASA	7,965342	68,72630275
Mp6	A104	MP	12/07/42	78	F	OS	Cataratta corticonucleare	pucker maculare non operato	/	8,643926	13,24972471
Ov1	A31	OVR	11/08/52	67	M	OS	Cataratta	OVP, Ozurdex		8,833663	154,3553
Ov2	A141	OVR	08/08/34	86	M	OS	Cataratta corticonucleare	esiti di occlusione venosa centrale della retina	Diabete NID, IRC	7,3085	84,8743467
M1	A3	Uveite	13/12/60	58	M	OS	Cataratta sottocapsulare posteriore	Ciclite eterocromica di Fuchs	/		

NUM	ID	CONTROLL	DoB	Età	SESSO	OCCHIO	PATOLOGIA PRINCIPALE	ALTRE PATO OCULARI	PATO SISTEMICHE	[P2X7r] pg/ml	SIERO[P2X7r] pg/ml
M2	A13	Uveite	22/04/39	80	F	OS	Cataratta nucleare	pregressa uveite OD, qualche gutta endoteliale, cornea verticillata da amiodarone	pacemaker, ipert.art., FA con bradi-tachicardia in tp Eliquis (NAO), artrite reumatoide		
M3	A27	MBL	25/12/37	81	F	OD	Cataratta	Esiti di MBL OD		63,90051	
M4	A66	Uveite	13/07/56	63	M	OD	Cataratta corticonucleare	Cheratouveite erpetica recidivante,conta < 2000	DMNID, tp asa		101,259995
M5	A113	Chertopati	30/05/30	90	F	OS	Cataratta corticonucleare	cornea verticillata per cordarone	tp cordarone, ipert.art	12,03962	66,71366487
M6	A196	Uveite	29/04/69	52	M	OD	Cataratta corticonucleare densa	pregressa uveite	tp anticoagulante orale	3,559049975	126,3906117

ID	DoB	Età	SESSO	OCCHIO	INTERVENTO	DATA INTERVENTO	MATERIALE PR	TOT materiale prelevato	num di campioni	PATOLOGIA PRINCIPALE	ALTRE PATO OCULARI	PATO SISTEMICHE	P2X7r pg/ml	II analisi [P2X7r]	media
V1	02/12/41	77	M	OS	Vitrectomia+peeling MER	27/03/19	Vitreo	0,6 ml	3 (x 0,2 ml)	Pucker maculare	pseudofachia OS	ipert.art.	4,949202		
V2	20/07/42	76	M	OD	Vitrectomia+endolaser+densiron	03/04/19	Vitreo	0,6 ml	3 (x 0,2 ml)	Distacco di retina	pseudofachia OO (2017), iniziale PVR superiore	ipert.art., prostatectomia (2017) in tp Bicalutamide	28,52198		
V3	23/03/43	76	M	OS	Vitrectomia+endolaser+densiron	11/04/19	Vitreo	0,8 ml	4 (x 0,2 ml)	Distacco di retina, macula OFF, rotture multiple inf, temp e nasali in periferia	pseudofachia OO (9 aa fa)	pregresso IMA+STENT (2011), tp ASA, DMNID	12,02505	198,539	105,282
V4	03/02/36	83	F	OD	Vitrectomia	02/10/19	Vitreo	0,5 ml	1 (x 0,5 ml)	Pucker maculare		tp ASA, Ipert. Art			
V5	10/03/43	76	F	OS	Vitrectomia	08/10/19	Vitreo	0,5 ml	1 (x 0,5 ml)	Pucker maculare+ foro lamellare		ticlopidina	7,986313	9,82101	8,903662
V6	11/03/49	70	M	OD	Vitrectomia	06/11/19	Vitreo	0,5 ml	1 (x 0,5 ml)	Pucker maculare			14,28002	16,78426	15,53214
V7	04/01/43	76	F	OD	Vitrectomia+FACO	20/11/19	Vitreo	0,5 ml	1 (x 0,5 ml)	Pucker maculare	Cataratta CN operata contestualmente	ipert. Art	8,282802	11,55426	9,918531
V8	02/10/39	80	M	OS	Vitrectomia	27/11/19	Vitreo	0,5 ml	1 (x 0,5 ml)	Distacco di retina			94,7421	95,53115	95,13663

ID	DoB	Età	SESSO	OCCHIO	INTERVENTO	DATA INTERVENTO	MATERIALE PR	TOT materiale prelevato	num di campioni	PATOLOGIA PRINCIPALE	ALTRE PATO OCULARI	PATO SISTEMICHE	P2X7r pg/ml	II analisi [P2X7r]	media
V9	19/10/62	57	F	OD	Vitrectomia+FACO	27/11/19	Vitreo	0,5 ml	1 (x 0,5 ml)	Pucker maculare+ foro lamellare	cataratta	tiroidectomia totale, allergia: potassio bicromato, cafezolina	23,26482	24,61351	23,93917
V10	02/12/37	82	M	OD	Vitrectomia	28/01/20	Vitreo	0,5 ml	1 (x 0,5 ml)	Distacco di retina			20,91764		
V11	22/01/49	71	F	OD	Vitrectomia	04/02/20	Vitreo	0,5 ml	1 (x 0,5 ml)	Distacco di retina			33,3787	31,12467	32,25168
V12	17/01/48	72	M	OS	Vitrectomia	05/02/20	Vitreo	0,5 ml	2 (x 0,5 ml)	Pucker in esiti di ddr	pregresso DDR		59,51961	68,99106	64,25533
V13	06/04/46	74	M	OS	VVP+peeling MER	29/09/20	Vitreo	0,6 ml	3 (x 0,2 ml)	Pucker maculare OS	Pseudofachia	Ipert. art, tp Clopidogrel	89,80207	49,0337	69,41789
V14	28/11/44	75	F	OD	VVP+peeling MER+FACO+IOL	29/09/20	Vitreo			Pucker maculare OD	Cataratta CN operata contestualmente		69,16676	84,67285	76,9198
V15	20/06/39	81	M	OD	VVP+peeling MER+FACO+IOL	30/09/20	Vitreo	0,2 ML	1 (x 0,2 ml)	Pucker maculare OD	Cataratta CN operata contestualmente		23,16345		
V16	18/05/59	61	F	OS	Vitrectomia	01/10/20	Vitreo	0,4 ml	2 (x 0,2 ml)	DDR totale	Pseudofachia		75,32348	212,0329	143,6782
V17	02/10/35	85	M	OS	FACO+IOL	09/10/20	Vitreo			Pucker maculare	Cataratta operata contestualmente	Diabete NID, tp ASA	42,76113	98,13544	70,44829

ID	DoB	Età	SESSO	OCCHIO	INTERVENTO	DATA INTERVENTO	MATERIALE PR	TOT materiale prelevato	num di campioni	PATOLOGIA PRINCIPALE	ALTRE PATO OCULARI	PATO SISTEMICHE	P2X7r pg/ml	II analisi [P2X7r]	media
V18	19/08/47	73	F	OD	Vitrectomia+FACO+IOL	13/10/20	Vitreo	0,6 ml	3 (x 0,2 ml)	Foro maculare	Cataratta CN operata contestualmente	/	45,02459		
V19	09/12/50	69	F	OD	Vitrectomia+FACO+IOL	13/10/20	Vitreo	0,8 nml	4 (x0,2 ml)	emovitreo in retinopatia diabetica proliferante	Cataratta operata contestualmente, pregresso laser trattamento PRP per retinopatia diabetica	Diabete ID, ipert.art.	16,94868		
V20			M	OS	Vitrectomia	13/10/20	Vitreo	0,8 nml	4 (x0,2 ml)	Distacco di retina regmatogeno	Pseudofachia	ipert.art.	44,32794	143,2582	93,79308
V21	06/08/59	61	F	OS	Vitrectomia+FACO+IOL	15/10/20	Vitreo	0,3 ml	1 (x 0,2 ml) + 1 (0,1 ml)	Distacco di retina regmatogeno	Cataratta CN operata contestualmente	/	16,77624	123,4691	70,12265
V22	05/05/48	72	F	OD	FACO+IOL	20/10/20	Vitreo	0,9 ml	3 (x 0,2 ml) + 1 (0,3 ml)	Distacco diretina regmatogeno	Cataratta CN operata contestualmente	/	10,74763		

ID	DoB	Età	SESSO	OCCHIO	INTERVENTO	DATA INTERVENTO	MATERIALE PR	TOT materiale prelevato	num di campioni	PATOLOGIA PRINCIPALE	ALTRE PATO OCULARI	PATO SISTEMICHE	P2X7r pg/ml	II analisi [P2X7r]	media
V22 bis	16/03/39	81	M	OS	Vitrectomia	22/10/20	Vitreo	0,9 ml	3 (x 0,2 ml) + 1 (0,3 ml)	emovitreo in retinopatia diabetica proliferante, edema maculare diabetico	Retinopatia diabetica ?	/		284,5732	
V23	28/06/33	87	M	OS	Vitrectomia e FS	27/10/20	Vitreo	2 ml	4 (x 0,5 ml)	IOL sublussata	/	ipert.art., tp clopidogrel	10,9197	173,7668	92,34324
V24	07/08/53	67	M	OS	Vitrectomia+FACO+IOL	03/11/20	Vitreo	0,7 ml	2 (x 0,2 ml) + 1 (x 0,1 ml)	pucker maculare	Cataratta CN operata contestualmente	allergia tachipirina, ipert.art., tp ASA	4,216871		
V25	27/03/50	70	M	OS	Vitrectomia	03/11/20	Vitreo	0,8 nml	4 (x0,2 ml)	emovitreo in retinopatia diabetica proliferante, edema maculare diabetico	pseudofachia	Diabete ID, tp clopidogrel, ipert.art.	30,77806	8,339797	19,55893
V26	04/03/51	69	M	OS	Vitrectomia	05/11/20	Vitreo	0,2 ml	1 (x 0,2 ml)	DDR con emovitreo	pseudofachia	ipert.art., IPB	54,09694	14,19096	34,14395
V27	29/01/68	53	F	OS	Vitrectomia+FACO+IOL	05/01/21	Vitreo	0,7 ml	2 (x 0,2 ml) + 1 (x 0,1 ml)	DDR e pucker maculare	Catarattna CN operata contestualmente		50,08051	254,633	63,90051
V28	07/08/46	74	M	OS	Vitrectomia+FACO+IOL	14/01/21	Vitreo	0,8 nml	4 (x0,2 ml)	Foro maculare	Cataratta CN operata contestualmente	ipert.art.	24,7193	237,3591	7,3085

ID	DoB	Età	SESSO	OCCHIO	INTERVENTO	DATA INTERVENTO	MATERIALE PR	TOT materiale prelevato	num di campioni	PATOLOGIA PRINCIPALE	ALTRE PATO OCULARI	PATO SISTEMICHE	P2X7r pg/ml	II analisi [P2X7r]	media
V29	23/04/41	80	M	OD	Vitrectomia	10/02/22	Vitreo	1,5 ml	3 (x0,5ml)	DDR temporale e inferiore recidivato	pseudofachia, pregresso piombaggio radiale+ laser	/	22,1267		
V30	29/04/43	78	F	OS	Vitrectomia+FACO+IOL	10/02/22	Vitreo	0,6 ml	2 (x 0,3 ml)	DDR regmatogeno macula OFF	Cataratta CN operata contestualmente	ipert.art.	27,83359		
V31	17/03/32	89	F	OS	Vitrectomia+FS	16/02/22	Vitreo	1 ml	5 (x 0,2 ml)	Residui lenticolari	Afachia, bassa conta endoteliale	ipert.art., tp clopidogrel, cardiopatia ipertensiva, decadimento cognitivo	22,47224		
V32	25/04/41	80	M	OS	Vitrectomia+FACO+IOL	17/02/22	Vitreo	0,4 ml	2 (x 0,2 ml)	Pucker e foro maculare OS	Cataratta CN	tp ticlodipina	21,09033		
V33	01/02/44	78	M	OD	Vitrectomia+FACO+IOL	17/02/22	Vitreo	0,2 ml	1 (x 0,2 ml)	Pucker maculare OD	Cataratta CN	allergia amoxicillina	54,44647		
V34	13/12/56	65	M	OD	Vitrectomia+FACO+IOL	22/02/22	Vitreo	0,8 ml	4 (x 0,2 ml)	Pucker maculare OD	Cataratta	Diabete NID, ipert.art,tp ASA, IMA con stent	20,91764		
V35	05/08/48	73	M	OD	Vitrectomia+FACO+IOL	24/02/22	Vitreo	0,6 ml	3 (x 0,2 ml)	DDR trazionale in RD	Cataratta, retinopatia diabetica proliferante	Diabete	122,573		

ID	DoB	Età	SESSO	OCCHIO	INTERVENTO	DATA INTERVENTO	MATERIALE PR	TOT materiale prelevato	num di campioni	PATOLOGIA PRINCIPALE	ALTRE PATO OCULARI	PATO SISTEMICHE	P2X7r pg/ml	II analisi [P2X7r]	media
V36	02/06/63	59	F	OD	Vitrectomia	04/03/22	Vitreo	1,5 ml	3 (x 0,5 ml)	DDR con corda sottoretinica, pieghe retiniche rigide	/	Fibromialgia, ipert. art.	18,32855		
V37	27/01/71	51	M	OD	Vitrectomia	08/03/22	Vitreo	0,4 ml	1 (x 0,4 ml)	Pucker maculare OD	/ pseudofachia	microcitemia	19,7091		
V38	23/04/46	75	M	OS	Vitrectomia+FACO+IOL	08/03/22	Vitreo	0,4 ml	2 (x 0,2 ml)	Pucker maculare OS	Cataratta, glaucoma tp Imolast	ipert.art., tp ASA, pregresso TIA	24,0277		
V39	31/05/53	68	M	OS	Vitrectomia+FACO+IOL	09/03/22	Vitreo	0,4 ml	2 (x 0,2 ml)	Pucker maculare OS	Cataratta, glaucoma, ambliopia OS	ipert.art.	20,22698		
V40	09/03/44	78	F	OS	Vitrectomia+FACO+IOL	15/03/22	Vitreo	0,6 ml	2 (x 0,3 ml)	Pucker maculare OS	Cataratta	ipert.art.	19,88171		
V41	09/02/68	54	F	OD	Vitrectomia+FACO+IOL - CONTROLLARE	15/03/22	Vitreo	0,8 ml	4 (x 0,2 ml)	Pucker maculare OD	Cataratta	ipert.art.	15,56948		
V42	17/12/48	73	F	OD	Vitrectomia	16/03/22	Vitreo	0,4 ml	2 (x 0,2 ml)	DDR regmatogeno macula OFF	Pseudofachia	/	23,50912		
V43	19/06/67	55	M	OS	Vitrectomia	19/03/22	Vitreo	0,6 ml	3 (x 0,2 ml)	DDR regmatogeno macula OFF	Pseudofachia OS, pregresse cheratotomie radiali OO, pregresso DDR OD con ftisi bulbare, nistagmo	ipert.art.	18,67362		

ID	DoB	Età	SESSO	OCCHIO	INTERVENTO	DATA INTERVENTO	MATERIALE PR	TOT materiale prelevato	num di campioni	PATOLOGIA PRINCIPALE	ALTRE PATO OCULARI	PATO SISTEMICHE	P2X7r pg/ml	II analisi [P2X7r]	media
V44	28/10/48	73	M	OS	Vitrectomia	08/04/22	Vitreo	0,8 ml	4 (x 0,2 ml)	DDR post-traumatico + emovitreo	/	Diabete NID, ipert.art,tp ASA	102,7564		
V45	21/11/32	89	M	OS	Vitrectomia	09/04/22	Vitreo	2 ml	4 (x 0,5 ml)	DDR regmatogeno macula OFF	Pseudofachia OO (da circa 20 aa)	ipert.art., ateromasia TSA	24,0277		
V46	18/08/58	63	M	OD	Vitrectomia	26/04/22	Vitreo	0,4 ml	2 (x 0,2 ml)	DDR regmatogeno macula OFF	Cataratta nucleare	no tp farmacologica	23,85483		
V47	05/03/77	45	M		Vitrectomia	27/04/22	Vitreo	0,6 ml	3(x0,2 ml)	DDR regmatogeno macula OFF	Pseudofachia	no tp farmacologica	17,29358		
V48	02/08/59	62	M	OS	Vitrectomia	28/04/22	Vitreo	0,6 ml	3(x0,2 ml)	DDR regmatogeno macula OFF			17,46605		
V49	21/01/40	82	F	OS	Vitrectomia	06/05/22	Vitreo	0,7 ml	2(x 0,2 ml) + 1 (x 0,3 ml)	DDR regmatogeno, schisi-distacco inferiore con foro	Cataratta operata contestualmente, conta endoteliale bassa	splenectomia, stato ansioso,	16,77624		
V50	01/11/03	19	M	OD	Vitrectomia	06/05/22	Vitreo	0,6 ml	3(x 0,2 ml)	CE endobulbare	/	/	22,1267		

UM	ID	CONTROLLI/PATOLOGIE	DB	BA	SESSO	OCCHIO	PATOLOGIA PRINCIPALE	ALTRE PATOLOGIE OCULARI	PATOLOGIE SISTEMICHE	VEGF(pg/ml	FIBRO(pg/ml
C1	V1	Controllo	02/12/41	77	M	OS	Pucker maculare	pseudofachia OS	ipert.art.	4,95	
C2	V4	Controllo	03/02/36	83	F	OD	Pucker maculare		tp ASA, Ipert. Art		
C3	V5	Controllo	10/03/43	76	F	OS	Pucker maculare+ foro lamellare		ticlopidina	8,90	209,10645
C4	V6	Controllo	11/03/49	70	M	OD	Pucker maculare			15,53	268,047
C5	V7	Controllo	04/01/43	76	F	OD	Pucker maculare	Cataratta CN operata cont	ipert. Art	9,92	73,09391
C6	V9	Controllo	19/10/62	57	F	OD	Pucker maculare+ foro lamell	cataratta	tiroidectomia totale, a	23,94	71,6349
C7	V13	Controllo	06/04/46	74	M	OS	Pucker maculare OS	Pseudofachia	Ipert. art, tp Clopidogr	69,42	126,9581878
C8	V14	Controllo	28/11/44	75	F	OD	Pucker maculare OD	Cataratta CN operata con	testualmente	76,92	
C9	V15	Controllo	20/06/39	81	M	OD	Pucker maculare OD	Cataratta CN operata con	testualmente		
C10	V17	Controllo	02/10/35	85	M	OS		Cataratta operata contest	Diabete NID, tp ASA	70,45	130,5057269
C11	V18	Controllo	19/08/47	73	F	OD	Foro maculare	Cataratta CN operata cont	/	45,02459006	
C12	V24	Controllo	07/08/53	67	M	OS	pucker maculare	Cataratta CN operata cont	allergia tachipirina, ipe	4,216871	
C13	V28	Controllo	07/08/46	74	M	OS	Foro maculare	Cataratta CN operata cont	ipert.art.	7,3085	35,68191337
C14	V32	Controllo	25/04/41	80	M	OS	Pucker e foro maculare OS	Cataratta CN	tp ticlodipina	21,09032837	42,2630522
C15	V33	Controllo	01/02/44	78	M	OD	Pucker maculare OD	Cataratta CN	allergia amoxicillina	54,44646638	55,26629218
C16	V34	Controllo	13/12/56	65	M	OD	Pucker maculare OD	Cataratta	Diabete NID, ipert.art,	20,91763741	
C17	V37	Controllo	27/01/71	51	M	OD	Pucker maculare OD	/ pseudofachia	microcitemia	19,7090984	114,4695829
C18	V38	Controllo	23/04/46	75	M	OS	Pucker maculare OS	Cataratta, glaucoma tp Im	ipert.art., tp ASA, preg	24,0277041	130,3707559
C19	V39	Controllo	31/05/53	68	M	OS	Pucker maculare OS	Cataratta, glaucoma, ambl	ipert.art.	20,22697991	64,57200352
C20	V40	Controllo	09/03/44	78	F	OS	Pucker maculare OS	Cataratta	ipert.art.	19,88171494	78,52111855
C21	V41	Controllo	09/02/68	54	F	OD	Pucker maculare OD	Cataratta	ipert.art.	15,5694838	59,93102851
R1	V2	DDRR	20/07/42	76	M	OD	Distacco di retina	pseudofachia OO (2017), k	ipert.art., prostatector	28,52198	
R2	V3	DDRR	23/03/43	76	M	OS	Distacco di retina, macula OF	pseudofachia OO (9 aa fa)	pregresso IMA+STENT,	105,28	
R3	V8	DDRR	02/10/39	80	M	OS	Distacco di retina			95,14	135,3573
R4	V10	DDRR	02/12/37	82	M	OD	Distacco di retina			20,91763741	94,97764
R5	V11	DDRR	22/01/49	71	F	OD	Distacco di retina			32,25	48,50898
R6	V12	DDRR	17/01/48	72	M	OS	Pucker in esiti di ddr	pregresso DDR		64,26	63,87126
R7	V20	DDRR			M	OS	Distacco di retina regmatoge	Pseudofachia	ipert.art.	93,79	117,2744481
R8	V21	DDRR	06/08/59	61	F	OS	Distacco di retina regmatoge	Cataratta CN operata cont	/	70,12	171,8646485
R9	V22	DDRR	05/05/48	72	F	OD	Distacco diretina regmatoger	Cataratta CN operata cont	/	10,74763117	131,2634
R10	V26	DDRR	04/03/51	69	M	OS	DDR con emovitreo	pseudofachia	ipert.art., IPB	34,14	18,991528

LUX	ID	CONTROLLI/PATOLOGIE	DOB	ETÀ	SESSO	OCCHIO	PATOLOGIA PRINCIPALE	ALTRE PATOLOGIE/ALTRI	PATOLOGIE SISTEMICHE	PCR (Y/N) [pg/ml]	VEGF (Y/N) [pg/ml]
R11	V27	DDRR	29/01/68	53	F	OS	DDR e pucker maculare	Cataratta CN operata contestualmente		63,90	
R12	V29	DDRR	23/04/41	80	M	OD	DDR temporale e inferiore re	pseudofachia, pregresso p	/	22,12669763	18,00082074
R13	V30	DDRR	29/04/43	78	F	OS	DDR regmatogeno macula OF	Cataratta CN operata cont	ipert.art.	27,83359379	52,4610428
R14	V36	DDRR	02/06/63	59	F	OD	DDR con corda sottoretinica,	/	Fibromialgia, ipert. art	18,32854831	34,53642325
R15	V42	DDRR	17/12/48	73	F	OD	DDR regmatogeno macula OF	Pseudofachia	/	23,50911983	39,98864982
R16	V43	DDRR	19/06/67	55	M	OS	DDR regmatogeno macula OF	Pseudofachia OS, pregress	ipert.art.	18,67362215	121,3296574
R17	V44	DDRR	28/10/48	73	M	OS	DDR post-traumatico + emov	/		102,7563565	NO PRELIEVO EMATICO
R18	V45	DDRR	21/11/32	89	M	OS	DDR regmatogeno macula OF	Pseudofachia OO (da circa	ipert.art., ateromasia T	24,0277041	42,47707145
R19	V46	DDRR	18/08/58	63	M	OD	DDR regmatogeno macula OF	Cataratta nucleare	no tp farmacologica	23,85483201	68,50238483
R20	V47	DDRR	05/03/77	45	M		DDR regmatogeno macula OF	Pseudofachia	no tp farmacologica	17,29358132	17,6486379
R21	V48	DDRR	02/08/59	62	M	OS	DDR regmatogeno macula OFF			17,46604932	128,5611974
R22	V49	DDRR	21/01/40	82	F	OS	DDR regmatogeno, schisi-dist	Cataratta operata contestu	splenectomia, stato an	16,7762409	28,27425182
D1	V19	RDP	09/12/50	69	F	OD	retinopatia diabetica prolifer	Cataratta operata contestu	Diabete ID, ipert.art.	16,94867711	155,3687565
D2	V22 bis	RDP	16/03/39	81	M	OS	emovitreo in retinopatia diab	Retinopatia diabetica ?	/	284,5732323	
D3	V25	RDP	27/03/50	70	M	OS	retinopatia diabetica prolifer	pseudofachia	Diabete ID, tp clopidog	19,56	31,30210168
D4	V35	RDP	05/08/48	73	M	OD	retinopatia diabetica con DDR	Cataratta, retinopatia diab	Diabete	122,5729914	36,88144244
M1	V23	Miscellanea	28/06/33	87	M	OS	IOL sublussata	/	ipert.art., tp clopidogre	92,34	196,1652632
M2	V31	Miscellanea	17/03/32	89	F	OS	Residui lenticolari	Afachia, bassa conta endot	ipert.art., tp clopidogre	22,47223924	46,25832321
M3	V50	Miscellanea	01/11/03	19	M	OD	trauma penetrante con CE en	/	/	22,12669763	81,74574871